

The role of the FtsA protein in *Bacillus subtilis* cell division

Joana Maria Da Silva Santos



A thesis submitted in fulfilment of the requirements
for the degree of Doctor of Philosophy

October 2011

The iThree Insitute
University of Technology, Sydney NSW,
Australia

Certificate of Authorship/Originality

I certify that the work in this thesis has not previously been submitted for a degree nor has it been submitted as part of requirements for a degree except as fully acknowledged within the text.

I also certify that the written preparation of the thesis, and all experimental work associated with it has been carried out solely by me, unless otherwise indicated.

Finally, I certify that all information sources and literature used are acknowledged in the text.

Joana Santos, October 2011

Acknowledgements

My life during the past few years has been full of professional and personal experiences. Being a PhD student was challenging and rewarding, shaping the scientist I dreamt to be. During this journey there are a few important people to thank. First and foremost, I would like to acknowledge Professor Liz Harry. I thank Liz for giving me the opportunity to work on such an interesting project; and for her encouragement and guidance throughout the time as her student. I will not forget the contagious excitement that Liz shared with me during scientific discussions, in our meetings; an inspiring way to do science. Liz helped me to develop into a scientist, using creativity and critical thinking, always believing in me. I finally wish to thank her for the invaluable time and effort spent on the reading and excellent commenting of this thesis.

I wish to acknowledge Frederico Gueiros-Filho and Gonçalo Real for kindly providing strains. I am thankful to the members of the Harry lab for their interesting input and assistance in all matters of science, for the stimulating discussions and for their fun and relaxing company making it a fantastic group to work with. These people are Adeline Quay, Kylie Turner, Patricia Quach, Jo Packer, Janniche Torsvik, Torsten Theis, Rebecca Rashid, Phoebe Peters, Michael Strauss, Andrew Liew, Jaye Lu and Michelle Tu. An individual thanks to Leigh Monahan for his precious unofficial mentoring and Sinead Blaber for being such a beautiful person and my friend. A special thank you goes to Christopher Rodrigues for being my PhD brother and a true friend.

Importantly, on a personal note I would like to thank my parents, Lurdes and António Santos, and my brothers, Rui and André Santos, for their unconditional love and support. Obrigada Mãe e Pai. Este doutoramento não existiria sem o vosso amor e apoio incondicional para perseguir os meus sonhos, e por isso dedico-vos esta tese. Lastly, I would like to thank my partner, Gavin Matanis, for his patience and encouragement, and for his help with the proof-reading and formatting of this thesis.

Contents

Certificate of Authorship/Originality.....	ii
Acknowledgements	iii
Contents	iv
Figures.....	ix
Tables	x
Publications	xii
Abbreviations	xiii
Abstract.....	xvi
Chapter 1	1
1.1 Preface.....	2
1.2 <i>Bacillus subtilis</i>: A study case	3
1.2.1 The vegetative cell cycle	4
1.2.2 Sporulation and the spore outgrowth system	6
1.3 Cell division	6
1.3.1 The FtsZ protein.....	7
1.3.2 The Z ring.....	9
1.3.2.1 The biochemistry of the Z ring.....	9
1.3.2.2 Dynamics of the Z ring	11
1.3.3 Cellular localisation of the Z ring	13
1.4 Regulation of cell division	15
1.4.1 The Min system.....	16
1.4.2 Nucleoid occlusion.....	18
1.4.3 Positioning of Z ring at the division site in <i>B. subtilis</i>	19

1.4.3.1 The coordination between DNA replication and cell division	21
1.5 Proteins affecting Z ring assembly	22
1.5.1 ZapA	24
1.5.2 SepF	25
1.5.3 EzrA	26
1.6 The FtsA protein	27
1.6.1 FtsA structure and biochemistry	28
1.6.2 The interaction of FtsA with FtsZ	31
1.6.3 FtsA function in cell division	32
1.6.3.1 The role of FtsA in <i>E. coli</i> cell division	32
1.6.3.2 FtsA functions in <i>B. subtilis</i> cell division	34
Chapter 2	37
2.1 Chemicals, reagents and solutions	38
2.2 <i>B. subtilis</i> strains and growth conditions	39
2.2.1 Testing the status of the <i>amyE</i> locus of <i>B. subtilis</i>	42
2.2.2 Depletion of FtsA using the P _{xyt} inducible promoter	42
2.3 Preparation and transformation of competent <i>B. subtilis</i> cells ...	43
2.4 Preparation and germination of <i>B. subtilis</i> spores	43
2.5 DNA methods	44
2.5.1 Extraction and purification of DNA from <i>B. subtilis</i>	44
2.5.2 Agarose gel electrophoresis of DNA	45
2.5.3 Purification of DNA from agarose gels	45
2.5.4 Determination of DNA concentration	46
2.6 Microscopy Methods	46
2.6.1 Immunofluorescence microscopy (IFM)	46
2.6.2 Live cell fluorescence microscopy	47

2.6.2.1 Preparation of cells for nucleoid and membrane visualisation.....	48
2.6.2.2 Time-lapse of live fluorescence cells	48
2.6.3 Phase contrast and fluorescence microscopy	49
2.6.4 Cell scoring and statistics.....	49
2.6.5 Fluorescence Recovery after Photo-Bleaching (FRAP).....	50
2.7 Protein methods	51
2.7.1 Denaturing polyacrylamide gel electrophoresis (SDS-PAGE).....	51
2.7.2 Western blot analysis	51
2.7.2.1 Whole cell protein extraction for Western blot analysis	52
2.7.2.2 Western transfer	52
2.7.2.3 Immunodetection.....	52
2.8 Suppliers of chemicals, reagents and equipment.....	53
Chapter 3	56
3.1 Introduction.....	57
3.1.1 Background on the <i>ftsA</i> story	57
3.1.2 Chapter Aims	59
3.2 Results	60
3.2.1 Characterisation of the <i>ftsA</i> null strain during vegetative growth.....	60
3.2.1.1 Analysis of cellular FtsA levels in <i>ftsA</i> -modified <i>B. subtilis</i> strains	64
3.2.2 Z ring formation in the absence of FtsA during spore outgrowth.....	65
3.2.3 Construction of an <i>ftsA</i> in-frame deletion strain (SU506).....	69
3.2.4 Construction of <i>ftsA</i> -complementation strains (SU630 and SU631)	73
3.2.5 Complementation of <i>ftsA</i> rescues cell division	73
3.2.5.1 <i>ftsA</i> null complementation strain (SU630).....	74
3.2.5.2 <i>ftsA</i> in-frame complementation strain (SU631)	74
3.2.6 Outgrowth spore system under FtsA-depletion conditions.....	75
3.2.6.1 Spore outgrowth of the <i>ftsA</i> in-frame complementation strain (SU631).....	75

3.2.7 The Z ring persists at midcell during transient FtsA depletion.....	78
3.3 Discussion	81
3.3.1 Why doesn't the absence of FtsA cause complete cell division inhibition? ..	83
3.3.2 The function of FtsA in later stages of cell division?	86
Chapter 4	88
4.1 Introduction.....	89
4.1.1 Chapter Aims	90
4.2 Results	90
4.2.1 Construction of GFP-DivIB fusion strains.....	91
4.2.2 Characterisation of GFP-DivIB fusion strains	91
4.2.3 Recruitment and localisation of DivIB in the absence of FtsA.....	94
4.2.4 Septum formation in the absence of FtsA	98
4.3 Discussion	102
4.3.1 FtsA is not required for DivIB recruitment. What is the primary function of FtsA?	103
4.3.1.1 Role of FtsA in recruitment of other downstream divisome proteins?	103
4.3.1.2 Role of FtsA in recruitment of later proteins, after DivIB (and related proteins) assembly?	104
4.3.1.3 Role of FtsA in Z ring constriction through direct interaction with FtsZ?.....	105
Chapter 5	107
5.1 Introduction.....	108
5.1.1 Overview of the FRAP technique	109
5.1.2 Chapter aims.....	110
5.2 Results	111
5.2.1 Introducing an FtsZ-GFP fusion protein into an FtsA-depletion background	111
5.2.2 Time-lapse microscopy of FtsZ-GFP in FtsA-depleted cells.....	113

5.2.2.1 Different fates for the Z rings formed in the absence of FtsA	116
5.2.4 Z ring dynamics is decreased in the absence of FtsA	121
5.2.4.1 FtsZ turnover in the Z ring is slower in the absence of FtsA	122
5.3 Discussion	125
5.3.1 FtsA may directly affect Z ring constriction by influencing FtsZ dynamics within the ring	127
5.3.1.1 Affecting FtsZ turnover during constriction	127
5.3.1.2 Tethering the Z ring to the cell membrane during constriction.....	128
5.3.2 FtsA may affect Z ring constriction through effects on the conformation or activity of other divisome proteins.....	130
5.3.2.1 FtsA might be required to recruit MinC and thereby allow Z ring constriction.	130
Chapter 6	133
Supplementary Material	141
References.....	142

Figures

Figure 1.1 Electron micrograph of a <i>B. subtilis</i> cell undergoing cell division.....	3
Figure 1.2 <i>B. subtilis</i> cell division.....	5
Figure 1.3 Z ring localisation	9
Figure 1.4 FtsZ polymerisation and assembly of the Z ring.	10
Figure 1.5 Model for FtsZ polymerisation and assembly into a Z ring, during the cell cycle of <i>B. subtilis</i>	15
Figure 1.6 The Min system in <i>B. subtilis</i>	17
Figure 1.7 The combined action of the Min system and nucleoid occlusion in Z ring positioning.....	20
Figure 1.8 Divisome assembly pathways in <i>B. subtilis</i> and <i>E. coli</i>	22
Figure 1.9 Network of stabilisers and destabilisers of Z ring formation.....	23
Figure 1.10 Alignment sequence of FtsA.....	29
Figure 1.11 Crystal structure of FtsA protein from <i>Thermotoga maritima</i>	30
Figure 1.12 Visualisation of FtsA in <i>B. subtilis</i> cells.....	35
Figure 3.1 Genetic constructs of <i>ftsA</i> -modified strains	62
Figure 3.2 Z ring localisation in the absence of FtsA	63
Figure 3.3 Western analysis of native FtsA presence in <i>B. subtilis</i>	65
Figure 3.4 Z ring localisation in the absence of FtsA in outgrown spores.....	68
Figure 3.5 Z ring localisation in the new <i>ftsA</i> in-frame deletion strain.....	70
Figure 3.6 Z ring localisation in the absence of FtsA in outgrown spores.....	72
Figure 3.7 Z ring localisation in <i>ftsA</i> in-frame complementation (SU631) cells during spore outgrowth.....	77
Figure 3.8 Z ring localisation in <i>ftsA</i> null complementation after depletion of FtsA. ...	80
Figure 3.9 Z ring formation and constriction in wild-type and <i>ftsA</i> mutant <i>B. subtilis</i> cells	82
Figure 4.1 GFP-DivIB localisation visualised by live cell microscopy	94
Figure 4.2 GFP-DivIB localisation in SU636 outgrown spores.....	95
Figure 4.3 DivIB localisation to midcell is delayed in the absence of FtsA	97
Figure 4.4 Frequency of cell lengths for septum formation	98
Figure 4.5 Septum formation in SU636 outgrown spores.....	101
Figure 5.1 Schematic illustrating the FRAP technique	110
Figure 5.2 FtsZ-GFP localisation in the absence of FtsA	113

Figure 5.3 Time-lapse microscopy of FtsZ–GFP localisation in <i>B. subtilis</i> SU570 (<i>ftsZ-gfp</i>) cells.....	116
Figure 5.4 Time-lapse microscopy of FtsZ–GFP localisation in <i>B. subtilis</i> SU638 (FtsA-depleted) cells.....	117
Figure 5.5 Time-lapse microscopy of FtsZ–GFP localisation in <i>B. subtilis</i> SU638 (FtsA-depleted) cells.....	119
Figure 5.6 Time-lapse microscopy of FtsZ–GFP localisation in <i>B. subtilis</i> SU638 (FtsA-depleted) cells.....	120
Figure 5.7 FRAP of a Z ring in control FtsZ-GFP <i>B. subtilis</i> cell.....	122
Figure 5.8 Overall FRAP in Z ring fluorescence intensity for <i>B. subtilis</i> cells (<i>ftsZ-gfp</i>).	123
Figure 5.9 FRAP of a Z ring in <i>ftsA</i> -depleted FtsZ-GFP <i>B. subtilis</i> cell.....	124
Figure 5.10 Overall FRAP in Z ring fluorescence intensity for <i>B. subtilis</i> cells (<i>ftsA</i> -depleted <i>ftsZ-gfp</i>).	125

Tables

Table 2.1 Commonly used aqueous buffers and solutions.....	38
Table 2.2 <i>B. subtilis</i> strains.....	40
Table 2.3 <i>B. subtilis</i> growth media.....	41
Table 2.4 Antibiotics used for selection in <i>B. subtilis</i>	41
Table 2.5 Antibodies used for primary and secondary detection for both IFM and western blot analysis.....	47
Table 2.6 Suppliers of chemicals, reagents and equipment.....	53
Table 3.1 Quantitative analysis of FtsA ⁺ (SU456), <i>ftsA</i> null (SU457), wild-type (SU5) and <i>ftsA</i> in-frame (SU506) cell lengths during mid-exponential vegetative growth.....	61
Table 3.2 Quantitative analysis of FtsA ⁺ (SU456) and <i>ftsA</i> null (SU457) cells average cell lengths during spore outgrowth.....	66
Table 3.3 Quantitative analysis of wild-type (SU5) and <i>ftsA</i> in-frame deletion (SU506) average cell lengths during spore outgrowth.....	71
Table 3.4 Cell lengths and Z ring/ μm at several time points after FtsA depletion, during vegetative growth. Quantitative analysis of wild-type (parental strain, SU456) and <i>ftsA</i>	

null complementation (SU630) cell lengths (μm), with standard error of the mean values (SEM), for sequential time points after depletion of FtsA.....	79
Table 4.1 Average cell lengths of SU633 (<i>gfp-divIB</i>) and SU636 (<i>gfp-divIB ftsA</i> compl.) strains.....	93
Table 4.2 Frequency of DivIB localisation and septum formation in <i>gfp-divIB ftsA</i> complementation strain (SU636).....	96
Table 5.1 Average cell lengths of SU570 (<i>ftsZ-gfp</i>) and SU638 (<i>ftsZ-gfp ftsA::cat P_{xyl}-ftsA</i>) strains.....	112
Table 5.2 Frequency of Z ring fates in FtsA-depleted cells (SU638; <i>ftsZ-gfp ftsA::cat P_{xyl}-ftsA</i>), during time-lapse fluorescence microscopy.....	117

Publications

J. Santos and E. J. Harry (2012). The role of the FtsA protein in *Bacillus subtilis* cell division (manuscript in preparation).

Conference proceedings

J. Santos and E. J. Harry – July, 2010 – Annual Scientific Meeting & Exhibition of the Australian Society of Microbiology – Sydney, Australia – **Oral Presentation** – Bacterial Cell Division: an “early” protein acting at a “late” stage.

J. Santos and E. J. Harry – November, 2009 – Light in Life Sciences Conference of Fluorescent Applications in Biotechnology and Life Sciences' (FABLS) Network – Melbourne, Australia – **Poster Presentation** – Life cell imaging: a fluorescent look into the function of a bacterial protein, in *Bacillus subtilis*.

J. Santos and E. J. Harry – July, 2009 – Prokaryotic Development Conference of the American Society of Microbiology – Cambridge, Massachusetts, USA – **Poster Presentation** – Unravelling the function of the bacterial cell division protein FtsA, in *Bacillus subtilis*.

J. Santos and E. J. Harry – July, 2008 – Annual Scientific Meeting & Exhibition of the Australian Society of Microbiology – Melbourne, Australia – **Oral Presentation** – The role of FtsA protein in *Bacillus subtilis* cell division.

J. Santos, A. Porta Cubas, and E. J. Harry – November, 2007 – Royal North Shore Hospital Annual Meeting – Sydney, Australia – **Poster Presentation** – Unravelling the role of an Actin-like bacterial cell division protein.

Abbreviations

A(x)	absorbance (where x = wavelength in nanometres)
A	alanine
aa	amino acid
Ab	antibody
<i>B.</i>	<i>Bacillus</i>
β	beta
bp	base pair(s)
BP	band pass
BSA	bovine serum albumin
cm	centimetres
Cm ^R	chloramphenicol resistance
DAPI	4'6-diamidino-2-phenylindole
DNA	deoxyribonucleic acid
DTT	dithiothreitol
dTTP	deoxythymidine 5''-triphosphate
<i>E.</i>	<i>Escherichia</i>
ECT	electron cryotomography
ECL	enhanced chemiluminescence
<i>ermC</i>	erythromycin resistance gene
<i>et al.</i>	and others
FITC	fluorescein isothiocyanate
FRAP	fluorescence recovery after photobleaching
FRET	fluorescence energy resonance transfer
<i>fts</i>	filamentation temperature sensitive
<i>g</i>	centrifugal force
g	gram(s)
GFP	green fluorescent protein
GMD	germination medium defined
GTP	guanosine 5'-triphosphate
h	hour(s)
IFM	immunofluorescence microscopy

Ig	Immunoglobulin
IPTG	isopropyl-1-thio- β -D-galactopyranoside
kD	kilo Dalton(s)
L	litre(s)
LP	long pass
M	milli- (10 ⁻³)
M	moles per litre
min	minute(s)
MQW	Milli-Q purified water
MSA	mineral salts A
MTS	membrane targeting sequence
N	nano- (10 ⁻⁹)
NA	numerical aperture
N/A	not applicable
<i>Neo</i>	neomycin resistance gene
NO	nucleoid occlusion
OD _x	optical density at (x refers to the wavelength in nm)
<i>P</i>	probability
<i>Pspac</i>	IPTG-inducible promoter
<i>Pxyl</i>	xylose-inducible promoter
PAGE	polyacrylamide gel electrophoresis
PBS	phosphate buffered saline
<i>Phleo</i>	phleomycin resistance gene
PCR	polymerase chain reaction
pH	power of Hydrogen
PSF	point spread function
RNA	ribonucleic acid
RNase	ribonuclease A
ROW	reverse osmosis purified water
rpm	revolutions per minute
<i>S.</i>	<i>Streptomyces</i>
sec	second(s)
SDS	sodium dodecyl sulfate
SEM	standard error of the mean

SMM	spizizen minimal medium
spp.	species
spec	spectinomycin
T	thymine
TBAB	tryptose blood agar base
TDE	2,2'-thiodiethanol
TEMED	N,N,N'',N''-tetramethyl-ethylenediamine
tet	tetracycline
thy-	thymine auxotroph
Tris	tris(hydroxymethyl)methylamine
Trp	L-Tryptophan
ts	temperature sensitive
U	units (enzyme activity)
UV	ultraviolet
V	volt(s)
v/v	volume per volume
W	watt
w/v	weight per volume
YFP	yellow fluorescent protein
2D	2-dimensional
3D	3-dimensional
μ	micro- (10 ⁻⁶)

Abstract

Bacterial cell division involves the invagination of the membrane and the cell wall to form a septum at midcell, between two replicated chromosomes. From a molecular perspective, the main event in cell division is the formation of a circumferential structure, the Z ring, formed by polymerisation of the tubulin-like FtsZ protein. The Z ring recruits a multi-protein complex to the division site, forming a division apparatus that eventually constricts as the septum forms. FtsA, a eukaryotic actin homologue, is another division protein, known to interact directly with FtsZ. It has been proposed that FtsA promotes Z ring formation; however its exact role has remained unknown. This thesis investigates how FtsA affects the Z ring and cytokinesis in the Gram-positive model organism, *Bacillus subtilis*.

Interestingly, FtsA is essential in *Escherichia coli*, the Gram-negative model organism, but not in *Bacillus subtilis*. Rather, deletion of the *ftsA* gene in vegetatively-growing *B. subtilis* cells causes a significant reduction in Z ring formation and cell division is severely diminished while cell growth is maintained, resulting in cell filamentation (long cells without septa). To confirm that this phenotype is due to the inability of FtsZ to efficiently form rings, Z ring formation was examined in the absence of FtsA, during the first round of cell division following *B. subtilis* spore germination. Surprisingly the Z rings formed with wild-type efficiency. However, unlike wild-type cells that showed subsequent constriction of these Z rings leading to septum formation, Z rings did not constrict immediately in the *ftsA* mutant and persisted into the second cycle of division. These results reveal for the first time that, unlike *E. coli*, FtsA is not required for Z ring formation in *B. subtilis*.

To understand the delay in Z ring constriction, further experiments were conducted to determine if the recruitment of downstream division proteins to the Z ring is affected in the absence of FtsA. The live-cell microscopy data confirmed that the recruitment of DivIB, and presumably other downstream division proteins that are co-recruited with DivIB, is delayed in *ftsA*-mutant cells, but occurs with wild-type efficiency. However, after recruitment of DivIB, Z ring constriction and septation are still inefficient in the absence of FtsA. These observations indicate a primary role for FtsA in *B. subtilis* in the

later stages of division, that is, after the division apparatus has assembled. This work reveals a novel perspective on the function of this protein.

In an attempt to further explore how Z ring constriction is affected by FtsA, microscopy studies were designed to analyse this cell process. Different Z ring constriction defects were observed in *ftsA*-mutant cells. Importantly, it was shown that, in the absence of FtsA, constriction is either significantly delayed or never occurs, resulting in destabilisation of the Z ring, indicating that FtsA is required for efficient Z ring constriction in *B. subtilis*. This finding raised the possibility that FtsA may be affecting the dynamics of the Z ring during cytokinesis. To verify this, the rate of FtsZ turnover in Z rings of *ftsA*-mutant cells was investigated. The results demonstrated a decrease in the rate of the FtsZ turnover in the Z ring in the absence of FtsA, possibly enough to cause an effect on Z ring constriction.

Chapter 1

§

Introduction

1.1 Preface

Cell division is an essential mechanism for life, prokaryotic or eukaryotic. Bacterial cell division is known to be a tightly regulated event, both spatially and temporally, following specific stages until a septum is formed, splitting the cell into two compartments that give rise to two new daughter cells (Figure 1.1). In the case of *Bacillus subtilis*, the organism studied in this work, and other rod-shaped bacteria, cell septation occurs precisely at the centre of the cell, ensuring that each new cell has an identical morphology and genetic identity. For decades, mainly due to established techniques of electron microscopy, bacteria were considered a simple “amorphous bag of enzymes”, with no complex internal structure or organisation. Years later, and after extended investigation, the complex but elegant bacterial life cycle and its regulatory processes are finally becoming better understood. This increased knowledge is mainly due to recent developments in cell biology methods (Phair and Misteli, 2001; Wells, 2004; Meyer and Dworkin, 2007; Kolin and Wiseman, 2007; Fu *et al.*, 2010; Li and Xie, 2011). Green fluorescent protein (GFP) fusion technology and immunofluorescence microscopy techniques are now allowing the visualisation and monitoring of fundamental bacterial processes in time and space. Interestingly, unlike eukaryotes that have separate and sequential cell cycle events, the prokaryotic cell cycle often has overlapping events. This characteristic makes it an even more challenging process to study. The current knowledge about bacterial cells has shown that they are highly organised at the level of protein localisation. Moreover, not only cell division, but other essential processes such as DNA replication, chromosome segregation, and cell growth and differentiation, are dependent on specific protein localisation at the right time and place (for reviews see: Errington *et al.*, 2003; Weiss, 2004; Goehring and Beckwith, 2005; Margolin, 2005; Harry *et al.*, 2006; Adams and Errington, 2009; Shapiro *et al.*, 2009; Erickson *et al.*, 2010).

The fundamental nature of understanding bacterial cell division is not only for learning about basic biology, but also for more practical applications. The identification of mechanisms and essential proteins involved in cell division has opened a new area of antimicrobial research at a time when effective antibiotics are becoming rare. The discovery and development of novel antibiotics that target this essential process are

therefore invaluable (for reviews see: Lappchen *et al.*, 2005; Stokes *et al.*, 2005; Paradis-Bleau *et al.*, 2007; Haydon *et al.*, 2008; Lock and Harry, 2008).

Most of the research on bacterial cell division is centred on three model organisms; the Gram-negatives *Escherichia coli* and *Caulobacter crescentus*, and the Gram-positive *B. subtilis*. A great deal of information is therefore being collected, including their complete genome sequence and the subsequent functions of many encoded proteins that are sometimes specific to a particular organism. This thesis is focused on cell division in *B. subtilis*, with the specific aim of examining the role/s of a particular protein, FtsA, in this process.

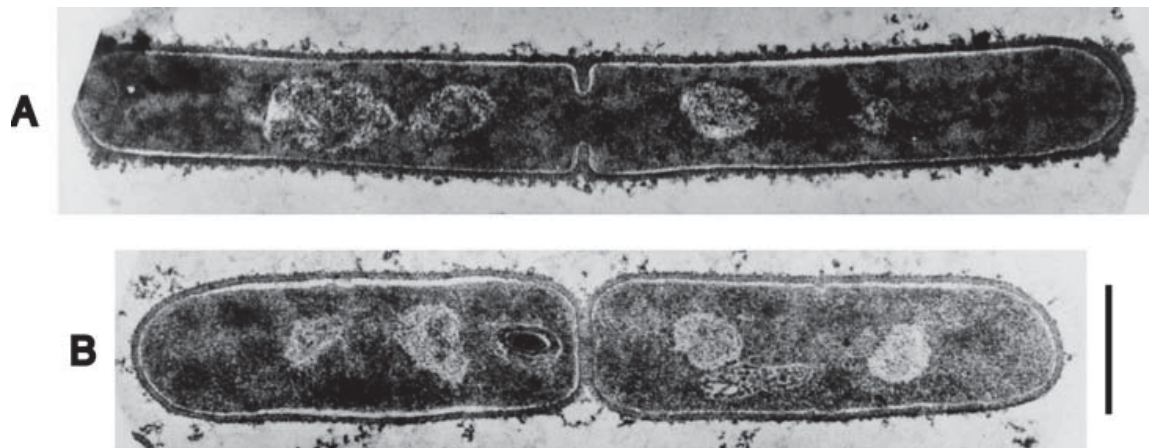


Figure 1.1 Electron micrograph of a *B. subtilis* cell undergoing cell division. A) The septum is being formed at the midcell site between two replicated nucleoids. B) The septum is fully formed; cell division is complete and the cells separate once the septal cell wall is hydrolysed. The nucleoids are visible as light coloured material within the dark cytoplasm. Scale bar represents 1 μm for both images. Figure taken from Callister (1982).

1.2 *Bacillus subtilis*: A study case

The genus *Bacillus* has been a target of scientific interest since the nineteenth century. Its introduction into science history became meaningful when Louis Pasteur used *Bacillus anthracis* as the first antibacterial vaccine, and Robert Koch was able to develop postulates making a connection between microorganisms and infectious diseases.

The importance of *Bacillus* was recognised further with its role in several infections in both humans and animals. Due to its importance and complexity, *B. subtilis* is a fundamental model for several mechanisms including cell division and development, regulation of genetic expression and metabolic processes (Errington, 2003). Fourteen years ago, the complete genome publication of *B. subtilis* by Kunst *et al.* (1997) made it possible to have an in-depth knowledge of the mechanisms of genetic and protein expression. *Bacillus subtilis* has become an excellent model bacterium for Gram-positive organisms, bringing new perspective to the microbiology field. Furthermore, the vast understanding about this organism has been generating new applications in food microbiology and it is already being heavily used in industry. A good example of this is the use of *B. subtilis* as a source of enzymes, such as subtilisin for the production of detergents (Gupta *et al.*, 2002).

1.2.1 The vegetative cell cycle

The life cycle of *B. subtilis* includes different pathways, depending on the environmental factors to which it is exposed. When there is a good supply of nutrients, cells follow the vegetative cycle; while stressful conditions promote a survival process called sporulation. There is also an alternative lifestyle pathway, in which individual cells undergo a development process to a communal growth in biofilms or colonies (Lemon *et al.*, 2008). Vegetative cell division in Gram-positive bacteria, such as *B. subtilis*, involves elongation of the rod-shaped cell along its long axis until it reaches double length (Errington and Daniel, 2002). Before cell division can occur, the single circular chromosome, which in most bacteria is condensed into a structure known as the nucleoid, undergoes replication (Lemon *et al.*, 2002). DNA replication involves the assembly of the replication machinery (initiation) and DNA synthesis (elongation) until all DNA is replicated (termination) (Lemon *et al.*, 2002). The newly-replicated chromosomes are then separated and segregated to opposite halves of the cell. Parallel to this chain of events, and prior to cell division, a multi-protein complex, called the divisome, is assembled at midcell to allow cytokinesis (Margolin, 2000; Errington *et al.*, 2003; Goehring and Beckwith, 2005; Harry *et al.*, 2006).

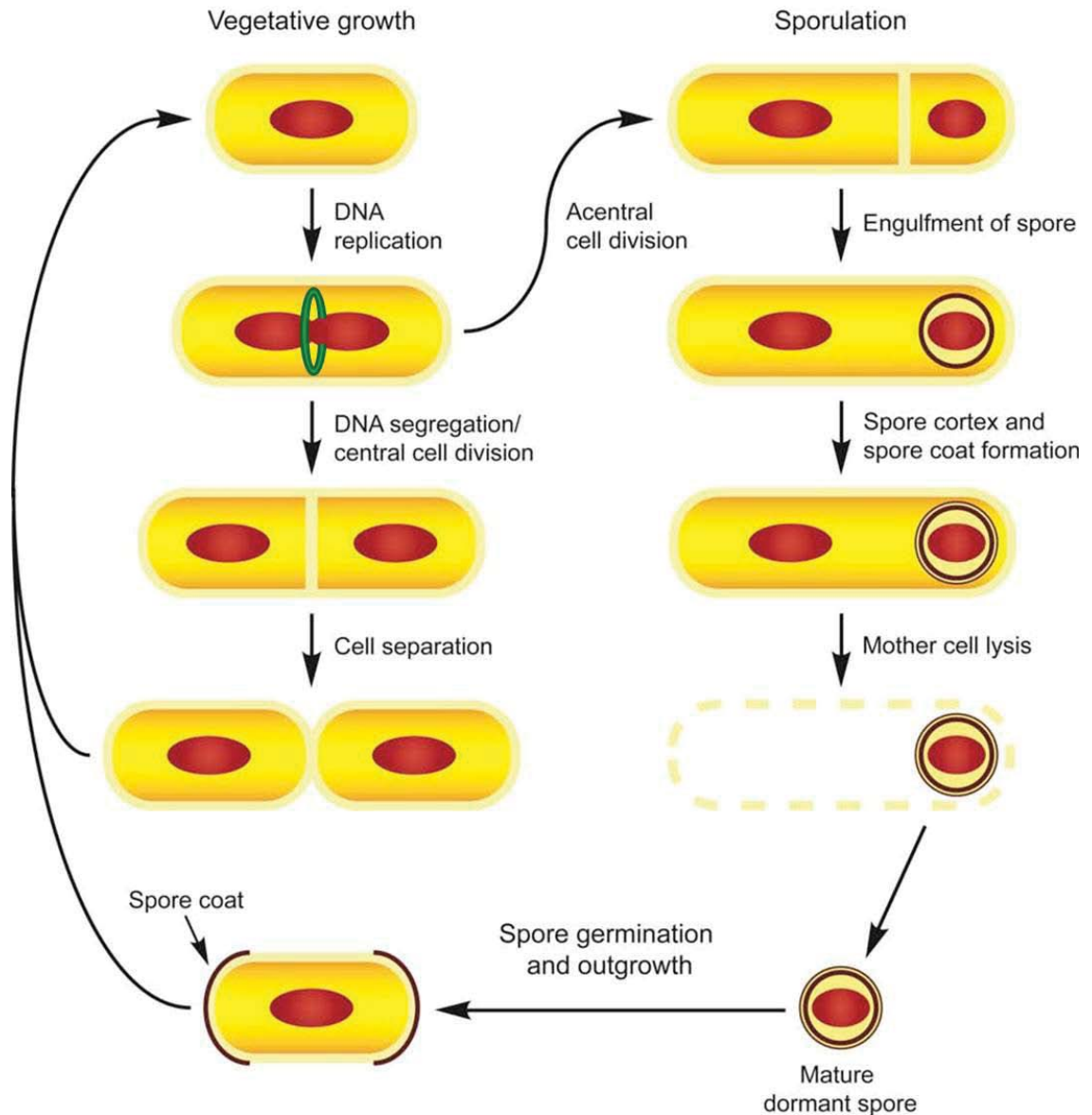


Figure 1.2 *B. subtilis* cell division. Vegetative growth (left) occurs under conditions of nutrient availability, with the cells dividing at midcell between two replicated chromosomes (red) and producing two identical daughter cells. The first event that triggers cell division is the initiation of DNA replication. Towards the end of a round of DNA replication and chromosome segregation, the Z ring forms precisely at midcell, followed by the recruitment of all the division proteins to the division site. The last stage of cell division involves Z ring constriction with ingrowth of the cell envelope layers, both membrane and cell wall (ingrowth causes formation of the septum). Finally the cell wall in the septum is hydrolysed to physically separate the two new daughter cells. Sporulation (right) occurs in response to starvation, giving rise to a dormant spore. The cells form an asymmetric septum that encloses one replicated nucleoid close to one of the cell poles, forming the forespore. This forespore is then engulfed by the larger mother cell, completes its maturation and is released through lysis of the mother cell. Once the external nutrient conditions become favourable, spore germination begins. Spore outgrowth allows the new cells to re-enter the vegetative cycle. Adapted from Monahan (2008).

1.2.2 Sporulation and the spore outgrowth system

In response to starvation, *B. subtilis* cells can switch to an alternative differentiation pathway called sporulation, which results in the formation of a metabolically dormant spore (Hauser and Errington, 1995). This ensures the viability of the species. The mature spore is highly resistant to extreme conditions such as intense heat, radiation, chemical exposure and pressure (recently reviewed by: Eichenberger, 2007). The sporulation process involves the formation of an asymmetric septum close to one of the cell poles, dividing the cell into a larger cell (mother cell) and a smaller compartment (forespore) (Figure 1.2), each enclosing one replicated nucleoid. The process continues with the engulfment of the forespore by the mother cell and formation of the spore cortex and the spore coat. The mature spore is then released from the mother cell by cell lysis, remaining viable for long periods of time (Nicholson, 2003). When external conditions for growth improve, spore germination begins giving rise to a new vegetative cycle (Figure 1.2) (Errington and Daniel, 2002; Gueiros-Filho, 2007).

The event of spore germination provides a remarkable tool for scientists to study cell cycle processes in bacteria. This is because the spores can be germinated under conditions that offer a relatively synchronous cell culture system (Harry *et al.*, 1999; Barák *et al.*, 2005). Most importantly, spore germination in this organism uniquely allows the possibility to examine the first cell cycle uncomplicated by prior division events (Harry, 2001).

1.3 Cell division

Cell division in rod-shaped bacteria involves the invagination of the membrane and the cell wall to form a septum at midcell, between two replicated and segregated chromosomes (Harry *et al.*, 2006). Subsequent hydrolysis of the septal cell wall gives rise to two genetically equal daughter cells. Prior to division, over two dozen proteins are recruited and assembled to the midcell site in a hierarchical mode, in *E. coli*, and there is a similar number in *B. subtilis* (de Boer, 2010). These proteins form a multi-protein complex called the divisome, and at least ten of them are considered to be fundamental for driving cell constriction (Errington, 2003; de Boer, 2010). Several of these proteins

were identified over 30 years ago, specifically in *B. subtilis* and *E. coli*, when some thermosensitive mutants defective in cell division were isolated (van de Putte *et al.*, 1964; Hirota *et al.*, 1968; Nukushina and Ikeda, 1969). Under conditions of high temperature, the mutant cells continue to elongate and replicate DNA without formation of division septa, resulting in long filamentous cells that eventually die by cell lysis. The genes that carried these mutations were classified with the prefix *fts*, firstly in *E. coli* and later in *B. subtilis*, as they cause the formation of long filaments at the non-permissive temperature (filamentous temperature sensitive). However, not all the divisome proteins are named with the prefix *fts*. A brief description of the divisome proteins is presented later in this introduction. However, the focus of this thesis is on two division proteins, FtsZ and FtsA. Thus, more detailed information on both proteins is outlined in the next sections. FtsZ is the first protein to assemble at midcell and is the master regulator of cell division (for reviews see: Errington *et al.*, 2003; Rothfield *et al.*, 2005; Harry *et al.*, 2006; Lutkenhaus, 2007; Adams and Errington, 2009). Despite of exhaustive investigation on this protein and its functions, many questions regarding FtsZ remain unresolved. FtsA is also a protein that localises early at the division site, and although its importance is clear, its exact functions throughout the division process are not well understood.

1.3.1 The FtsZ protein

FtsZ is an essential protein for cell division, being highly conserved among almost all bacteria (Begg and Donachie, 1985; Rothfield *et al.*, 1999; Margolin, 2000; Kobayashi *et al.*, 2003; Margolin and Bernander, 2004; Vaughan *et al.*, 2004). A few exceptions include some intracellular species of *Chlamydia* (Stephens *et al.*, 1998; Kalman *et al.*, 1999; Vaughan *et al.*, 2004), and some free-living bacterial species, including *Ureaplasma urealyticum* (Glass *et al.*, 2000). The mechanism by which cell division occurs in species that lack *ftsZ* is unknown. An intriguing FtsZ-independent process has been studied in *B. subtilis* L-forms, cells without cell wall, which appear to divide by membrane extrusion (Leaver *et al.*, 2009).

At the structural and functional level, FtsZ is regarded as the ancestor of eukaryotic tubulin, a cytoskeletal protein (Bermudes *et al.*, 1994; Erickson, 1995; Addinall and Holland, 2002). This homology is based on the strong similarity at the level of their

tertiary structure (Löwe and Amos, 1998; Romberg and Levin, 2003), since these proteins only share less than 10% sequence identity (Erickson, 2007). Early cell division studies have shown that the disruption of *ftsZ* in *E. coli* is not obtainable but an FtsZ-depleted mutant led to a filamentous phenotype (Lutkenhaus *et al.*, 1980; Dai and Lutkenhaus, 1991). Similarly, FtsZ depletion in *B. subtilis* resulted in severe filamentous cells with an inability to form central or asymmetric septa required for vegetative growth and sporulation, respectively (Beall and Lutkenhaus, 1992; Partridge and Wake, 1995). This filamentous phenotype is presumably due to the absence of the Z rings (see below) which are required for cell division. Also, in these cells, chromosome replication or segregation is not impaired (Bi *et al.*, 1991; Dai and Lutkenhaus, 1991; Wang and Lutkenhaus, 1993; Harry *et al.*, 2006). Such observations demonstrate that FtsZ is required for division but is not involved in chromosomal events. The FtsZ-depleted cells become extremely filamentous and eventually lyse, causing cell death (Beall and Lutkenhaus, 1992).

The high conservation and essentiality of FtsZ in bacteria soon made this protein an ideal drug target in the continuous search for new antibiotics (Lappchen *et al.*, 2005; Stokes *et al.*, 2005; Paradis-Bleau *et al.*, 2007; Haydon *et al.*, 2008; Lock and Harry, 2008; Monahan *et al.*, 2011). This antibacterial approach is also extremely relevant, since currently there are no drugs that specifically target cell division proteins, and antibiotics with new modes of action are urgently needed. The application of FtsZ as a potential drug target highlights the relevance that basic research has in all clinical aspects of new science discoveries. As this work shows, new and more detailed information on how the mechanisms of bacterial cell division occur is of high importance.

1.3.2 The Z ring

Two decades ago, a study about FtsZ marked a new era in protein localisation and function in bacteria. Bi and Lutkenhaus (1991) showed that FtsZ assembles into a ring-like structure and localises on the inside of the cytoplasmic membrane at midcell, during the early stages of *E. coli* cell division. From then on, the structure was called the FtsZ ring, or just simply the Z ring. These studies were performed by immunoelectron

microscopy, and were later confirmed using more sensitive techniques such as immunofluorescence microscopy (IFM) and live-cell microscopy using fluorescent protein fusions (Harry *et al.*, 1995; Addinall *et al.*, 1996; Levin and Losick, 1996; Ma *et al.*, 1996). This Z ring has also been observed and studied in different bacteria, including *B. subtilis* (Figure 1.3; Wang and Lutkenhaus, 1993). These initial studies also showed that FtsZ was the first bacterial cytokinesis protein to be localised to the division site in cells and that the Z ring was positioned at midcell prior to septum formation. Thus, the Z ring marks the position of the future division site and stays with the leading edge of the nascent septum as cytokinesis occurs. Besides the spatial regulation, the temporal regulation of Z ring assembly seems to provide an important control over the timing of cell division (Margolin, 2005; Harry *et al.*, 2006).

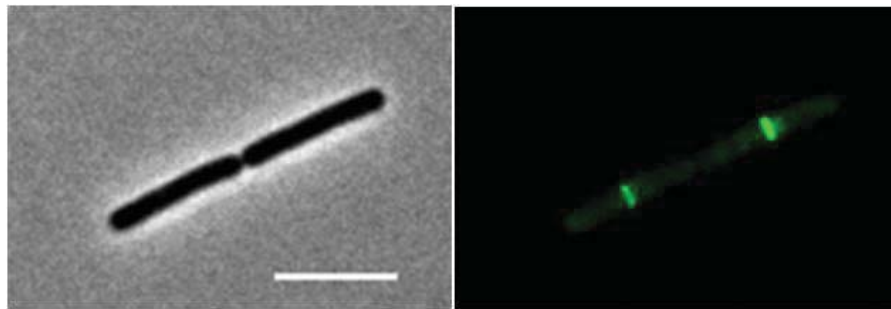


Figure 1.3 Z ring localisation. Z rings visualised by fluorescence microscopy in vegetatively-growing live cells of *B. subtilis*, containing an FtsZ-GFP fusion protein (green fluorescent protein of FtsZ; right panel). The left panel is a phase-contrast image of the same cells shown on the right. Scale bar represents 5 μm . Image from this work; strain SU570 (Table 2.2).

1.3.2.1 The biochemistry of the Z ring

The process of Z ring formation and constriction is still not completely understood. Z ring formation is thought to involve hydrolysis of GTP (Romberg and Levin, 2003; Harry *et al.*, 2006; Huecas *et al.*, 2007; Erickson *et al.*, 2010). However, recent observations suggest that at least initial Z ring constriction might not fully require GTP hydrolysis to occur (Osawa and Erickson, 2011). FtsZ proteins have GTP-binding and GTPase activity *in vitro*, which is thought to be active during polymerisation into tubulin-like protofilaments (Wang and Lutkenhaus, 1993; Wang *et al.*, 1997; Oliva *et*

al., 2004; Erickson *et al.*, 2010). In the presence of GTP *in vitro*, FtsZ monomers can reversibly assemble into protofilaments, head-to tail linear polymers of FtsZ (Nogales *et al.*, 1998). This assembly has been shown to be directional, with subunits of FtsZ being added at the minus-end of the previous added protein (Figure 1.4A and B; Osawa and Erickson, 2005). Furthermore, *in vitro*, FtsZ polymerisation is dependent on the concentration of FtsZ present (Rivas *et al.*, 2000). This suggests that, *in vivo*, FtsZ may be able to self-assemble into a Z ring if the FtsZ concentration is sufficiently high. Interestingly, Lu *et al.* (2000) have demonstrated that GTP-bound protofilaments have a straight conformation while those bound to GDP have a curved conformation, suggesting that GTPase activity *in vivo* may cause conformational changes in the protofilaments within Z ring. How this GTPase activity actually acts on the protofilaments is still unclear, although it seems that GTP hydrolysis is a rate-limiting step in FtsZ subunit turnover and can cause instability and disassembly of FtsZ polymers (Mukherjee and Lutkenhaus, 1999; Romberg and Mitchison, 2004; Oliva *et al.*, 2004; Weiss, 2004).

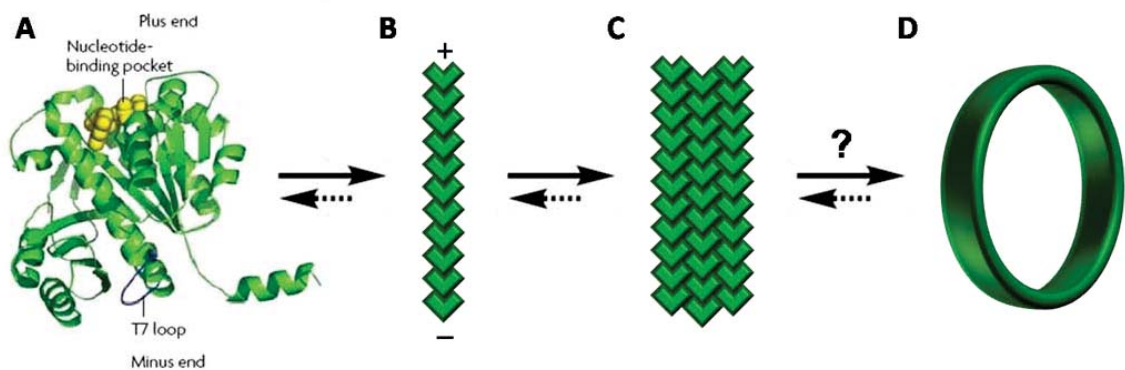


Figure 1.3 FtsZ polymerisation and assembly of the Z ring. (A) The crystal structure of *Methanococcus jannaschii* FtsZ bound to GDP (yellow spheres) and showing the T7 loop in blue. [The crystal structure from *B. subtilis* has also been solved and is similar (Oliva *et al.*, 2007)]. (B) FtsZ monomers are associated through head-to-tail interactions, forming a linear protofilament with a distinct ‘plus’ and ‘minus’ end. (C) FtsZ protofilaments associate laterally to form higher-order structures, which are arranged to form (D) the completed Z ring. The protofilaments within the Z ring are thought to follow some higher-order of arrangement, although the fine details of this structure are not well understood (illustrated by the question mark). FtsZ assembly is a completely reversible process, as indicated by the reverse arrows. In the cell, this equilibrium is controlled by a several FtsZ-binding proteins that either promote or inhibit FtsZ polymerisation (see later). Adapted from Harry *et al.* (2006).

FtsZ protofilaments can laterally associate *in vitro* creating higher-ordered structures such as ribbons/sheets, helical tubes or protofilament bundles (Bramhill and Thompson, 1994; Erickson *et al.*, 1996; Yu and Margolin, 1997; Löwe and Amos, 1999; Oliva *et al.*, 2003; Margolin, 2005; Dajkovic and Lutkenhaus, 2006; Harry *et al.*, 2006). These lateral associations differ from those of tubulin, and it is therefore unlikely that FtsZ protofilaments form structures similar to microtubules (Oliva *et al.*, 2003; Dajkovic and Lutkenhaus, 2006; Harry *et al.*, 2006). It is still not known which of the FtsZ higher-ordered structures seen *in vitro* are relevant *in vivo* and therefore, which are important for FtsZ function. It is thought that the FtsZ protofilaments can also laterally associate within the *in vivo* Z ring (Figure 1.4C; Stricker *et al.*, 2002; Monahan *et al.*, 2009). However, there is some controversy about this matter (Ghosh and Sain, 2008; Erickson, 2009; Osawa *et al.*, 2009). Several studies have suggested that lateral interactions of protofilaments are responsible for Z ring constriction. The increase of this lateral bonding and sliding of the protofilaments can generate contraction and a decrease of the ring circumference (Oliva *et al.*, 2007; Dajkovic *et al.*, 2008; Scheffers, 2008; Lan *et al.*, 2009). According to Ghosh and Sain (2008), the decrease of the ring radius appears to be an important factor for the correct constriction of the Z ring. However, their theoretical model for this suggestion is based on lateral bonds connecting protofilaments that are perpendicular to the membrane, an unlikely feature for Z ring dynamics (reviewed in: Erickson, 2009). In contrast to the above studies, other works are rejecting the importance of lateral associations of FtsZ protofilaments, considering them unable to allow for the fast FtsZ dynamics to occur; questioning their existence *in vivo* (reviewed in: Erickson, 2009). The alternative hypothesis is that a conformational change from straight to curved FtsZ protofilaments generates the constriction force (Osawa *et al.*, 2009; Erickson, 2009). The bending force exerted by FtsZ protofilaments can induce the curved conformation. This has been demonstrated using liposomes with FtsZ assembling in contractible Z rings (Osawa *et al.*, 2009).

1.3.2.2 Dynamics of the Z ring

Observations of Z ring formation provide an even more complex level to the field. They revealed that the Z ring is not a static structure, but rather highly dynamic, with

continuous remodelling of itself both before and during its constriction (Stricker *et al.*, 2002; Rueda *et al.*, 2003; Anderson *et al.*, 2004). Supporting the idea of dynamic turnover is the observation that a high concentration of FtsZ in *E. coli* promotes the GTP-dependent assembly of FtsZ protofilaments into dynamic polymers *in vitro* (Gonzalez *et al.*, 2003). In most situations only one Z ring per cell is observed, which incorporates only ~30% of the cellular pool of FtsZ molecules (Stricker *et al.*, 2002; Anderson *et al.*, 2004). These FtsZ subunits are rapidly exchanged between the Z ring and a cytoplasmic pool of FtsZ due to destabilisation of FtsZ polymers, driven by the GTPase activity of FtsZ (Addinall and Holland, 2002; Harry *et al.*, 2006; Huecas *et al.*, 2007; Lan *et al.*, 2007; Erickson, 2007; Niu and Yu, 2008; Mingorance *et al.*, 2010). Fluorescence recovery after photobleaching (FRAP) analysis in both *B. subtilis* and *E. coli* has demonstrated that FtsZ turnover within the Z ring has an approximate half-time of 8-9 seconds (Stricker *et al.*, 2002; Anderson *et al.*, 2004). *In vitro* FRET (fluorescence resonance energy transfer) measurements also showed a similar FtsZ turnover with a half-time of 7 seconds (Chen and Erickson, 2005). Some studies suggested that Z ring dynamics may derive from the exchange of molecules along the length of the polymer, or only at the ends of FtsZ polymers (Mingorance *et al.*, 2005; Shih and Rothfield, 2006). However, more recent experiments using atomic force microscopy (AFM) point to fragmentation and re-annealing of FtsZ protofilaments at locations within the Z ring, supporting the possibility that FtsZ dynamics occur along the entire length of the polymers (Mingorance *et al.*, 2005; Shih and Rothfield, 2006; Mingorance *et al.*, 2010).

It is still not clear how the process of Z ring constriction occurs. Since Z ring dynamics seem to be important for its function, are they responsible for Z ring constriction? FtsZ turnover in a normal Z ring is considered fast due to its GTPase activity. Although as mentioned above, this GTP hydrolysis seems to be a limiting factor in the turnover rate of single FtsZ protofilaments *in vitro* (Romberg and Mitchison, 2004; Weiss, 2004). It has been shown that an *ftsZ* mutant, with low GTPase activity *in vitro* (de Boer *et al.*, 1992; RayChaudhuri and Park, 1992), has a 3-fold slower Z ring turnover than wild-type (Anderson *et al.*, 2004). Nonetheless, cell division occurs normally. The observations of this mutant seem to discard the idea that a high FtsZ turnover rate is delivering enough energy for Z ring constriction. However, a recent study brings some clarity to the subject. Osawa and Erickson (2011) have shown that Z rings can still assemble and

generate initial constriction without GTP hydrolysis, but constriction stops when the Z rings become rigid. Their work with assembled Z rings in tubular liposomes proposed that the constant exchange of FtsZ subunits, mediated by GTP hydrolysis, creates openings in the dynamic Z ring, which in turn allows constriction to occur (Osawa and Erickson, 2011). Different perspectives for Z ring constriction have also been raised, including the possibility that septal peptidoglycan synthesis could drive the inward invagination of the cell wall, while the Z ring constriction is a passive event. This seems unlikely since invagination of the cytoplasmic membrane can occur when septal wall synthesis is blocked (Daniel *et al.*, 2000), and bacteria without a cell wall still have functional FtsZ, implying that Z ring constriction does not require wall ingrowth (Wang and Lutkenhaus, 1996). These findings seem to point to another force-generating source, like an unidentified motor-like protein (Bramhill, 1997; Erickson, 1997; Ryan and Shapiro, 2003), but it is still unknown what the source is and how it works on the Z ring to constrict to bring about cytokinesis.

1.3.3 Cellular localisation of the Z ring

For normal cell division to occur it is imperative that the Z ring is assembled at the midcell site, in order to orchestrate the following events that lead to the production of viable daughter cells. For more than ten years, the field of fluorescence microscopy has presented new and improved ways to observe Z ring formation, its dynamics *in vivo* and its functionality in bacterial cells. Techniques such as immunofluorescence microscopy, using specific antibodies for protein-labelling, or live cell fluorescence microscopy, using fluorescent protein tags, have been relentlessly applied ever since.

Initial fluorescence microscopy studies in *E. coli*, suggested that FtsZ assembles into a ring-like structure (Z ring) on the inner cytosolic membrane (Bi and Lutkenhaus, 1991; Addinall and Lutkenhaus, 1996; Addinall and Lutkenhaus, 1997). FtsZ monomers localise at midcell and polymerise bi-directionally to produce an arc and then a closed circle (Bi and Lutkenhaus, 1991; Addinall and Lutkenhaus, 1996; Addinall and Lutkenhaus, 1997; Sun *et al.*, 1998). However more recently, other FtsZ structures, such as FtsZ helices (or spirals), have added a more complex perspective regarding Z ring formation. These FtsZ helices were first thought to be abnormal. However, there are

strong indications that FtsZ helices are a genuine form of FtsZ localisation in bacteria. Addinall and Lutkenhaus (1996) showed functional FtsZ structures that caused helically constricting septa in an *E. coli* *ftsZ* mutant; and later, Thanedar and Margolin (2004) identified FtsZ helices in wild-type *E. coli* cells. FtsZ helices have since been observed *in vivo* in several bacteria including *E. coli* (Stricker and Erickson, 2003; Thanedar and Margolin, 2004), *B. subtilis* (Feucht and Errington, 2005; Peters *et al.*, 2007; Monahan *et al.*, 2009), *C. crescentus* (Thanbichler and Shapiro, 2006), and *Mycobacterium tuberculosis* (Chauhan *et al.*, 2006). Fluorescence microscopy studies in *E. coli* also demonstrated that FtsZ helices are highly mobile, capable of extending across the entire length of the cell, and exhibit rapid movement within the helical pattern (Thanedar and Margolin, 2004). Moreover, these helices were found to form during all stages of the cell cycle, even before Z ring assembly, suggesting that FtsZ helices are an important feature of Z ring formation. Besides vegetatively growing cells, FtsZ helices were also observed in sporulating cells of *Streptomyces coelicolor* (Grantcharova *et al.*, 2005) and of *B. subtilis* (Ben-Yehuda and Losick, 2002). In *B. subtilis* these form during the switch from medial to asymmetric division in the early stages of sporulation.

The recent new model for Z ring formation in *B. subtilis* shown in Figure 1.5 was developed by Peters *et al.* (2007). The model results from observing patterns of FtsZ localisation using time-lapse microscopy and deconvolution, and from identifying two structural precursors of the Z ring, a long-extended FtsZ-helix and a short FtsZ-helix. Using the spore outgrowth system, FtsZ was first localised as dynamic helix extending over the entire length of the newborn cell (Figure 1.5A). Later this long helix appeared to remodel itself into a shorter helical structure within the central area of the cell (Figure 1.5B). This central helix seems to persist until it is reorganised into a dynamic but stable Z ring at midcell (Figure 1.5C). Once constriction of the Z ring occurs, FtsZ emerges out of the Z ring in the same helical pattern, going through the same remodelling process and finally accumulating into a new Z ring at the division sites of the new cells. This study did not fully explain how the helical structures of FtsZ protofilaments are rearranged between the long-to-short helix and helix-to-ring. New studies suggest that it occurs through a process of lateral interactions between protofilaments (mentioned above in section 1.3.2.1). Monahan *et al.* (2009) have shown that a temperature-sensitive FtsZ mutant of *B. subtilis*, *ts1*, does not form Z rings due to a defect in lateral associations between FtsZ protofilaments. This causes these FtsZ protofilaments to be

trapped in a short helical structure. Interestingly, this group also demonstrated that the overproduction of ZapA (a stabiliser of Z ring assembly) rescues this *tsI* mutant *in vivo*, by stimulating lateral interactions (Monahan *et al.*, 2009), supporting the idea that lateral interactions stimulate remodelling of the short FtsZ helix into a ring.

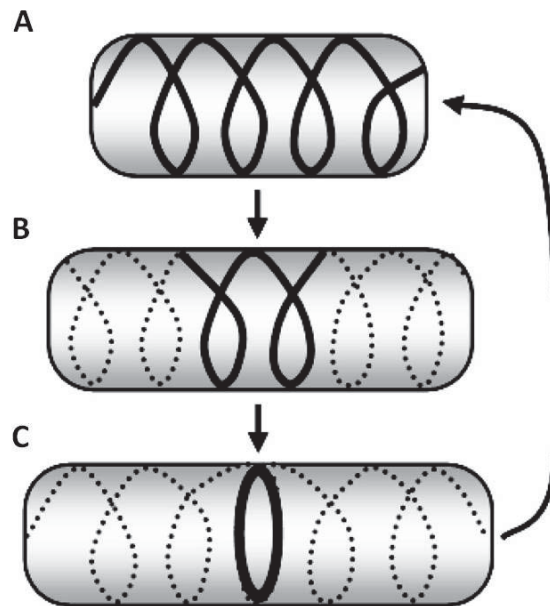


Figure 1.4 Model for FtsZ polymerisation and assembly into a Z ring, during the cell cycle of *B. subtilis*. (A) At early times, a long helical structure is formed throughout the length of the cell. (B) Later, the long helix is remodelled into a short intermediate helix, occupying the central region of the cell. (C) Lastly, the short helix is again remodelled into the Z ring at the division site at midcell. Solid lines indicate the dominant location and pattern of FtsZ at the different stages of the cell cycle, with dotted lines denoting a lower concentration of FtsZ, representing a permanent helix. Adapted from Peters *et al.* (2007).

1.4 Regulation of cell division

The regulation of Z ring formation must be tightly coordinated in both spatial and temporal terms in order to produce identical and viable daughter cells. This section will discuss the proteins that appear to influence where and when division occurs. There are many factors that regulate cell division, including regulatory proteins and systems that work at different levels. These work together to provide an overall coordination that ensures cell division maintains precision generation after generation. Several proteins

are known to affect Z ring assembly in various ways. These include positive regulators such as ZapA, FtsA and ZipA; negative regulators such as Noc and Min and EzrA (see section 1.5; Beall and Lutkenhaus, 1992; Margolin, 2000; Gueiros-Filho and Losick, 2002; Romberg and Levin, 2003; Hamoen *et al.*, 2006; Claessen *et al.*, 2008). Absence of just one of these factors does not seem to strongly affect either viability or assembly of the Z ring (Anderson *et al.*, 2004), and their regulatory function is not directly related to Z ring positioning at midcell. In this section, two of the factors known to regulate Z ring formation, by preventing Z ring assembly at inappropriate locations in the cell beside the midcell, will firstly be discussed. These are the Min system and nucleoid occlusion (NO). Both mechanisms are regarded as negative regulatory factors (or destabilisers of the Z ring; Figure 1.9). Several lines of evidence suggest that these factors are involved in positioning of the division site (Errington *et al.*, 2003; Rothfield *et al.*, 2005; Harry *et al.*, 2006; Lutkenhaus, 2007; Adams and Errington, 2009). However, a recent study has suggested that the main function of the Min and NO systems is to ensure that the division site is utilised efficiently, by making sure that the Z ring forms at midcell (Rodrigues and Harry, unpublished results). Both these systems have been studied mainly in the model organisms' *B. subtilis* and *E. coli*, revealing some differences in their function between these organisms. Therefore, for the purpose of this thesis, only the information relevant to *B. subtilis* cell division will be discussed. The role of chromosome replication in positioning the Z ring is also discussed.

1.4.1 The Min system

In order to prevent aberrant Z ring formation at the cell poles, the cells have a mechanism called the Min system, a group of proteins that localise to the poles to inhibit FtsZ polymerisation in this region during vegetative growth. Thus, in the absence of the Min system, cell division occurs at the cell poles as well as midcell. This results in the production of both cells that are longer than normal as well as anucleate minicells (Reeve *et al.*, 1973; Romberg and Levin, 2003). The Min system in *B. subtilis* is composed of four proteins, MinD, MinC, MinJ and DivIVA. MinD, a membrane-bound protein, forms a complex with MinC, an inhibitory protein of FtsZ polymer assembly (Margolin, 2000; Romberg and Levin, 2003; Scheffers, 2008), recruiting it to the inner membrane. DivIVA, an essential *B. subtilis* protein, is the topological specificity factor

for the Min system at the cell poles (Cha and Stewart, 1997; Edwards and Errington, 1997). MinJ, a recently identified protein, seems to mediate a connection between MinD and DivIVA (Patrick and Kearns, 2008; Bramkamp *et al.*, 2008).

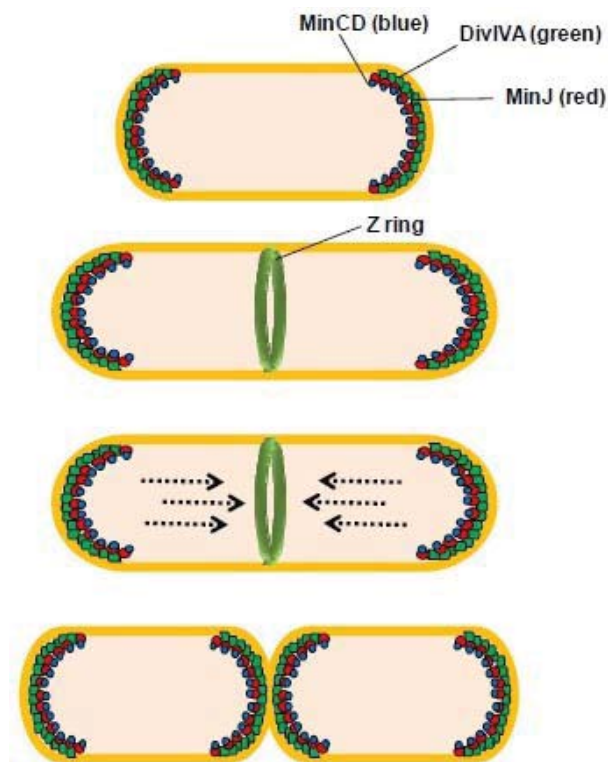


Figure 1.5 The Min system in *B. subtilis*. DivIVA pilots the MinCD division inhibitory complex (red) to the cell poles. This allows Z ring formation to occur only at the midcell site. Once the Z ring and the complex of division proteins have been assembled, DivIVA recruits the MinCDJ complex to midcell. When division is complete, DivIVA retains MinCDJ at the new and old poles so that division is again inhibited at the poles in the two daughter cells. The overall effect is the concentration of MinCDJ is highest at the poles and lowest at midcell. Adapted from Rodrigues (2011).

The Min system in *B. subtilis* functions at the level of Z ring assembly via a gradient mechanism. The concentration of the MinCD complex (with DivIVA and MinJ) is found highest at the poles preventing Z ring formation there; and lowest at the centre of the cell, ensuring midcell Z ring formation and efficient cell division (Figure 1.6; Marston *et al.*, 1998; Marston and Errington, 1999; Margolin, 2000). The classic perspective is that the protein gradient in the cell is static, although recent studies have questioned this idea (Barák *et al.*, 2008; Gregory *et al.*, 2008). One study has shown

MinD co-localisation with the cytoplasmatic membrane in a helical pattern throughout the cell (Barák *et al.*, 2008). Later, MinC dynamic behaviour was also observed between the cell pole and the midcell site (Gregory *et al.*, 2008). At a later stage in the cell cycle, after assembly of the division proteins (divisome), the Min proteins are recruited to the midcell site (Edwards and Errington, 1997; Marston *et al.*, 1998; Marston and Errington, 1999), possibly by interaction with the division proteins (Marston and Errington, 1999; Hamoen and Errington, 2003; Harry and Lewis, 2003). This localisation at midcell is important to ensure that the Min proteins are already present at the new cell poles upon cell division (Marston and Errington, 1999). DivIVA restricts MinCD at these nascent poles after septation, allowing the midcell site of the new cells to be free for Z ring assembly (Marston and Errington, 1999). However, a more recent study has found a different function for MinC in *B. subtilis* (Gregory *et al.*, 2008). They suggest that MinC prevents double division events in the presence of Z rings, by preventing extra Z rings forming adjacent to the midcell Z ring, thereby preventing Z rings forming at the nascent poles that result from septum formation.

1.4.2 Nucleoid occlusion

It is known that the nucleoid, or bacterial chromosome, has an inhibitory effect on Z ring formation. This is called the nucleoid occlusion (NO) effect (Woldringh *et al.*, 1990; Woldringh *et al.*, 1991; Margolin, 2000). This phenomenon exists presumably to prevent Z ring formation over the nucleoid, thus avoiding guillotining of the DNA by the septum prior to its complete replication and separation of the two chromosomes. Originally, it was believed that the Z ring was prevented from forming over any part of the nucleoid only by the nucleoid occlusion inhibitory effect. It has been observed in several studies that Z rings almost never localise in the same cell area occupied by an intact, unsegregated nucleoid (Yu and Margolin, 1999; Gullbrand and Nordstrom, 2000; Margolin, 2001; Sun and Margolin, 2001). Furthermore, when the replicated chromosomes segregate, a DNA-free gap is formed in the centre of the cell, providing what is called the relief of nucleoid occlusion (Yu and Margolin, 1999). This is thought to be the reason why FtsZ assembly can occur precisely at midcell, at the proper time in the cell cycle (Woldringh *et al.*, 1991; Rothfield *et al.*, 2005). Recently, Wu and

Errington (2004) have identified a DNA-binding protein, Noc, in *B. subtilis*; while a similar protein, SlmA, was found in *E. coli* (Bernhardt and de Boer, 2005). The primary role of Noc and SlmA is to prevent guillotining of the DNA by the septum under various conditions, for example when DNA replication is disturbed. These studies showed that, although not essential, the absence of Noc/SlmA together with inhibition of DNA replication allows the formation of central Z rings over the chromosome, leading to guillotining of the partially replicated chromosome by the division septum (Wu and Errington, 2004). Similarly, a *noc* deletion in cells with a defective Min system resulted in accumulation of the FtsZ protein at many positions along the length of the cell, including over the nucleoid, severely reducing the viability of the cells (Wu and Errington, 2004). Recently the regions of the chromosome at which the Noc and SlmA proteins bind in their respective organisms have been identified. These are called SlmA-binding sequences (SBSs) and Noc-binding sequences (NBSs), in *E. coli* and *B. subtilis* respectively (Wu *et al.*, 2009; Cho *et al.*, 2011). These sequences were shown to enhance negative regulation of the FtsZ assembly by the SlmA and Noc proteins (Wu *et al.*, 2009; Cho *et al.*, 2011). Interestingly, the inhibitory activity of these proteins seems to be dependent on the interaction with the identified DNA regions. These sequences are localised throughout the chromosome but become less abundant closer to its terminus region, which remains at midcell at the late stage of replication (Wu *et al.*, 2009). This position provides a way for allowing Z ring formation to occur when most of the chromosome segregates close to the end of the round of replication, thus offering a mechanism of specific spatial regulation and timing control for nucleoid protection during cell division (Wu *et al.*, 2009; Cho *et al.*, 2011).

1.4.3 Positioning of Z ring at the division site in *B. subtilis*

In the recent years, a model for the timing and placement of the Z ring at the division site has been proposed (Figure 1.7), combining nucleoid occlusion and the Min system as the factors responsible for blocking aberrant FtsZ localisation in the entire cell and allowing division to occur only at midcell, at the correct time (Errington *et al.*, 2003; Rothfield *et al.*, 2005; Harry *et al.*, 2006; Lutkenhaus, 2007; Adams and Errington, 2009; Rudner and Losick, 2010).

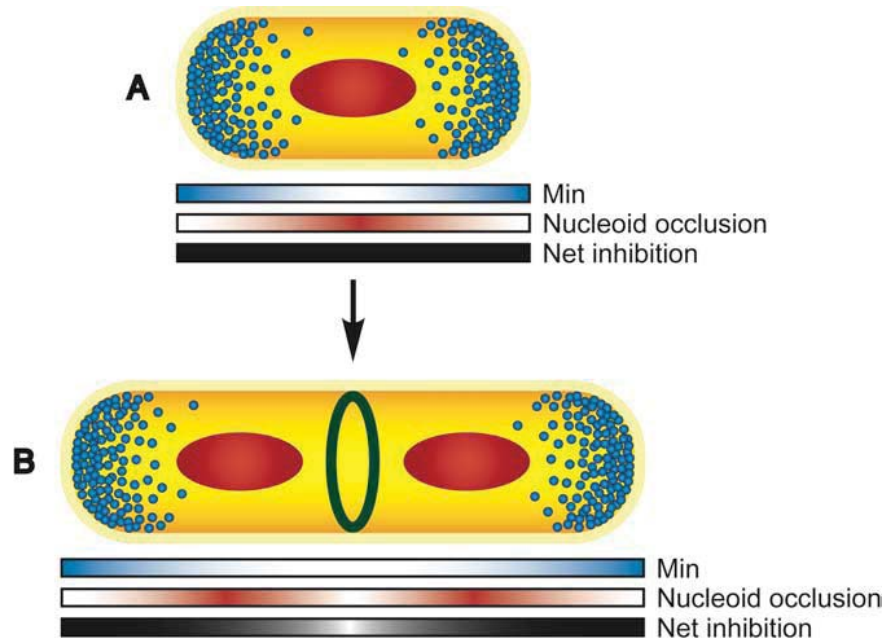


Figure 1.6 The combined action of the Min system and nucleoid occlusion in Z ring positioning. (A) Early in the cell cycle, the Min system and nucleoid occlusion proteins together block Z ring formation throughout the entire cell (total net inhibition as indicated by the solid black line). The nucleoid (red) occupies the central region, while the Min proteins (blue) are located mainly at the cell poles. (B) According to the nucleoid occlusion model of Woldringh *et al.* (1990, 1991), the segregation of replicated chromosomes results in a DNA-free gap at midcell later in the cell cycle, generating a relief of the inhibitory effect (clear spot centred in the black line), thus allowing the Z ring (green) to form at this position. Image taken from Monahan (2008).

This combined action of the Min system and nucleoid occlusion is widely accepted as the mechanism by which *B. subtilis* cells position the Z ring precisely at midcell and at the right time in the cell cycle. Interestingly, neither the Min system nor the Noc protein are essential in *B. subtilis*. Recently, some studies seem to challenge the idea that these are the sole factors. It has been shown previously that MinC and MinD are not required for the precise positioning of Z rings at midcell in *B. subtilis* (Migocki *et al.*, 2002). Furthermore, in a study discussed above, by Wu and Errington (2004), it was demonstrated that in *B. subtilis* cells deprived of both Noc protein and the Min system (double *min noc* mutant), the Z rings form very infrequently and division is defective, resulting in long cells. Importantly, they also shown that over-expression of FtsZ could restore normal cell division in the double *min noc* mutant (Wu and Errington, 2004). Very recently, it was found that, in a similar situation of complete absence of both these systems, Z ring could still be positioned precisely at midcell in *B. subtilis*, (Rodrigues and Harry, unpublished data). In addition, several bacteria do not have the inhibitory

Noc or Min homologues (Margolin, 2005; Harry *et al.*, 2006). It has been demonstrated that in *Staphylococcus aureus*, which does not contain a Min system, the Noc protein is not essential (Veiga *et al.*, 2011). All these observations suggest that the relief of nucleoid occlusion and/or the Min system is not sufficient or even required for the FtsZ to assemble precisely at midcell. Consequently, they highlight the possibility that other factors are required for the positioning of the Z ring in *B. subtilis* and other bacteria. An idea emerging points to the link between DNA replication and cell division.

1.4.3.1 The coordination between DNA replication and cell division

It has been established that Z ring formation occurs before the end of chromosome replication and segregation in *E. coli* and *B. subtilis* (Wu *et al.*, 1995; Den Blaauwen *et al.*, 1999). This suggests that when the cell triggers the initiation of DNA replication by a cell cycle signal, it may also be stimulating the cell into producing a Z ring, or at least identifying where the division site is (Margolin, 2001). Furthermore, chromosome replication may direct the localisation of the Z ring (Moriya *et al.*, 2010). Using the outgrown spore system of *B. subtilis*, new data has led to the proposal of a new mechanism for positioning the Z ring that links it to progress of the initiation phase of DNA replication. It has been suggested that the midcell division site becomes increasingly potentiated for Z ring formation as DNA replication initiation progresses (Moriya *et al.*, 2010). Once initiation is complete, the midcell site is fully potentiated (i.e. competent for Z ring assembly). However, Z ring formation does not occur yet due to nucleoid occlusion (Moriya *et al.*, 2010).

1.5 Proteins affecting Z ring assembly

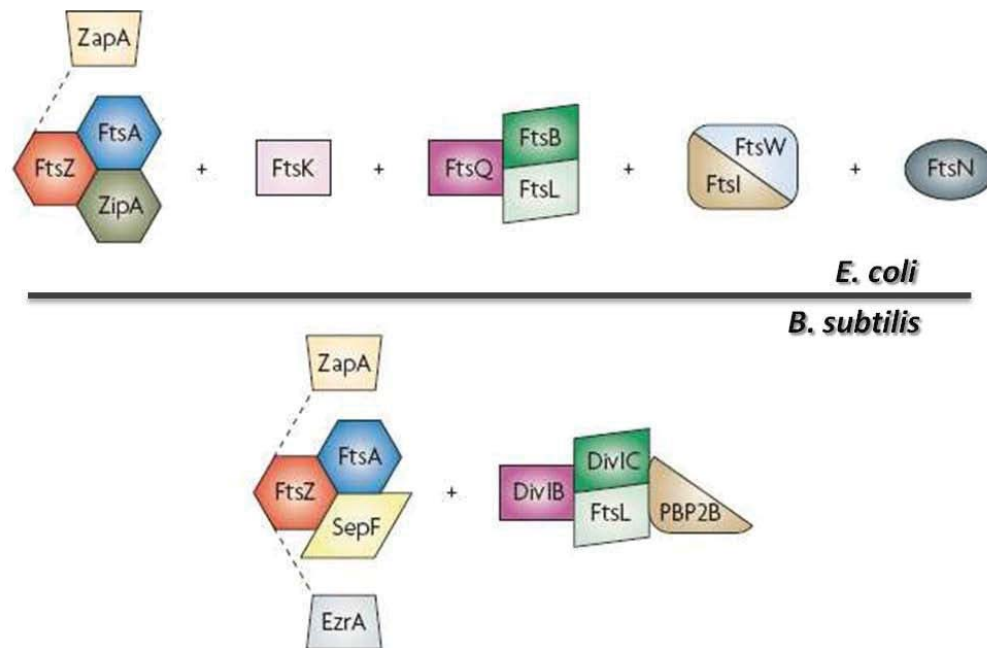


Figure 1.7 Divisome assembly pathways in *B. subtilis* and *E. coli*. In *B. subtilis*, the assembly process occurs in two stages, while in *E. coli* the pathway appears to be a linear recruitment process. Only the well characterised proteins of the divisome are depicted in this figure. The shape and colour of the boxes represent protein homologous between the two organisms. *B. subtilis* has no equivalent of the *E. coli* ZipA or FtsN proteins, and the FtsK homologue (SpoIIIE) is not required for division. The EzrA protein of *B. subtilis* has a similar topology to ZipA, but it is not required for division. The time of recruitment of the FtsW homologue in *B. subtilis* is not known, and so it is not shown for simplicity. Dotted lines indicate proteins which are not required to recruit downstream cell division proteins. All of the proteins which are recruited to the divisome are dependent on the initial formation of the Z ring composed of FtsZ. Adapted from Lock and Harry (2008).

Z rings do not assemble on their own *in vitro*. *In vivo* FtsZ polymerisation is highly dynamic and is modulated by several FtsZ-interacting proteins that are part of a protein complex known as the divisome (Dajkovic and Lutkenhaus, 2006; Harry *et al.*, 2006; Lock and Harry, 2008; de Boer, 2010). The divisome consists of proteins involved in the process of cell division and assemble at the Z ring in two sequential steps (see Figure 1.8). This recruitment pathway in *B. subtilis* appears to involve two main steps: FtsZ and the FtsZ-binding proteins (FtsA, ZapA, EzrA and SepF) that assemble early and are involved in the tight regulation of Z ring assembly; and then the other sub-complex of proteins, mainly membrane-bound proteins, that assemble later and are required for

septum formation (DivIB, FtsL, DivIC, FtsW, PBP 2B, GpsB/YpsB) (Figure 1.8; reviewed in: Errington *et al.*, 2003; Weiss, 2004; Goehring and Beckwith, 2005; Harry *et al.*, 2006; Lock and Harry, 2008; de Boer, 2010). The early sub-complex of FtsZ-interacting proteins also interact with each other, as seen with bacterial and yeast two-hybrid experiments and immune-precipitation, in both *B. subtilis* and *E. coli* (Errington *et al.*, 2003; Goehring and Beckwith, 2005; Lock and Harry, 2008). Most of these proteins have homologues present in *E. coli*. In addition, there are some septum formation proteins in *E. coli* that are not present in *B. subtilis* (Figure 1.8). Although the exact functions of most of these proteins is not known, they seem to be involved in several different events of the cell division process, including Z ring formation and stability, recruitment and stability of the divisome at the division site and division septum formation (Errington *et al.*, 2003; Goehring and Beckwith, 2005; Harry *et al.*, 2006).

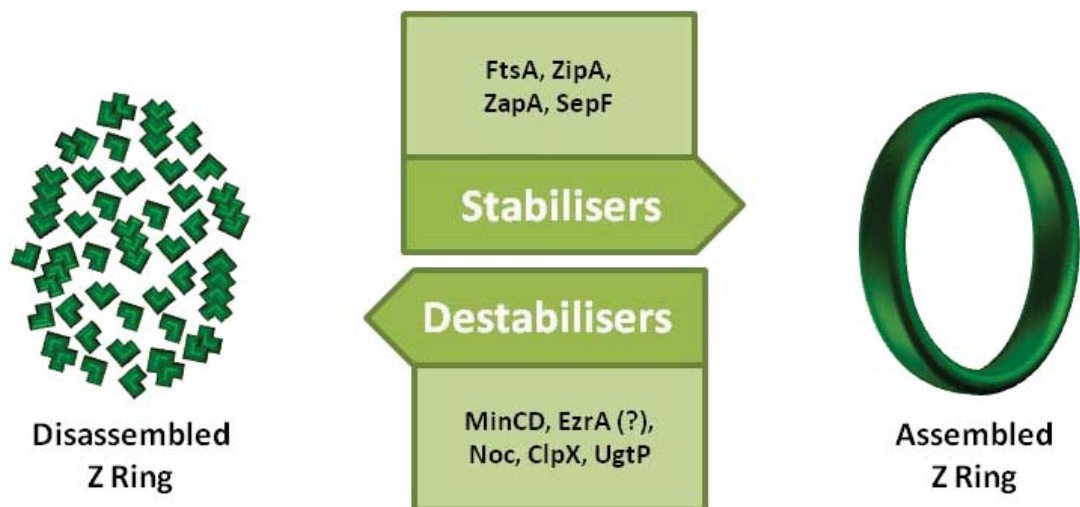


Figure 1.8 Network of stabilisers and destabilisers of Z ring formation. Z ring formation is the result of a complex network of several positive and negative regulators that act as stabilisers or destabilisers. FtsA appears to be an important part of the group of proteins that promotes Z ring formation. ZipA is found in *E. coli*, while Noc and SepF are found in *B. subtilis*. Adapted from Romberg and Levin (2003).

Among the several functions played by the division proteins, it appears that there is a complex network of positive and negative factors that tightly regulate Z ring formation (Figure 1.9). The proteins in this network seem to function in either stabilising or destabilising Z ring formation in each round of cell division. It is postulated that within

this network, Z ring formation occurs when positive-acting factors (stabilisers) are activated concurrently to switch its direction towards Z ring assembly (Lutkenhaus, 2009). ZapA, found in *B. subtilis* and *E. coli*, appears to stabilise FtsZ polymers and thus promote Z ring formation *in vivo* (Gueiros-Filho and Losick, 2002). ZipA, found exclusively in *E. coli*, is also a positive regulator of Z ring formation (RayChaudhuri, 1999). In contrast, several proteins found in *B. subtilis* are believed to be negative regulators of Z ring formation, including EzrA, MinC, UgtP and ClpX (Levin *et al.*, 1999; Weart *et al.*, 2005; Weart *et al.*, 2007; Scheffers, 2008). Most of the main regulators of Z ring formation are not essential for Z ring formation by themselves, as midcell Z ring assembly occurs in their absence; however, often double mutants are unviable (Shapiro and Losick, 2000). Another important protein is FtsA, which might also function as Z ring promoter and is the main focus of this thesis.

Interestingly, some of these proteins, namely FtsA, ZipA and EzrA, interact with the C-terminal tail of FtsZ (Ma *et al.*, 1996; Ma and Margolin, 1999; Singh *et al.*, 2007). Thus, the conserved C-terminus of FtsZ appears to function as a common interaction site for stabilisers and destabilisers of FtsZ activity. Furthermore, the assembly and function of the Z ring is understood to be regulated, at least in part through competition of these proteins for the binding to a common site on FtsZ.

The section below is a brief discussion about the main proteins relevant to Z ring assembly and stability in *B. subtilis*, with the exception of FtsA, which is discussed in more detail in section 1.6.

1.5.1 ZapA

ZapA is a widely conserved non-essential protein that was first identified in *B. subtilis* (Gueiros-Filho and Losick, 2002). ZapA is recruited early to the Z ring and acts as a positive modulator (stabiliser, Figure 1.9) of FtsZ assembly *in vivo* (Gueiros-Filho and Losick, 2002). It appears to do this by decreasing the concentration of FtsZ needed for Z ring formation and subsequently promoting FtsZ polymerisation into higher-ordered structures *in vitro*. Deletion of *zapA* does not show an abnormal phenotype nor does it affect viability under normal conditions. However, ZapA becomes fundamental for cell

division to occur properly when there is a reduction in cellular FtsZ levels or loss of another FtsZ regulatory protein (EzrA; Gueiros-Filho and Losick, 2002). *In vitro*, ZapA directly binds FtsZ, stimulating the lateral associations of FtsZ protofilaments into bundles (Gueiros-Filho and Losick, 2002; Low *et al.*, 2004; Small *et al.*, 2007), and cross-links FtsZ polymers (Dajkovic *et al.*, 2010). It is still unknown how ZapA uses this ability in the cell but possibilities include helping to drive Z ring formation, enhancing the stability of the ring or even its dynamics.

1.5.2 *SepF*

Recently, the same FtsZ-interacting protein was identified in *B. subtilis* by two different groups; Hamoen *et al.* (2006) named it SepF, while Ishikawa *et al.* (2006) called it YlmF. SepF (the preferred name) is a conserved protein among Gram-positive bacteria and Cyanobacteria, and localises to the division site in an FtsZ-dependent manner (Hamoen *et al.*, 2006; Ishikawa *et al.*, 2006). The absence of SepF in *B. subtilis* cells produces abnormal, wider septa, which are formed slowly, mildly affecting cell division (Hamoen *et al.*, 2006; Ishikawa *et al.*, 2006). Interestingly, the depletion of either FtsA or EzrA (other FtsZ regulators) in the *sepF* mutant seems to result in a synthetic lethal effect and cell death (Hamoen *et al.*, 2006; Ishikawa *et al.*, 2006). Ishikawa *et al.* (2006) also analysed the over-expression of SepF in a *B. subtilis ftsA* mutant and showed that it suppresses the defect in Z ring formation and cell division, proposing that SepF might have an overlapping role with FtsA in cell division. Currently, the known function of SepF is as a positive regulator of Z ring assembly and dynamics, promoting lateral associations between FtsZ protofilaments, stabilising them and increasing bundling of FtsZ polymers (Singh *et al.*, 2008). Very recently, it was demonstrated by electron microscopy (EM) that purified SepF can assemble into rings capable of bundling FtsZ protofilaments and generating microtubule-like structures (Gündoğdu *et al.*, 2011). This new data, together with the initial defect observed in septal formation, seems to support the idea that SepF assists with Z ring stability for efficient septal ingrowth and cell division (Haeusser and Margolin, 2011; Gündoğdu *et al.*, 2011).

1.5.3 EzrA

EzrA was first identified as a negative regulator of Z ring assembly (destabiliser protein, Figure 1.9) in *B. subtilis* (Levin *et al.*, 1999). It was first identified during a screen for extragenic suppressors of a temperature-sensitive *ftsZ-gfp* allele. One suppressor was found to be point mutation in *ezrA* that resulted in a truncated EzrA protein, restoring cell division at a non-permissive temperature (Levin *et al.*, 1999). However, more recent studies have presented some contradicting evidence for this function. In these studies, *ezrA* has been inactivated or deleted causing a delay in cell division (Chung *et al.*, 2004; Claessen *et al.*, 2008). The requirement of EzrA for efficient division in *B. subtilis* suggests that this protein may also be a positive regulator of cell division.

EzrA is conserved in Gram-positive bacteria that have a low GC-content (Levin *et al.*, 1999). EzrA co-localises with FtsZ at the nascent septal site, although it can also localise at the cell poles and throughout the cytoplasmic membrane by an N-terminal transmembrane domain (Levin *et al.*, 1999; Chung *et al.*, 2004). The deletion of *ezrA* in *B. subtilis* cells results in a decrease in the minimum intracellular FtsZ concentration necessary for Z ring assembly, which in turn promotes the formation of multiple Z rings located at midcell as well as aberrant polar sites (Levin *et al.*, 1999). In contrast, overproduction of the EzrA protein arrests Z ring formation and cytokinesis (Haeusser *et al.*, 2004). Additional studies have shown that EzrA interacts directly with FtsZ *in vitro* and prevents FtsZ polymerisation (Haeusser *et al.*, 2004; Chung *et al.*, 2007; Singh *et al.*, 2007). This in turn has generated another study that shows a direct interaction between EzrA and PBP1, a cell wall protein, and the possibility that EzrA might promote the recruitment of PBP1 to the division site (Claessen *et al.*, 2008). The absence of EzrA causes thinner and elongated cells, probably mediated partly by the mislocalisation of PBP1 (Claessen *et al.*, 2008).

According to the above data, one of the functions of EzrA is to block Z ring assembly at inappropriate cellular locations. However, for a Z ring to form correctly at midcell the inhibitory effect of EzrA must be overcome specifically at midcell, possibly by the counter-effect of a positive regulator of FtsZ assembly. Interestingly, while EzrA prevents the polymerisation of FtsZ *in vitro*, it does not affect the already assembled polymers (Haeusser *et al.*, 2004). This suggests that the formed Z ring may be resistant

to EzrA activity, allowing the interaction and co-localisation of EzrA to the Z ring once it has formed.

How does EzrA work to fulfil the two seemingly contradictory functions? The paradox can be partly solved if the effect of EzrA on Z ring formation is not restricted to a single round of cell division: more precisely, if the negative effects of EzrA on a round of Z ring formation become positive for the next. It has been proposed that EzrA contributes to Z ring remodelling by accelerating the disassembly of Z ring (Gueiros-Filho and Losick, 2002).

Some studies have also led to the suggestion of another role for EzrA in assisting with the turnover dynamics of the Z ring at midcell. This is thought to be the link the two seemingly contradictory functions of EzrA. In other words the negative regulation exerted by EzrA during Z ring formation becomes positive in later stages of cell division, contributing to the remodelling and disassembly of Z rings (Chung *et al.*, 2004). Those studies have shown that EzrA can promote the turnover and disassembly of pre-formed FtsZ polymers by enhancing the GTPase activity of FtsZ (Gueiros-Filho and Losick, 2002; Chung *et al.*, 2007; Singh *et al.*, 2007). However, earlier observations showed that the absence of EzrA has only a modest effect on slowing the Z ring assembly dynamics (Anderson *et al.*, 2004), contrasting with the above assumption.

1.6 The FtsA protein

Although considered to be one of the main proteins in cell division, a great deal less is known about FtsA than FtsZ. FtsA has homologues in a wide range of bacteria, being the second most conserved protein after FtsZ (Margolin, 2000; Harry *et al.*, 2006). Interestingly, bacteria that don't have FtsZ don't have FtsA either, and this may highlight the importance of the interaction between these two proteins. In fact, the *ftsA* gene is typically located immediately adjacent to *ftsZ* on the bacterial chromosome and transcribed within the same operon (Lutkenhaus and Donachie, 1979; Robinson *et al.*, 1984; Gholamhoseinian *et al.*, 1992; Gonzy-Tréboul *et al.*, 1992; Tamames *et al.*, 2001). The balance between FtsA and FtsZ protein levels *in vivo* seems to be controlled by the positioning of the genes in the operon (Feucht and Lewis, 2001; Rueda *et al.*,

2003), essential for viability, at least in *E. coli* (Donachie *et al.*, 1979; Dai and Lutkenhaus, 1992; Dewar *et al.*, 1992; Begg *et al.*, 1998). Most of the detailed studies have been done in *E. coli*, where FtsA is an essential protein; although some information is also available for *B. subtilis*. In *B. subtilis*, FtsA is not essential for viability, but an *ftsA* mutant exhibits a filamentous phenotype (Beall and Lutkenhaus, 1992; Jensen *et al.*, 2005), but is essential for efficient sporulation (Beall and Lutkenhaus, 1992; Kemp *et al.*, 2002). FtsA interacts with FtsZ prior to Z ring formation and localises to the Z ring early in the division process in an FtsZ-dependent manner (Addinall and Lutkenhaus, 1996; Ma *et al.*, 1996; Wang *et al.*, 1997; Hale and de Boer, 1999; Feucht *et al.*, 2001; Jensen *et al.*, 2005). This co-localisation occurs by interaction to the C-terminal tail of FtsZ protein (Wang *et al.*, 1997; Din *et al.*, 1998; Ma and Margolin, 1999; Yan *et al.*, 2000; Di Lallo *et al.*, 2003).

1.6.1 FtsA structure and biochemistry

Molecular studies on FtsA have shown that this protein is a member of the ATPase superfamily, which contains proteins like actin, hexokinase and the Hsp70 family of heat shock proteins (Bork *et al.*, 1992). It was later confirmed, by the crystal structure of FtsA from *Thermotoga maritime* (Figure 1.11), that this protein resembles the eukaryotic cytoskeletal protein actin, including an ATP-binding cleft (van den Ent and Löwe, 2000). In fact, like actin, FtsA from *B. subtilis*, *E. coli* and *S. pneumoniae* has been shown to bind ATP *in vitro* (Sanchez *et al.*, 1994; van den Ent and Löwe, 2000; Yim *et al.*, 2000; Feucht *et al.*, 2001; Lara *et al.*, 2005). Interestingly, ATPase activity in FtsA has only been reported *in vitro* in *B. subtilis* (Sanchez *et al.*, 1994; Feucht *et al.*, 2001; Adams and Errington, 2009). The function of this adenosine triphosphate (ATP) hydrolysis is still not known for FtsA, and the significance of this activity *in vivo* is unclear. This could be due to the absence of other as yet unidentified proteins required for this ATPase activity to occur. The significance of the structural similarity of FtsA to actin is unclear. The three-dimensional fold of FtsA presents four subdomains designated as 1A, 1C, 2A and 2B (Figure 1.11; van den Ent and Löwe, 2000). Subdomain 1C is unique to FtsA, which is essential for its function *in vivo*, and has been suggested to be involved in FtsA polymerisation (van den Ent and Löwe, 2000; Corbin

et al., 2004; Rico *et al.*, 2004). Subdomain 2B of FtsA seems to contain the site necessary for interaction with FtsZ (Pichoff and Lutkenhaus, 2007). Also, the conserved C-terminal amphipathic helix in subdomain 1A of FtsA has been found to be responsible for anchoring the protein to the membrane, and the deletion of this helix results in FtsA inactivation in *E. coli* (Pichoff and Lutkenhaus, 2005).

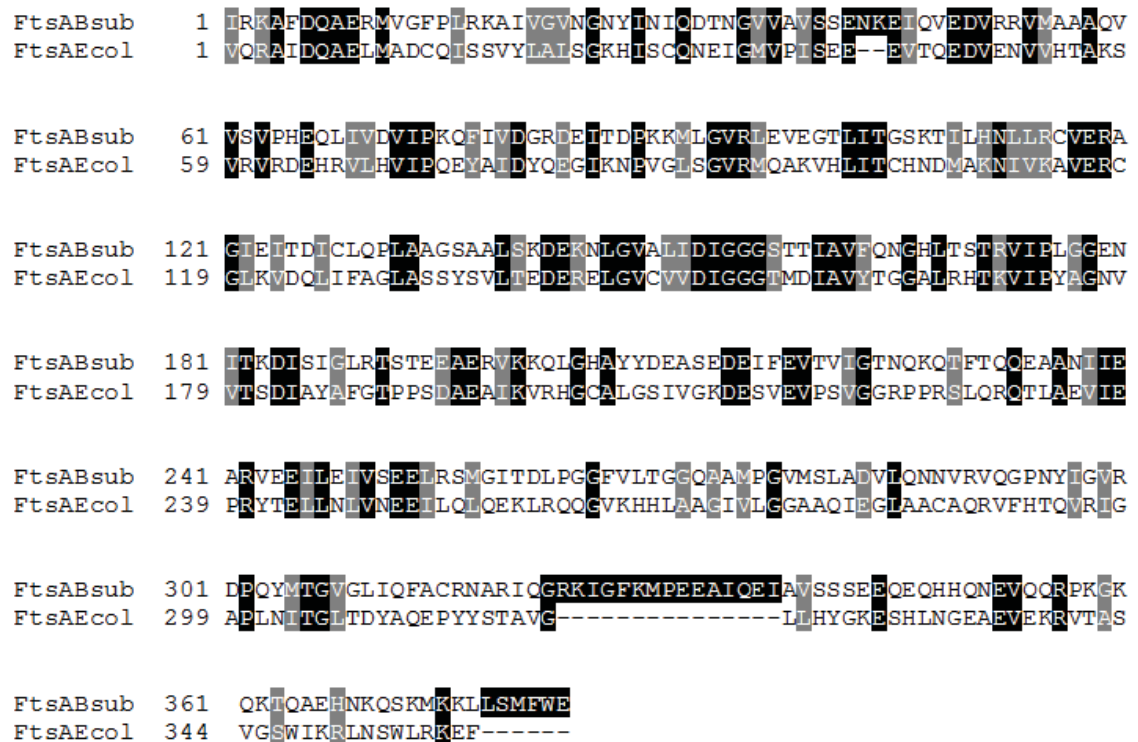


Figure 1.9 Alignment sequence of FtsA. The figure shows the alignment of the FtsA sequences from *B. subtilis* and *E. coli*, obtained using the program ClustalW. The residues have been highlighted using the program Boxshade 3.21, from the most conserved (in black) to similar residues (in grey) and the less conserved (in white). The two sequences share 33.9% of identity with 4.2% gap frequency.

Despite sharing a primary amino acid similarity of 33.9% (Figure 1.10), it is believed that in *E. coli* and *B. subtilis*, FtsA does not share the cytoskeleton functionality of the eukaryotic actin, since bacteria have proteins that play that structural role: MreB and Mbl (Jones *et al.*, 2001). This is supported by the finding that the absence of FtsA in bacterial cells does not result in any shape change to the cells. Furthermore, unlike actin, FtsA from most prokaryotes has not been shown to polymerise. The known exception is FtsA from *Streptomyces pneumonia* that polymerises into helical structures *in vitro*, in a nucleotide-dependent manner (Lara *et al.*, 2005). However, FtsA from this species does not support any ATP hydrolysis; and this absence of ATPase activity causes the

polymers to be highly stable and not dynamic (Lara *et al.*, 2005). However, yeast two-hybrid and bacterial two-hybrid data have shown that FtsA self-interacts (Yim *et al.*, 2000; Di Lallo *et al.*, 2003; Rico *et al.*, 2004; Karimova *et al.*, 2005; Pichoff and Lutkenhaus, 2007), while *in vivo* studies have suggested that FtsA forms dimers in *B. subtilis* (Feucht *et al.*, 2001). Moreover, a more recent study has demonstrated that the dimerisation or oligomerisation ability of FtsA is critical for its function and has a stability effect on the integrity of the Z ring (Shiomi and Margolin, 2007). In this work, they found out that the monomer form of FtsA has an innate inhibitory activity on FtsZ assembly, while the dimer form of FtsA has not, although its effects are not yet understood (Shiomi and Margolin, 2007). The two FtsA subunits in the dimers can bind to two independent FtsZ protofilaments, cross-linking them (Pichoff and Lutkenhaus, 2007; Shiomi and Margolin, 2007). Therefore, it has been proposed that if FtsA is present as dimers or oligomers its ability to promote Z ring integrity appears enhanced (Shiomi and Margolin, 2007).

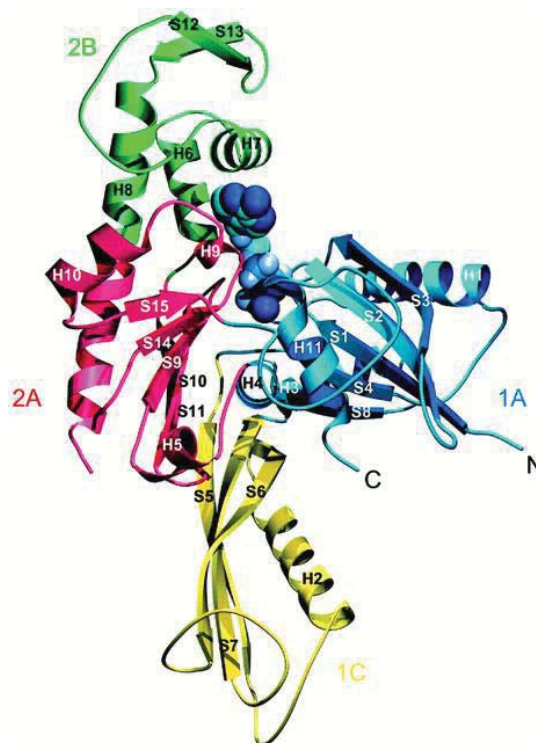


Figure 1.11 Crystal structure of FtsA protein from *Thermotoga maritima*. Each of the domains of FtsA can be divided into two subdomains. By analogy to actin, these subdomains have been designated 1A, 1C, 2A and 2B. FtsA contains a unique domain, 1C, which is essential for FtsA function *in vivo*, and has been suggested to be involved in FtsA polymerisation. It also houses an ATP binding ‘cleft’ formed by the 1A, 2A and 2B subdomains. Image sourced from van den Ent and Lowe (2000).

1.6.2 The interaction of FtsA with FtsZ

In vivo, the ratio of FtsA to FtsZ is critical for cell division. This ratio has been calculated using quantitative immunoblotting techniques and results showed a similar ratio factor of 1:5 (FtsA:FtsZ) for both *B. subtilis* and *E. coli* cells (Feucht *et al.*, 2001; Rueda *et al.*, 2003) and a much higher ratio of 1:1.5 in *S. pneumoniae* cells (Lara *et al.*, 2005). Although the physiological significance of these differences is not clear, several studies suggest that these ratios must be maintained *in vivo* for efficient Z ring formation (Dai and Lutkenhaus, 1992; Dewar *et al.*, 1992; Rueda *et al.*, 2003). Furthermore, it is important to consider that the ratios measured might not stoichiometrically translate to the *in vivo* FtsA-FtsZ ratio in the septal ring, taking into account the distribution of both FtsA and FtsZ molecules in the cytoplasm and in the Z ring (Errington, 2003). *In vivo*, slight fluctuations in the FtsA-FtsZ ratio, by over-expression or depletion of one of the proteins levels, result in cell division inhibition and consequent filamentation in both *E. coli* and *B. subtilis* (Wang and Gayda, 1990; Beall and Lutkenhaus, 1991; Beall and Lutkenhaus, 1992; Wang *et al.*, 1993; Ma *et al.*, 1996; Jensen *et al.*, 2005). However, when both proteins are concurrently over-expressed, the frequency of midcell Z rings increases, confirming the dependency of this ratio for normal cell division (Dewar *et al.*, 1992; Dai and Lutkenhaus, 1992; Begg *et al.*, 1998).

Early studies *in vitro* using yeast-two-hybrid assays have suggested that FtsA interacts directly with FtsZ; more specifically via the C-terminus of FtsZ (Ma *et al.*, 1996; Wang *et al.*, 1997; Din *et al.*, 1998; Ma and Margolin, 1999; Yan *et al.*, 2000; Di Lallo *et al.*, 2003). One study showed FtsA failing to localise to the midcell site of FtsZ-depleted cells, suggesting that FtsA might be recruited after Z ring assembly (Feucht *et al.*, 2001). However, while FtsA recruitment to the division site requires FtsZ, the *in vivo* complexes that result from the FtsA-FtsZ interaction were later studied in *B. subtilis* and *E. coli*, indicate that FtsA co-localises with the FtsZ ring at the division site (den Blaauwen *et al.*, 1999; Addinall and Lutkenhaus, 1996; Ma *et al.*, 1996; Feucht *et al.*, 2001; Rueda *et al.*, 2003; Jensen *et al.*, 2005). Immunofluorescence microscopy and protein cross-linking techniques were also used to determine the timing and localisation of these complexes in outgrown spores of *B. subtilis*, controversially showing that these complexes form prior to Z ring formation (Jensen *et al.*, 2005).

1.6.3 FtsA function in cell division

Despite the biochemical information already obtained regarding FtsA, little is known about its cytological role. FtsA is essential in *E. coli*, since depletion of FtsA causes loss of viability (Addinall *et al.*, 1996; Hale and de Boer, 1999). In contrast, it is non-essential in *B. subtilis*, although an *ftsA* deletion mutant has a dramatically reduced number of Z rings, showing that it is important for cell division (Beall and Lutkenhaus, 1992; Jensen *et al.*, 2005).

1.6.3.1 The role of FtsA in *E. coli* cell division

The loss of FtsA in *E. coli* does not appear to affect the ability of FtsZ to form normal Z rings (Addinall *et al.*, 1996; Hale and de Boer, 1999). The reason for this might be attributed to the presence of an additional essential protein in *E. coli*, ZipA (Hale and de Boer, 1997). ZipA also binds FtsZ and has an overlapping function of the FtsA protein (Pichoff and Lutkenhaus, 2002). ZipA seems to promote Z ring formation *in vivo*, since it is involved in the bundling of FtsZ protofilaments *in vitro*, and suppresses an *ftsZ* mutation that is known to cause unstable Z ring formation (RayChaudhuri, 1999). Studies of protein inactivation support the notion of similar and complementary functional roles of these proteins in *E. coli*. Pichoff and Lutkenhaus (2002) demonstrated that depletion or inactivation of either FtsA or ZipA in this bacterium still resulted in Z ring formation. However, when both proteins were simultaneously inactivated, new Z rings could not form and pre-formed Z rings become destabilised and disassembled (Pichoff and Lutkenhaus, 2002). Further studies have confirmed these results by showing that, in *E. coli*, a single point mutation in *ftsA* bypasses the lethal effect of the absence of ZipA, allowing the cells to survive and divide normally (Geissler *et al.*, 2003). This gain-of-function mutation (a single residue alteration in a conserved residue in FtsA, R286W), known as FtsA*, is fully functional, since it can replace wild-type FtsA with almost no effect on cell viability (Geissler *et al.*, 2003), FtsA* seems to function by accelerating the re-assembly of the Z ring, as seen in thermosensitive cells after shifting between non-permissive and permissive temperatures, and generally enhancing the structural integrity of the Z ring (Geissler *et al.*, 2003; Geissler *et al.*, 2007). Summarising this data, the overlapping role of the FtsA

and ZipA proteins is clear, with FtsA being able to support the formation and stabilisation of the FtsZ ring *in vivo* just as ZipA might through the bundling of FtsZ protofilaments, as observed *in vitro* (RayChaudhuri, 1999; Geissler *et al.*, 2003; Geissler *et al.*, 2007). However, it is still unknown whether FtsA can promote bundling or polymerisation of protofilaments, partially because of the difficulty of obtaining FtsA in a purified form on its own.

FtsA seems to have three main functions in *E. coli* that are important in different stages of cell division. At an early stage of cell division, FtsA is fundamental for promoting Z ring stability. This is possible due to the ability of FtsA to interact with FtsZ, the cytoplasmic membrane and with itself; thus tethering FtsZ and Z ring to the membrane. The second role of FtsA appears to be in the recruitment of several downstream division proteins, essential for proper cell division. Lastly, although there is little direct evidence, FtsA also seems to play a direct role in Z ring constriction once the divisome has fully matured (Beuria *et al.*, 2009; de Boer, 2010).

As mentioned above, the first role for FtsA is the tethering of the Z ring to the membrane, an important event required for proper cell division. FtsA was previously considered to be a cytosolic protein because it did not contain any clear membrane-interacting sequences. However, Pla *et al.* (1990) have shown that ~30% of cellular FtsA is located in the cytoplasmic membrane, predicting some association with the membrane. Much later, Pichoff and Lutkenhaus (2005) identified an amphipathic helix within the FtsA protein from *E. coli* as a membrane-targeting sequence that allows FtsA to associate with the membrane. Moreover, at least in *E. coli*, this helix is essential for FtsA function, and was further shown to successfully replace the MTS (membrane-targeting sequence) of MinD, another membrane protein (Pichoff and Lutkenhaus, 2005). This further supports the prediction that FtsA inserts into the membrane via its MTS and the possibility that FtsA actually tethers FtsZ and the Z ring to the membrane.

Another role for FtsA in *E. coli* is thought to be the recruitment of FtsK and consequentially the later-acting cell division proteins, such as FtsQ, FtsL, FtsB, FtsI, and FtsN to the division site (Pichoff and Lutkenhaus, 2002; Corbin *et al.*, 2004; Rico *et al.*, 2004). However, an interesting study has shown that the recruitment of these late division proteins by FtsA can be bypassed by the premature targeting of the division protein FtsQ to the Z ring (Goehring *et al.*, 2005), thus restoring localisation of

downstream proteins in cells lacking FtsA and/or FtsK. One exception to this bypass was the recruitment of the final division protein, FtsN, which still requires the presence of FtsA at midcell (Goehring *et al.*, 2005; Goehring *et al.*, 2006). An interpretation of these results is that, in fact, FtsA seems to be required for the recruitment of at least some late division proteins. An interesting and relevant observation was that, although recruitment of some later division proteins was bypassed, cell division was not restored in the cells (Goehring *et al.*, 2005; Goehring *et al.*, 2006). That is, even when the Z ring is formed and the later-acting division proteins have been recruited, an *ftsA* mutant is not able to divide. This suggests that FtsA may also play an additional role in *E. coli* cell division, perhaps during Z ring constriction. Accordingly, a recent study has shown that FtsA* (a gain-of-function mutation in FtsA, see above) was able to disassemble pre-formed FtsZ polymers *in vitro* in an ATP binding-dependent manner (Beuria *et al.*, 2009), suggesting that FtsA* acts on FtsZ polymers *in vivo*, possibly during Z ring constriction.

1.6.3.2 *FtsA* functions in *B. subtilis* cell division

Much less is known about the function/s of FtsA in *B. subtilis*. At the time of commencing this thesis, current evidence presented below suggested that FtsA can directly stimulate Z ring assembly and/or help to maintain the structural integrity of the formed Z ring. An *ftsA* mutant of *B. subtilis* results in highly filamentous cells (Beall and Lutkenhaus, 1989; Beall and Lutkenhaus, 1992; Jensen *et al.*, 2005). Jensen *et al.* (2005) showed that the *ftsA*-deleted cells have a vastly decreased frequency of Z ring formation; only ~10% of Z rings formed. The remainder of FtsZ localisations were either helical patterns or diffuse areas of FtsZ localisation between nucleoids. Therefore, some Z rings formed in these cells, and the *ftsA* deletion is not lethal, there seems to be an absolute requirement of FtsA for efficient Z ring assembly in *B. subtilis* (which does not contain a ZipA homolog). Accordingly, chemical cross-linking experiments demonstrated that the FtsA protein binds FtsZ prior to Z ring formation, consistent with a direct role for FtsA in the assembly of the ring (Jensen *et al.*, 2005). Furthermore, 10% of apparently correctly formed Z rings seem to account for sustaining cell division and therefore cell viability (Jensen *et al.*, 2005). This observation implies that there may be

another protein performing a similar function to FtsA in *B. subtilis*. Two recent studies have identified a protein, SepF (or YlmF), that might be filling this role (see section 1.5.2; Ishikawa *et al.*, 2006; Hamoen *et al.*, 2006), since over-production of SepF rescues an *ftsA* null mutant. It is still unknown if SepF, in *B. subtilis*, is performing an analogous function to ZipA in *E. coli*.

In contrast to *E. coli*, *B. subtilis* FtsA does not seem to be absolutely required for the recruitment of later-assembling division proteins. Although no experiments have been conducted regarding the localisation dependency of FtsA by the later division proteins (Errington *et al.*, 2003), the infrequent cell division observed in the absence of FtsA seems to justify the assembly of the divisome, even if not wild-type efficiently, independent of FtsA. Furthermore, as mentioned in the above paragraph, the over-expression of *sepF* can fully complement the *ftsA*-deletion phenotype (Ishikawa *et al.*, 2006), indicating that *B. subtilis* FtsA is not be absolutely required for the localisation of later acting division proteins.

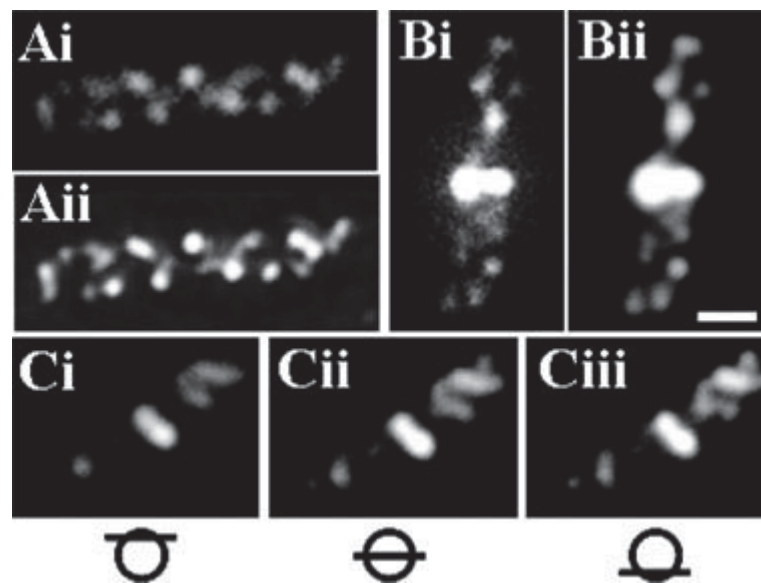


Figure 1.12 Visualisation of FtsA in *B. subtilis* cells. Images were obtained by immunofluorescence microscopy and additional three-dimensional deconvolution was performed for a higher resolution imaging. **(A and B)** Images **(i)** show the original fluorescence image and images **(ii)** show the corresponding deconvolved image. **(A)** Cell with an FtsA helix, but no ring of FtsA. **(B)** Cell with a ring of FtsA and an FtsA helix. **(C)** Different focal planes of a deconvolved cell showing the top **(i)**; middle **(ii)**; and bottom **(iii)**. Scale bar represents 1 μm . Image from Peters *et al.* (2007).

Quantification of the number FtsA molecules in *B. subtilis* cells suggests that they may be able to form a circumferential ring structure that constricts with the invaginating membrane (Feucht *et al.*, 2001). This suggestion is supported by immunofluorescence microscopy data, showing FtsA ‘band’ and ‘dot’ structures at the midcell site, much like the Z ring during constriction (Feucht *et al.*, 2001). Furthermore, imaging and additional deconvolution of vegetatively-growing wild-type cells of *B. subtilis* have shown that FtsA also seems to form frequent helical structures identical in appearance to those of FtsZ, as well as FtsA rings (Figure 1.12; Peters *et al.*, 2007). The FtsA localisation pattern observed was reportedly less intense than that observed for FtsZ, probably due to the lower concentration of FtsA relative to FtsZ in the cells (see section 1.6.2; Feucht *et al.*, 2001). It is important, however, to acknowledge the difficulty of assigning localization information from microscopy images, demonstrated by the recent re-interpretation of MreB adjacent helical structures now as mobile, fragmented horizontal bands perpendicular to the length of the cell (Garner *et al.*, 2011).

A last piece of information about *B. subtilis* FtsA is that it can hydrolyse ATP *in vitro* (Sanchez *et al.*, 1994; Feucht *et al.*, 2001), which tempts to suggest that the energy derived from ATP hydrolysis is used either for polymerisation of FtsA or to provide constrictive power to the Z ring during septum formation.

Finally, observation of sporulation in *B. subtilis* in the absence of FtsA suggests one more role for FtsA specifically in this organism. An *ftsA* disruption in *B. subtilis* cells causes reduced sporulation efficiency compared to that of wild-type cells, with between 25% and 50% less viable spores depending on the sporulation method used (Beall and Lutkenhaus, 1992). The defective sporulation phenotype was shown to be correlated with a deficiency in the activation of the mother-cell-specific sigma-factor σ^E and, as observed by electron microscopy, this caused improper formation of the polar septum. Interestingly, the isolation of an *ftsA* mutant, FtsA-D265G, showed normal vegetative division but a deficiency in sporulation, with sporulating cells being able to form the asymmetric septum, but were impaired in the engulfment process (Kemp *et al.*, 2002). In this mutant, fluorescence microscopy and electron microscopy showed that the midcell vegetative septa formed normally, while the polar (asymmetric) septa were abnormally thin (Kemp *et al.*, 2002). These early studies suggested that FtsA may be playing two distinct roles, depending on the cell cycle processes.

Chapter 2

§

Material and Methods

2.1 Chemicals, reagents and solutions

Chemicals and reagents used in this work were typically analytical reagent (AR) grade and were obtained from Amresco, BDH Chemicals or Sigma unless otherwise specified. Commonly used aqueous buffers and solutions are listed in Table 2.1.

Table 2.1 Commonly used aqueous buffers and solutions.

<i>Buffer/solution</i>	<i>Constituents^a</i>
GTE	50 mM glucose, 20 mM Tris-HCl, 10 mM EDTA, pH 7.5
Lysis buffer	10 mM MgCl ₂ , 500 µg/mL lysozyme, 300 µg/mL henylmethylsulfonyl fluoride (PMSF), 100 µg/mL DNase I, 1X TE
MSA	8 mM K ₂ HPO ₄ , 4.4 mM KH ₂ PO ₄ , 1.5 mM (NH ₄) ₂ SO ₄ , 340 mM Na ₃ C ₆ H ₅ O ₇ ·2H ₂ O
PBS	137 mM NaCl, 10.1 mM Na ₂ HPO ₄ , 2.7 mM KCl, 1.8 mM KH ₂ PO ₄
PC buffer (10X)	0.63 mM trisodium citrate (Na ₃ C ₆ H ₅ O ₇ ·2H ₂ O), 6.1 mM K ₂ HPO ₄ , 4.4 mM KH ₂ PO ₄ ; pH 7
SDS-PAGE loading buffer	62.5 mM Tris-HCl, 10% glycerol (v/v), 5% 2-mercaptoethanol, 2% SDS (sodium dodecyl sulfate), 0.1% bromophenol blue, pH 6.8
TBE	89 mM Tris-HCl, 89 mM boric acid, 2.5 mM EDTA, pH 8.3
TBS	137 mM NaCl, 20 mM Tris-HCl, pH 7.6
TE	10 mM Tris-HCl, 1 mM EDTA, pH 8.0
TES	200 mM Tris-HCl, 100 mM NaCl, 5 mM EDTA, pH 7.5
Trace metals	50 mM CaCl ₂ , 5 mM MnCl ₂ , 1.6 mg/mL FeCl ₃ ·6H ₂ O, 430 mg/mL CuCl ₂ ·2H ₂ O, 170 mg/mL ZnCl ₂ , 60 mg/mL CoCl ₂ ·6H ₂ O, 60 mg/mL Na ₂ MoO ₄ ·2H ₂ O
XS buffer (2X)	pre-heated to 65°C; 2% (w/v) potassium ethyl xanthogenate, 1.6 M ammonium acetate, 0.2 M Tris-HCl, pH 7.4, 36 mM EDTA, 2% SDS
Western lysis buffer	10 mM MgCl ₂ , 500 µg/mL lysozyme, 300 µg/mL

	phenylmethylsulfonyl fluoride, 100 µg/mL DNase I, 1xTE
Western transfer buffer	49.6 mM Tris, 384 mM glycine, 20% (v/v) methanol

^aAll buffers and solutions were made up in Milli-Q® purified water (MQW; Millipore) and are listed at the normal working concentration (1x). All percentages are given as weight per volume (w/v) unless otherwise noted.

2.2 *B. subtilis* strains and growth conditions

All *B. subtilis* strains used in this thesis are listed in Table 2.2. For those strains produced as part of this work, experimental details regarding strain construction are described in the text when the strains are first used.

Growth media used to cultivate *B. subtilis* cells are shown in Table 2.3. Unless otherwise noted, cells were grown on Antibiotic medium 3 (also known as Penassay broth; PAB) plates or in PAB broth. Spores were germinated and outgrown in Germination Medium Defined (GMD). Broth cultures were incubated with vigorous shaking in a gyratory water-bath (G76; New Brunswick) and growth was monitored by recording the absorbance at 600 nm (A_{600}) using a spectrophotometer (UV-120-02; Shimadzu). All media was supplemented with L-tryptophan (50 µg/mL), and when required thymine (20 µg/mL), glucose, xylose or isopropyl-1-thio- β -Dgalactopyranoside (IPTG), as specified in the text. Antibiotics were used for selection as described in Table 2.4. *B. subtilis* strains were stored as stationary phase cultures suspended in 16% (v/v) glycerol at -80°C .

Table 2.2 *B. subtilis* strains.

Strain	Genotype ^a	Reference/Source
SU5	168 <i>trpC2</i>	E. Nester
SU456	<i>trpC2 ftsZ::(phleo P_{spac}-ftsZ)</i>	Jensen <i>et al.</i> (2005)
SU457	<i>trpC2 ftsZ::(phleo P_{spac}-ftsZ) ftsA::cat</i>	Jensen <i>et al.</i> (2005)
SU506	<i>trpC2 ΔftsA::cat</i> (in-frame)	A. Cubas, Harry Lab
SU570	<i>trpC2 ftsZ::ftsZ-gfp spc</i>	P. Peters, Harry Lab
SU630	<i>trpC2 ftsZ::(phleo P_{spac}-ftsZ)</i> <i>ΔftsA::cat amyE::P_{xyl}-ftsA neo</i>	SU632 → SU457 (this study)
SU631	<i>trpC2 ΔftsA::cat</i> (in-frame) <i>amyE::P_{xyl}-ftsA neo</i>	SU632 → SU506 (this study)
SU632	<i>trpC2 amyE::P_{xyl}-ftsA neo</i>	SU5 → FG718 (this study)
SU633	<i>trpC2 thrC::P_{spac}-gfp-divIB erm</i>	SU5 → AH3580 (this study)
SU636	<i>trpC2 ΔftsA::cat</i> (in-frame) <i>amyE::P_{xyl}-ftsA neo</i> <i>thrC::P_{spac}-gfp-divIB erm</i>	SU531 → AH3580 (this study)
SU638	<i>trpC2 ftsZ::ftsZ-gfp spc ftsA::cat</i> (in-frame) <i>amyE::P_{xyl}-ftsA neo</i>	SU531 → SU570 (this study)
FG718	<i>ΔftsA amyE::P_{xyl}-ftsA cat</i>	Tavares <i>et al.</i> , 2008
AH3580	<i>trpC2 ΔdivIB::cat thrC::P_{spac}-gfp-divIB erm</i>	G.Real (unpublished)

^aAntibiotic resistance genes are expressed as follows: *cat*, chloramphenicol; *erm*, erythromycin; *phleo*, phleomycin; *spec*, spectinomycin; *neo*, neomycin.

Table 2.3 *B. subtilis* growth media.

Medium	Constituents ^a
Germination medium defined (GMD)	80 mM K ₂ HPO ₄ , 44 mM KH ₂ PO ₄ , 15 mM (NH ₄) ₂ SO ₄ , 3.4 mM sodium citrate, 0.5% glucose, 0.3% monosodium glutamate, 0.3% asparagine, 0.05% Bacto casamino acids, 0.02% MgSO ₄ ·7H ₂ O
MD medium	8.7 mg/mL K ₂ HPO ₄ , 5.2 mg/mL KH ₂ PO ₄ , 0.9 mg/mL Na ₃ C ₆ H ₅ O ₇ ·2H ₂ O, 1.9% glucose, 3 mM MgSO ₄ , 2.5 g/mL K-glutamate, 11 mg/mL (NH ₄) ₂ Fe(SO ₄) ₂ ·H ₂ O, trace metals, pH 7
MDCH medium	MD and 50 mg/mL L-tryptophan, 1% casein hydrolysate, pH 7
Penassay Broth (PAB)	1.75% Bacto antibiotic medium 3
Spizizen minimal medium (SMM)	1.4% K ₂ HPO ₄ , 0.6% KH ₂ PO ₄ , 0.5% D-glucose, 0.2% (NH ₄) ₂ SO ₄ , 0.14% MgSO ₄ ·7H ₂ O, 0.1% Bacto casamino acids, 0.1% tri-sodium citrate dihydrate, 1xtrace metals
Sporulation agar	0.8% Bacto nutrient broth, 0.1% KCl, 1 mM Ca(NO ₃) ₂ , 500 µM NaOH, 10 µM MnCl ₂ , 1 µM FeSO ₄ , 300 µg/mL MgSO ₄ ·7H ₂ O, 1.5% agar
Tryptose blood agar base (TBAB)	3.3% tryptose blood agar base

^aAll media were made up in reverse osmosis purified water (ROW) and sterilised by autoclaving or 0.2 µm filtration. Tryptone, yeast extract and TBAB were obtained from Amyl Media. Agar, tryptose, Bacto antibiotic medium 3, Bacto casamino acids and Bacto nutrient broth were from Difco. All percentages are given as w/v. Media was supplemented with 50 mg/mL L-tryptophan.

Table 2.4 Antibiotics used for selection in *B. subtilis*.

Drug/antibiotic	Working concentration ^a (µg/mL)
Chloramphenicol	5
Erythromycin	0.5-1
Phleomycin	2
Neomycin	1-2
Spectinomycin	40-80

“Stock solutions were prepared by dissolving antibiotics either in 95% ethanol (chloramphenicol and erythromycin), MQW (spectinomycin) or 95% methanol (phleomycin) and filter sterilised (0.2 µm filter). Antibiotics were stored at -20°C or 4°C.

2.2.1 Testing the status of the *amyE* locus of *B. subtilis*

Genetic manipulation of *B. subtilis* often involves insertion of gene cassettes into the *amyE* locus. The *amyE* gene encodes an alpha-amylase which breaks down starch. To test if *amyE* has been disrupted (indicative of gene cassette insertion), *B. subtilis* cells were patched onto TBAB plates containing 1% (w/v) starch and incubated overnight at 37°C. Plates were then stained by vapourising 3-5 iodine crystals in the inverted plate lids. In the vicinity of cells containing a functional *amyE* gene, the agar remained colourless, while for cells carrying an inactivated *amyE* gene, the agar stained purple. This is due to the fact that iodine complexes with starch, and that starch is degraded in the presence of a functional *amyE* gene.

2.2.2 Depletion of *FtsA* using the P_{xyl} inducible promoter

Several strains used in this work contain the P_{xyl} xylose-inducible promoter. This promoter was used to control *ftsA* induction in several strains (see Table 2.2). To deplete the FtsA protein in *B. subtilis* cells and check the effect of its depletion on cell division, cells were grown in the absence of xylose as follows. A volume of exponentially-growing cells grown in the presence of xylose was removed from the culture so that a new culture grown in the absence of xylose would initiate with an OD600 ~ 0.05. Before transferring this volume of cells to the culture media without xylose, the cells were washed twice by centrifugation and resuspension in media without xylose. This step removes residual amounts of xylose from the cell pellet. Next the cell pellet was resuspended in the media without xylose and the same concentration of glucose was added to maintain repression of the promoter by occupying the subtract' binding site. The cell culture was then grown for 2 - 3 hours to deplete the P_{xyl} inducible-promoter. Simultaneously as a control, the above procedure was performed but instead cells were

transferred to culture media with xylose. The cells were then prepared for microscope visualisation.

2.3 Preparation and transformation of competent *B. subtilis* cells

In culture, *B. subtilis* cells naturally acquire competence for DNA uptake as they enter the stationary phase of growth (Cutting and Vander Horn, 1990). Taking advantage of this fact, competent *B. subtilis* cells were prepared. A single colony of the parent strain to be made competent was freshly cultivated the night before at 37°C, in Penassay broth (PAB) supplemented with auxotrophic requirements. MDCH medium (10 mL, see Table 2.3) was inoculated with the fresh culture to an A_{600} of 0.1 and incubated at 37°C, with shaking until the cells reached stationary phase ($A_{600} \sim 1.2$). An equal volume of the cell culture was added to MD medium (MDCH medium minus tryptophan and casein hydrolysate) and shaken for a further hour at the appropriate temperature to fully induce competence. Competent cells (500 μ L) were aliquoted into culture tubes and donor chromosomal DNA (see section 2.6.1) was added (20 μ L - 50 μ L, ~ 200 -250 μ g), along with a no DNA control. These tubes were shaken for 1 hr. The entire sample was then pelleted for 2 min at 12 000 g, resuspended into 200 μ L of Cg (see Table 2.1), vortexed, and 100 μ L plated and spread onto PAB plates supplemented with the appropriate auxotrophic requirements and antibiotic. These were incubated at 37°C overnight or 30°C for 1 - 2 days, until colonies of transformants appeared.

2.4 Preparation and germination of *B. subtilis* spores

B. subtilis spores were prepared using a method based on that of Callister and Wake (1974). An overnight culture was prepared by inoculating 10 mL PAB with a single colony of *B. subtilis*. This was incubated overnight in a giratory water-bath at 30°C. The overnight culture was subsequently used to inoculate 10 mL of fresh PAB to an $A_{600} \sim 0.05$ and incubated at 37°C with aeration. Early stationary phase cells (0.5 mL at

A600~1-2) were spread onto a sporulation agar plate (18 cm petri dish) and incubated in a 30°C oven until ~80% cells had formed phase-bright mature spores, as determined by phase-contrast microscopy (usually 7-10 days). Spores were harvested by resuspension in sterile ROW and centrifugation at 12 000 g at 4°C for 10 min. Spores were washed twice in ROW then resuspended in 30 mL TE buffer containing lysozyme (1 mg/mL; Sigma) and incubated at 37°C with shaking for 1 hour. SDS [2% (w/v)] was added and incubated at 37°C for a further 20 min. The resuspension was centrifuged at 12 000 g at 4°C for 10 min and the pellet was washed with sterile ROW until only phase-bright spores remained, as determined by phase-contrast microscopy (usually ~8 times). Spores were stored in sterile ROW at 4°C. The concentration of spores was estimated by absorbance, given that 10^{10} spores/mL equals $A_{625} \sim 50$. Spores were germinated at a concentration of 2×10^8 spores/mL in germination medium defined (GMD) with aeration at 34°C.

2.5 DNA methods

2.5.1 Extraction and purification of DNA from *B. subtilis*

B. subtilis chromosomal DNA was extracted and purified based on the method of Errington (1984) with modifications as follows. Starting from a 10 mL saturated culture, *B. subtilis* cells were sedimented, washed once with 1.0 mL TES (Table 2.1) and then resuspended in 500 μ L TES. 25 μ L of lysozyme (10 mg/mL in TES) and 5 μ L RNase (10 mg/mL in TES) were then added and the mixture was incubated for 30 min at 37°C. Following the subsequent addition of 50 μ L of pronase (10 mg/mL in TES) and 30 μ L of the detergent sarkosyl [30% (v/v)], incubation was continued for a further 30 min. 600 μ L of chloroform:isoamylalcohol (24:1) was then added to the lysed cells and the preparation was gently mixed by inversion on a rotator for 10 min. After subsequent 10 min incubation on ice, followed by centrifugation at 10000 g for 5 min, the aqueous phase was removed and the above chloroform extraction repeated. Several additional extractions were then performed using 600 μ L volumes of phenol:chloroform:isoamylalcohol (25:24:1) to remove any remaining protein contaminants (see: Sambrook *et al.*, 1989). These were followed by a final chloroform extraction. The

DNA was precipitated by adding of 2.5 volumes of ethanol (-20°C) and inverting the tube several times. The precipitated DNA was then centrifuged briefly, washed with ice-cold 70% (v/v) ethanol and dried *in vacuo*. Finally, the pellet was dissolved in 100 µL TE (Table 2.1) and stored at 4°C.

2.5.2 Agarose gel electrophoresis of DNA

Agarose gels were prepared on a horizontal slab gel apparatus (8.0 cm × 5.5 cm; 20 mL gel volume) or a wide gel apparatus (8.0 × 13.5 cm; 60 mL gel volume). Agarose (type 1: low electroendosmosis; Sigma) at 1% (w/v) was dissolved in electrophoresis buffer (TBE; Table 2.1) and gels were cast with a well-forming comb in place. DNA loading buffer (Table 2.1) was added to DNA samples prior to loading into the pre-cast wells. Bacteriophage λ DNA pre-cut with *Hind*III (New England Biolabs) was used for size standards, enabling the size estimation of DNA fragments greater than 1 kb. For fragments less than 1 kb, GeneRuler® 100 bp DNA Ladder Plus (Fermentas) was used. Agarose gels were run submerged under a volume of electrophoresis buffer that lay 2-5 mm above the surface of the gel at 60V (3.45-4.83 V/cm) for 1-2 h. After electrophoresis, gels were stained in 2 µg/mL ethidium bromide for ~20 min followed by destaining in ROW for ~20 min. Stained gels were exposed to short wavelength UV light (254 nm) using a transilluminator (EC-40; UltraLum) and recorded as a digital image using a charge-coupled device (CCD) camera (EDAS 290; Kodak) linked to Kodak 1D molecular imaging software, version 4.5 (Kodak).

2.5.3 Purification of DNA from agarose gels

DNA was purified from agarose gel slices using the QIAquick® gel extraction kit (Qiagen). Purification was carried out according to the manufacturer's instructions, and involved first melting the agarose gel slice, adsorbing the DNA onto a silica membrane, washing, and finally eluting into 30-50 µL MQW.

2.5.4 Determination of DNA concentration

DNA concentrations were determined spectrophotometrically as described by Sambrook *et al.* (1989).

2.6 Microscopy Methods

2.6.1 Immunofluorescence microscopy (IFM)

IFM was used for the detection of FtsZ protein in various strains of *B. subtilis* under various conditions as described in the in subsequent chapters. The method used was adapted from that reported in Harry *et al.* (1995). Multi-well microscope slides (ICN Biochemicals) were prepared for cell adhesion by incubating the wells with 0.1% solution of poly-L-lysine (Sigma) for 2 min, aspirating the wells dry and rinsing twice with MQW. Slides were allowed to dry completely before applying cell samples. Vegetative cells and outgrown spores were fixed using methanol (as described by: Teleman *et al.*, 1998). Mid-exponential phase vegetative cells or outgrown spores (1 mL) were concentrated by centrifugation and resuspension in 500 μ L PBS. This was then added to 10 mL ice-cold methanol (-20°C), mixed by inversion and fixed at -20°C for 1 hr. Fixed cells were washed three times in 0.5 mL PBS by centrifugation in a microfuge (12 000 *g*, 5 min) and the supernatant discarded and then resuspended in 90 μ L GTE. Cells were permeabilised with the addition of lysozyme in GTE (to a final concentration of 1 mg/mL) and immediately added to the wells on the multi-well slide. Cells were then incubated for 2-3 min and lysozyme excess liquid was removed from the slides by aspiration until dry. A blocking solution containing 2% (w/v) bovine serum albumin (BSA) and 0.05% (v/v) Tween 20 in PBS was added to each well and incubated for a further 15 min before washing with PBS. After this point, wells were kept moist. Slides were washed once with PBS. 10 μ L aliquots of rabbit polyclonal anti-FtsZ serum (primary antibody as gift from S. Moriya), diluted 1:10000 in PBS containing 1% (w/v) BSA, were then placed onto each well and incubated at 4°C overnight in a humidified container. The following morning, the primary antibody solution was aspirated off and the slide washed ten times with PBS. Wells were then blocked by the addition of 5% (v/v) goat serum (Jackson Immunoresearch) in PBS for 30 min. After washing once

more with PBS, 10 μ L aliquots of Alexa 488-conjugated goat-anti-rabbit IgG (Molecular Probes), diluted 1:10000 in PBS containing 1% (w/v) BSA, were added to each well and incubated with the cells at room temperature for 1 h in the dark. Wells were washed ten times with PBS and the slide was mounted with 50% (v/v) glycerol (in PBS) and a coverslip. The edges of the coverslip were sealed with nail polish. FtsZ was then detected using fluorescence microscopy (Section 2.8.2). Images were acquired as described in Section 2.8.3. Slides were stored at -20°C .

Table 2.5 Antibodies used for primary and secondary detection for both IFM and western blot analysis.

<i>Antibody raised against</i>	<i>Source</i>	<i>Origin</i>	<i>Dilution used</i>		<i>Antibody type</i>
			<i>IFM</i>	<i>Western blotting</i>	
FtsZ (primary)	S. Moriya	Rabbit	1:10 000	N/A	Whole serum
FtsA (primary)	S. Jensen	Rabbit	1:50	N/A	Whole serum/ Purified antibody
Rabbit Ig (secondary)	Molecular Probes	Goat	1:10 000	N/A	Alexa 488
Rabbit Ig (secondary)	Promega	Goat	N/A	1:1 000	Alkaline Phosphatase
Mouse Ig (secondary)	Molecular Probes	Goat	1:10 000	N/A	Alexa 568

2.6.2 Live cell fluorescence microscopy

To examine the *in vivo* localisation of various GFP fusion proteins, live cells expressing the fusion of interest in culture were collected and immobilised on agarose-coated microscope slides as follows. First, a 1.5×1.6 cm rectangular well was created on the surface of the glass slide using a 65 μ L Gene Frame (ABgene; slides were obtained from Livingstone). Agarose (type 1; Sigma) was dissolved at 2% (w/v) in the same medium used to culture the cells (including supplements and/or inducers) and 65 μ L of this solution was applied to the centre of the well. A coverslip was immediately placed on top and the agarose was allowed to solidify within the well for ~ 5 min, producing a flat

“agarose pad”. To mount cells for fluorescence microscopy, the coverslip was gently lifted away and 3 μL of live cell culture was placed on the surface of the agarose pad. When using outgrown spores the sample was briefly spun to concentrate the cells (10 sec at 6700 g). The coverslip was then reapplied and the cells were viewed immediately.

2.6.2.1 Preparation of cells for nucleoid and membrane visualisation

Often it was necessary to examine the localisation/conformation of the nucleoid during IFM and live-cell fluorescence microscopy experiments. For this purpose, the fluorescent DNA stain, 4'6-diamidino-2-phenylindole (DAPI; Invitrogen), was used. DAPI was added directly to the secondary antibody solution for IFM or to culture medium (2 min prior to collection) for live cell microscopy, at a final concentration of 0.2 $\mu\text{g}/\text{mL}$. Also for visualisation of division septum, the fluorescent dye FM4-64 (Invitrogen) was added to the cell culture 30 minutes prior collection at a final concentration of 1 $\mu\text{g}/\text{mL}$.

2.6.2.2 Time-lapse of live fluorescence cells

Image acquisition was performed on live cells prepared as in section 2.6.2. In addition, live cell time-lapse experiments must be conducted using a heated microscope stage equipped with an objective heater, heatable universal mounting frame and an achromatic condenser (Zeiss), set at the optimal growth temperature (either 30, 34 or 37°C). Due to rapid bleaching of the GFP fluorophore during time-lapse image acquisition, a 2x2 binning factor was applied to the AxioCam MRm camera for all time-lapse experiments. Binning increases the sensitivity of fluorescence detection, enabling the use of shorter exposure times and thereby preserving the signal for longer. However, this comes at the cost of lowering the pixel resolution, resulting in lower quality images than those obtained without binning. Additionally a gain factor of 3 was used and the frame size was halved. Both of these measures were used to maximize the ability of the camera to capture fluorescence. Due to the relatively low fluorescence and a significant amount of photobleaching of the GFP signal during time-lapse acquisition, a relatively short

exposure time for fluorescence image acquisition (generally 50-200 ms, depending on the signal source) was used. These constraints enabled satisfactory acquisition of ~100 images throughout the period of the time-lapse. The resultant images in the time-lapse sequence were aligned in AxioVision 4.5. The aligned time-lapse image sequence was also re-sampled using the 3×3 Cubic Spline algorithm in AxioVision 4.5 to smooth the outline of the featured cell in the time-lapse and generally improve the appearance of the image.

2.6.3 Phase contrast and fluorescence microscopy

Fixed and live mounted cells were observed using a Zeiss AxioPlan 2 fluorescence microscope equipped with a 100xPlan ApoChromat phase-contrast objective (numerical aperture 1.4; Zeiss) and an AxioCam MRm cooled CCD camera (Zeiss).

The light source for fluorescence excitation was a 100 W high pressure mercury lamp passed through the following filter blocks: for visualising Alexa 488 (Filter set 09, Zeiss; 450-490 nm band pass (BP) excitation filter, 515 nm LP barrier filter), for visualising DAPI (Filter set 02, Zeiss; 365 nm excitation filter, 420 nm LP barrier filter), for GFP (Filter set 41018, Chroma Technology; 450-490 nm BP excitation filter, 495 nm beamsplitter, 500 nm LPbarrier filter) and for FM4-64 (Filter set 14, Zeiss; 506 nm excitation filter, 750 nm LP barrier filter). All images were collected using an AxioCam MRm camera. Image acquisition was generally performed at room temperature. Image processing was performed using AxioVision 4.5 or 4.6 software (Zeiss) and scoring of these images was performed within AxioVision. Images were exported as TIFF or JPEG files.

2.6.4 Cell scoring and statistics

Pixel to μm scaling for images collected by an AxioCam MRm camera were used to calculate cell lengths from digital images. Correct scaling conversions for digital images were calibrated using images of a slide micrometer (Zeiss) collected under a Plan ApoChromat (100x NA 1.4; Zeiss) objective lens on a Zeiss AxioPlan 2 microscope by

an AxioCam MRm camera. Cell lengths were measured directly from digital micrographs (untreated images) using AxioVision software, versions 4.5 and 4.6 (Zeiss) with the appropriate scaling. Numerical values for each cell length were exported from AxioVision software as a text file, and imported into Excel (Microsoft) for final analysis and graph production. Excel was used to calculate mean, standard deviation, standard error of the mean (SEM) and the number of cells counted for each data set. Statistical analyses included t-test and “Kolmogorov-Smirnov” test were carried out using Excel. The KS test is non-parametric and distribution free and was used to seek the difference in the frequency of cell lengths when DivIB is localised at midcell in wild-type and mutant strains. All statistics were performed using a 95% confidence interval, where $p < 0.05$ indicates a statistically significant difference between the comparisons made.

2.6.5 Fluorescence Recovery after Photo-Bleaching (FRAP)

Fluorescence recovery after photo-bleaching was performed on live cells prepared as normal (section 2.6.2). However, because FRAP experiments require multiple slides, cultures were re-diluted with continued shaking at 30°C temperature in order to maintain a log-phase culture. Images were acquired using a CFI Apo TIRF (100x NA 1.49, Nikon) objective lens on a Nikon A1 confocal microscope, with a temperature-controlled stage set up for 30°C, at Microbial Imaging Facility at UTS. Exposures for fluorescence intensity acquisition were done for 400 ms, while the photo-bleaching laser was set at 50% power for 50 ms pulses. Time series were typically taken over 1 min with exposures every 2 sec. Quantifications of the fluorescence intensity in 1 µm wide photo-bleached Z rings and other regions at each time point were acquired using NIS-Elements Software. For each measured Z ring, background intensity was subtracted and a correction factor was applied for overall photo-bleaching of the sample during observation. Recovery half times, achieved by applying curve fitting analysis, and statistical t-tests were determined using ImageJ and GraphPad Prism 5 softwares.

2.7 Protein methods

2.7.1 Denaturing polyacrylamide gel electrophoresis (SDS-PAGE)

Proteins were analysed by SDS-PAGE using the discontinuous pH, glycine/SDS gel system of Laemmli (1970). Polyacrylamide gels (70.0 × 80.0 × 1.5 mm) were assembled in a vertical apparatus (Mighty Small II® SE250; Hoefer). A stacking gel consisting of 4% (w/v) acrylamide (37.5:1, acrylamide:N,N-methylene-bis-acrylamide; BioRad), 0.1% (w/v) SDS, 0.1% (w/v) ammonium persulfate, 0.1% (v/v) N,N,N',N'-tetramethylethylenediamine (TEMED; ProSciTech), 125 mM Tris-HCl, pH 6.8, was cast with a well-forming comb in place over a resolving gel consisting of 10% (w/v) acrylamide (37.5:1, acrylamide:N,N-methylene-bis-acrylamide; BioRad), 0.1% (w/v) SDS, 0.1% (w/v) ammonium persulfate, 0.1% (v/v) TEMED, 375 mM Tris-HCl, pH 8.8. Samples were prepared in SDS-PAGE loading buffer (Table 2.1) and incubated at 95-100°C for 5 min prior to loading. Mark 12® wide range protein markers (Invitrogen) were used for size standards when gels were to be stained with Coomassie Brilliant Blue R250 (see below), while SeeBlue® pre-stained markers (Invitrogen) were used for gels to be prepared for Western blotting (Section 2.7.2).

Each gel was run at 20 mA in an electrophoresis buffer of 192 mM glycine, 25 mM Tris-HCl, pH 8.3, 0.1% (w/v) SDS until the tracking dye (bromophenol blue) neared the bottom of the resolving gel (~60-75 min). Following electrophoresis, the gel was either prepared for Western blotting (Section 2.7.2) or fixed in a destain solution [30% (v/v) methanol, 10% (v/v) acetic acid] for 15 min, then stained with 0.125% (w/v) Coomassie Brilliant Blue R250 (made up in destain solution) for 4-16 h before finally destaining with 2 or 3 changes of destain solution over 3-4 h.

2.7.2 Western blot analysis

Western blotting experiments were performed in this study to examine the cellular level of FtsA in four *B. subtilis* strains (SU5, SU456; SU457 and SU506; Table 2.2) grown under specific conditions (see Section 3.2.1.1, Chapter 3).

2.7.2.1 Whole cell protein extraction for Western blot analysis

Protein samples were prepared for Western blotting by cell lysis as follows. First, 5 mL of live culture was harvested by centrifugation at 3000 *g* for 5 min and the pellet was resuspended in a volume of Western lysis buffer (Table 2.1) calculated such that the A_{590} would be ~20 if resuspended using an equivalent volume of the original medium. The mixture was incubated at 37°C for 10 min. SDS was then added to 1% (w/v) and the incubation was continued at room temperature for a further 2 min. At this time SDS-PAGE loading buffer (Table 2.1) was added to a concentration of 1x and the samples were stored at -20°C until needed. Thawed samples were further diluted (if necessary) with 1x SDS PAGE loading buffer and incubated at 95-100°C for 5 min prior to loading 20 μ L onto a denaturing polyacrylamide gel (Section 2.7.1).

2.7.2.2 Western transfer

The procedure used for Western transfer was based on that previously reported by Otter *et al.* (1987) for small proteins. After running the desired samples on a polyacrylamide gel (Section 2.7.1), the gel was incubated in ice-cold Western transfer buffer (Table 2.1) for 15 min. An electro-transfer apparatus (Mini Trans-Blot; BioRad) for transfer of the proteins to a nitrocellulose membrane (BioTrace® NT; Gelman Sciences) was then assembled using fibre pads, filter paper, membrane and gel (all pre-incubated in ice-cold Western transfer buffer). Transfer was performed at 4°C and 30V for ~16 h on a magnetic stirrer.

2.7.2.3 Immunodetection

Following Western transfer, detection of FtsZ was performed using the Enhanced Chemi-Luminescence (ECL) Western blotting detection system (Amersham Biosciences) according to the manufacturer's instructions. First, the nitrocellulose membrane was air-dried and equilibrated in TBS (Table 2.1) at room temperature for 5 min. The membrane was then blocked in TBS + milk (containing 5% (w/v) skim milk powder) for 2 h with rocking. After removing the blocking buffer, the membrane was

incubated for 1 h in a primary antibody solution made up of rabbit polyclonal anti-FtsZ serum (S. Moriya) diluted 1:10000 in TBS + milk. The membrane was then washed three times for 10 min in TBS + milk and incubated for 1 h with a goat anti-rabbit horseradish peroxidase-conjugated secondary antibody (Promega) diluted 1:2500 in TBS + milk. After four 5 min washes in TBS, the membrane was incubated with detection reagents for the ECL reaction as per the manufacturer's instructions (Amersham Biosciences), then exposed to autoradiography film (Hyperfilm ECL; Amersham Biosciences) for 1 min in the dark. The film was immersed in Kodak GBX developer (Kodak) until protein bands developed to the desired intensity, rinsed in MQW, and then fixed in Kodak GBX fixer until the background became transparent.

A digital image of the film was acquired with a CCD camera (EDAS 290; Kodak) and band intensities were analysed by densitometry using Kodak 1D molecular imaging software, version 4.5 (Kodak).

2.8 Suppliers of chemicals, reagents and equipment

Table 2.6 Suppliers of chemicals, reagents and equipment.

Supplier	Full name and location
ABgene	ABgene Limited, Epsom, UK
Adobe Systems	Adobe Systems Incorporated, Mountain View, USA
Alpha Innotech	Alpha Innotech Corporation, San Leandro, CA, USA
Amersham Biosciences	Amersham Biosciences International, Little Chalfont, UK
Amresco	Amresco Incorporated, Solon, USA
Amyl Media	Amyl Media Proprietary Limited, Moorabbin, Australia
BDH Chemicals	BDH Chemicals Australia Proprietary Limited, Kilsyth, Australia
BioRad	BioRad Laboratories, Hercules, USA

Chroma Technology	Chroma Technology Corporation, Rockingham, USA
Clontech	Clontech Laboratories Incorporated, Palo Alto, USA
Difco	Difco Laboratories, Detroit, USA
Fermentas	Fermentas Life Sciences Incorporated, Burlington, Canada
GE Healthcare	GE Healthcare, Uppsala, Sweden
Genomed	Genomed Incorporated, St Louis, USA
ICN Biochemicals	ICN Biochemicals Australasia Proprietary Limited, Sydney, Australia
Invitrogen	Invitrogen Life Technologies, Carlsbad, USA
Kodak	Eastman Kodak Company, Rochester, USA
Livingstone	Livingstone International Proprietary Limited, Sydney, Australia
Microsoft	Microsoft Corporation, USA
Millipore	Millipore Corporation, Bedford, USA
Molecular Devices	Molecular Devices, Sunnyvale, CA, USA
Molecular Probes	Molecular Probes Incorporated, Eugene, USA
New Brunswick	New Brunswick Scientific Company, Edison, USA
New England Biolabs	New England Biolabs Incorporated, Beverly, USA
Nikon	Nikon Instruments Inc., USA
Novex	NOVEX, San Diego, CA, USA
Promega	Promega Corporation, Madison, USA
ProSciTech	ProSciTech, Thuringowa, Australia
Qiagen	Qiagen Incorporated, Chatsworth, USA
Roche	Roche Diagnostics GmbH, Mannheim, Germany
Sigma	Sigma Chemical Company, St Louis, USA

Thermo Fisher Scientific	Thermo Fisher Scientific, Inc., Waltham, MA, USA
UltraLum	UltraLum Incorporated, Claremont, USA
Zeiss	Carl Zeiss Incorporated, Oberkochen, Germany

Chapter 3

§

*Z ring formation in the absence of the FtsA
protein in Bacillus subtilis*

3.1 Introduction

Bacterial cell division begins with the formation of a cytoskeletal structure, the Z ring, at midcell between two replicated chromosomes. Once formed, the FtsZ ring acts as a molecular scaffold to recruit several other proteins to the division site in a hierarchical order to form a multi-complex, named the divisome. The Z ring undergoes constriction as septum formation occurs to separate the two new daughter cells. Z ring formation and constriction are tightly regulated events in time and space, being essential for correct division and survival of the cell.

It has been proposed that FtsA, an early division protein, is required for efficient Z ring formation by directly interacting with FtsZ. However, its exact role remains elusive. The work presented in this chapter attempts to add more information on this subject by studying the behaviour of *B. subtilis* cells lacking FtsA.

3.1.1 Background on the ftsA story

The FtsA protein has been studied mostly in *E. coli*, where it is an essential protein, although some information has also been gathered from studies on *B. subtilis*. Following the literature observations it seems that FtsA plays different functions in these two organisms.

In *E. coli*, there are three main functions for FtsA: to promote Z ring formation and stability, recruitment of several downstream division proteins and a direct role in septal invagination possibly by affecting Z ring constriction. Early in cell division FtsA interacts directly with FtsZ and it is dependent on FtsZ for localisation to the Z ring (Addinall and Lutkenhaus, 1996; Feucht *et al.*, 2001; Peters *et al.*, 2007). In *E. coli*, the loss of FtsA does not affect the ability of FtsZ to form normal Z rings (Addinall *et al.*, 1996; Hale and de Boer, 1999), probably due to the overlapping function of an additional essential protein, ZipA, which also binds FtsZ. Studies have confirmed the complementary roles of ZipA and FtsA. Depletion or inactivation of either protein results in Z ring formation. However simultaneous inactivation of both proteins inhibits formation of new Z rings and causes destabilisation and disassembly of preformed Z

rings (Pichoff and Lutkenhaus, 2002; Geissler *et al.*, 2003; Geissler *et al.*, 2007). The earlier function for FtsA in *E. coli* is to anchor FtsZ and the Z ring to the membrane, promoting Z ring formation and being essential for its stability. This is possible because FtsA interacts directly with FtsZ through C-terminal tail of FtsZ (Wang *et al.*, 1997; Ma and Margolin, 1999; Di Lallo *et al.*, 2003); and interacts with the cytoplasmic membrane by an amphipathic helix (Pichoff and Lutkenhaus, 2005). Another function for FtsA in *E. coli* is to recruit the later-acting cell division proteins to the division site (Pichoff and Lutkenhaus, 2002; Corbin *et al.*, 2004; Rico *et al.*, 2004). However, this recruitment can be bypassed by fusing the subdomain 1C of FtsA to FtsZ and partially suppress a thermosensitive *ftsA* mutation (Corbin *et al.*, 2004), suggesting that the placement of the divisome at the midcell site is not the main function of FtsA in these cells. Interestingly, this bypass for FtsA did not rescue cell division, suggesting that FtsA also plays an additional role in *E. coli* division, perhaps during Z ring constriction. This role is still not very clear, but studies suggest that it could happen through the tethering mechanism that would allow the invagination of the membrane during Z ring constriction (Hale and de Boer, 1997; Weiss, 2004). Also, the oligomerisation ability of FtsA at midcell could somehow assist the protofilament dynamics in the FtsZ ring, assisting with Z ring integrity, as suggested by Shiomi and Margolin (2007).

Much less is known about the functions of FtsA in *B. subtilis*. At the time of commencing this thesis, available evidence pointed to a main role for FtsA in promoting Z ring assembly and stability. The last detailed study regarding *B. subtilis* FtsA was done by Jensen *et al.* (2005), conducted in the same group of this present thesis. Jensen *et al.* have shown that an *ftsA*-deletion mutant of *B. subtilis* has a significantly decreased frequency of Z ring formation. Compared to wild-type cells, these mutant cells are quite filamentous (~3-fold longer), indicating an impairment in cell division (Jensen *et al.*, 2005), a phenotype seen previously by Beall and Lutkenhaus (1992). Unlike *E. coli* cells, the *ftsA* deletion is not lethal for *B. subtilis* cells; however the frequency of Z ring formation is only ~10% of that in wild-type cells, showing an absolute requirement of FtsA for efficient Z ring assembly in *B. subtilis* (Jensen *et al.*, 2005). Accordingly, chemical cross-linking experiments point out that the FtsA protein binds FtsZ prior to Z ring formation, consistent with a direct role for FtsA in the assembly of the Z ring (Jensen *et al.*, 2005). Interestingly, the observation of some Z rings still able to form in the absence of FtsA implies that there may be an additional protein sharing the function

of FtsA in *B. subtilis*. The SepF protein has been indicated as a good candidate (see section 1.5.2; Ishikawa *et al.*, 2006; Hamoen *et al.*, 2006), since over-production of the SepF seems to rescue an *ftsA* mutant.

Jensen *et al.* (2005) was the first study that really focused on the effects of FtsA on Z ring frequency, and gathered more information regarding its role as a facilitator of Z ring formation and stability. However, it is still unclear what caused the filamentous phenotype in the absence of FtsA. The present work tries to address this gap in the current knowledge, by taking advantage of the spore outgrowth system as a unique tool for uncovering the direct consequence of lacking a single component of the divisome on FtsZ assembly and septum formation. The results obtained here, with the observation of the formation of the first Z rings in the cells, emphasise the importance of understanding how the phenotype was raised.

3.1.2 Chapter Aims

The primary objective of the work presented in this chapter was to determine the reason for the low frequency of Z rings in *B. subtilis* cells in the absence of FtsA. The *ftsA*-deletion phenotype is characterised by significant cell filamentation (inhibition of division) and a significant (3-fold) reduction in Z ring formation. The main question that immediately arises regarding the lack of Z rings in the absence of FtsA is whether this reflects a lack of Z ring assembly altogether or whether Z rings actually form in the absence of FtsA but are unstable, resulting in their disassembly. To investigate this, the first round of cell division following spore germination in *B. subtilis* was examined to determine the frequency of formation of the first Z ring in cells in a system uncomplicated by previous division events. Surprisingly, in the absence of FtsA in germinated spores, the first Z rings formed with wild-type efficiency. However, unlike wild-type cells that showed subsequent constriction of these Z rings leading to septum formation, in the *ftsA*-deleted strain the Z rings did not constrict immediately and persisted into the second cycle of division. Further analysis confirmed that the observed phenotype was in fact due to the absence of FtsA in the cells. Collectively, these data strongly suggest that there is no absolute requirement of FtsA for efficient Z ring formation, with Z ring constriction being severely affected. This seems to contradict the

assumed role for FtsA and thus reveals a novel perspective on the function of this protein in *B. subtilis*.

3.2 Results

3.2.1 Characterisation of the *ftsA* null strain during vegetative growth

To determine whether the low frequency of Z rings in the absence of FtsA is due to the lack of Z ring formation or due to their formation and then subsequent destabilisation, an *ftsA*-deletion strain was used. This strain (SU457) had been created in previous work (Jensen *et al.*, 2005) and was available for this work. The SU457 strain, from now on referred to as the *ftsA* null strain, was constructed by replacing the 1051-bp of the *ftsA* gene with an 800-bp chloramphenicol resistance gene (*cat*). In *B. subtilis*, the *ftsA* and *ftsZ* genes are normally co-transcribed from three identified promoters (Beall and Lutkenhaus, 1991; Gholamhoseinian *et al.*, 1992; Gonzy-Tréboul *et al.*, 1992). Two promoters, P1 and P3, are dependent on the vegetative sigma factor (σ^A) and are expressed mainly during growth. The third promoter, P2, is controlled by another sigma factor (σ^H) which is active during growth but more strongly around the onset of sporulation (Gonzy-Tréboul *et al.*, 1992). All promoters are found upstream of *ftsA* (P_{ftsAZ}), specifically in the *sbp-ftsA* intergenic region (Gonzy-Tréboul *et al.*, 1992). The transcription regulation of all promoters was maintained in the new deletion strain. To enable controlled *ftsZ* transcription, the *ftsZ* gene was placed under the control of the IPTG-inducible promoter P_{spac} (Beall and Lutkenhaus, 1991), producing the final construct in strain SU457 (*ftsA::cat P_{spac}-ftsZ*; Figure 3.1). The parental SU457 strain is SU456(P_{spac} -*ftsZ*; Figure 3.1), used in this work as the control strain, and is from now on referred to as the FtsA⁺ strain (Jensen *et al.*, 2005). This strain derives from the strain BB11 (Beall and Lutkenhaus, 1991), which was created by inserting a plasmid containing the ribosome-binding site and the first 147 codons of the *ftsZ* gene downstream of the *spac* promoter control. An important genetic construction detail is that the BB11 strain had phleomycin resistance, which was then replaced by chloramphenicol resistance by Jensen *et al.* (2005). The FtsA⁺ strain is the wild-type counterpart of the *ftsA* null mutant and any difference between these strains can only be

due to the absence of *ftsA*. In all previous experiments and those described here, both strains are normally grown in rich liquid media (PAB; Chapter 2, Table 2.3) at 37°C and samples are analysed when the cells reach the mid-exponential phase of growth. The presence of 1mM IPTG during growth is always required for P_{spac} -*ftsZ* induction to maintain approximately wild-type levels of cellular FtsZ in the cells and show normal growth and division (Jensen *et al.*, 2005). As previously reported by Jensen *et al.* (2005), *ftsA* null cells had a slower growth rate when compared to FtsA⁺ cells, with an approximate 1.5-fold longer doubling time; and also presented a lower OD₆₀₀ reading at stationary phase, probably due to some observed cell lysis in this mutant.

To confirm the cellular morphology of SU456 (FtsA⁺) and SU457 (*ftsA* null), cells of these strains were fixed in methanol and visualised by phase-contrast microscopy. The FtsA⁺ strain was morphologically indistinguishable from its parent strain, SU5 (wild-type; from the laboratory background strain *B. subtilis* 168, see Table 2.2), at 37°C. This FtsA⁺ strain displayed short cells, characteristic of a normal (wild-type) frequency of cell division (Figure 3.2 Ai) with an average cell length of 4.2 µm ± 0.06 (± standard error of the mean), compared to wild-type (SU5) which was 4.3 µm ± 0.07 (Table 3.1). As expected, the *ftsA* null strain formed long filamentous cells (Figure 3.2 Bi) with an average cell length of 24.5 µm ± 1.29, with some cell lysis observed. These filaments still had infrequent visible septa, confirming that cell division is not entirely blocked in this mutant, but its rare occurrence causes the cells to become long filaments. This work is consistent with published work from Jensen *et al.* (2005).

Table 3.1 Quantitative analysis of FtsA⁺ (SU456), *ftsA* null (SU457), wild-type (SU5) and *ftsA* in-frame (SU506) cell lengths during mid-exponential vegetative growth.^a

	FtsA ⁺	<i>ftsA</i> null	Wild-type	<i>ftsA</i> in-frame
Average cell length (µm ± SEM)	4.2 ± 0.06	24.5 ± 1.29	4.3 ± 0.07	16.8 ± 0.89
% Z rings	53	19	47	8
Z ring/cell length (µm)	0.24	0.07	0.23	0.09

^aCultures were grown in rich media PAB to mid-exponential phase at 37°C. Strains SU456 and SU457 were grown in the presence of 1mM IPTG. SEM refers to standard error of the mean.

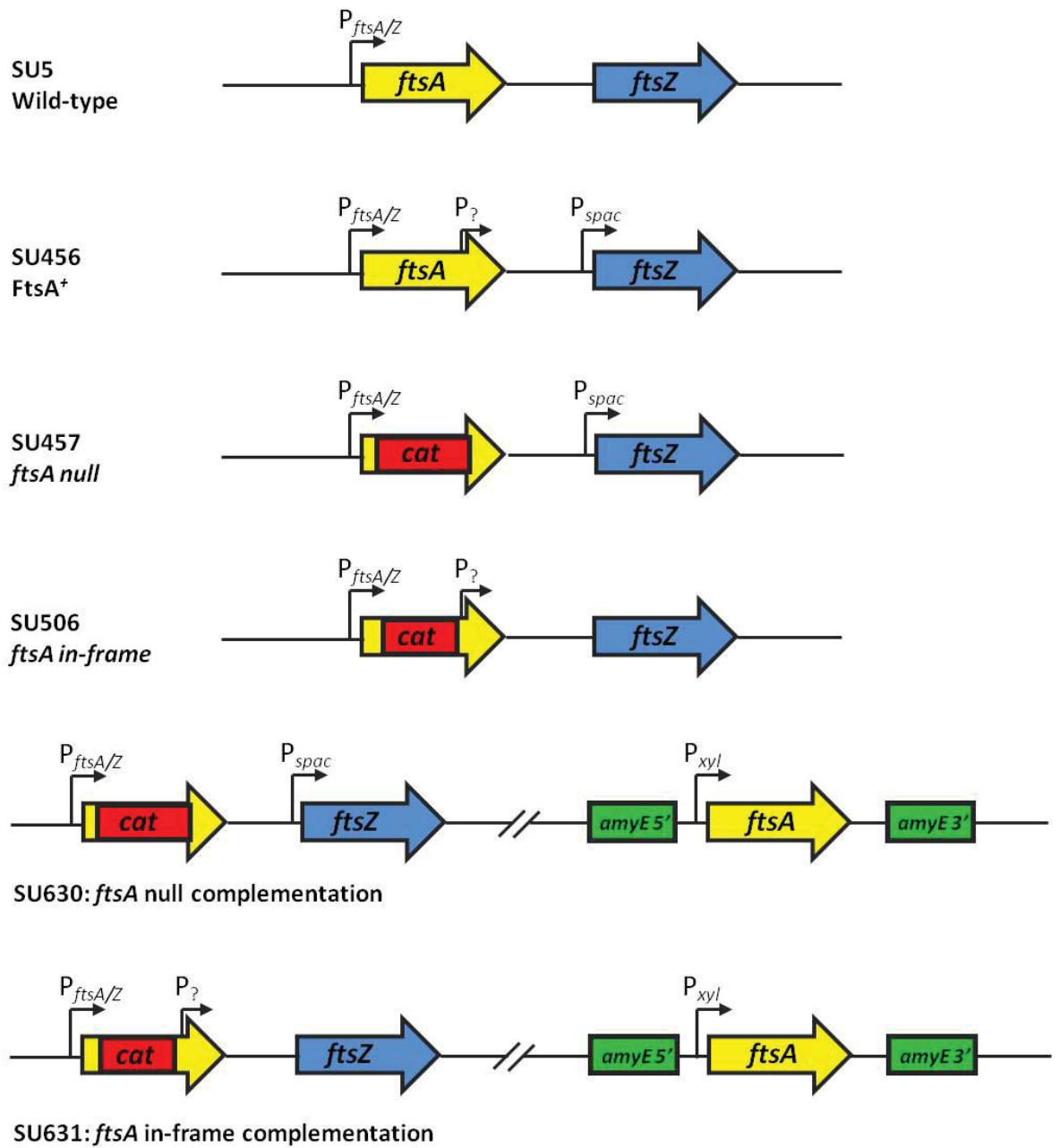


Figure 3.1 Genetic constructs of *ftsA*-modified strains. Control strains are represented first as SU5 (wild-type) and SU456 (FtsA⁺); followed by the *ftsA*-deleted strains as SU457 (*ftsA* null) and SU506 (*ftsA* in-frame); and the complementation strains in last as SU630 (*ftsA* null complementation) and SU631 (*ftsA* in-frame complementation). Both SU457 and SU630 have an 800-bp *cat* gene replacing the 1051-bp of the *ftsA* gene and an IPTG-inducible promoter (P_{spac}) driving *ftsZ* transcription. In contrast, both SU506 and SU631 strains have a *cat* gene without its promoter and terminator sequences and 1.4kb upstream and downstream flanking regions complementary to *ftsA*. Part of the downstream region was kept because it may contain a fourth putative *ftsZ* promoter (see Beall *et al.*, 1988). Also, the absence of the *cat* terminator sequence in these strains allows the transcription of *ftsZ* gene by its native promoters. Genuine or putative promoter sequences are marked with black arrows with $P_{ftsA/Z}$ representing the three promoters upstream of *ftsA* and $P_?$ representing the putative fourth promoter. // represents non-contiguous sequence.

To confirm Jensen's results (Jensen *et al.*, 2005), FtsZ and Z rings were visualised in the presence and absence of FtsA. Therefore, both the *ftsA* null and FtsA⁺ strains were grown as mentioned above, collected for methanol fixation at mid-exponential phase and processed for immunofluorescence microscopy using anti-FtsZ antiserum. In wild-type cells (SU5), the FtsZ protein assembles as a Z ring at midcell under these conditions. The proportion of cells with Z rings in the wild-type population is 47%. In the FtsA⁺ strain (Figure 3.2 Aii) the proportion of cells in the population containing midcell Z rings was 53%. The *ftsA* null strain showed a similar frequency of midcell Z rings as reported previously by Jensen *et al.* (2005). In these filamentous cells, only 19% of the cells in the population at mid-exponential phase had a midcell Z ring. Additionally, although these filamentous cells contained several nucleoid-free regions, only one Z ring per cell was observed (see arrow in Figure 3.2 Bii). This equates to a Z ring frequency of 0.07 rings per μm in cells when there is no FtsA present, compared to 0.24 Z rings per μm for the FtsA⁺ strain (Table 3.1). Thus in the absence of FtsA, the frequency of Z rings is decreased by 3-fold.

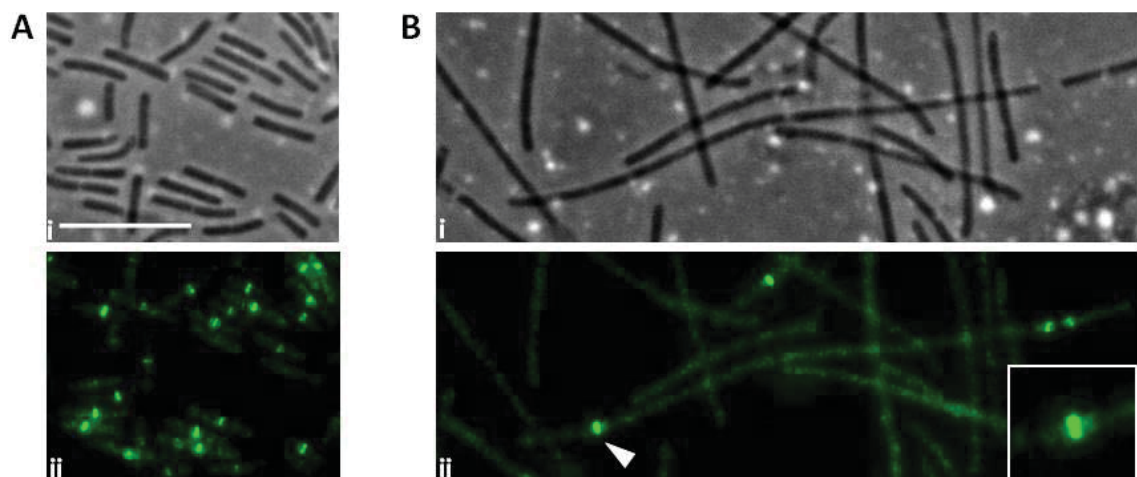


Figure 3.2 Z ring localisation in the absence of FtsA. Cultures were grown in the presence of 1mM IPTG to mid-exponential phase at 37°C. **(A)** The FtsA⁺ strain (SU456) shows wild-type phenotype with short dividing cells, with an average cell length of $4.2 \mu\text{m} \pm 0.06$ (SEM). **(B)** The *ftsA* null strain (SU457) shows a filamentous phenotype, with an average cell length of $24.5 \mu\text{m} \pm 1.29$ (SEM), caused by a defect in cell division. These cells divide with lower frequency but continue to grow into long filaments. Cells were fixed with methanol and processed for immunofluorescence microscopy (phase-contrast images are shown in i) and FtsZ localisation as green fluorescence is shown in ii) (this work). Scale bar represents 10 μm for all images.

3.2.1.1 Analysis of cellular FtsA levels in *ftsA*-modified *B. subtilis* strains

To confirm the absence of cellular FtsA in *ftsA*-deleted strains, a quantitative Western blot analysis was performed (Figure 3.3). During this present work two different *ftsA*-deleted constructs were used: the *ftsA* null strain (SU457) previously mentioned; and an in-frame *ftsA*-deletion strain (SU506). Experiments performed with this strain are presented later in this chapter. Cells of both *ftsA*-deleted strains and their corresponding control strains were grown in the absence or presence (1mM) of IPTG and examined at the mid-exponential phase of vegetative growth. Whole cell lysates of these samples were prepared and ‘optical density equivalents’ (as determined by the optical density of the cultures at the time of collection) were used for Western blotting. However, to quantitatively compare the intensities of different bands on the Western blot, it was first necessary to establish the linear range of detection i.e. the range of band intensities over which a change in protein concentration generates a proportional change in intensity. To this end, a series of dilutions were prepared for the cell lysate of the wild-type strain (SU5) and then subjected to Western blotting using anti-FtsA antibodies. The observed band intensities were then plotted against various sample dilutions to determine the linear range of detection for FtsA (data not shown). To compare FtsA levels among the different cell lysates, Western analysis was carried out after an appropriate dilution of the samples, such that the band intensities would be predicted to lie within this pre-determined linear range. A representative Western blot is shown in Figure 3.3. As expected, the control strains (SU5 and SU456) exhibited a band on the blot (Figure 3.3) that, by comparison to protein size standards, corresponds to native FtsA (~50 kDa). The FtsA antibody is polyclonal and while able to detect the FtsA protein, it is not uniquely specific to it and multiple bands are observed on the blot (Figure 3.3). However, the main finding was that neither *ftsA*-deleted strains, SU457 and SU506 (referred in the later section 3.2.3), showed a band of molecular mass equal to FtsA, showing that, as expected, the gene deletions in these strains completely prevent production of FtsA.

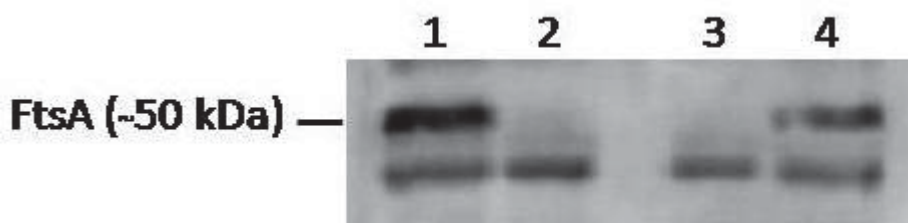


Figure 3.3 Western analysis of native FtsA in *B. subtilis*. Cells were grown in PAB media for 2 h at 37°C. Whole cell lysates were run at a 1 in 2 dilution, facilitating detection of wild-type FtsA within the linear range. Both control strains (SU5 and SU456) were also analysed. FtsA band size was estimated by comparison to the proteins markers added (not shown) (1) SU5, wild-type. (2) SU506, *ftsA* in-frame deletion. (3) SU457, *ftsA* null. (4) SU456, FtsA⁺.

3.2.2 Z ring formation in the absence of FtsA during spore outgrowth

The previous sections have confirmed that when the FtsA protein is not present, there is a significant reduction (3.4-fold) in the frequency of Z ring formation per μm . To determine whether the low frequency of Z rings in the absence of FtsA is due to their lack of formation or due to their formation and subsequent destabilisation, the spore outgrowth system was used. This experiment was carried out in spores of the *ftsA* null strain (SU457) and its control strain FtsA⁺ (SU456). *B. subtilis* spores are mature when they become phase-bright when viewed by phase-contrast microscopy (see Chapter 2, section 2.6.3). Sporulation was induced on Sporulation Agar as described in Chapter 2 (see also Table 2.3) and the spores were harvested and washed after 8 days of incubation at 30°C. At this point, a high quality spore preparation should contain around 90% phase-bright spores, although the deletion strains normally contained significantly less phase-bright spores due to its inefficient cell division, as observed by phase-contrast microscopy and estimated spectro-photometrically (see Chapter 2, section 2.6.3).

For spore outgrowth (details in Chapter 2, section 2.4), the spores were germinated in GMD media (Table 2.3) at 34°C and samples were taken every 30 minutes and prepared for immunofluorescence microscopy to visualise Z rings. Following 120 minutes of incubation, approximately 78% of outgrown cells of the FtsA⁺ strain had a midcell Z ring positioned between two replicated nucleoids. Cells with a Z ring had an average cell length of $3.0 \pm 0.05 \mu\text{m}$ (see Table. 3.2 and Figure 3.4 FtsA⁺). This first generation of cells continue to elongate with subsequent Z ring constriction and cell division. The

cycle then begins again, giving rise to a population of cells of similar, normal length. Consequently, FtsA⁺ cells at later times of spore outgrowth are the same phenotype as earlier times (images not shown) and the Z ring frequency (number of Z rings per cell) maintains close to 80% (see Table. 3.2).

Surprisingly, when the *ftsA* null strain was analysed under the same growth conditions, the frequency of Z ring formation was the same as FtsA⁺ cells (~80%) at the same time points. All Z rings were located at midcell between two replicated nucleoids. After 120 minutes, the average cell length was the same as cells of the FtsA⁺ strain ($3.1 \pm 0.07 \mu\text{m}$; Table 3.2; Figure 3.4 120'i, ii, iii and iv). According to this analysis, Z ring formation in the absence of FtsA is as efficient as in wild-type cells. However, in contrast to the FtsA⁺ strain, at 150 minutes following spore germination, the majority of the Z rings in the *ftsA* null cells (SU457) do not appear to constrict (see Figure 3.4 150'i, ii, iii and iv). Rather, they remain at midcell. This is supported by the observation that most of the cells did not divide, although cell elongation and DNA replication appeared normal (see Figure 3.4 150'iii, showing the nucleoids stained with DAPI). These cells thus elongated to an average cell length of $5.6 \pm 0.13 \mu\text{m}$, while for the same time point the wild-type cells (FtsA⁺, SU456; Table 3.2) had an average cell length of $3.3 \pm 0.04 \mu\text{m}$.

Table 3.2 Quantitative analysis of FtsA⁺ (SU456) and *ftsA* null (SU457) cells average cell lengths during spore outgrowth.^a

	120'		150'		180'		210'	
	FtsA ⁺	<i>ftsA</i> null	FtsA ⁺	<i>ftsA</i> null	FtsA ⁺	<i>ftsA</i> null	FtsA ⁺	<i>ftsA</i> null
Cell lengths	3.0	3.1	3.3	5.6	3.6	6.9	3.7	7.2
± SEM	0.05	0.07	0.04	0.13	0.05	0.20	0.06	0.20
% Z ring	78	68	82	81	79	80	82	78
Z ring/μm	0.30	0.29	0.29	0.15	0.27	0.12	0.26	0.11

^aSpores were germinated and outgrown in germination media (GMD) at 34°C. SU457 strain was grown in the presence of 1mM IPTG. Values for cell lengths are presented as an average, SEM referring to its standard error of the mean.

To examine the fate of the *ftsA* null cells after several cell cycles, later time points were observed. As shown in Figure 3.4, at 210 minutes after spore germination, the *ftsA* null cells become longer with average cell length of $7.2 \pm 0.20 \mu\text{m}$. Additionally, although the percentage of individual cells containing a Z ring remained high, at 78%, these cells presented several nucleoid-free regions, which are potential sites for Z ring assembly, but unexpectedly only one Z ring per cell is observed (Figure 3.4 210' iv). Indeed, during the first cell cycle (at 120 minutes) in *ftsA* null cells Z ring localisations occurred at a frequency of 0.29 localisations per μm which is similar to the Z ring/ μm ratio in FtsA⁺ cells (~ 0.30 throughout spore outgrowth). However, this frequency decreases 2.6-fold in the null mutant strain, reaching 0.11 Z rings/ μm at 210 minutes of spore outgrowth. These results clearly show that FtsA is not essential for efficient Z ring assembly at the first division site following spore germination. However, this first Z ring does not constrict, and also Z ring formation does not occur at subsequent division sites, causing the cells to become longer than wild type cells. Some division still occurs however since the *ftsA* mutant is still viable.

Further time points were observed (data not show) to confirm that after several more generations, the phenotype of the *ftsA* null strain resembles that of the filamentous phenotype characteristic of vegetative cells observed previously for the *ftsA* null strain that has a average cell length of $24.5 \mu\text{m}$ (reported above). Thus the differences in Z ring frequency observed between the first cell cycle following spore germination and vegetatively-growing cells are likely not to be due to some genetic modification of the cells during the preparation of spores.

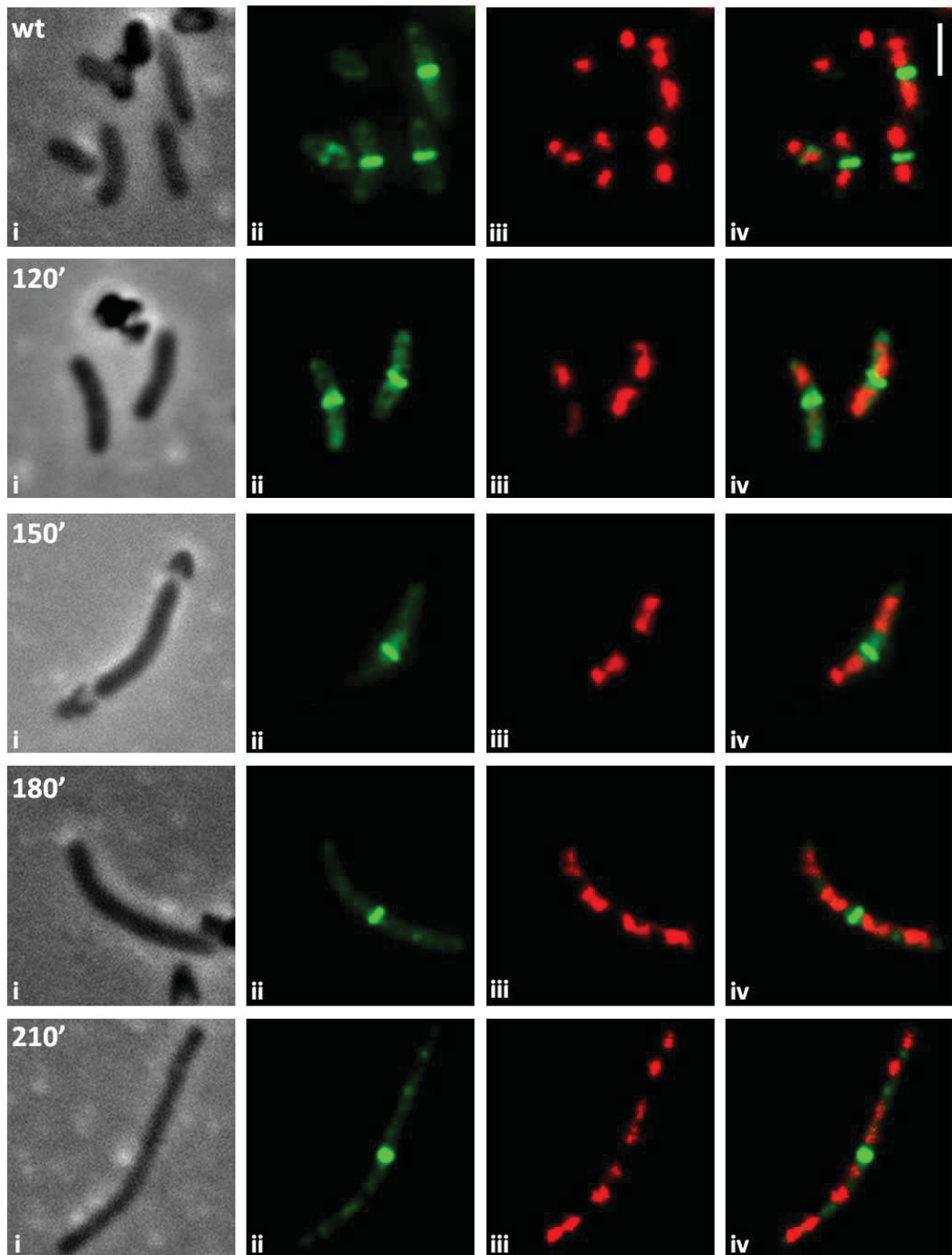


Figure 3.4 Z ring localisation in the absence of *FtsA* in outgrown spores. *FtsA*⁺ (SU456) and *ftsA* null (SU457) spores were germinated in GMD medium with 1mM of IPTG for *FtsZ* expression, at 34°C. Samples were taken every 30 minutes and cells were immediately fixed with methanol and prepared for immunofluorescence microscopy. Nucleoids were stained with DAPI. Panels labelled i depict phase-contrast images, while those labelled ii and iii show the corresponding *FtsZ* (green) and nucleoid (red) localisation patterns, respectively. Panels designated iv depict an overlay of ii and iii. (WT) The *FtsA*⁺ control strain shows short dividing cells (at 120 minutes after germination), with an average cell length of $3.0 \mu\text{m} \pm 0.05$ (SEM). All other images are referent to the *ftsA* null strain during sequential times of the spore outgrowth. These cells divide with lower frequency and continue to grow into long filaments. Scale bar represents $2 \mu\text{m}$ for all images.

3.2.3 Construction of an *ftsA* in-frame deletion strain (SU506)

The work done with the FtsA⁺ and *ftsA* null strains involved constant induction of P_{spac} -*ftsZ* to maintain cellular levels of FtsZ that were similar to those in wild-type cells. However, it is possible that the expression of *ftsZ* during vegetative growth and spore germination in *B. subtilis* could be different. Therefore, the constitutive expression of *ftsZ* due to induction of the P_{spac} promoter driving the *ftsZ* gene in the *ftsA* null strain could possibly account for the unexpectedly high frequency of Z rings observed in outgrown spores. In other words, there could be an abnormally high level of FtsZ specifically in outgrown spores under these conditions that gives rise to such a high frequency of Z rings in the first cycle following spore germination, while not having an effect on vegetative cells of the same strain. To test whether this is the case, a modified version of the *ftsA* null strain (SU457) was created by Ana P. Cubas previous to this study (unpublished work) and was available for the present work. In this new strain, the *cat* gene, which replaces *ftsA*, is placed in-frame with the coding region of the *ftsZ* gene and it allows *ftsZ* gene expression to be controlled by its native promoters. In this strain *ftsA* was replaced with an insertion of a chloramphenicol (*cat*) gene cassette, without its transcription terminator, promoter and RBS (ribosome-binding sequence), all of which replaced the *ftsA* gene in the SU457 strain; and with 1.4kb upstream and downstream flanking regions complementary to *ftsA*. The reason why part of the downstream region was kept was due to the possibility that it contains a fourth putative *ftsZ* promoter (Beall *et al.*, 1988). In this new deletion strain, from now on referred to as the *ftsA* in-frame deletion strain (SU506), all three identified native promoters, $P_{ftsA/Z}$, within the *ftsA* coding region are maintained (Figure 3.1). The stop codon of the *cat* gene was present to prevent the fusion of the product of the *cat* gene with the product of the downstream *ftsZ* gene the FtsZ protein. Also, the absence of the *cat* terminator sequence in these strains allows the transcription of *ftsZ* gene by its native promoters. The control strain for this work is the wild-type strain SU5, from now on referred to as the wild-type strain (Figure 3.1). Both strains are vegetatively grown in rich liquid media (PAB; Chapter 2, Table 2.3) at 37°C.

Prior to performing the germinated spore experiments to test for Z ring frequency in this strain, the cellular morphology of these strains during vegetative growth was examined to see if a similar phenotype was observed between the *ftsA* null strain and this new

strain. To investigate the cellular morphology of these strains, cells were fixed in methanol and visualised by phase-contrast microscopy. As shown in Figure 3.5, cells of the wild-type strain, SU5, were short, characteristic of a normal frequency of cell division (Figure 3.5 Ai), with an average cell length of $4.3 \mu\text{m} \pm 0.07$. As expected, the *ftsA* in-frame deletion strain formed long filamentous cells (Figure 3.5 Bi) with an average cell length of $16.8 \mu\text{m} \pm 0.89$ compared to $24.5 \mu\text{m} \pm 1.29$ for the *ftsA* null strain. These filaments still presented infrequent visible septa, confirming that cell division is not entirely blocked in the absence of FtsA, but the infrequent division causes the cells to become long filaments.

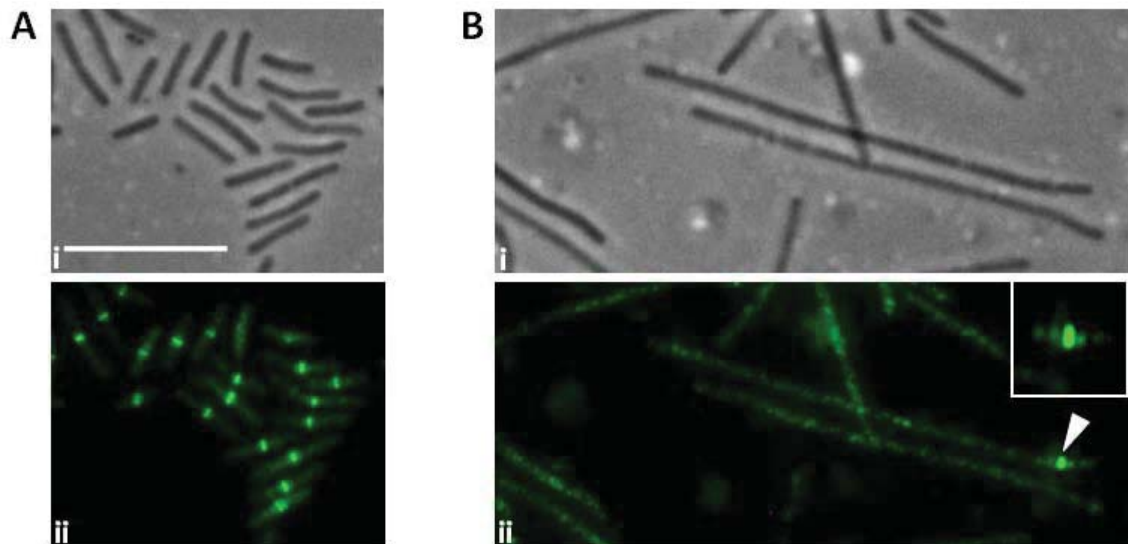


Figure 3.5 Z ring localisation in the new *ftsA* in-frame deletion strain. Cultures were grown to until mid-exponential phase of vegetative cycle at 37°C. **(A)** The wild-type strain (SU5) shows short dividing cells, with an average cell length of $4.3 \mu\text{m} \pm 0.07$ (SEM). **(B)** The *ftsA* in-frame strain (SU506) shows a filamentous phenotype, with an average cell length of $16.8 \mu\text{m} \pm 0.89$ (SEM), caused by a defect in cell division. These cells divide with lower frequency but continue to grow into long filaments. Cells were fixed with methanol and processed for immunofluorescence microscopy (Phase-contrast images, i) and FtsZ localisation, (green fluorescence, ii). Scale bar represents $10 \mu\text{m}$ for all images. SEM is referred to standard error of the mean.

To visualise FtsZ and the Z rings in the presence and absence of FtsA, both wild-type and *ftsA* in-frame strains were grown to mid-exponential phase, collected for methanol fixation and processed for immunofluorescence microscopy using anti-FtsZ antiserum (details in Chapter 2, section 2.6.1). In the wild-type cells, Z rings were visualised by microscopy as bright fluorescent bands at midcell (Figure 3.5 Aii). Z rings were present

in 47% of the cell population at mid-exponential phase. Cells of the *ftsA* in-frame strain had Z rings; however, the frequency of Z rings per cell was dramatically decreased. At mid-exponential phase only 8% of cells in the population had a Z ring. Furthermore, although these filamentous cells contained several nucleoid-free regions, only one Z ring per cell was observed (see arrow in Figure 3.5 Bii). So in this case, in the absence of FtsA, the Z ring localisations occurred at a low frequency of 0.09 localisations per μm , a 2.6-fold decrease when compared to the frequency of 0.23 Z rings per μm for the wild-type strain (see Table 3.1). These data show that the phenotype observed earlier in vegetatively growing cells of the *ftsA* null strain is not due to *ftsZ* expression being controlled by the P_{spac} promoter. Further, these results confirm that the observed phenotype was caused only by the absence of the FtsA protein.

To determine whether Z rings in the *ftsA* in-frame strain can form with the same frequency as wild-type cells during spore germination, spores of both wild-type and *ftsA* in-frame strains were prepared as described in section 3.2.2 so that formation of the first Z ring could be analysed. Again, both strains showed the same results as the previous set of strains, with FtsA⁺ strain and wild-type strain behaving similar, but most importantly with *ftsA* in-frame deletion strain showing the same phenotypic behaviour and morphology as the *ftsA* null strain (Figure 3.4 and Figure 3.6; Table 3.2 and Table 3.3). This fully supports the idea that those first Z rings seen in outgrown spores of the *ftsA* null strain were not a product of abnormally high levels of FtsZ caused by the presence of the P_{spac} promoter upstream of *ftsZ* but a valid event in the absence of FtsA.

Table 3.3 Quantitative analysis of wild-type (SU5) and *ftsA* in-frame deletion (SU506) average cell lengths during spore outgrowth.^a

	120'		150'		180'		210'	
	WT	<i>ftsA</i> in-frame	WT	<i>ftsA</i> in-frame	WT	<i>ftsA</i> in-frame	WT	<i>ftsA</i> in-frame
Cell lengths	2.8	3.2	2.9	4.3	3.0	6.4	3.4	8.5
± SEM	0.07	0.07	0.07	0.13	0.06	0.20	0.07	0.19
% Z ring	64	67	73	75	65	69	68	70
Z ring/μm	0.23	0.21	0.23	0.16	0.21	0.11	0.18	0.08

^aSpores were germinated and outgrown in germination media (GMD) at 34°C. Values for cell lengths are presented as an average, SEM referring to its standard error of the mean.

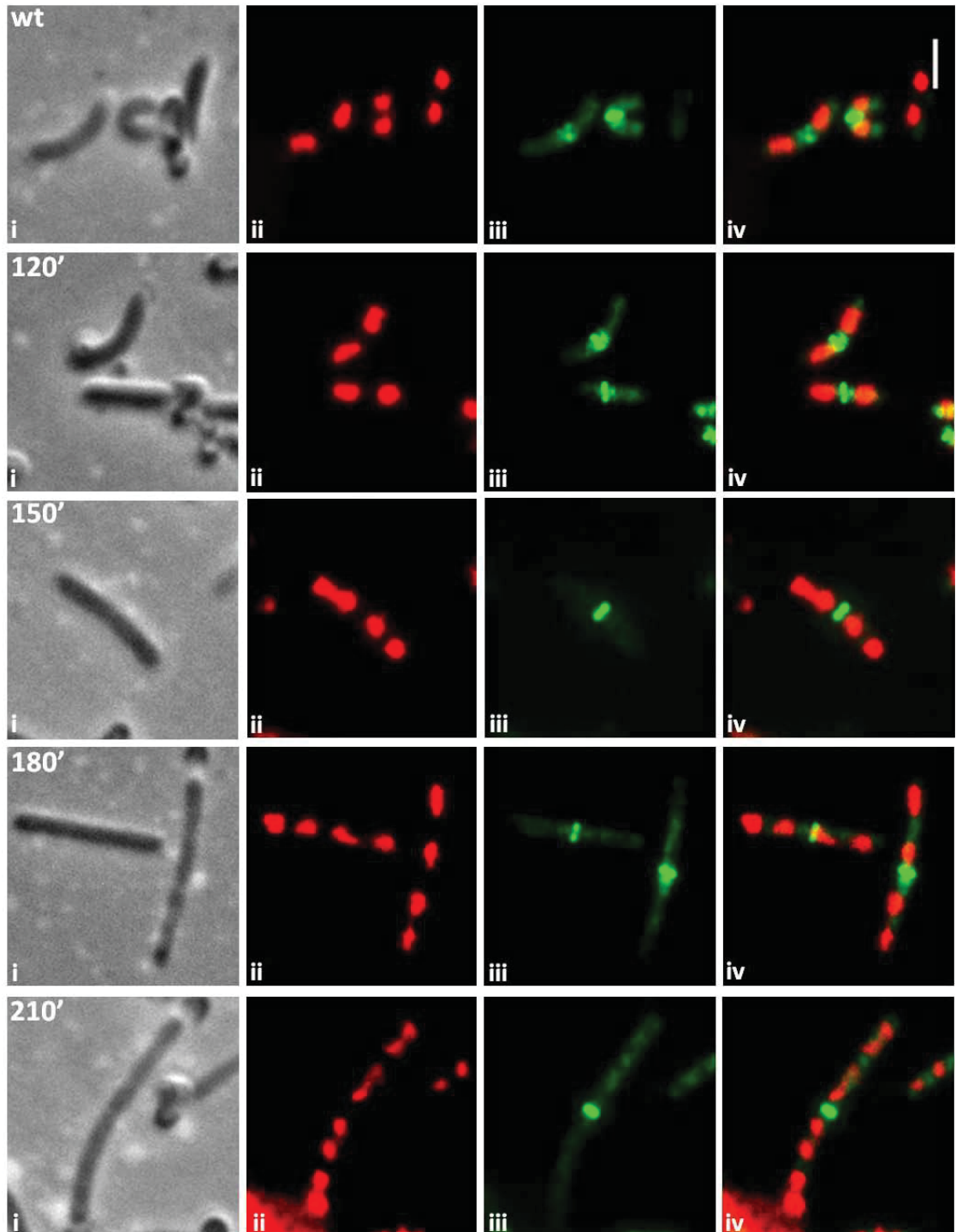


Figure 3.6 Z ring localisation in the absence of *FtsA* in outgrown spores. Wild-type (SU5) and *ftsA* in-frame deletion (SU506) spores were germinated in GMD medium, at 34°C. Samples were taken every 30 minutes and cells were immediately fixed with methanol and prepared for immunofluorescence microscopy. Nucleoids were stained with DAPI. Panels labelled i depict phase-contrast images, while those labelled ii and iii show the corresponding FtsZ (green) and nucleoid (red) localisation patterns, respectively. Panels designated iv depict an overlay of ii and iii. (WT) The wild-type control strain shows short dividing cells, with an average cell length of $2.8 \mu\text{m} \pm 0.07$ (SEM) (at 120 minutes after germination). All other images are referent to the *ftsA* in-frame deletion strain during sequential times of the spore outgrowth. These cells divide with lower frequency and continue to grow into long filaments. Scale bar represents $2 \mu\text{m}$ for all images.

3.2.4 Construction of *ftsA*-complementation strains (SU630 and SU631)

A common problem encountered when some genes are deleted from a bacterial genome is that the phenotype observed is not a direct consequence of the gene's absence, but is due to another genetic modification that suppresses this phenotype. In the present situation it is important to confirm that the phenotypes observed in the *ftsA*-deleted strains (SU457 and SU506) during vegetative growth and during spore outgrowth are solely due to the absence of the *ftsA* gene and not due to any suppressor mutations. A common method to confirm the veracity of such phenotypes is to introduce a copy of the gene at a location in the chromosome that is different to its original locus and determine if this rescues the mutant phenotype. This is known as complementation.

For this purpose, both *ftsA*-deletion strains (SU457 and SU506) were complemented, to confirm that both types of gene deletions could be complemented successfully. This resulted into two new strains, *ftsA* null complementation (SU630) and *ftsA* in-frame complementation (SU631). These *ftsA* complementation strains were constructed by firstly transforming competent cells of the wild-type strain (SU5) with chromosomal DNA of the strain FG718 (Tavares *et al.*, 2008), resulting in the insertion of P_{xyl} -*ftsA* through double homologous crossover at the *amyE* locus (Figure 3.1). This new strain (SU632; SU5 *amyE*:: P_{xyl} -*ftsA*) was then used to harbour the *ftsA* deletions, applying the same method as the construction of SU457 and SU506 (see sections 3.2.1 and 3.2.3 above). The resulting new *ftsA* complementation strains are SU630 (SU5 *ftsZ*:: P_{spac} -*ftsZ* *ftsA*::*cat* *amyE*:: P_{xyl} -*ftsA*) and SU631 (SU5 *ftsA*::*cat* in-frame *amyE*:: P_{xyl} -*ftsA*) respectively (Figure 3.1). It is important to identify that this last step (inserting *ftsA* deletions) was done in the presence of xylose to induce the P_{xyl} -*ftsA* promoter and ensure that the new clones would not undergo stress caused by the absence of FtsA.

3.2.5 Complementation of *ftsA* rescues cell division

Upon constructing both strains, SU630 (*ftsA* null complementation) and SU631 (*ftsA* in-frame complementation), a number of experiments were performed to confirm the proper induction and repression of the xylose-inducible promoter and examine the phenotypic effects.

3.2.5.1 *ftsA* null complementation strain (SU630)

The SU630 strain was initially characterised without any FtsA production to ensure that the *ftsA* null filamentous phenotype was still occurring. The xylose-inducible promoter should not be active if there is no xylose available. However, 0.5% glucose was used for complete promoter repression for two consecutive exponential phases of vegetative growth to ensure that all FtsA produced from the overnight culture would be completely depleted. The cells were also cultivated in the presence of 1mM IPTG for FtsZ production at wild-type levels. *ftsA* null complementation cells in which *ftsA* is being repressed had an average length of $16.03 \pm 0.75 \mu\text{m}$ (total of 132 cells were measured). This is shorter than the average cell length of the *ftsA* null strain of $24.5 \mu\text{m}$ (SU457; Table 3.1). However, the filamentous phenotype was still obtained showing successful repression of the xylose-promoter.

FtsA production was then induced in strain SU630. In this case, the presence of FtsA should restore normal cell division. The complementation of the *ftsA* null phenotype was achieved in vegetative growth in rich media PAB with 1mM IPTG by inducing FtsA production with 0.5% xylose at 37°C. *ftsA* complementation cells in which *ftsA* was induced had an average length of $5.9 \pm 0.10 \mu\text{m}$ (total of 234 cells were measured), showing that the parental phenotype (SU456) with a reported average cell length of $4.2 \mu\text{m}$ (Table 3.1) was rescued. The successful complementation of the *ftsA* deletion with FtsA demonstrates that the *ftsA* null phenotype observed previously was solely caused by the absence of FtsA, and that no additional mutations had occurred that interfere with the FtsA phenotype.

3.2.5.2 *ftsA* in-frame complementation strain (SU631)

This second *ftsA* complementation was made to confirm that cell division could also be rescued in the *ftsA* in-frame deletion strain. The SU631 strain was characterised in the same way as the previously described SU630 strain. However, in this strain there is no addition of IPTG since the *ftsZ* gene is under its native promoter. *ftsA* in-frame complementation cells in which *ftsA* is being repressed had an average length of $12.8 \pm 0.69 \mu\text{m}$ (total of 130 cells were measured). This result is somewhat shorter but still

similar to the previously determined average cell length of the *ftsA* in-frame deletion strain (SU506) of 16.8 μm (see table 3.1), showing that the filamentous phenotype was obtained also in this strain, showing successful repression of the xylose-promoter.

ftsA complementation cells in which *ftsA* is being induced were then analysed. These had an average length of $5.4 \pm 0.11 \mu\text{m}$ (total of 126 cells were measured) showing that cell division was fully rescued. As with the SU630 strain, the results obtained with this SU631 strain confirm that the filamentous phenotype could be complemented with FtsA thus validating the premise that the phenotypes of both the *ftsA* null and *ftsA* in-frame deletion strains are caused by the absence of FtsA.

3.2.6 Outgrowth spore system under FtsA-depletion conditions

As mentioned before, the absence of FtsA in *B. subtilis* cells not only creates important cell division defects during its vegetative cycle, but also creates a major inefficiency of the sporulation process. Using the previously described *ftsA*-deleted strains (*ftsA* null, SU457; and *ftsA* in-frame, SU506) it was possible to obtain spore preparations although in very low yields. Therefore, the construction of the *ftsA* complementation strains offered the opportunity to control the FtsA available in the cells and produce a high yield of spores without this complication. To obtain efficient production of spores, $P_{\text{xyI}}-ftsA$ is induced giving wild-type conditions for sporulation to occur. On the other hand, spore outgrowth studies are conducted with $P_{\text{xyI}}-ftsA$ repressed to completely deplete FtsA. These experiments were performed in both *ftsA* complementation strains, and again, both strains behaved in a similar manner. To avoid repetition, only the *ftsA* in-frame complementation strain (SU631) results are presented below.

3.2.6.1 Spore outgrowth of the *ftsA* in-frame complementation strain (SU631)

Spores of SU631 strain were prepared and germinated as described in Chapter 2, section 2.4. Spore germination and outgrowth was done in the presence of either 0.5% xylose (for *ftsA* induction) or 0.5% glucose (for *ftsA* repression) at 34°C, to promote wild-type

cell behaviour or *ftsA*-deletion behaviour, respectively. This resembles the previous results obtained for the non-complementation *ftsA* deletion strains (see Figure 3.4 and Figure 3.6). Samples were collected at 30 min intervals, after 120 minutes of incubation, for immunofluorescence microscopy (IFM) to visualise FtsZ. For each time point collected, around 100 outgrown cells were scored. At 120 minutes of incubation, the first Z rings were formed in the absence of FtsA. As expected, *ftsA* complementation spores, germinated with and without *ftsA* being expressed, and Z rings were present in the population at wild-type frequency (~80%) formed during the first cell cycle (see first and second row of images of Figure 3.7).

As observed for the non-complementing *ftsA* in-frame deletion strain (Figure 3.6), after the first Z rings have formed at midcell in the absence of FtsA, with the same efficiency and precision as in wild-type cells, they do not follow the same behaviour as wild-type. These Z rings, instead of constricting and allowing a septum formation, remained as midcell rings for at least 2 generations. Hence, the behaviour of the *ftsA* complementation spores germinated without FtsA is in accordance with what was previously reported for spore outgrowth of *ftsA*-deleted strains. Accordingly, there is an increase of nucleoids in the cells (see Figure 3.7 columns iii), where cell elongation and DNA replication continues at a normal rate, but division is almost absent and *ftsA*-repressed cells eventually become filamentous with only one Z ring present at midcell. Thus, while Z rings can form in the absence of FtsA, they persist for more than a cell cycle. These results confirm previous suggestions in the spore outgrowth studies in *ftsA* in-frame (SU506) and *ftsA* null (SU457) spores; that FtsA is not required for Z ring formation, during the first division cycle, but may play a role in Z ring constriction.

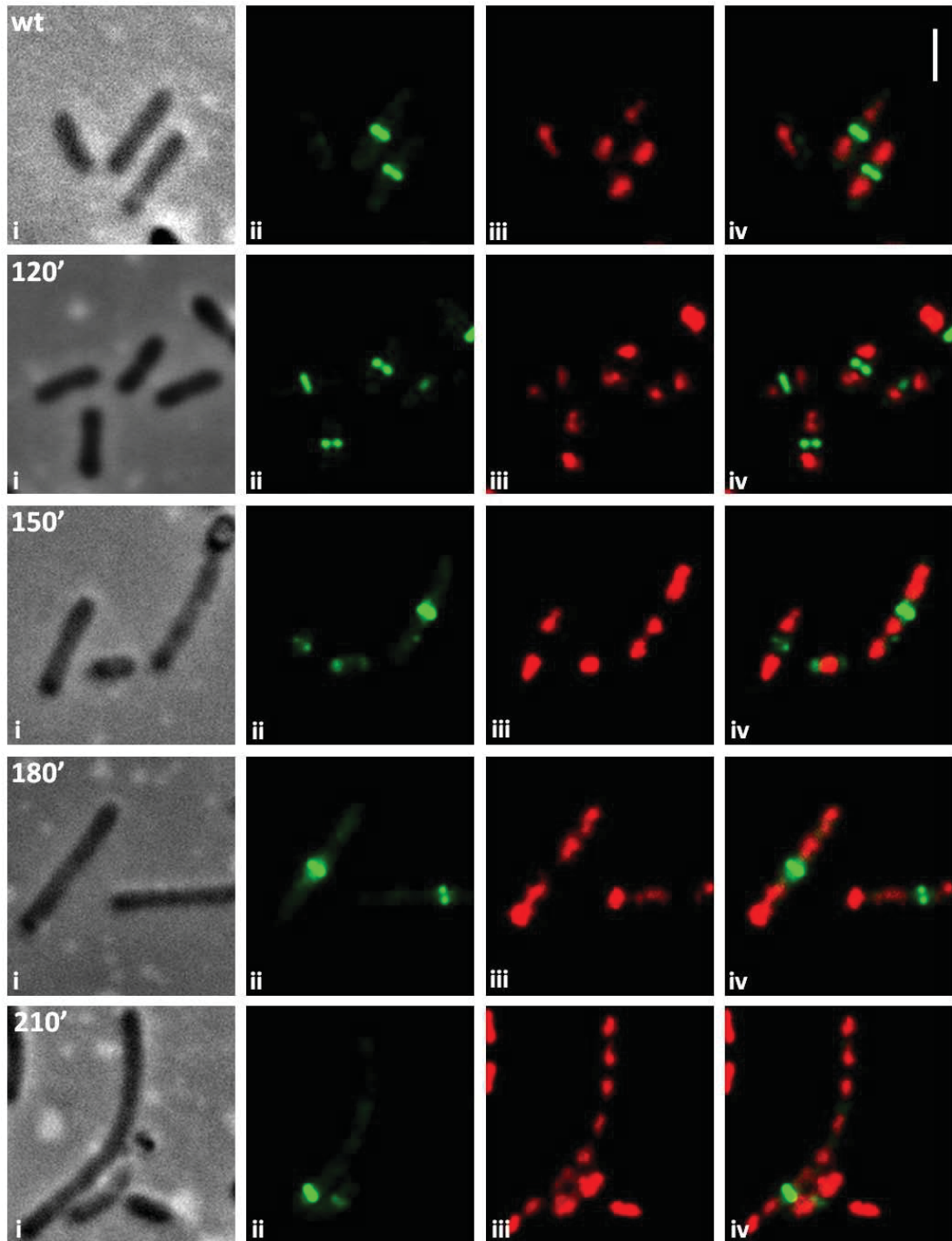


Figure 3.7 Z ring localisation in *ftsA* in-frame complementation (SU631) cells during spore outgrowth. Spores were germinated in GMD medium, in the presence and absence of *FtsA*, at 34°C. Samples were taken every 30 minutes and cells were immediately fixed with methanol and prepared for immunofluorescence microscopy (IFM). Nucleoids were stained with DAPI. Panels labelled i depict phase-contrast images, while those labelled ii and iii show the corresponding *FtsZ* (green) and nucleoid (red) localisation patterns, respectively. Panels designated iv depict an overlay of ii and iii. (wt) The first row of images shows the wild-type behaviour of when *ftsA* is induced, with short dividing cells, at 120 minutes after germination. The remaining rows of images report the sequential time points analysed of when *ftsA* is being repressed, and shows a progression of the filamentous phenotype caused by a defect in cell division. Scale bar represents 2 μm for all images.

3.2.7 The Z ring persists at midcell during transient FtsA depletion

The discovery that, during spore outgrowth, *ftsA* deletion mutants are able to assemble Z rings at the first division site with wild-type efficiency is a unique and clearly important finding. Further, when these same outgrown cells are analysed after many cell cycles during vegetative growth there is still just one Z ring in each cell (in the majority of the cases). The observations so far suggest that when FtsA is absent from the cells the Z rings are able to form normally, but they don't constrict. Furthermore, the defect in Z ring constriction appears to be preventing new Z rings from forming at potential division sites. Thus long cells with just one central Z ring are present, and this explains why after many generations, vegetatively-growing *ftsA*-deleted cells have very few Z rings.

To test this idea, the spore outgrowth was mimicked in vegetative cells by growing them up in the presence of FtsA and then transiently removing it. This was achieved using an *ftsA* complementation strain in which FtsA is induced during vegetative growth and then FtsA is depleted from the cells by repressing its production. For this purpose, *ftsA* null complementation cells (SU630) were grown with *ftsA* induction, in PAB media with 0.5% xylose and 1mM IPTG, until mid-exponential phase. At this point, the cell culture underwent repeated washes to remove all traces of xylose and the cells were then resuspended in fresh PAB media with 0.5% glucose and 1mM IPTG for complete repression of *ftsA* (for more details of the experimental procedures, see Chapter 2). The start of *ftsA* repression was considered the initial time of depletion (t_0) and samples were collected every 30 minutes for immunofluorescence microscopy (Figure 3.8). As a control to this experiment, the parental strain (SU456) was grown under the same conditions as those described above for SU630. The analysis of cell lengths and Z rings is presented in Table 3.4. When both conditions are compared, the results for *ftsA* repression during vegetative growth show a clear filamentous phenotype evolving with time. Initially (t_0), the cells appeared normal and Z ring frequency was similar to wild-type. Observation of the cells after 30 minutes of depletion showed the cells becoming longer, at which point the Z rings would normally be constricting for cell division to occur. However, 60 minutes after the start of *ftsA* repression, it becomes clear that the Z rings formed in the cells persist and do not constrict. The cells continue replicating their DNA (Figure 3.8 images $t_{60\text{iii}}$ and $t_{90\text{iii}}$) and cell elongation, eventually becoming

filamentous. The Z rings remained in the centre of the elongating cell, indicating a lack of constriction as seen with spore outgrowth. As expected the number of Z rings per μm during FtsA depletion decreases with time (see Table 3.4).

Table 3.4 Cell lengths and Z ring/ μm at several time points after FtsA depletion, during vegetative growth. Quantitative analysis of wild-type (parental strain, SU456) and *ftsA* null complementation (SU630) cell lengths (μm), with standard error of the mean values (SEM), for sequential time points after depletion of FtsA.

	t₀		t₃₀		t₆₀		t₉₀	
	wt	<i>ftsA</i>	wt	<i>ftsA</i>	wt	<i>ftsA</i>	wt	<i>ftsA</i>
Av. cell length	3.6	3.4	3.6	4.7	3.6	8.2	3.7	12.3
± SEM	0.05	0.08	0.04	0.35	0.05	0.46	0.06	0.74
% Z ring	75	68	71	79	72	78	70	85
Z ring/cell length	0.21	0.20	0.19	0.17	0.20	0.10	0.19	0.07

Finally, this experiment shows that when FtsA is depleted Z rings formed in the next cell cycle do not constrict (see cell lengths in Table 3.4 and microscopy images in Figure 3.8). Furthermore, the time-point observations with vegetative-growing cells are entirely consistent with the spore outgrowth experiments. This is consistent with the proposed hypothesis that FtsA is not required for Z ring formation during vegetative growth or spore outgrowth.

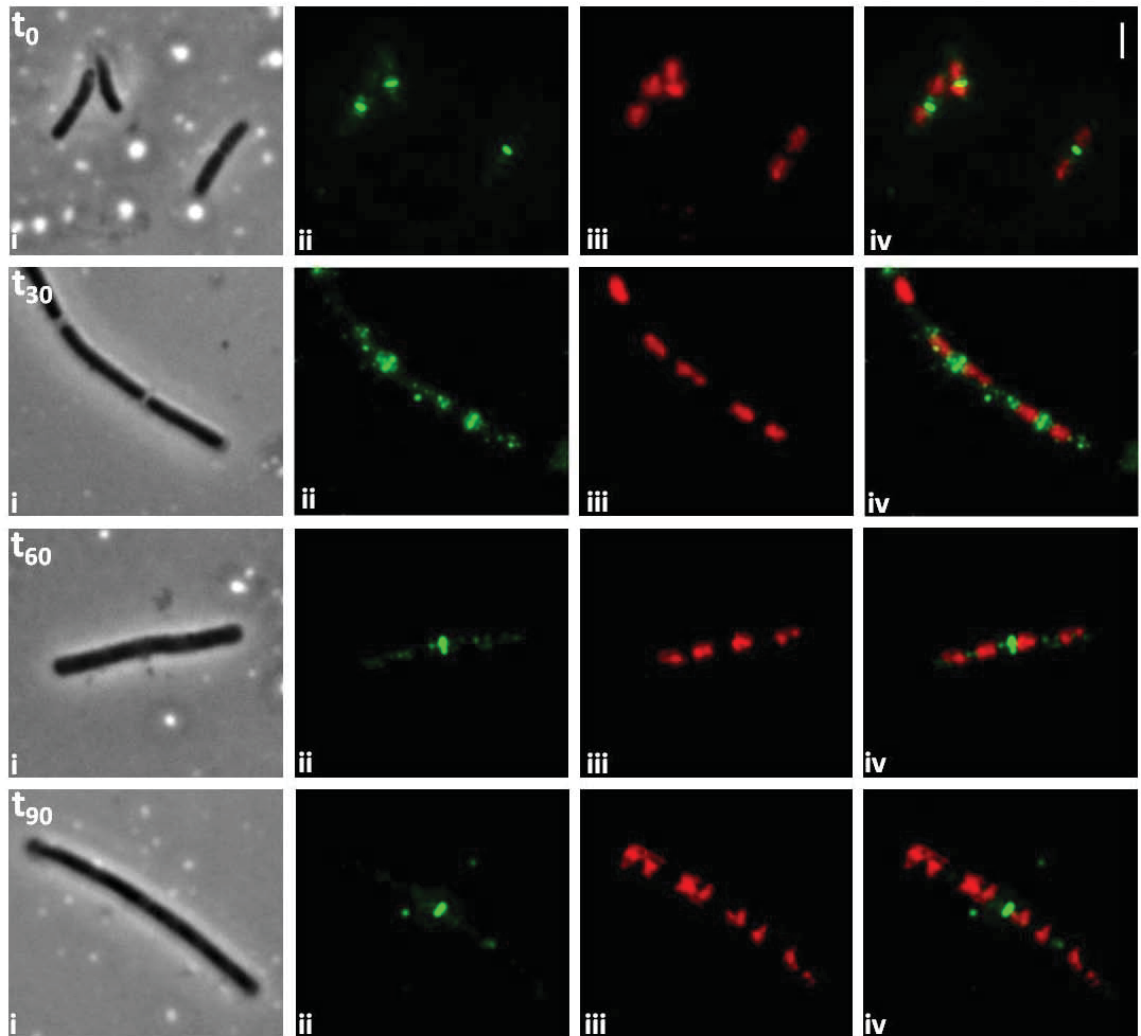


Figure 3.8 Z ring localisation in *ftsA* null complementation after depletion of FtsA. Cells were cultivated in PAB media with 1mM IPTG at 37°C, for vegetative growth. Samples were taken every 30 minutes and cells were immediately fixed with methanol and prepared for immunofluorescence microscopy (IFM). Nucleoids were stained with DAPI. Panels labelled i depict phase-contrast images, while those labelled ii and iii show the corresponding FtsZ (green) and nucleoid (red) localisation patterns, respectively. Panels designated iv depict an overlay of ii and iii. The first row of images shows the wild-type behaviour of when *ftsA* is induced, with short dividing cells. The remaining rows report the sequential time points analysed of when *ftsA* is being repressed and show a progression of the filamentous phenotype caused by a defect in cell division. Scale bar represents 2 μm for all images.

3.3 Discussion

The understanding of a protein function can be achieved by studying the phenotype of the cells in its absence. In the case of the *FtsA* protein, it is known that its absence in *B. subtilis* cells leads to a defect in cell division. The interesting aspect of this phenotype is that the cells become filamentous but only a few *Z* rings are present. This phenotype in the absence of *FtsA* was previously reported by Jensen *et al.* (2005) and became the starting point of this work.

It has been recently shown that *FtsZ* and *FtsA* associate prior to *Z* ring formation; and that, although it is possible to observe *FtsZ* localised throughout the *ftsA*-deleted filamentous cells, *Z* rings are drastically reduced during vegetative growth (Jensen *et al.*, 2005). In *E. coli*, it was also confirmed that there is a requirement for either *FtsA* or *ZipA* for tethering the *Z* ring to the cell membrane; and that *Z* ring is still formed in the presence of either protein, but *Z* ring formation is completely abolished (with cell death as result) when both *FtsA* and *ZipA* are absent (Pichoff and Lutkenhaus, 2002). The absence of *ZipA* in *B. subtilis* seems to leave the entire responsibility of *Z* ring formation and membrane-anchoring to *FtsA*.

In this chapter, an extensive analysis of *Z* ring formation in *ftsA*-deletion strains was carried out to study the observed low frequency of *Z* rings. Surprisingly, the reason for the lack of *Z* rings was due to an unpredicted cause. The *Z* rings were able to form normally and remained stable for some time. However, most of them were not able to constrict (see diagram in Figure 3.9). It was shown for the first time that *FtsA* is not required for *Z* ring assembly as previously suggested, but it seems instead to be required for its constriction.

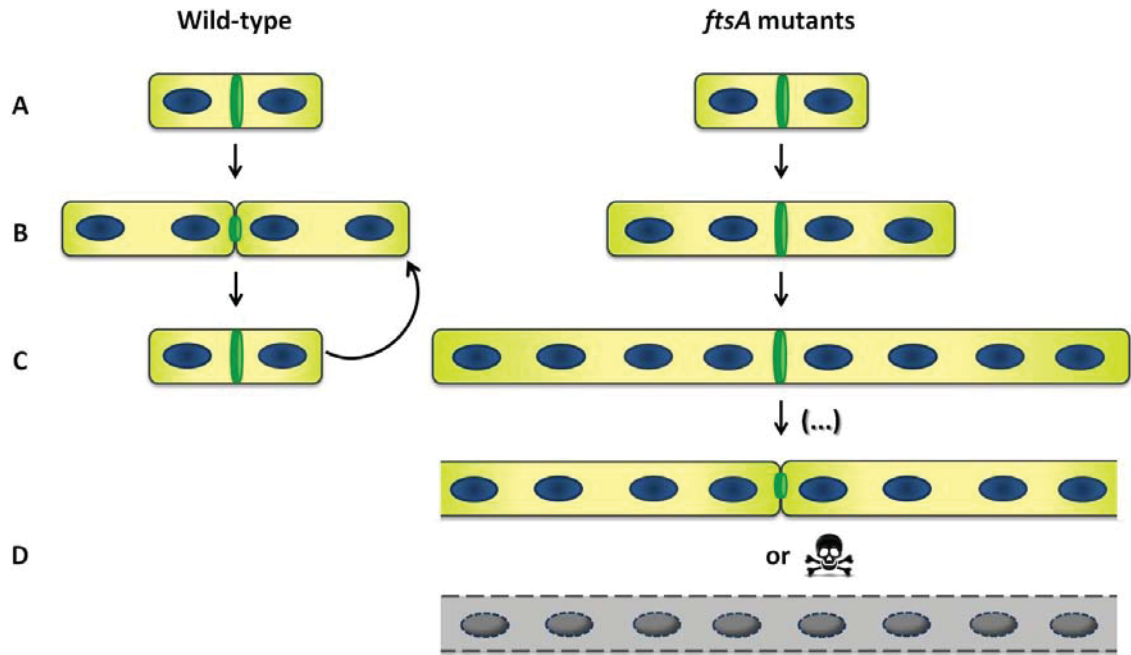


Figure 3.9 Z ring formation and constriction in wild-type and *ftsA* mutant *B. subtilis* cells. (A) The first Z ring (in green) is formed efficiently in both wild-type and *ftsA* mutant cells between two nucleoids (in dark blue). Z ring formation is not affected by the absence of FtsA. (B) Completion of the first cell cycle. In wild-type cells the Z ring constricts giving rise to two new daughter cells, while in *ftsA*-deleted cells the Z ring persists unconstricted at midcell. (C) In wild-type cells, the following cell cycles are a repetition of the previous ones (half-circle arrow), with each cell elongating, duplicating its DNA and dividing into two new daughter cells. In *ftsA* mutants, frequent cell division does not occur. The cell elongation and DNA replication processes continue normally, giving rise to longer cells. The filamentous phenotype becomes evident. (D) After several generations [(...) symbol], some cells eventually constrict, keeping the mutant viable, while others ultimately die (grey cell). The number of generations before a cell constricts its Z ring and divides, or dies, does not seem to be specific for the *ftsA* mutants.

During vegetative growth, there is an accumulation of events that occur during previous cell cycles making it difficult to study a single occurrence before a phenotype is established. In other words, if after several generations cells are observed to be filamentous, it is not known how this occurred. Such information is important in determining the cause of the phenotype and therefore the function of the gene whose absence gave rise to such a phenotype. Therefore in this work, the focus of the study was to investigate what happens to Z ring formation in the first cell cycle following the absence of FtsA. The spore outgrowth system was chosen for its special ability to present an isolated cell cycle. The first round of cell division following spore germination in *B. subtilis* was examined to study formation of the first Z rings in the absence of FtsA. Unexpectedly, the first Z rings formed with wild-type efficiency.

However, unlike wild-type cells that showed subsequent constriction of these *Z* rings leading to septum formation, in *ftsA*-deleted cells the *Z* rings did not constrict immediately and persisted into the second cycle of division.

Following these new findings with the spore outgrowth system, it was important to confirm three facts. Firstly, it needed to be demonstrated that the genetic constructs used, in which the *ftsZ* gene was not under control of its native promoters, were not the cause for the highly efficient formation of *Z* rings observed in spore outgrowth. To confirm this, an *ftsA* in-frame mutation was made, allowing *ftsZ* to be expressed normally. The results were the same. Secondly, it needed to be demonstrated that the efficient formation of the first *Z* ring formed in outgrown spores in the absence of FtsA was not a unique characteristic of the spore outgrowth system used in these studies (although this is valuable information in its own right). To confirm this, FtsA was transiently depleted in vegetatively-growing cells and the fate of *Z* rings monitored to confirm that the formation of the first *Z* rings was not a unique characteristic of the spore outgrowth system used in these studies. Furthermore, it validated the extremely valuable resource the spore outgrowth system can be in examining an isolated cell cycle. Thirdly, it needed to be demonstrated that the FtsA⁻ phenotypes observed during vegetative and spore outgrowth were only due to the absence of FtsA in the cells. To confirm this, the *ftsA* deletion strains were complemented with a copy of *ftsA* under an inducible-promoter at a non-essential locus, to rescue cell division and *Z* ring defects. The complementation experiments showed that when FtsA is restored to the cells, the wild-type phenotype is re-established.

3.3.1 Why doesn't the absence of FtsA cause complete cell division inhibition?

Previous work in *E. coli* (Pichoff and Lutkenhaus, 2005) suggests that FtsA is the main protein needed to tether the *Z* ring to the membrane because of its C-terminal amphipathic helix, essential for FtsA function; and because it is a widely conserved protein in bacteria. There are two main differences between *E. coli* and *B. subtilis* in this matter. In *E. coli*, FtsA is known to be essential to cell division and either FtsA or ZipA needs to be present for a normal *Z* ring formation (Pichoff and Lutkenhaus, 2002;

Pichoff and Lutkenhaus, 2005). In *B. subtilis* however, FtsA is not essential although there is no ZipA homolog (Beall and Lutkenhaus, 1992). The results shown in this chapter clearly demonstrate that in *B. subtilis* the Z rings are not only able to form in the absence of FtsA but seem to persist in the cell for several cell cycles. So, how are these Z rings being stabilised and maintaining attachment to the bacterial membrane in *B. subtilis*? A valid hypothesis could be that some other protein is assisting FtsA with this specific function, namely SepF or EzrA. This is discussed below.

SepF is a recently identified protein of the divisome complex that interacts with itself and FtsZ (Ishikawa *et al.*, 2006). SepF appears to be required for proper septum morphology (Hamoen *et al.*, 2006) suggesting a role in later stages of cell division. Also recently, it has been shown that SepF assembles into large rings that seem to regulate the arrangement of FtsZ filaments into the higher order structures necessary for correct synthesis of the septum (Gündoğdu *et al.*, 2011). According to Ishikawa *et al.* (2006), the over-expression of SepF in *B. subtilis* can rescue the *ftsA* mutant phenotype, restoring cell division. When both the proteins were absent, in an *ftsA sepF* double mutant, Z ring formation was abolished, leading to the consequential cell death. These results led the authors to propose that SepF shares a role with the early division protein FtsA, thus becoming important in the early stages of cell division. The present work has demonstrated that Z ring formation and stability are not affected in the absence of FtsA, going against the complementary function of SepF and FtsA proposed by Ishikawa *et al.* (2006). However, it is not known if the Z rings observed in their work did not form in the first place or they did but subsequently disassembled and disappeared, like FtsA⁻ cells observed here, resulting in filamentous cells unable to divide. Consequentially, an interesting question arises: does the first Z ring form with wild-type efficiency in outgrown spores of the *ftsA sepF* double mutant? Applying the same methodology as presented early in this chapter's results section (section 3.2.2), could answer whether Z ring formation can occur in the absence of these two proteins, FtsA and SepF. If Z rings were able to form in the first cell cycle, SepF would not have a role in their formation. However, because no Z rings are observed during vegetative growth, it could be assumed that SepF would be involved in the fate of the normally-formed Z rings. If it was found that the first Z rings failed to form in outgrown spores in the absence of SepF and FtsA, this would strongly suggest that SepF has a role in Z ring formation and even perhaps its stability. Since SepF doesn't appear to be membrane-bound, it would be

expected no changes in Z ring formation in its absence, excluding SepF of performing a Z ring-tethering function.

As an alternative to SepF, EzrA, a membrane-anchored protein, could also be assisting in Z ring formation. EzrA is a regulator of Z ring assembly and dynamics (Levin *et al.*, 1999). It achieves this regulation by interacting directly with FtsZ proteins at the membrane and preventing polymerisation and aberrant Z ring formation. Although this specific function of EzrA is to stop Z ring formation, it is targeted mainly at the poles and other non-midcell positions. It also acts by sustaining the dynamics of midcell Z rings by destabilising FtsZ assembly at midcell (Haeusser *et al.*, 2004). It is known that EzrA has a negative effect on Z ring assembly, making its role as positive modulator of Z ring attachment to the membrane not intuitive. However, EzrA is a transmembrane protein with topology similar to ZipA (Levin *et al.*, 1999; Mosyak *et al.*, 2000), which is known to tether the Z ring to the membrane in the lack of FtsA in *E. coli* (Pichoff and Lutkenhaus, 2002). Also, like FtsA, EzrA interacts with the C-terminal end of FtsZ (Singh *et al.*, 2007), which suggests competition between positive and negative regulators that share the same binding site. These common characteristics support the possibility of EzrA having a role in anchoring Z rings to the membrane, helping cell division to occur when it is impaired by the absence of other membrane-anchoring proteins (such as FtsA). One follow-up experiment would be to analyse an *ftsA ezrA* double mutant. Ishikawa *et al.* (2006) have shown that this double mutation is not lethal to *B. subtilis* cells, although they have stated that it caused cell filamentation (no images provided). It seems that EzrA is not essential for playing this Z ring-anchoring role in *ftsA*-deleted cells. However, a relevant future study would be to determine if the *ftsA ezrA* double mutant vegetative cells present some or all Z rings at the division sites. Also, would the first Z rings still be able to form in outgrown spores of this double mutant? This information would more clearly identify the role EzrA plays in Z ring formation, stability and constriction. The analysis of SepF and EzrA as possible factors responsible for the tethering of the Z ring to the membrane, disclosed a *sepF ezrA* double mutant in *B. subtilis* (Hamoen *et al.*, 2006). Interestingly, this double mutant is synthetically lethal, but despite that, the Z rings are still formed and the later stages of division are affected. Taking into account the results presented in this chapter regarding the non-requirement for FtsA for Z ring formation and the work done by Hamoen *et al.* (2006), it seems plausible that none of these three proteins (FtsA, SepF and EzrA) are

fundamental for tethering the Z ring to the membrane. Alternatively, could it be possible that FtsZ is tethering itself to the membrane? A recent review by Erickson *et al.* (2010) considers this to be a likely possibility. They suggest that because the C-terminal peptide of FtsZ is quite conserved among bacteria, including those that do not having a candidate binding protein, it might be able to bind the membranes even though it does not present an amphipathic helix. Whether this is true or not it would be an exciting thought to follow up. One experimental suggestion could be to use techniques as fluorescence resonance energy transfer (FRET) or atomic force microscopy (AFM) to detect possible protein-lipid interactions, as FtsZ and the cell membrane.

3.3.2 The function of FtsA in later stages of cell division?

After observing that the first Z rings were able to form efficiently in *B. subtilis* outgrown spores in the absence of FtsA, the follow-up analysis showed that the Z rings seem to persist in the cells for several cell cycles with a low frequency of constriction. These results suggest a role for FtsA in Z ring constriction, contrasting with the previously suggested role for FtsA in Z ring formation in this organism (Jensen *et al.*, 2005). According to the literature, in *E. coli* FtsA takes on different roles throughout the various stages of cell division. Specifically, FtsA is involved in Z ring assembly and stability, recruitment of downstream proteins, and Z ring constriction (Geissler *et al.*, 2003; Corbin *et al.*, 2004; Rico *et al.*, 2004; Geissler and Margolin, 2005; Goehring *et al.*, 2005; Pichoff and Lutkenhaus, 2005; Shiomi and Margoli, 2007; Pichoff and Lutkenhaus, 2007). As previously mentioned, FtsA shares the important function of Z ring tethering and assembly to midcell in *E. coli*. In its absence, although Z rings still form, cell division is impaired. This seems to suggest a later role for FtsA in Z ring constriction. In support of this idea, work done by Goehring *et al.* (2005) shows that the premature targeting of cell division proteins to the Z ring in an *E. coli ftsA* mutant does not rescue cell division. This was done by bypassing the requirement of FtsA for FtsQ localisation to the division site. Given this information, the results of this chapter clearly reveal that *B. subtilis* FtsA has more in common with *E. coli* FtsA than previously thought. It is shown for the first time that FtsA is not required for Z ring assembly in *B. subtilis* and that the main defect appears to be in a later stage of constriction. Feucht *et*

al. (2001) also favour this role for FtsA in *B. subtilis* cell division with their cytological and biochemical characterisation of the protein. They have shown that FtsA is present in *B. subtilis* at a constant ratio of 1:5 with FtsZ; that is a sufficient quantity to assemble into a complete ring. This characteristic, together with a membrane targeting sequence and homology to the structural protein actin, suggests a direct structural role for FtsA in cell division. They have also demonstrated that *B. subtilis* FtsA is able to bind and hydrolyse ATP. This could be required for enhancing *Z* ring dynamics and together with GTP hydrolysis, by FtsZ, could also be important for efficient *Z* ring constriction (more details in Chapter 5).

At this point, despite considering the strong possibility that the *ftsA* mutant phenotype is due to a defect in *Z* ring constriction, it is important to understand exactly what is happening to the *Z* rings that are formed and persist in the cells. It is also fundamental to determine what other checkpoints are being affected during cell division in the absence of FtsA. Are the later division proteins still being assembled at midcell? The next chapter will answer these questions and bring new important information to the subject.

Chapter 4

§

*DivIB recruitment and septum formation in
the absence of FtsA*

4.1 Introduction

The novel results presented in the previous chapter inevitably lead to new and exciting questions regarding the roles for *FtsA* in *B. subtilis* cell division. Fundamentally, the new data has shown that the absence of *FtsA* in the cells does not affect *Z* ring formation. Importantly, those efficiently-formed *Z* rings showed a very low frequency of constriction, implying that the primary role for *FtsA* is not in *Z* ring formation but during the later stages of cell division. *FtsA* plays multiple roles in *E. coli* (reviews: Errington, 2003; Harry *et al.*, 2006; Adams and Errington, 2009; de Boer, 2010), with the main function being attributed to promoting *Z* ring formation and its stability, by anchoring it to the membrane. This was also assumed to be the role for *FtsA* in *B. subtilis*. However, the results in Chapter 3 demonstrated that this is not the case, with *Z* ring formation occurring efficiently in the absence of *FtsA* in this organism. Another event of *E. coli* cell division that seems to require *FtsA* is the recruitment of several downstream division proteins, namely the recruitment of *FtsK* and consequentially the later cell division proteins, *FtsQ*, *FtsL*, *FtsB*, *FtsI*, and *FtsN* to the division site (Pichoff and Lutkenhaus, 2002; Buddelmeijer and Beckwith, 2004; Corbin *et al.*, 2004; Rico *et al.*, 2004). It has been strongly suggested that *FtsA* is also recruiting the later division proteins (members of the divisome) to the *Z* ring in *B. subtilis* cells, although no experimental data is available regarding the dependency on *FtsA* for localisation of the later division proteins (Errington *et al.*, 2003).

After *Z* ring and the early division proteins, such as *FtsA*, have assembled at midcell, the later division proteins localise together at the division site, forming the divisome (Goehring and Beckwith, 2005; Harry *et al.*, 2006). Importantly, at least some of these later division proteins, including *FtsQ*, *FtsL*, and *FtsB*, in *E. coli*; and *DivIB*, *FtsL* and *DivIC*, in *B. subtilis*, are thought to be interdependent for recruitment, forming a stable pre-complex before localising to the division site (Errington, 2003; Buddelmeijer and Beckwith, 2004; Karimova *et al.*, 2005; Gamba *et al.*, 2009). Taking into account this interconnectivity between the late division proteins, and *DivIB* is thought to be a chaperone to other proteins (Harry *et al.*, 1993; Rowland *et al.*, 1997; Sanchez-Pullido *et al.*, 2003), *DivIB* was chosen in this work as a marker for divisome assembly.

4.1.1 Chapter Aims

The aim of the work in this chapter was to determine whether *FtsA* has a function in the recruitment of later-assembling divisome proteins in *B. subtilis*. *DivIB* protein was used as a reference for the assembly of these proteins, and the efficiency and timing of its recruitment in the absence of *FtsA* was analysed. The spore outgrowth system was again chosen to perform these experiments as it offers the ability to easily determine the timing of events through one cell cycle without the complication of previous divisions. The results obtained show that localisation of *DivIB*, and presumably the other later-assembly proteins to the midcell site, occurs with wild-type efficiency in the absence of *FtsA*. This confirms previous suggestions in *E. coli* (Goehring *et al.*, 2005), that *FtsA* is not essential for localisation of *DivIB* (i.e. the divisome). However, it was observed that this localisation was delayed, suggesting that *FtsA* is required for the correct timing of *DivIB* (and other proteins) recruitment. It was also shown that despite the normal efficiency of recruitment of *DivIB*, and presumably the other later-assembling division proteins, the frequency of septum formation was significantly reduced in the absence of *FtsA*, suggesting that *FtsA* is essential in *B. subtilis* for efficient septum formation after divisome assembly.

4.2 Results

Following the main findings of Chapter 3, it was imperative to determine what happens after *Z* ring assembly in cells lacking *FtsA*. It has been suggested that, in *B. subtilis* and in *E. coli*, *FtsA* plays a role in the recruitment of later-assembling division proteins to the *Z* ring (Ghigo *et al.*, 1999; Feucht *et al.*, 2001; Pichoff and Lutkenhaus, 2002; Errington *et al.*, 2003; Corbin *et al.*, 2004; Rico *et al.*, 2004). Therefore the recruitment and localisation of *DivIB*, as a representative of these divisome proteins, was examined in the absence of *FtsA* to establish if this event is the reason for the delay in *Z* ring constriction in *ftsA*-deleted cells.

4.2.1 Construction of GFP-DivIB fusion strains

To determine if the later-assembling divisome proteins are still being recruited to the Z ring in the absence of *FtsA*, the genetic construct, P_{spac} -*gfp-divIB*, available from Gonalo Real was used (AH3580 strain; Table 2.2). A new strain was constructed with *gfp-divIB* being expressed in the *ftsA* in-frame complementation strain background, SU636 (*ftsA::cat* in-frame *amyE::P_{xyl}-ftsA* *thrC::P_{spac}-gfp-divIB*; Table 2.2). It is important to mention that, although this fusion has been shown to be fully functional, the native *divIB* gene is still being expressed in these cells (non-published work by Gonalo Real). This is because attempts to knock out the native *DivIB* gene whilst expressing wild-type levels of *gfp-divIB* in an *ftsA*-deletion background resulted in a rescue of cell division and loss of the *ftsA* deletion filamentous phenotype. The reason for this is not very clear, although it is possible that the GFP tag on DivIB could alter the structure of the assembled divisome in some way and partially complement the lack of *FtsA* in the division process. While this is interesting in itself, the major focus was to determine whether DivIB could localise properly at midcell in the absence of *FtsA*. So the native *divIB* gene was kept intact and the *gfp-divIB* fusion was weakly expressed, using as little inducer as possible just to enable visualisation of DivIB by decorating it minimally with GFP-DivIB. The *gfp-divIB* expression was controlled by an inducible promoter, P_{spac} , at the non-essential *thrC* locus for visualisation with live cell microscopy. A control strain was also constructed by inserting *thrC::P_{spac}-gfp-divIB* into the wild-type (SU5) background. This control strain, named SU633, served to determine if the small level of GFP-DivIB production caused any changes to growth or cell division on its own.

4.2.2 Characterisation of GFP-DivIB fusion strains

Both the *gfp-divIB* strain and *gfp-divIB* *ftsA*-depleted strain (SU633 and SU636, respectively) were initially characterised during vegetative growth. The cells were grown in PAB (Chapter 2, Table 2.3) to mid-exponential phase at 34°C, which was found to be the functional optimal temperature the protein fusion, as reported by Gonalo Real (non-published). Cells were then prepared for live-cell microscopy (details in Chapter 2, section 2.6.2). 0.1 mM IPTG (inducer of the P_{spac} promoter) was

added to induce *gfp-divIB* expression and xylose or glucose (inducer and repressor of the P_{xyl} promoter, respectively) were used to control *ftsA* expression. At least 100 cells were analysed for each condition for the both strains, SU633 and SU636.

For SU633 (P_{spac} -*gfp-divIB*), in the absence of IPTG, there was no observable fluorescence in the cells which leads to the conclusion that expression of *gfp-divIB* from the P_{spac} promoter was being significantly repressed (data not shown). Under these conditions, cells had an average length of $5.9 \pm 0.16 \mu\text{m}$, which is slightly but not statistically significantly longer than wild-type cells ($5.1 \pm 0.07 \mu\text{m}$; Table 4.1). In the presence of 0.1mM of IPTG, the GFP-DivIB fusion protein in SU633 cells was observed as a fluorescent band at midcell (Figure 4.1, image Aii), demonstrating that P_{spac} -*gfp-divIB* was being induced and the protein product localising correctly. These cells had an average length essentially the same as that of the uninduced SU633 cells ($6.1 \pm 0.15 \mu\text{m}$) showing that the presence of the fusion protein was not altering the frequency of cell division.

For SU636 (P_{xyl} -*ftsA* P_{spac} -*gfp-divIB*), regardless of the addition or not of xylose for *ftsA* induction, the absence of IPTG also resulted in no observable fluorescence as seen in SU633 cells (data not shown). SU636 cells had an average length of $6.4 \pm 0.14 \mu\text{m}$ in the presence of xylose, reporting a similar phenotype as the SU633 (P_{spac} -*gfp-divIB*) control strain; whilst the presence of glucose successfully repressed the P_{xyl} -*ftsA* promoter and cells became filamentous, as expected, with an average cell length of $17.5 \pm 0.76 \mu\text{m}$ (Table 4.1). Importantly, when both native DivIB and fusion GFP-DivIB are present in the cells, there is no rescue of the *ftsA*-deleted phenotype, availing the use of this fluorescence fusion.

As shown in Figure 4.1B and C, the induction of P_{spac} -*gfp-divIB* in SU636 (P_{xyl} -*ftsA* P_{spac} -*gfp-divIB*) cells was successful and fluorescent bands were seen at midcell indicating the localisation of DivIB. Also there was no discernable effect on the *ftsA* complementation phenotype with the expression of GFP-DivIB. In the presence of xylose, the average cell length was of $6.7 \pm 0.13 \mu\text{m}$, comparable to the control conditions; while in the presence of glucose the *ftsA* mutant phenotype was observed with cells having an average length of $17.9 \pm 0.68 \mu\text{m}$ (Table 4.1).

Table 4.1 Average cell lengths of SU633 (*gfp-divIB*) and SU636 (*gfp-divIB ftsA* compl.) strains.^a

Media supplements	Strains	Average cell length ($\mu\text{m} \pm \text{SEM}$)
no IPTG	SU633 ($P_{\text{spac}}\text{-gfp-divIB}$)	5.9 ± 0.16
no IPTG; 0.5% xylose	SU636 ($P_{\text{xyI}}\text{-ftsA } P_{\text{spac}}\text{-gfp-divIB}$)	6.4 ± 0.14
no IPTG; 0.5% glucose	SU636 ($P_{\text{xyI}}\text{-ftsA } P_{\text{spac}}\text{-gfp-divIB}$)	17.5 ± 0.76
0.1mM IPTG	SU633 ($P_{\text{spac}}\text{-gfp-divIB}$)	6.1 ± 0.15
0.1mM IPTG; 0.5% xylose	SU636 ($P_{\text{xyI}}\text{-ftsA } P_{\text{spac}}\text{-gfp-divIB}$)	6.7 ± 0.13
0.1mM IPTG; 0.5% glucose	SU636 ($P_{\text{xyI}}\text{-ftsA } P_{\text{spac}}\text{-gfp-divIB}$)	17.9 ± 0.68

^aCultures were grown in PAB to mid-exponential phase at 34°C. SEM refers to standard error of the mean.

There are a few important remarks to make from the characterisation of these strains. Firstly, the *gfp-divIB* construct did not cause any observable changes to the filamentous phenotype of an *ftsA*-deleted strain (Table 4.1 and Figure 4.1). Secondly, the localisation of GFP-DivIB in SU633 and SU636 strains, in the presence of xylose, seems to be correctly positioned at midcell, as expected for DivIB. Finally, and by far most importantly, these experiments suggest that when FtsA is absent (SU636 strain in the presence of glucose), DivIB is still being recruited to the division site (Figure 4.1 C ii). Some degree of localisation to the existent Z rings in the *ftsA*-deleted strain was expected because there is still some cell division occurring and divisome assembly is essential for that. Employing the data from the above experiment, using the *gfp-divIB ftsA* complementation strain, SU636, it was determined that there is an average of 0.17 DivIB localisations/ μm in *ftsA*-induced vegetatively growing cells. In contrast, in *ftsA*-repressed cells the DivIB localisation diminishes to an average of 0.05 bands/ μm . These values are in fact similar to the number of Z rings per cell length (in μm) seen in the same background (*ftsA* in-frame complementation strain, SU631); with an average of 0.20 Z rings/ μm in the presence of FtsA, and an average of only 0.05 Z rings/ μm in the absence of FtsA. These results suggest that DivIB appears to be recruited to all Z rings that form in the absence of FtsA, suggesting that FtsA does not appear to be required for the efficient recruitment of DivIB to Z rings.

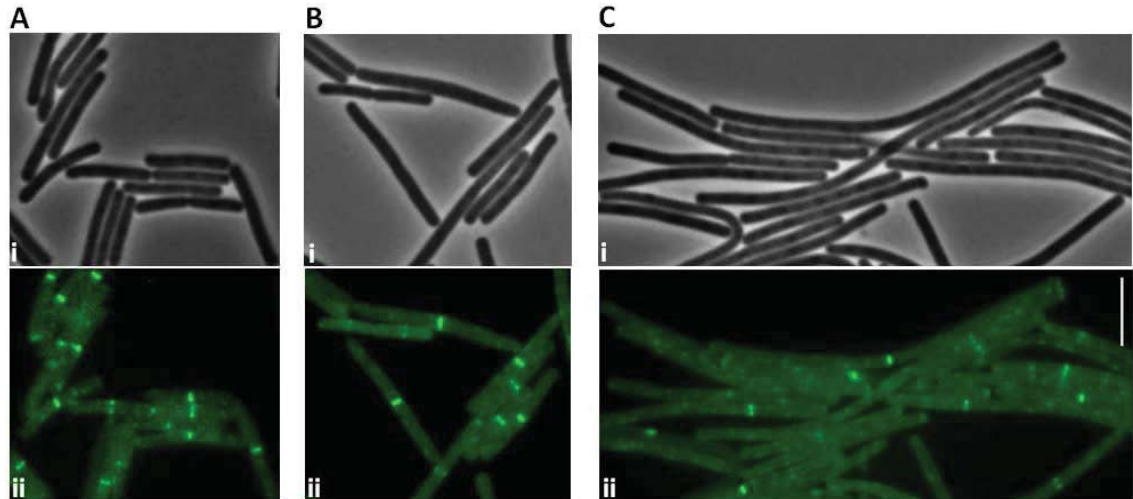


Figure 4.1 GFP-DivIB localisation visualised by live cell microscopy. *gfp-divIB* (SU633) and *gfp-divIB ftsA* complementation (SU636) vegetative cells were grown in PAB in the presence of 0.1mM IPTG. Panels labelled i depict phase-contrast images, whilst those labelled ii show DivIB localisation (green) as a midcell band. **(A)** Control strain harbouring *gfp-divIB*, SU633. **(B)** *gfp-divIB ftsA* complementation strain, SU636, in the presence of 0.5% xylose. **(C)** *gfp-divIB ftsA* complementation strain, SU636, in the presence of 0.5% glucose. Scale bar represents 5 μm for all images.

4.2.3 Recruitment and localisation of *DivIB* in the absence of *FtsA*

In order to confirm the above statement, it was necessary to measure DivIB recruitment when there is a higher frequency of Z rings in the population, as seen in outgrown spores. The key question at this point is if the delay in Z ring constriction is due to a delay in recruitment of downstream divisome components. To assess this, the spore outgrowth system was used. Spores of strain SU636 (*gfp-divIB ftsA* in-frame complementation) were prepared as described in Chapter 2, section 2.4, then germinated in GMD media (Chapter 2, Table 2.3) containing 0.1 mM IPTG (for *gfp-divIB* induction) and either 0.5% xylose (for *ftsA* induction) or 0.5% glucose (for *ftsA* repression) at 34°C. During spore outgrowth, samples were collected at 30 minute intervals starting at 3 hours after the onset of germination (at 180, 210 and 240 minutes) for live cell microscopy (see Chapter 2, section 2.6.2). Around 200 outgrown cells were scored and measured per sample. In outgrown spores of the *ftsA*-deleted complementation strain (SU631), Z rings usually start forming 120 minutes after germination, at an average cell length of $2.9 \pm 0.06 \mu\text{m}$. However, spores from different strains can germinate with different rates. In the case of strain SU636 (*ftsA* in-frame

complementation with *gfp-divIB*), the cells had an average cell length of $2.5 \pm 0.04 \mu\text{m}$ at 150 minutes, and $3.2 \pm 0.06 \mu\text{m}$ at 180 minutes when GFP-DivIB was first visualised.

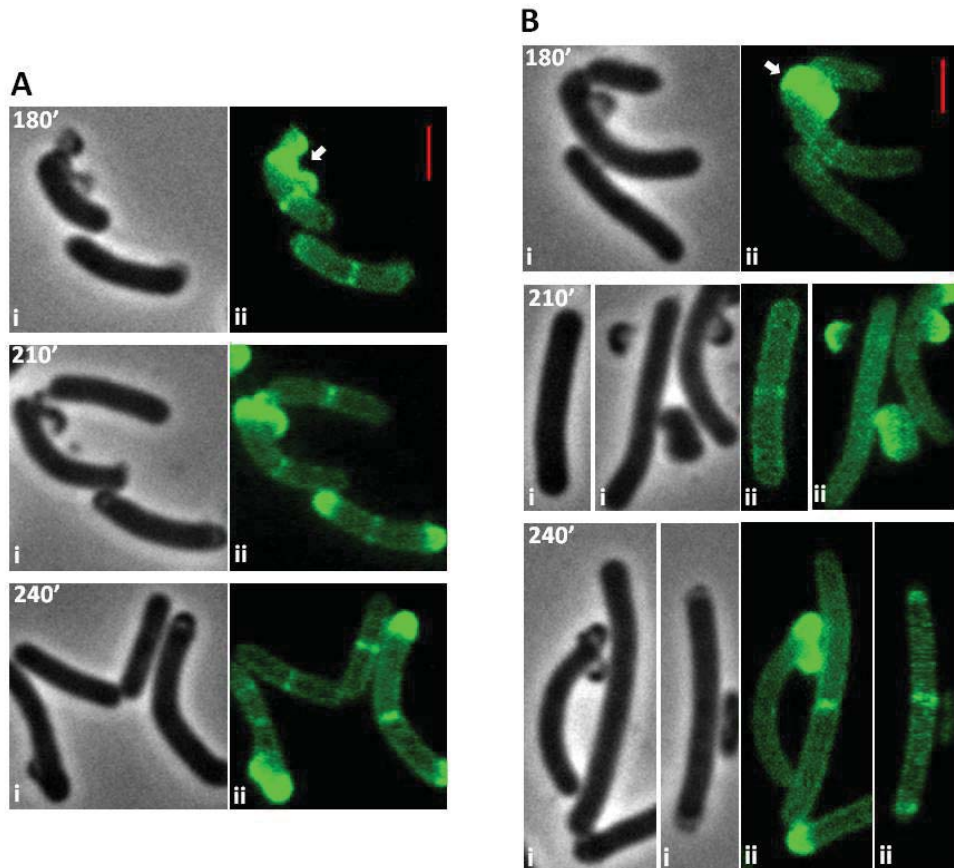


Figure 4.2 GFP-DivIB localisation in SU636 outgrown spores. *gfp-divIB ftsA* complementation spores (SU636) were germinated in GMD media at 34°C with 0.5% xylose for *ftsA* induction or 0.5% glucose for *ftsA* repression. Samples were taken every 30 minutes and cells were prepared on agarose pads for live cell microscopy. Panels labelled i depict phase-contrast images, whilst those labelled ii show DivIB (green) localisation as a midcell band. **(A)** *ftsA* induction conditions showing short dividing cells. **(B)** *ftsA* repression conditions showing progressively longer cells caused by a defect in cell division. These cells divide with lower frequency, so continue to grow into long filaments. Frequency of DivIB localisation in these cells is presented in Table 4.2. White arrows point to auto-fluorescent spore coats. Red scale bar represents 2 μm for all images.

Analysing the cells under *ftsA*-induced conditions, which are seen as the control experiment in this situation, DivIB localisation can be observed at the division site in a similar pattern as the Z ring (Figure 4.2 A). At 180 minutes of *ftsA*-induced outgrowth, 43% of the cells have DivIB localised at midcell. A constant proportion of the population with a GFP-DivIB fluorescent signal was detected at all time points

throughout the experiment when *FtsA* was induced (Table 4.2). As reported in Table 4.2, at 180 minutes of *ftsA*-repressed outgrowth, only 17% of the cells presented *DivIB* at midcell. However, at later times the fluorescent signal increases reaching 24% of the cell population at 210 minutes and 37% at 240 minutes. As shown above, when *FtsA* is produced, *DivIB* band frequency is 43%. This data shows that *DivIB* localisation at midcell is similar at the later time points suggesting that it becomes as efficient as wild-type. These data indicate that in the absence of *FtsA*, *DivIB* is recruited to midcell with wild-type efficiency although its recruitment is delayed.

Table 4.2 Frequency of *DivIB* localisation and septum formation in *gfp-divIB ftsA* complementation strain (SU636).^a

	<i>ftsA</i> induction		<i>ftsA</i> repression	
	<i>DivIB</i>	Septum	<i>DivIB</i>	Septum
180 min	43 %	8 %	17 %	0 %
210 min	42 %	30 %	24 %	3 %
240 min	44 %	32 %	37 %	6 %

^aCells were analysed during *ftsA* induction and repression for sequential periods of spore outgrowth. 200 outgrown cells were scored and measured per sample.

Although one of the reasons for using the spore outgrowth system is for its synchronicity, the times of sample collection do not necessarily mean that all cell cultures are at the same stage of the cell cycle. Therefore, to more accurately analyse the delay in protein recruitment in terms of the cell cycle, a comparison of the length of cells that exhibit GFP-*DivIB* at midcell both in the presence and absence of *FtsA* is required. This type of analysis is not possible with *ftsA*-deleted filamentous cells undergoing vegetative growth but is possible with the germinated spore system of *B. subtilis*. The cell length data presented in section 4.2.3 was therefore grouped into just two populations: *ftsA*-induced cells and *ftsA*-repressed cells, irrespective of the time at which each sample was collected. This data was then plotted as a distribution frequency graph (Figure 4.3, Panel A), with the frequency of *DivIB* localisation *versus* the cell length at which this localisation occurred. The graph clearly demonstrates that when *DivIB*

localisation occurs in the absence of *FtsA*, the cells are longer. In fact, the cells are on average 2.7µm longer (average cell length of 3.7 ± 0.03 µm and 6.4 ± 0.10 µm, in the presence and absence of *FtsA*, respectively) (Figure 4.3, Panel B). Employing the KS-test for statistical analysis, it was confirmed that the cell length distribution was significantly different ($P < 10^{-5}$) between the two situations, indicating that the cells are in a significantly later stage in the cell cycle when *DivIB* is recruited to the Z ring in the absence of *FtsA*. Furthermore, the frequency of cell lengths revealed a wider distribution in *ftsA*-depleted cell lengths when compared to the *ftsA*-induced cells. The small standard error of the mean for cell length of *ftsA*-induced cell (0.03; Figure 4.3, Panel B) shows that *DivIB* localisation occurs at a specific cell length and therefore, at an accurate time during the cell cycle. However, the wider distribution of cell lengths for *DivIB* localisation in *ftsA*-repressed cells (SEM of 0.10; Figure 4.3, Panel B) shows that this localisation occurs at different and mostly later times during the cell cycle.

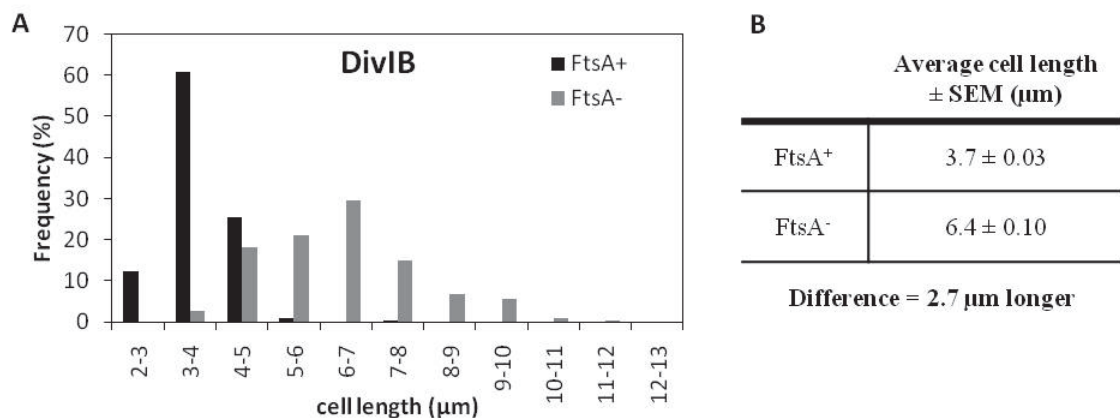


Figure 4.3 *DivIB* localisation to midcell is delayed in the absence of *FtsA*. (A) Graph shows the frequency of *DivIB* localisation per cell length in strain SU636 (*gfp-divIB ftsA* complementation), under *ftsA*-induction or *ftsA*-repression conditions (FtsA⁺ and FtsA⁻, respectively). The data was obtained through the course of 240 min of spore outgrowth. The samples collected at different the time points were group together for analysis of the population cell length distribution (shown as percentage of frequency). (B) Table shows the average cell length of each population of cells (FtsA⁺ and FtsA⁻) and its difference, showing the cell length delay in with *DivIB* localises in the absence of *FtsA*. SEM refers to standard error of the mean.

Collectively, the above data support the idea that *FtsA* is necessary for the correct timing of *DivIB* localisation, but does not appear to affect the efficiency of its

recruitment to the Z ring. As previously mentioned, it is known that some later division proteins (*DivIB*, *FtsL*, *DivIC* and *PBP2B*) in *B. subtilis* interact together to form a complex before assembling at the midcell site (Feucht *et al.*, 2001; Errington *et al.*, 2003; Buddelmeijer and Beckwith, 2004; Goehring and Beckwith, 2005). Also, except for *DivIB*, all other protein components are essential to division and the absence of one of them results in complete cell division inhibition. Based on this information, we can then suggest that the results presented above are valid not only for the recruitment and localisation of *DivIB* to the Z ring but also for the other later division proteins complex, showing that in the absence of *FtsA* the localisation of these proteins at the midcell Z ring is significantly delayed.

4.2.4 Septum formation in the absence of *FtsA*

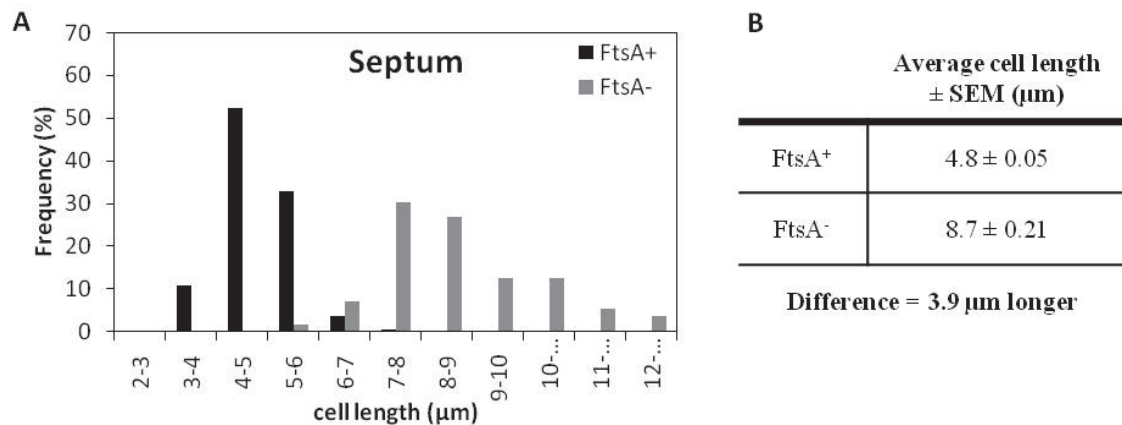


Figure 4.4 Frequency of cell lengths for septum formation. (A) Graph shows the frequency of septa formation per cell length in strain SU636 (*gfp-divIB ftsA* complementation), under *ftsA*-induction or *ftsA*-repression conditions (FtsA⁺ and FtsA⁻, respectively). The data was obtained through the course of 240 min of spore outgrowth. The samples collected at different the time points were group together for analysis of the population cell length distribution (shown as percentage of frequency). (B) Table shows the average cell length of each population of cells (FtsA⁺ and FtsA⁻) and its difference, showing the cell length delay in which septum forms after *DivIB* had localised, in the absence of *FtsA*. SEM refers to standard error of the mean.

The previous section demonstrated that in the absence of *FtsA* there is a delay in recruitment of the downstream divisome protein, *DivIB*, and probably other proteins such as *FtsL*, *DivIC* and *PBP2B*, as these are dependent on *DivIB* for their recruitment to the division site. However, regardless of this delay the level of *DivIB* recruitment

reaches approximately wild-type levels. Furthermore, the average cell length for *DivIB* localisation ($6.4 \pm 0.10 \mu\text{m}$) is not near as long as the cell length of the *ftsA* deleted strains. Taken into account these observations, the delay in *DivIB* recruitment does not explain why these *FtsA*-depleted cells are still defective in cell division and form filaments, since once *DivIB* is recruited, septation should proceed. Current evidence suggests that once the later-assembling division proteins are recruited, septation proceeds in *E. coli* (Rico *et al.*, 2010; Alexeeva *et al.*, 2010). In other words, the data suggest that *FtsA* has an additional role in cell division that occurs after the recruitment of *DivIB*.

In *E. coli*, the third role for *FtsA* appears to be *Z* ring constriction. A role for *FtsA* in *Z* ring constriction in *B. subtilis* was therefore examined. This involved the same procedure as that used to study *DivIB* localisation (see above section 4.2.3). The main alteration to this protocol was the addition of a membrane dye FM4-64 that enabled septum visualisation in live cells. SU636 (*gfp-divIB ftsA* complementation) spores were germinated at 34°C under conditions of both *ftsA*-induction (0.5% xylose) and *ftsA*-repression (0.5% glucose), with the constant induction of *gfp-divIB* (0.1 mM IPTG) to visualise *DivIB* localisation. During spore outgrowth, samples were collected at 30 minute intervals, 3 hours after the onset of germination (at 180, 210 and 240 minutes) for live cell microscopy (see Chapter 2, section 2.6.2). Approximately 200 outgrown cells were scored and measured per sample.

The data analysis presented in Table 4.2, and supported by the overall cell length frequencies in Figure 4.3 and Figure 4.4, clearly show an infrequency of septum formation after *DivIB* recruitment in the absence of *FtsA*. At 240 minutes of spore outgrowth, *DivIB* is maximally recruited (37%) in *ftsA*-repressed cells; however the septum formation is only present in 6% of the cells. This frequency is much lower when compared to the 32% of septation in the *ftsA*-induced cells, at the same time-point of 240 minutes. In other words, even after *DivIB* is been recruited in *ftsA*-repressed cells as efficiently as in wild-type (*ftsA*-induced cells), the septation process still occurs 5.3-fold less frequently compared to wild-type. Importantly, all the cells that have a division septum also show *DivIB* localisation, as expected.

The microscopy images shown in Figure 4.2 and Figure 4.5 correspond to the same cells at each time point, obtained using different fluorescence filters for GFP-*DivIB* and

membrane visualisation, respectively. These cells are a good representation of infrequent septation after *DivIB* recruitment, and also suggest a delay in the septation event. However, it is important to determine whether this delay is a consequence of the delay in *DivIB* recruitment, or whether it represents a further delay in a later stage of cell septation. The question here is whether the time between *DivIB* recruitment and septation is longer when *ftsA* expression is repressed compared to when *ftsA* expression is induced. To investigate this, the cell lengths of *ftsA*-induced cells and *ftsA*-repressed cells were compared. The analysis is similar to the one presented in section 4.2.3 when studying the delay in *DivIB* localisation. The cell length data that was previously reorganised in two populations, *ftsA*-induced cells and *ftsA*-repressed cells, disregarding the times at which each sample was collected (section 4.2.3), was again used to study the delay in septation. This data was then plotted on a frequency distribution graph showing the frequency of septum formation *versus* the cell length at which septation occurred. Figure 4.4 (above) shows that the cell length distribution of *ftsA*-repressed cells at the time of septum formation is quite different to the observed in *ftsA*-induced cells, extending through a larger range of cell lengths. This indicates a higher heterogeneity in the cells life-time when septation occurred. The graph also shows that the cell-length distribution of *ftsA*-repressed cells ($FtsA^-$, grey columns in Figure 4.4) is shifted to the right compared to the cell length distribution of *ftsA*-induced cells ($FtsA^+$, black columns in Figure 4.4), i.e. all cells were longer at the time of septation. This longer cell length suggests that, after *DivIB* localisation, septum formation is also delayed in the absence of *FtsA*.

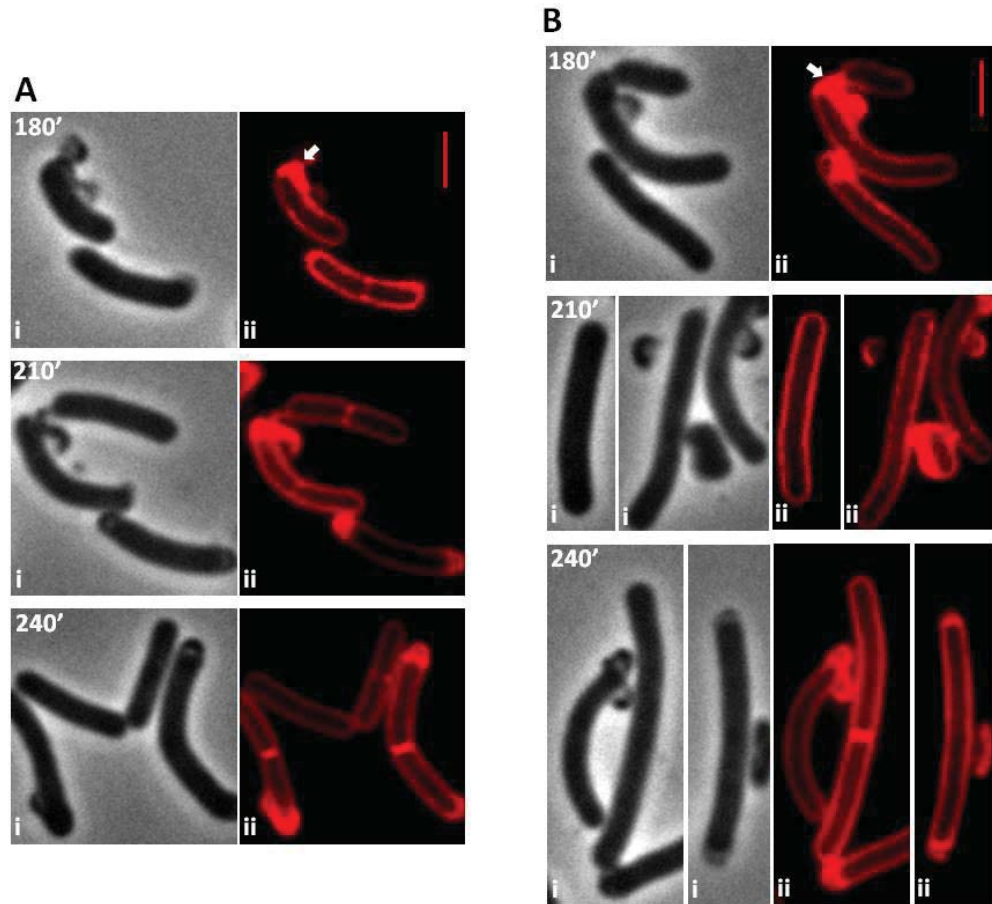


Figure 4.5 Septum formation in SU636 outgrown spores. *gfp-divIB ftsA* complementation spores were germinated in GMD media at 34°C with 0.5% xylose for *ftsA* induction or 0.5% glucose for *ftsA* repression. Samples were taken every 30 minutes and cells were prepared in agarose pads for live cell microscopy. Membranes were stained with FM4-64. Panels labelled i depict phase-contrast images, whilst those labelled ii show the septum (red) localisation. **(A)** *ftsA* induction conditions showing short dividing cells. **(B)** *ftsA* repression conditions showing progressively longer cells caused by a defect in cell division. These cells divide with lower frequency, but continue to grow into long filaments. Frequency of septum formation in these cells is presented in Table 4.2. White arrows point to auto-fluorescent spore coats. Red scale bar represents 2 μm for all images.

Further analysis of the cell length distribution data showed that when septation occurs the cells are on average 3.9 μm longer (Figure 4.4, Panel B). This almost 2-fold increase in cell length is obtained when comparing the average cell length of $4.8 \pm 0.05 \mu\text{m}$ and $8.7 \pm 0.21 \mu\text{m}$, in the presence and absence of *FtsA*, respectively. This confirms that the cells are at a significantly later stage of cell cycle when septation occurs in the absence of *FtsA*. Employing the KS-test for statistical analysis, it was established that the cell length distribution was significantly different ($P < 10^{-5}$) between the two populations (*ftsA*-induced and *ftsA*-repressed cells). Thus, this data indicates that in the absence of

FtsA, after *DivIB* recruitment, cells are significantly longer when the septum forms. Moreover, the difference of average cell lengths between *DivIB* localisation and septum formation, in the absence of *FtsA*, is 1.2 μm . Clearly, this attests for the delay in septation, independently of the time of localisation of the later division proteins.

Together, the results presented in this chapter showed that in the absence of *FtsA* in *B. subtilis* cells there is a significant delay in the recruitment of *DivIB* to the division site and, most likely the other later-assembling division proteins. The results also indicated that the absence of *FtsA* causes a significant delay in septum formation, which was shown to be independent from the delay in *DivIB* recruitment. More importantly however, it was determined an inefficiency in septation. These new findings reinforce the idea that *FtsA* plays a vital role in the later stages of cell division rather than in *Z* ring formation as previously thought.

4.3 Discussion

In Chapter 3 it was shown that *FtsA* is not required for the efficient assembly of the *Z* ring. Instead *FtsA* appears to be required for a later stage of division, perhaps affecting the proper recruitment and localisation of the downstream division proteins to the *Z* ring. In *E. coli*, *FtsA* has an essential role in recruiting downstream division proteins to the division site (namely, *FtsK*, *FtsQ*, *FtsI*, *FtsL*, and *FtsN*) (Ghigo *et al.*, 1999; Pichoff and Lutkenhaus, 2002; Corbin *et al.*, 2004; Rico *et al.*, 2004). It has been assumed that, in *B. subtilis*, *FtsA* plays the same role, but not much is known yet. Errington *et al.* (2003) presents a table of interdependency on localisation between various division proteins in *B. subtilis*; however, there is no information regarding protein localisation dependency on *FtsA* localisation, with the exception of *FtsZ* (Feucht *et al.*, 2001) and *FtsW* (Daniel and Wu, unpublished data). Furthermore, Feucht *et al.* (2001) stated that *FtsA* does not require *DivIB* for its localisation, but the opposite was not shown. Given this lack of information, the work presented in this chapter is of major importance.

To investigate whether the downstream recruitment of division proteins is affected in the absence of *FtsA*, and find out whether this is the cause of the *ftsA* mutant cell division defect, a fusion of GFP-*DivIB* was used as a marker for late divisome

recruitment. Therefore, using the GFP-DivIB fusion in the absence of FtsA, it was confirmed that FtsA is not required for DivIB recruitment. However, this was somewhat expected, taking into account that a fraction of FtsA mutant cells can still divide, albeit less frequently than normal. More significant was that the level of DivIB recruitment reached wild-type levels, despite the notable delay in the recruitment process. Thus, rather than being required for the localisation of DivIB, FtsA seems to be required for the timing of its localisation. Although live cell fluorescence imaging was a significant choice for this work, in the future it would be advantageous to use the immunofluorescence microscopy approach as further validation of these results.

Importantly, further analysis revealed that, even after the delayed arrival of DivIB to the division site, the septation event was still inefficient in the absence of FtsA. In summary, the data suggest that FtsA is required for the correct timing of DivIB recruitment, and possibly all downstream division proteins, perhaps by remodelling the Z ring to make it division competent, but is not absolutely required for its localisation. In addition, and very significantly, the results point to the possibility that FtsA is directly involved in the later stages of cell division, promoting efficient septum formation after divisome assembly.

4.3.1 FtsA is not required for DivIB recruitment. What is the primary function of FtsA?

The results in this chapter demonstrate that FtsA is not required for DivIB recruitment to the division site. However, this new information does not explain the delay in, and inefficiency of, septation in *ftsA* mutant cells. Discussed below are some possibilities for the primary function of FtsA, taking into account the results presented in this chapter.

4.3.1.1 Role of FtsA in recruitment of other downstream divisome proteins?

One possibility for the function of FtsA is the efficient recruitment of the other downstream divisome proteins, other than DivIB. According to the literature, the results presented here about DivIB localisation in the absence of FtsA can probably be

extrapolated for some later division proteins (DivIB, DivIC, FtsL and PBP 2B). Goehring and Beckwith (2005) validate the existence of a conserved sub-complex of proteins in bacteria including *B. subtilis* that includes DivIB, FtsL and DivIC (and in *E. coli*, the respective homologs, FtsQ, FtsL and FtsB). These proteins need one another for stability and assembly at the division site, with several studies demonstrating that these proteins interact directly with each other (Daniel and Errington, 2000; Katis *et al.*, 2000; Robson *et al.*, 2002; Errington *et al.*, 2003; Buddelmeijer and Beckwith, 2004; Goehring and Beckwith, 2005). PBP 2B, a *B. subtilis* penicillin-binding protein, is not considered to be part of the sub-complex of proteins (DivIB, FtsL and DivIC); however, its localisation to the division site is known to be interdependent with this sub-complex (Daniel *et al.*, 2000). Also, work done by Gamba *et al.* (2009) further elucidates the assembly pathway of the divisome proteins in *B. subtilis*, by studying its dynamics and temporal hierarchy, and providing *in vivo* evidence for two-step assembly of the divisome. With this in mind, it seems acceptable to assume that all four proteins are being recruited to the Z ring in the absence of FtsA. Nevertheless, for future work, it would be important to confirm this assumption for FtsL, DivIC and PBP 2B recruitment.

4.3.1.2 *Role of FtsA in recruitment of later proteins, after DivIB (and related proteins) assembly?*

The second suggestion for the function of FtsA is its possible requirement for the recruitment of other protein(s) that localise to the division site, later than the sub-complex of proteins mentioned above (DivIB, FtsL and DivIC; and PBP 2B). The DivIVA protein localises at the cell poles and at the new division sites after the divisome is assembled, functioning as a protein scaffold and site selection. Interestingly, although it is known that DivIVA recruits the Min system proteins, not much is known about its own recruitment and localisation. Supposedly, this happens by a signal or interaction with an early division protein or by detecting the cell membrane curvature (Lenarcic *et al.*, 2009; Oliva *et al.*, 2010; Lutkenhaus, 2009). Another important observation relates to the time of DivIVA localisation. According to Gamba *et al.* (2009), DivIVA localisation happens slightly after the localisation of other late division proteins to the division site. This suggests that the results obtained in this work,

regarding the divisome assembly in the absence of *FtsA*, cannot be extrapolated for *DivIVA* localisation. In this sense, it is possible that, without the presence of *FtsA* at midcell, *DivIVA* would lack the connection to the divisome, thus partially or completely obstructing its localisation and function. However, if *DivIVA* is still being recruited and localised to normal efficiency to the division site, then this would suggest that all divisome components are recruited to wild-type levels, in the absence of *FtsA*. For future work it would be important to check *DivIVA* recruitment and localisation in *ftsA*-depleted conditions.

4.3.1.3 Role of *FtsA* in *Z* ring constriction through direct interaction with *FtsZ*?

Although not much is known yet regarding the steps between divisome assembly and the events leading to actual cytokinesis (*Z* ring constriction, septum formation and cell wall synthesis), there is a general consensus that there might be an “as-yet-undiscovered” signal that connects them and triggers cytokinesis (Adams and Errington, 2009; Lutkenhaus, 2009; Rudner and Losick, 2010).

Another possibility that might explain the low frequency of septation in *FtsA* mutants, despite the eventual wild-type level of *DivIB* (and assumingly the divisome) recruitment, is the requirement of *FtsA* for efficient *Z* ring constriction. Since *FtsA* interacts directly with *FtsZ* (Feucht *et al.*, 2001; Jensen *et al.*, 2005), one likely function of *FtsA* seems to be in *Z* ring constriction, not via other division proteins, but by its direct interaction with the C-terminal tail of *FtsZ* (Ma *et al.*, 1996; Din *et al.*, 1998; Ma and Margolin, 1999; Yan *et al.*, 2000; Di Lallo *et al.*, 2003). Therefore, the inefficiency of this process would result in the lack of septation seen in the absence of *FtsA* in *B. subtilis*. Also, *FtsA* connects the *Z* ring to the membrane in *E. coli* (Pla *et al.*, 1990; Pichoff and Lutkenhaus, 2005; Shiomi and Margolin, 2008) and it is possible that *FtsA* can generate a mechanical and/or catalytic force on the *Z* ring during constriction (Sanchez *et al.*, 1994; Strahl and Hamoen, 2010) (see Section 5.3 of Chapter 5 for a follow up on this subject).

Overall, the results presented in this chapter are starting to reveal the role of FtsA in *B. subtilis* as a key protein in the later stages of cell division, specifically in Z ring constriction. The next chapter investigates this idea.

Chapter 5

§

*Examining a possible role for FtsA in Z ring
constriction*

5.1 Introduction

So far, it has been demonstrated that FtsA is not essential for the actual formation of Z rings in *B. subtilis*. Rather, FtsA seems to be responsible for the efficient timing of recruitment of DivIB, and possibly the divisome complex; and is essential for the normal frequency of cell septation after divisome assembly. However, an *ftsA* deletion is not lethal to the cells, although cell lengths are still long, implying that cell division still occurs at low frequency.

Z ring constriction seems very inefficient when FtsA is absent. Also, Z ring frequency between outgrown spores and vegetative cells is very different, and what happens to the formed Z rings is still unknown. However, there is still some division in cells in the absence of FtsA. Therefore, some of the Z rings must constrict. Why and how these cell events happen is investigated in this chapter. Understanding the fate of the remaining Z rings will aid in defining the role of FtsA in *B. subtilis* cell division.

How Z ring constriction occurs is still not solved. However, two main classes of models are being investigated (Erickson, 2009). One type of model is based on continuous protofilaments in the Z ring that overlap at the ends to form lateral bonds. The model proposes that when these ends slide, the lateral bonds increase, generating contraction of the Z ring (Lan *et al.*, 2009; Horger *et al.*, 2010). The other type of model proposes that protofilaments can undergo a conformational change, inducing them from straight to curved protofilaments, which in turn applies a bending force on the cell membrane causing constriction (Lu and Erickson, 1999; Erickson, 1997; Erickson and Stoffler, 1996; Li *et al.*, 2007; Allard and Cytrynbaum, 2009). The main point is that, independently of the model, the dynamics of the Z ring seem to be important for constriction (Erickson, 2009). These dynamics are determined by the turnover of FtsZ subunits that allow remodelling of FtsZ within the Z ring (Erickson *et al.*, 2010). To investigate if FtsA influences FtsZ dynamics, the turnover of FtsZ within the Z ring was analysed in *ftsA* mutants.

The dynamic nature of the Z ring, necessary for the constriction process, happens through continuous remodelling both before and during its constriction (Stricker *et al.*, 2002; Anderson *et al.*, 2004; Erickson *et al.*, 2010). Normally, cells in a population contain one central Z ring, which incorporates ~30% of the cellular pool of FtsZ

molecules, while the remaining FtsZ is free in the cytoplasm (Stricker *et al.*, 2002; Anderson *et al.*, 2004). The FtsZ subunits in the Z ring are constantly being recycled by exchanging with the FtsZ cytoplasmic pool, driven by the GTPase activity of FtsZ that destabilises the FtsZ polymers (Addinall and Holland, 2002; Harry *et al.*, 2006; Huecas *et al.*, 2007; Lan *et al.*, 2007; Erickson, 2007; Niu and Yu, 2008; Erickson *et al.*, 2010; Mingorance *et al.*, 2010). This exchange of FtsZ between the Z ring and the cytoplasm seems to occur rapidly and at the same rate before and during constriction (Stricker *et al.*, 2002), possibly by fragmentation and re-annealing of FtsZ protofilaments at locations within the Z ring (Mingorance *et al.*, 2005; Shih and Rothfield, 2006; Surovtsev *et al.*, 2008; Erickson *et al.*, 2010; Mingorance *et al.*, 2010). Fluorescence recovery after photobleaching (FRAP) analysis in both *B. subtilis* and *E. coli* has demonstrated that FtsZ turnover within the Z ring has an approximate half-time of 8-9 seconds (Stricker *et al.*, 2002; Anderson *et al.*, 2004). *In vitro* FRET (fluorescence resonance energy transfer) measurements also showed a similar FtsZ turnover with a half-time of 7 seconds in *E. coli* (Chen and Erickson, 2005). Several FtsZ-interacting proteins known to have a role in Z ring regulation do not appear to significantly influence FtsZ turnover in the ring (Anderson *et al.*, 2004). However, the role for FtsA in FtsZ turnover and Z ring dynamics has not been studied yet. The work in this chapter attempts to investigate this role and clarify the effect of FtsA in Z ring constriction using FRAP analysis.

5.1.1 Overview of the FRAP technique

One of the most common current techniques for studying protein kinetics was first developed almost 40 years ago and is called fluorescence recovery after photobleaching or FRAP (Axelrod *et al.*, 1976). Among other applications, this technique is used for detection of protein kinetic rates and mobility *in vivo* (Phair and Misteli, 2001; Lippincott-Schwartz *et al.*, 2001; Sprague and McNally, 2005). In FRAP experiments, a small region of interest (ROI) in a cell is selected and irreversibly photobleached using a high-intensity laser beam (Figure 5.1). GFP-fusion proteins are the best choice for this technique, since their bleaching does not seem to cause damage to the cells (Lippincott-Schwartz *et al.*, 2001). In fact, this technique turns part of the fluorescence-labelled

proteins undetectable, presenting a result that reflects the real behaviour *in vivo* (Phair and Misteli, 2001). The rate of fluorescence recovery of the bleached area is then measured at regular time intervals, using low intensity illumination microscopy (Figure 5.6). This recovery is a consequence of the movement of the unbleached fluorescent molecules from the surrounding areas into the photobleached area. The FRAP results are then analysed through the application of complex mathematical models to the recovery curve (Figure 5.1), available as useful functions in imaging and analytical softwares (as Image J and Grad Pad Prism 5). This analysis uses large amounts of quantitative information from the experimental procedure and offers a final qualitative view on the cellular process in question, including the rate of protein mobility, the presence of binding interactions, or how a particular mutation, cell defect or specific treatment affects the process.

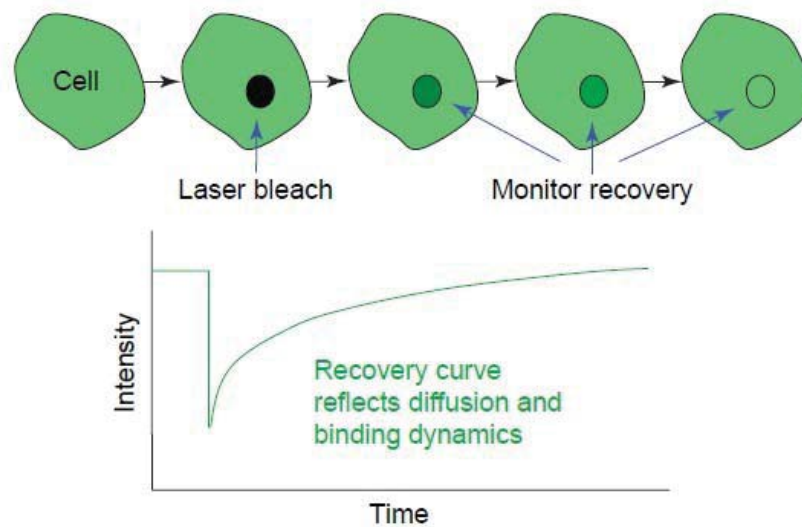


Figure 5.1 Schematic illustrating the FRAP technique. The region of interest in the cell is photobleached and the fluorescence recovery in the same region is monitored to determine the diffusion rate of the molecules translating their mobility or dynamics. Image taken from Sprague and McNally (2005).

5.1.2 Chapter aims

Chapters 3 and 4 showed that in *B. subtilis* cells, in the absence of FtsA, Z rings formed with wild-type efficiency in outgrown spores. Furthermore, although delayed, recruitment of DivIB, and likely other DivIB-dependent divisome components, occurs

as efficiently as wild-type. However, in vegetative cells that lack FtsA, there are very few Z rings and division is impaired. Therefore, the main question raised in this chapter is: What is the fate of the Z rings formed in the absence of FtsA? The results obtained in this chapter using time-lapse fluorescence microscopy are a strong indication that FtsA is required for efficient Z ring constriction. It was observed that the absence of FtsA gives rise to different Z ring fates, such as; normal constriction, disassembly, or Z rings persisting for long periods of time without constriction. These observations prompted further questions regarding the role of FtsA during Z ring constriction. Is FtsA affecting constriction by influencing the FtsZ turnover in the Z rings? The application of FRAP showed that FtsZ turnover in the Z ring decreases in the absence of FtsA. However, while it is significant, it is a small decrease of 1.6-fold. The observations presented in this chapter strongly support a role for FtsA in Z ring constriction. However, it is still not clear if this is a direct effect on Z ring dynamics through the direct interaction between FtsA and FtsZ, or an indirect effect on Z ring dynamics through an FtsA-induced alteration of other divisome proteins.

5.2 Results

5.2.1 Introducing an FtsZ-GFP fusion protein into an FtsA-depletion background

In an effort to better visualise the formation and fate of Z rings in *B. subtilis* cells in the absence of FtsA, an FtsZ-GFP fusion protein was used in this work for live cell microscopy. The *B. subtilis* strain SU570 (kindly provided by P. Peters, PhD thesis) has the only copy of *ftsZ* fused to *gfp* and its expression is controlled by the endogenous promoter (Levin *et al.*, 1999). A genetic modification was done by P. Peters in which the chloramphenicol cassette for antibiotic resistance was substituted by a spectinomycin cassette (Table 2.2; Chapter 2). The use of SU570 enables direct visualisation of all the FtsZ present in the cell and thus provides a genuine image of the Z ring in live cells. At 30°C, *B. subtilis* SU570 is able to utilise the fusion protein as the sole source of FtsZ required for division (Levin *et al.*, 1999; Figure 5.2).

The main advantage of using this fluorescence fusion (FtsZ-GFP) is that it enables the observation of all the FtsZ in the cell, rather than just a portion of the labelled protein in addition to the native protein as is sometimes used. Additionally, with all the FtsZ fluorescently labelled, the microscopy image is brighter and clearer. This strain was used to obtain a new FtsA-depletion strain containing this fusion, named SU638 (Table 2.2). To construct this strain, chromosomal DNA from SU570 was extracted and used to transform the *ftsA* in-frame complementation strain (SU631), under *ftsA*-induction conditions (presence of 0.5% xylose). The vegetative growth of both SU570 and SU638 strains was then analysed in rich media (PAB) at 30°C. At mid-exponential phase, the FtsZ-GFP (SU570) strain showed an average cell length of $7.5 \pm 0.12 \mu\text{m}$, similar to the average cell length of $8.1 \pm 0.14 \mu\text{m}$ for the *ftsZ-gfp ftsA*-inducible strain (SU638 with 0.5% xylose) (Fig. 5.2 and Table 5.1). The cell length analysis shows a longer mean cell length in the FtsZ-GFP (SU570) and FtsZ-GFP *ftsA*-induced (SU638) strains compared to wild-type (SU5) cells at 30°C ($5.6 \pm 0.10 \mu\text{m}$, P. Peters, PhD thesis). This is a significant difference in cell length, resulting in strains that are less efficient in cell division. However, for the purpose of this experiment, the fusion protein is used as a tool to analyse the efficiency of FtsZ-GFP recruitment in the presence and absence of FtsA, and therefore it would be unlikely to affect the conclusions drawn from it.

Table 5.1 Average cell lengths of SU570 (*ftsZ-gfp*) and SU638 (*ftsZ-gfp ftsA::cat P_{xyt}-ftsA*) strains.^a

Media supplements	Strains	Average cell length ($\mu\text{m} \pm \text{SEM}$)
None	SU570 (FtsZ-GFP)	7.5 ± 0.12
0.5% xylose	SU638 (FtsZ-GFP <i>ftsA</i> induced)	8.1 ± 0.14
0.5% glucose	SU638 (FtsZ-GFP <i>ftsA</i> repressed)	18.0 ± 0.67

^aCultures were grown in rich media PAB to mid-exponential phase at 30°C.

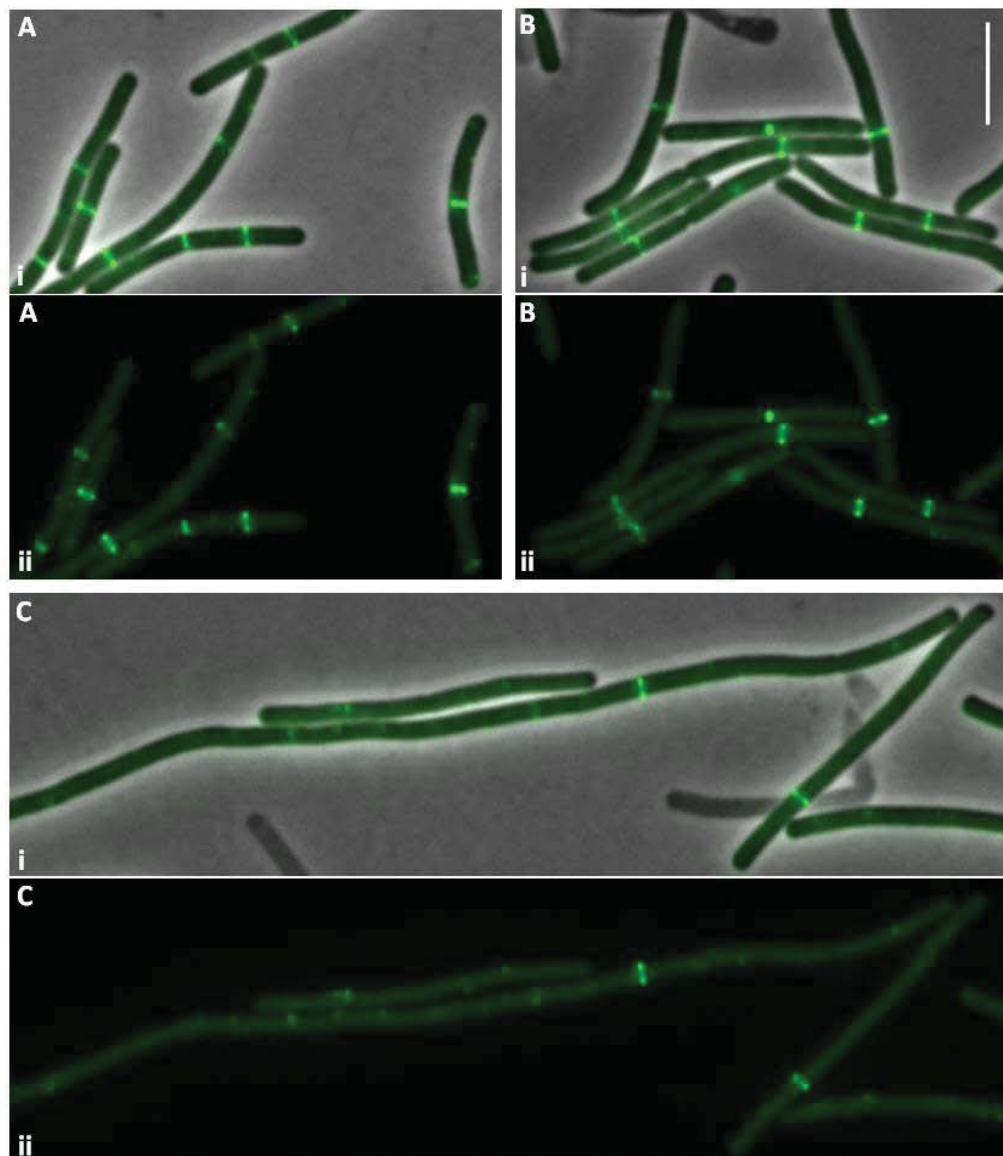


Figure 5.2 FtsZ-GFP localisation in the absence of FtsA. (A) The FtsZ-GFP (SU570) strain shows cells that are similar in length to wild-type cells, albeit a little longer, with an average cell length of $7.54 \mu\text{m} \pm 0.12$ (SEM). In this strain (SU570) 53% of the cells contain Z rings. (B) The FtsZ-GFP *ftsA*-induced (SU638 with 0.5% xylose) strain shows a similar phenotype to SU570, with an average cell length of 8.1 ± 0.14 (SEM) (C) The FtsZ-GFP *ftsA*-inducible strain (SU638) with *ftsA* expression repressed (with 0.5% glucose) shows a filamentous phenotype, with an average cell length of $18.0 \mu\text{m} \pm 0.67$ (SEM), caused by a defect in cell division. These cells divide with lower frequency but continue to grow into long filaments. This strain (SU638) presents 49% of the *ftsA*-induced cells with Z rings and 31% of the *ftsA*-repressed cells with Z rings. Vegetative growing cells were collected at mid-exponential phase at 30°C . Live cell microscopy: (i) Overlay of phase-contrast and FtsZ-GFP images; (ii) FtsZ-GFP localisation. Scale bar represents $5 \mu\text{m}$ for all images.

Z ring frequency is similar in strains SU570 (FtsZ-GFP, 53%) and SU638 (FtsZ-GFP *ftsA*-induced, 49%). However, the *ftsA*-repressed cells (SU638) had only 27% Z rings. These values are similar to those seen in the wild-type and *ftsA*-deletion strains in

Chapter 3 (see Table 3.1). The slight increase in Z ring frequency in strain SU570 is probably due to the different techniques used to visualise the Z rings; immunofluorescence microscopy vs fluorescent-fusion live cell microscopy. Importantly, the SU638 cells had the expected filamentous phenotype under *ftsA*-repressed conditions (0.5% glucose), with an average cell length of $18.0 \pm 0.67 \mu\text{m}$ (Fig. 5.2 and Table 5.1). The similar phenotype between SU638 strain and its parental strain SU631, both in the presence and absence of FtsA, leads to the conclusion that *ftsZ-gfp* expression does not affect the cell division process under these conditions (see section 3.2.5.2).

5.2.2 Time-lapse microscopy of FtsZ-GFP in FtsA-depleted cells

To investigate the fate of Z rings formed in the absence of FtsA, time-lapse microscopy was performed. The findings described here show a consistency in the difference between the Z ring frequency in outgrown spores and vegetatively growing cells, since the results below show that the Z rings are able to form efficiently in vegetatively-growing cells, but either fail to constrict, constrict slowly, or disassemble.

Time-lapse experiments were performed in exponentially-growing FtsZ-GFP FtsA-depleted vegetative cells (SU638) and in control FtsA⁺ cells containing FtsZ-GFP, in PAB media at 30°C, for time-lapse analysis of Z ring constriction. FtsA depletion was done using glucose (0.5%) for complete promoter repression for two consecutive exponential phases of vegetative growth, to ensure that all FtsA produced from the overnight culture would be completely depleted. Cells were collected at mid-exponential phase, placed on an agarose pad and images were taken every 5 minutes over a 150-min period. The experimental procedure presented some difficulties regarding cell growth on agarose pads. The cells were gently treated when transferred to the agarose pads, so as not to disturb their growth. However, in various time-lapse experiments the cells failed to continue their growth or its rate became too slow, resulting in non-measurable growth and more cell death. Problems often occurred with membrane staining of the cells with FM4-64 for septum visualisation. According to previous work done by Pogliano *et al.* (1999), the use of FM4-64 membrane stain is not detrimental for *in vivo* time-lapse microscopy. However, in this work the use of the

membrane stain became toxic for the cells, both wild-type and mutant. As soon as they were exposed to the fluorescent light, cell death occurred very quickly. After several attempts and different trial conditions, the decision was made to proceed with the experiments without membrane visualisation and focus on the vital information that could be gathered from the study of the Z rings during live cell microscopy.

Time-lapse experiments with FtsZ-GFP in an otherwise wild-type background (SU570) showed normal Z ring constriction. Although not all the Z rings were observed from formation until constriction, the minimum time before a Z ring constricts was ~60 minutes (as an example, see Z rings identified with green and red arrows in Figure 5.3). In total, 54 cells were analysed, with most of them behaving in a similar manner to the cells presented in Figure 5.3. The movie which corresponds to the time-lapse images of vegetative growing cells in Figure 5.3 is shown in Supplementary Material (Figure S5.1). Figure 5.3 shows examples of Z ring constriction (red and green arrows) in these cells. It is also possible to observe two new Z rings assembling in the daughter cells before the constricting Z ring disappears (Figure 5.3; red and green chevrons).

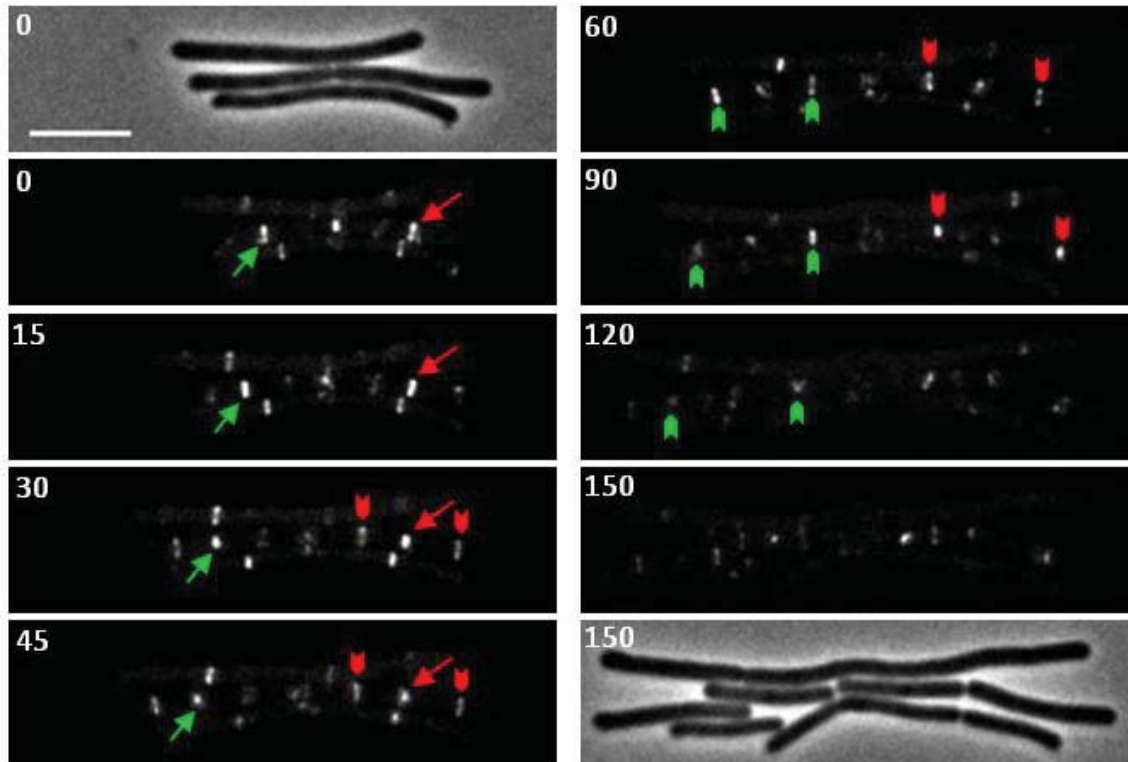


Figure 5.3 Time-lapse microscopy of FtsZ–GFP localisation in *B. subtilis* SU570 (*ftsZ-gfp*) cells. The cells were collected for microscopy analysis when the mid-exponential growth phase was reached in PAB at 30°C, and were then applied to agarose pads and viewed by fluorescence microscopy using a stage heated to 30°C. Images were acquired at 5-min intervals over a 150-min period. The red and the green arrows indicate different constricting Z rings in the cells. The chevrons indicate the new pairs of Z rings that are then observed to assemble in the corresponding daughter cells, within 60 minutes. Numbers represent time in minutes. Scale bar represents 5 μ m. The movie corresponding to these time-lapse images is shown in Supplementary Material (Figure S5.1).

5.2.2.1 Different fates for the Z rings formed in the absence of FtsA

Unlike the control strain, SU570 (*ftsZ-gfp*), not all Z rings constricted in the *ftsA*-depleted vegetatively growing cells of SU638 (*ftsZ-gfp ftsA*-inducible). In total, 40 cells were studied in the time-lapse experiments, all of which were observed to elongate for the duration of the observation period. Different fates for these Z rings were observed; most of them not seen in the wild-type FtsZ-GFP cells observed, with the exception of normal Z ring constriction (see below). The fates are described below with examples of each one in Figures 5.4, 5.5 and 5.6. Table 5.2 presents the schematic image and the frequency of each of the Z ring fates in these cells. The movies, corresponding to the time-lapse images of vegetatively-growing cells in Figures 5.4, 5.5 and 5.6, are shown in Supplementary Material (Figure S5.2, Figure S5.3 and Figure S5.4).

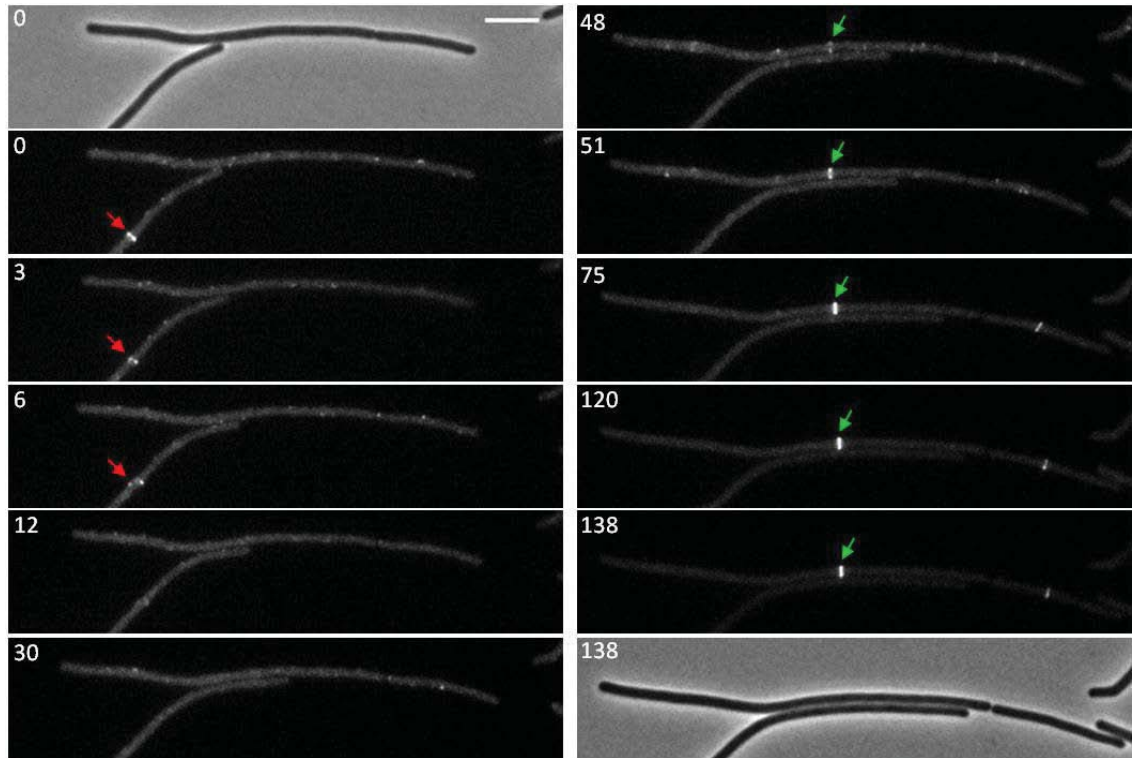


Figure 5.4 Time-lapse microscopy of FtsZ–GFP localisation in *B. subtilis* SU638 (FtsA-depleted) cells. Cells were collected for microscopy analysis when the mid-exponential growth phase was reached, and were then applied to agarose pads and viewed by fluorescence microscopy using a stage heated to 30°C. Red arrow points to a cell with a Z ring disassembling and then disappearing, while green arrow points to a cell with a non-constricting Z ring that persists for longer than any Z ring in the FtsA⁺ *ftsZ-gfp* strains (SU570). Numbers represent time in minutes. Images were acquired at 5 min intervals over a 140 min period. Scale bar represents 5 μm. The movies corresponding to these time-lapse images are shown in Supplementary Material (Figure S5.2).

Table 5.2 Frequency of Z ring fates in FtsA-depleted cells (SU638; *ftsZ-gfp ftsA::cat P_{xyl}-ftsA*), during time-lapse fluorescence microscopy.

Z rings (%)	Phenotype	Z ring schematic fate
13 cells, 32.5%	No constriction	
12 cells, 30%	Disappearance	
9 cells, 22.5%	Constriction/No septa	
6 cells, 15%	Slow constriction	

One observable fate for the Z rings that formed in some FtsZ-GFP FtsA-depleted cells (13 cells, 32.5%) was Z ring persistence throughout most of the time-lapse. An example of a non-constricting Z ring persisting for at least 90 minutes, is identified with a green arrow, in Figure 5.4; movie S5.2. This is despite the ability of the cells to continue to grow (elongate) under these conditions. A second fate observed in 30% of the cells (12 cells) was the disassembly of the Z ring without visible constriction. An example of a Z ring disassembling is identified with a red arrow, in Figure 5.4; movie S5.2. The third fate observed in 9 of the cells analysed (22.5%) was the apparent Z ring constriction inside the cell without visible cell division. However, without more information such as 3D data, this phenotype needs to be confirmed. It is presented here as an observation of what seems to be Z ring constriction with no septation, although it could also be interpreted as disassembly of the Z ring. An example of a slowly-constricting Z ring, without visible septation after 129 minutes, is identified with a red arrow, in Figure 5.5; movie S5.3. Lastly, on some occasions (6 cells, 15%), it was possible to observe normal Z ring constriction and cell division. It is not possible to calculate the exact duration of this process, since all the Z rings observed were already starting the process of constriction when the time-lapse analyses began. However, the Z rings persist for at least 100 minutes longer than the wild-type Z rings, (Figure 5.5). So the process of constriction is significantly delayed in the absence of FtsA compared to that in wild-type cells (see above). An example of Z ring constriction with cell division occurring is identified with a red arrow, in Figure 5.6; movie S5.4. It is important to note here that the FtsZ-GFP cells (SU570) divide normally. Another interesting observation regarding the FtsZ-GFP FtsA-depleted cells (SU638) is that only one new Z ring is formed per filament and also at a slower rate compared to the control FtsZ-GFP cells.

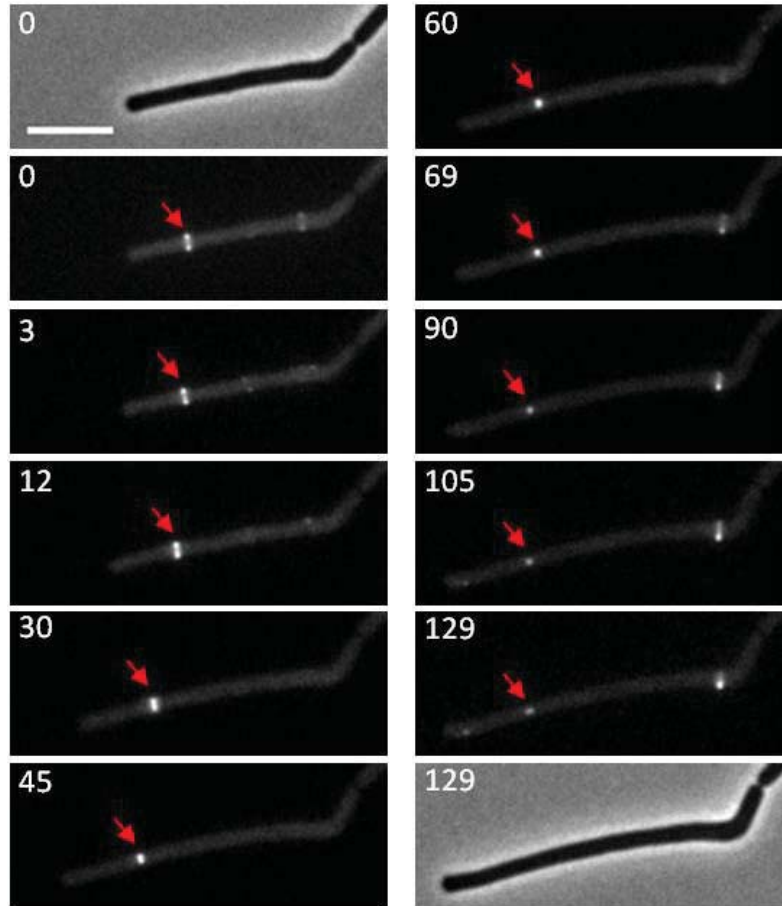


Figure 5.5 Time-lapse microscopy of FtsZ–GFP localisation in *B. subtilis* SU638 (FtsA-depleted) cells. Cells were collected for microscopy analysis when the mid-exponential growth phase was reached, and were then applied to agarose pads and viewed by fluorescence microscopy using a stage heated to 30°C. Red arrow points to a cell with a slow constricting Z ring but with no apparent cell wall constriction. Numbers represent time in minutes. Images were acquired at 5 min intervals over a 130 min period. Scale bar represents 5 μm . The movie corresponding to these time-lapse images is shown in Supplementary Material (Figure S5.3).

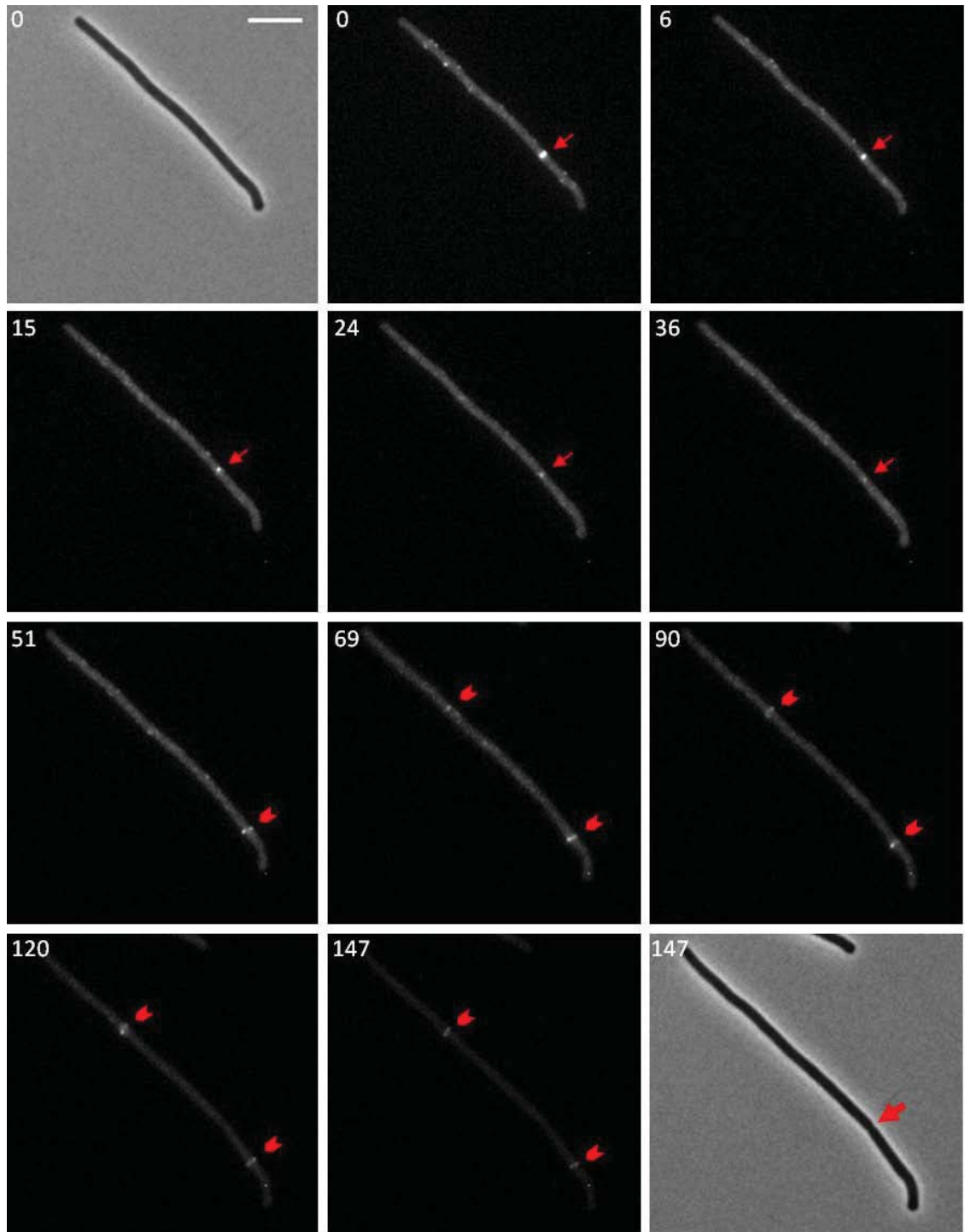


Figure 5.6 Time-lapse microscopy of FtsZ-GFP localisation in *B. subtilis* SU638 (FtsA-depleted) cells. Cells were collected for microscopy analysis when the mid-exponential growth phase was reached, and were then applied to agarose pads and viewed by fluorescence microscopy using a stage heated to 30°C. Red arrow points to a cell with a constricting Z ring with visible constriction, as seen in the image of phase-contrast. The chevrons indicate the new pair of Z rings that are then observed to assemble in the corresponding daughter cells, within 60 minutes. Numbers represent time in minutes. Images were acquired at 5 min intervals over a 150 min period. Scale bar represents 5 μ m. The movie corresponding to these time-lapse images is shown in Supplementary Material (Figure S5.4).

These time-lapse observations demonstrate that, in the absence of FtsA, Z rings clearly have different fates. In most cells (62.5%), Z ring constriction does not happen at all in the time-frame given, with either persistence of the Z ring or its disassembly without constriction. Thus the majority of Z rings that form in the absence of FtsA are not productive and do not lead to cell division. This further explains why the outgrown spores show wild-type timing and frequency of Z ring assembly and yet by the time they have gone through several generations of vegetative growth, the cells are quite long and there are very few Z rings. The findings described here support the idea proposed earlier in this chapter that FtsA is required for efficient Z ring constriction. The observation that Z ring disassembly in the absence of FtsA in particular seems to suggest that FtsA plays a role in FtsZ stabilisation. Furthermore, the observation of different fates of the Z rings formed in the absence of FtsA suggests that FtsA is also involved in FtsZ dynamics within the ring. This is investigated below.

5.2.4 Z ring dynamics is decreased in the absence of FtsA

In the absence of FtsA Z ring constriction is slow and infrequent. It was then hypothesised that it might be due to a change in the Z ring dynamics. According to Anderson *et al.* (2004), the rate of FtsZ turnover in the Z ring appears to be directly related to FtsZ protofilament stability. Furthermore, changes to this turnover may affect its normal constriction. Their work only found minor changes in FtsZ turnover, in both *B. subtilis* and *E. coli* organisms, when some division proteins were deleted (ZapA, EzrA and MinCD), but none of these mutants show a severe effect on Z ring stability and constriction as the *ftsA* mutant (Varley and Stewart, 1992; Levin *et al.*, 1999; Gueiros-Filho and Losick, 2002). Also, reviews on the subject by Adams and Errington (2009) and Osawa and Erikson (2011) propose that there is a high rate of FtsZ turnover in the Z ring and that this is directly related to its constriction. Is it possible that the highly inefficient Z ring constriction in the absence of FtsA is due to a decreased rate of FtsZ turnover in the Z ring? FtsA might be directly involved with this cell event and this would explain why the Z rings persist for several cell cycles without constricting. To investigate Z ring dynamics in the presence and absence of FtsA in the cell, the rate of

FtsZ turnover in the Z ring was measured *in vivo* using fluorescence recovery after photobleaching (FRAP).

5.2.4.1 FtsZ turnover in the Z ring is slower in the absence of FtsA

FRAP analysis was conducted on the same strains used for the above-mentioned time-lapse experiments examining the fate of Z rings. During several independent experiments, 17 cells were analysed as a wild-type control (FtsZ-GFP, SU570) and 57 cells were analysed in the absence of FtsA (FtsA-depletion FtsZ-GFP, SU638). The details of sample preparation, FRAP settings and analysis are described in Chapter 2. NIS-Elements (Nikon), ImageJ and GradPad Prism 5 software was applied for a complete FRAP analysis.

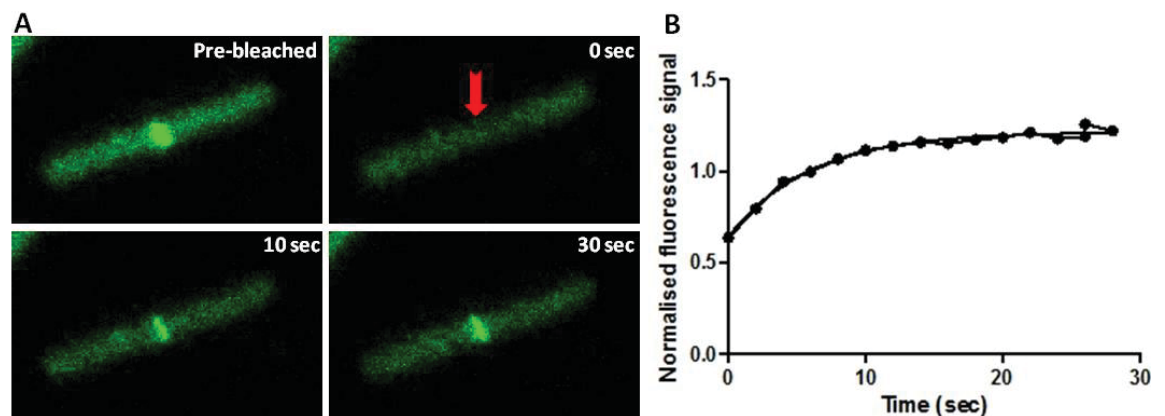


Figure 5.7 FRAP of a Z ring in control FtsZ-GFP *B. subtilis* cell. (A) Time-lapse series of fluorescence images show the time course of recovery. The red arrow shows the ring bleached. Images were taken every 2 sec using a Nikon A1 Confocal microscope under a CFI Apo TIRF (100× NA 1.49, Nikon) objective lens and were analysed with NIS-Elements Software. (B) Intensity of the photobleached region overtime, graphic directly obtained using Graph Prism software. The data points have been corrected for background and photobleaching during the acquisition period. The points represent the fluorescence data, and the solid line is the predicted recovery curve given the first-order rate constant, k . The half-time recovery for this series was 4.1 sec.

Figure 5.7 shows an example of FRAP analysis in FtsZ-GFP cells (SU570) serving as a control for the FtsA-depletion analysis. The fluorescence intensity of each Z ring was measured before, during and after its bleaching. An example of the image obtained is

presented in Figure 5.7A, with the cell in question having a cell length of 5.9 μm . The subsequent FRAP analysis of the fluorescent signal, is shown in Figure 5.7B, and the determined half-time recovery of FtsZ molecules in the Z ring is 4.1 seconds. All FtsZ-GFP cells analysed this way had a mean cell length of $7.0 \pm 0.95 \mu\text{m}$ and a mean half-time recovery of FtsZ molecules in the Z ring of 3.3 ± 0.3 seconds (see graph in Figure 5.8). This value is lower than the one obtained by Anderson *et al.* (2004), which was 8 ± 3 (SD) seconds; however, the experimental and microscopy setup were different. The reasons for this may lie in the choice of genetic construct and the temperature set up during the experiment. Anderson *et al.* (2004) expressed low levels of the FtsZ-GFP fusion, along with the normal level of endogenous FtsZ. This would result in most of the FtsZ proteins in the rings not actually being accounted for in the measurement. Another possible factor for the slower half-time recovery in their work could be the choice of operating at room temperature (25-26°C) instead of the strain optimal temperature of 37°C.

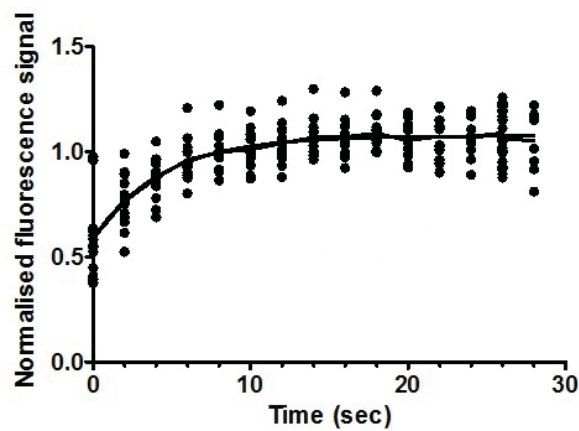


Figure 5.8 Overall FRAP in Z ring fluorescence intensity for *B. subtilis* cells (*ftsZ-gfp*). SU570 cells presented an average cell length of $6.97 \pm 0.95 \mu\text{m}$ and the average recovery half time of FtsZ molecules in the Z ring for this strain was 3.3 sec (17 cells analysed).

FRAP analysis for the study of FtsZ dynamics using the FtsA-depleted FtsZ-GFP strain (SU638) was done on 57 cells. Figure 5.9 shows an example of the image obtained (A), with the cell in question having a cell length of 23.7 μm ; and the subsequent FRAP analysis of the fluorescent signal (B). The half-time recovery of FtsZ molecules in the Z ring was determined to be 5.1 seconds. When all FtsA-depleted FtsZ-GFP cells were

taken into account, they presented an average cell length of $19.7 \pm 1.09 \mu\text{m}$. FRAP analysis of all the cells established an average half-time recovery of FtsZ molecules in the Z ring of 5.2 ± 0.2 seconds (see graph in Figure 5.10), which is *1.6-fold* slower than the control cells. This difference in FtsZ turnover was shown to be statistically significant when a t-test was applied using GraphPad Prism 5 software. This work suggests that the absence of FtsA results in a small but significant decrease in FtsZ turnover in the Z ring.

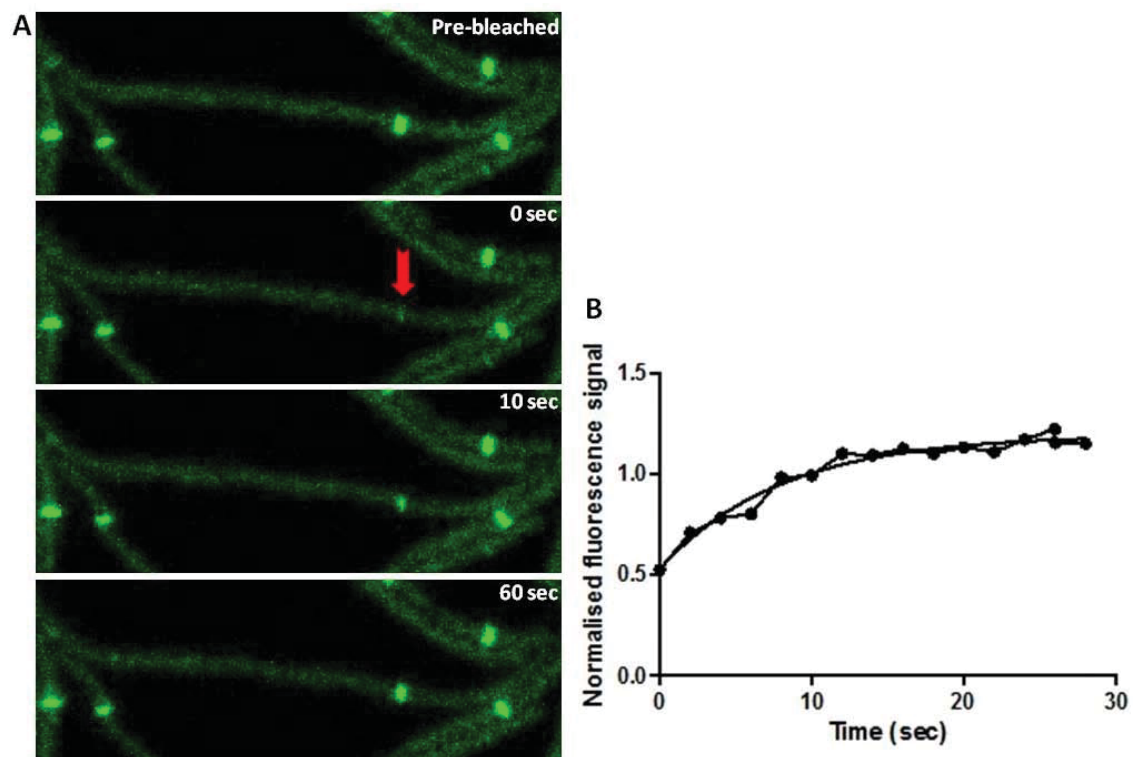


Figure 5.9 FRAP of a Z ring in *ftsA*-depleted FtsZ-GFP *B. subtilis* cell. **(A)** Time-lapse series of fluorescence images show the time course of recovery. The red arrow shows the ring bleached. Images were taken every 2 sec using a Nikon A1 Confocal microscope under a CFI Apo TIRF (100 \times NA 1.49, Nikon) objective lens and were analysed with NIS-Elements Software. **(B)** Intensity of the photobleached region overtime. The data points have been corrected for background and photobleaching during the acquisition period. The points represent the fluorescence data, and the solid line is the predicted recovery curve given the first-order rate constant, k . The recovery half time for this series was 5.1 sec.

When analysing the cells, it came to our attention that the half-time of recovery seemed to vary with the cell length, with the Z rings in longer cells taking longer to recover. It seemed plausible that shorter cells will have newer Z rings; while the Z rings in longer

cells would have been there for more cell cycles. To understand if the age of the Z rings (assumed by the length of the cells from last data) could influence its dynamics the data was reorganised according to cell lengths. The cells shorter than 10 μm (10 cells) presented an average cell length of $7.7 \pm 0.22 \mu\text{m}$ and a half-time of recovery of 3.9 ± 0.4 seconds, which is not statistically significant compared to control values. However, cells that are longer than 10 μm (47 cells) had an average cell length of $22.3 \pm 0.98 \mu\text{m}$ and an average half-time of recovery of 5.5 ± 0.2 seconds. In this case, the difference is statistically relevant when comparing to control values, raising it to *1.7-fold* slower than cells with FtsA present. This further suggests that FtsA can affect the FtsZ turnover in the Z rings, since in its absence the assembled Z rings have a significantly lower turnover of FtsZ.

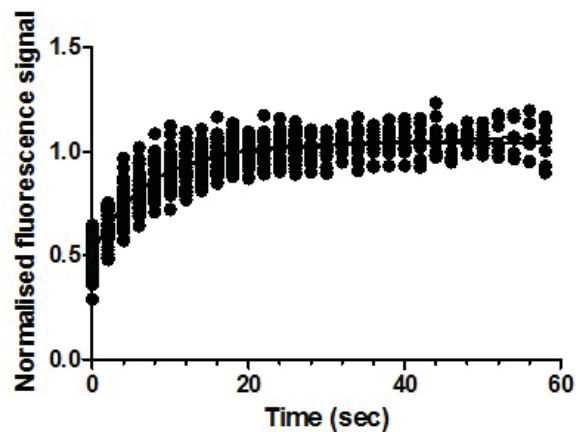


Figure 5.10 Overall FRAP in Z ring fluorescence intensity for *B. subtilis* cells (*ftsA*-depleted *ftsZ-gfp*). SU638 cells presented an average cell length of $19.7 \pm 1.09 \mu\text{m}$ and the average recovery half time of FtsZ molecules in the Z ring for this strain was 5.2 sec (57 cells analysed).

5.3 Discussion

The results in Chapter 3 and Chapter 4 point to the possibility that FtsA is required for Z ring constriction. In this chapter, this possibility was examined more directly; firstly by investigating the fate of the Z rings that form and persist during the cell cycle in the absence of FtsA, and secondly by examining the rate of FtsZ turnover in the Z ring in the absence of FtsA. Time-lapse microscopy of FtsA-depleted cells demonstrated that

some Z rings can undergo normal, albeit slower, constriction with apparently normal septum formation and separation of cells. However, in most cells lacking FtsA the Z rings followed different fates. In some cases (15%), the Z ring constriction process appeared to be very slow, causing a significant delay in cell division. Although it is not possible to determine exactly how much longer it takes to constrict, it seems to be delayed by at least an hour compared to wild-type cells. The minimum time before a Z ring constricts in wild-type cells was ~60 minutes (Figure 5.3), while in the absence of FtsA the Z rings persist for at least 129 minutes (Figure 5.5). In other cases, Z rings persisted in the cells for long periods of time without any noticeable constriction. Yet, others appeared to disassemble without constriction, or even constricted without visible cell separation. Together these observations indicate that, in the absence of FtsA, constriction is either significantly delayed or never occurs, and results in destabilisation of the Z ring.

To gain more molecular insight into the involvement of FtsA in Z ring constriction, the rate of FtsZ turnover in FtsA-depletion mutant Z rings was investigated using FRAP. This line of approach was in part propelled by the observations made in the time-lapse studies, as well as the idea that a certain level of FtsZ turnover appears to be required for Z ring constriction (Li *et al.*, 2007; Adams and Errington, 2009; Mingorance *et al.*, 2010; Osawa and Erikson, 2011). FtsA, through its direct interaction with FtsZ may be altering the rate of turnover in the Z ring (i.e. slowing it down), such that constriction is not as efficient. FRAP analysis demonstrated that the rate of FtsZ turnover in the Z rings is 1.6-fold slower in FtsA-depleted cells. Importantly, although the difference in the turnover rate is small, it is significant, and it may be enough to cause an effect on Z ring constriction. Also, the decrease in FtsZ turnover in the ring is more significant in longer cells, possibly because the Z rings have been present in the cells for long periods of time. This exciting result points to the role of FtsA in promoting efficient Z ring constriction.

What is the significance of the observations described above, regarding the fates of the Z rings and the FtsZ turnover rates, in light of what is currently known about Z ring constriction? Furthermore, is it possible to extrapolate about the role for FtsA in Z ring constriction? To attempt an answer to these questions, the following sections deal with distinct possibilities regarding the role that FtsA might play in the Z ring constriction.

5.3.1 FtsA may directly affect Z ring constriction by influencing FtsZ dynamics within the ring

Z ring constriction is inefficient in the absence of FtsA. How might FtsA ensure efficient constriction of the Z ring? One possibility is that FtsA has a direct role in the process of constriction through its direct interaction with FtsZ. This interaction could either assist with FtsZ turnover in the Z ring, affecting its dynamics; or provide a membrane tether for the Z ring that is required for its contraction.

5.3.1.1 Affecting FtsZ turnover during constriction

The data collected from the FRAP experiments presented in this chapter point to the possibility that FtsA is required for rapid turnover of FtsZ in the Z ring during its constriction. Z ring constriction is a complex process and several models have been put forward to explain it (see General Introduction, Chapter 1). A common central aspect of these models is that Z ring constriction is dynamic. The dynamic nature of Z ring constriction is in part related to the fact that FtsZ monomers are continuously being exchanged within the FtsZ protofilaments (Mukherjee and Lutkenhaus, 1994; Mukherjee and Lutkenhaus, 1998). In the study from Anderson *et al.* (2004), the FtsZ turnover rates in the Z rings of *ezrA* and *minCD* mutant cells of *B. subtilis* were statistically significantly decreased, and to similar extents to the rates presented for *ftsA* mutant in this Chapter (1.5-1.75-fold and 1.6-fold slower, respectively). This small but significant change in FtsZ turnover lead the authors to suggest that it would only cause modest effects on Z ring dynamics, and that a possible role in FtsZ turnover would not be sufficient to affect the assembly and disassembly of FtsZ protofilaments in the Z rings (Anderson *et al.*, 2004). However, several *in vitro* and *in vivo* observations suggest that the FtsZ-binding proteins tested above are important in Z ring assembly rather than constriction. EzrA is a negative regulator of the Z ring, acting before and during Z ring assembly; ZapA is a positive regulator of the Z ring, promoting lateral association of FtsZ protofilaments during Z ring formation; and MinC is part of an inhibitory system of the Z ring (the Min system) that acts at the cell poles before Z ring formation and at midcell once the Z ring is formed to prevent extra Z rings in this region (Gueiros-

Filho and Losick, 2002; Haeusser, *et al.*, 2004; Gregory *et al.*, 2008). The current work presented in this thesis has shown that, in contrast to these proteins, the absence of FtsA seems to act towards the later stages of division, affecting Z ring constriction, not its assembly. Although speculative, it is possible that the FtsZ turnover during constriction may be different from that during the early stages of Z ring assembly. In this case, the effect of the FtsZ-interacting proteins in the FtsZ turnover can also be different, thus separating the effect of FtsA in Z ring dynamics from that of other studied division proteins.

FtsA may be assisting in the FtsZ turnover needed for Z ring dynamics during constriction. One way it might achieve this could be through its ATPase activity that, together with the GTP-hydrolysis of FtsZ, could drive the dynamics and subsequent constriction of Z rings (de Boer *et al.*, 1992; Ray-Chaudhuri and Park, 1992; Mukherjee *et al.*, 1993; Shapiro, 1993). An interesting characteristic of FtsA is its ability to bind and hydrolyse ATP (Feucht *et al.*, 2001). Beuria *et al.* (2009) demonstrated that a hypermorphic *E. coli* mutant of FtsA (FtsA*) was able to partially disassemble pre-formed FtsZ polymers *in vitro*, which transitioned from long, straight polymers to short, curved protofilaments. This effect was dependent on ATP or ADP binding to FtsA*. Wild-type FtsA did not show the same effect on the FtsZ polymers, but that might indicate that under normal cellular conditions, FtsA may depend on other factors for its ATP hydrolysis activation. It is therefore possible that the FRAP analysis results, i.e. the slower FtsZ turnover rate seen in FtsA-depleted cells, could be due to the absence of the ATPase activity of FtsA. This further suggests that the ATPase activity of FtsA might affect the length distribution of FtsZ polymers within the ring, assisting with the constant remodelling of the Z ring necessary for proper Z ring constriction.

5.3.1.2 Tethering the Z ring to the cell membrane during constriction

Another way for FtsA to directly affect the process of Z ring constriction could be by providing a membrane tether for the Z ring, required for its contraction. It is known that FtsA has a conserved C-terminal amphipathic helix that anchors the protein to the membrane, and essential for its function in *E. coli* (Pichoff and Lutkenhaus, 2005). Also, FtsA binds to the C-terminal peptide of FtsZ (Ma and Margolin, 1999; Pichoff and

Lutkenhaus, 2007). Thus, FtsA tethers FtsZ to the membrane. The hypothesis raised here is that this tethering of FtsZ to the membrane by FtsA is essential for efficient Z ring constriction. Osawa *et al.* (2008) cleverly showed that FtsZ could form a constricting Z ring in liposomes, as long as a direct tether to the membrane was provided. This experiment was done without FtsA, but showed that for normal cell division FtsZ requires a membrane-targeting amphipatic helix, most likely from FtsA. Since it has been shown earlier in this thesis that FtsA is not required for Z ring assembly, it seems plausible to assume that the requirement of the membrane anchor of FtsA is mostly important for Z ring constriction.

Further supporting this suggestion is the most intriguing of the observed Z ring fates in the absence of FtsA, the apparently normal constriction of Z rings in the absence of septation. This phenotype, observed in 23% of the analysed cells, was unexpected and it would be difficult to predict from what was observed in outgrown spores, since this constriction did not result in visible septation or in any cell defect visible in isolated microscopy images. This phenotype seems to support a role for FtsA in coupling Z ring constriction with cell wall ingrowth. The anchoring of the Z ring to the membrane could then occur directly by FtsA, while the interaction with the cell envelope could occur indirectly between FtsA and some peptidoglycan-binding proteins. Because FtsA has a transmembrane anchor, it may act as a connection between the septal cell wall synthesising machinery and Z ring constriction. One possible protein for this interaction is YpsB. YpsB (or GpsB) is a newly discovered division protein that localises at the divisome significantly after Z ring formation and is required for recruitment of PBP1 to the divisome in *B. subtilis* (Claessen *et al.*, 2008). Interestingly, *ypsB* has a synthetic effect when combined with an *ftsA* mutation (Tavares *et al.*, 2008). These observations suggest that YpsB contributes to efficient septum formation, by regulating septal wall synthesis; a function possibly impaired in the absence of FtsA (Tavares *et al.*, 2008). Therefore, YpsB may interact with FtsA, assisting in its ability to influence Z ring constriction, while linking it to cell wall synthesis.

5.3.2 FtsA may affect Z ring constriction through effects on the conformation or activity of other divisome proteins

If FtsA is not directly involved in FtsZ turnover in the Z ring, another possible explanation for the inefficient Z ring constriction could be that FtsA is required to ensure the correct divisome assembly, necessary for proper Z ring constriction. As already discussed in Chapter 4, there is a possibility that, in the absence of FtsA, one or more divisome components downstream of DivIB are not being recruited to midcell, disabling Z ring constriction. Some examples already referred to in Chapter 4 include peptidoglycan-binding proteins (PBPs) or YpsB. Another possibility is that all divisome components are recruited, but one or more of those are incapable of interacting with FtsZ in the absence of FtsA to enable efficient constriction.

5.3.2.1 FtsA might be required to recruit MinC and thereby allow Z ring constriction

As already mentioned in Chapter 4, it is possible that the divisome complex is not properly assembled in the absence of FtsA, suggesting that FtsA is required for the recruitment of a divisome protein downstream of DivIB. The idea raised here is that the absence of FtsA may be reducing the efficiency of Z ring constriction by preventing some later-acting division protein to carry out its role during Z ring constriction.

One hypothesis is that FtsA keeps DivIVA, and thus MinC, at the division site, counteracting their inhibitory activity, and helping to promote efficient constriction. Work from Gregory *et al.* (2008) shows that, while not as long as *ftsA*-deletion cells, cells lacking *minCD* are also long. One of the reasons that *minCD* mutant cells are longer is because the interdivisional times in these cells are variable and very heterogeneous relative to wild-type. This raised the possibility that Z rings in the absence of Min are staying for long periods of time at the division site (Gregory *et al.*, 2008). This suggests that Min is required to control the timing of Z ring constriction. Min's role in constriction is further highlighted by the fact that MinC-GFP is observed on both sides of the Z ring, and appears to rotate around the Z ring (Gregory *et al.*, 2008). Their *minCD* mutant phenotype is quite similar to what is observed in the

absence of FtsA, with Z rings persisting at the midcell site until eventual constriction. It is possible that FtsA has a similar role to MinC in promoting Z ring constriction. If DivIVA is not localising at midcell in the absence of FtsA (hypothesis already discussed in section 4.3), it would compromise the recruitment of MinC and inhibit proper cell division by delaying Z ring constriction.

Another related possibility is that, in the absence of FtsA, the competition between positive and negative regulators is not efficient. For example, in *E. coli*, overproduction of MinCD has been shown to displace FtsA from the Z ring, probably by competing with the conserved C-terminal tail of FtsZ, and eventually resulting in the disruption of the Z ring (Shen and Lutkenhaus, 2009). Without FtsA to compete with MinC for the interaction with FtsZ polymers (Pichoff and Lutkenhaus, 2005; Shen and Lutkenhaus, 2009), a more effective division inhibition occurs in the cells. Furthermore, it has been shown by Dajkovic *et al.* (2008) that MinC reduces the integrity of FtsZ protofilaments by preventing lateral interactions. As suggested earlier, FtsA may be controlling cellular balance of the lateral association/dissociation of FtsZ protofilaments during constriction, by counteracting the inhibitory activity of Min in the lateral associations between FtsZ polymers (Dajkovic *et al.*, 2008).

Lastly, a recent publication by van Baarle and Bramkamp (2010) suggests an interesting role for Min system that supports the need for competition between positive and negative regulators of the Z ring. They propose that the main role for the Min system is to ensure that only one round of cell division occurs per cell cycle. It is proposed that Min achieves this by preventing the formation of minicells through promoting the disassembly of the divisome just after cytokinesis (van Baarle and Bramkamp, 2010). In other words, the absence of FtsA could enhance the inhibitory function of the Min system, affecting Z ring constriction.

This chapter presents new information regarding the defects that the absence of FtsA causes in Z ring dynamics and raises a few possibilities regarding how FtsA is involved in the process of Z ring constriction. There are currently different models that attempt to explain the mechanisms behind the process of Z ring constriction (Ghosh and Sain, 2008; Strahl and Hamoen, 2010; Erickson *et al.*, 2010; Mignorance *et al.*, 2010); however, more information is needed for a complete understanding of the subject. In light of the above results and suggestions, it can be strongly hypothesised that FtsA has

a role in Z ring constriction. This role can be through a direct interaction with FtsZ, assisting the FtsZ turnover in the Z ring, or providing a membrane tether for the Z ring required for its contraction. It is also hypothesised FtsA has an indirect effect on Z ring constriction, most probably by ensuring the correct divisome assembly or even making the interaction of some divisome components to FtsZ accessible.

Chapter 6

§

General Discussion

Bacterial cell division involves the formation of a septum at midcell between two replicated chromosomes. Division begins with the polymerisation of FtsZ into a Z ring, followed by the assembly of several division proteins forming a complex, the divisome. The Z ring eventually constricts as the septum forms during cytokinesis. Formation and constriction of the Z ring involves a complex network of regulatory proteins and mechanisms to ensure the spatial and temporal control of the events. During the last 20 years, extensive research has been carried out using both *in vivo* and *in vitro* approaches, with focus on the Z ring as the key player of cell division. Although comprehensive information has been gathered from various laboratories, it is still unclear how many of the Z ring-related processes occur and how they are regulated.

The work presented in this thesis focuses on the role of FtsA, a highly conserved division protein, and how it affects the Z ring and the process of cell division in the Gram-positive model organism, *B. subtilis*. Prior to this work, most of the studies concerning FtsA were done in *E. coli*, the Gram-negative model organism. These studies identified several important features of FtsA, most of them cautiously extrapolated to other organisms. Studies on *E. coli* also proposed three separate functions for FtsA in cell division, namely in Z ring assembly, divisome recruitment and Z ring constriction. However, the *B. subtilis ftsA* null phenotype and the cell division differences between the organisms hint that the role of FtsA may not be exactly the same in the two organisms. Studies examining the function of FtsA in *B. subtilis* had been the subject of studies initiated approximately 20 years ago, and very few had been performed during the last decade. As a result, this important division protein is still poorly understood. It had been proposed that FtsA, an early division protein, promotes Z ring assembly and stability by directly interacting with FtsZ. However, its exact role in *B. subtilis* was elusive.

The last comprehensive study regarding *B. subtilis* FtsA was done by Jensen *et al.* (2005), and was performed in the same group as this present thesis. They showed that the absence of FtsA in *B. subtilis* cells caused a significant decrease infrequency of Z ring formation (only 10% of Z rings were formed) and cell filamentation (~3-fold longer than wild-type). The conclusion at the time was that FtsA was required for efficient Z ring assembly in *B. subtilis* (Jensen *et al.*, 2005). However, the presence of some Z rings in the cells and the cause for the filamentous phenotype of *ftsA* null cells were not

elucidated. The starting point of the present work was this gap in the knowledge of why so few *Z* rings are formed in the absence of FtsA in vegetative cells and what this can tell us about the function of FtsA in *B. subtilis*.

To address these questions it was crucial to investigate the origin of the *ftsA* null phenotype (Chapter 3). Normally, filamentous phenotypes are caused by the accumulation of defects throughout several vegetative cell cycles. To examine the formation of the first *Z* ring in cells with the absence of FtsA, it is highly advantageous to employ a system that is uncomplicated by previous division events, such as the spore outgrowth system. Thus, the first round of cell division following spore germination in *B. subtilis* was analysed in *ftsA*-deleted cells. Surprisingly, in the absence of FtsA, the first *Z* rings formed with wild-type efficiency. An immediate conclusion was that there is no absolute requirement of FtsA for efficient *Z* ring formation. This contradicts the assumed role for FtsA in *B. subtilis* in *Z* ring assembly and brings some speculation about what is tethering the *Z* ring to the membrane. It has been shown that in *E. coli* FtsA serves as the principal membrane anchor for the *Z* ring, although ZipA also shares this function (Pichoff and Lutkenhaus, 2005). Since FtsA is also a membrane-binding protein and it has been shown to interact with FtsZ before *Z* ring formation in *B. subtilis*, it was assumed that it would be responsible for such a function in this organism too (Jensen et al., 2005). Proteins such as SepF or EzrA are potentially good candidates for this role, but some observations, such as SepF being a cytoplasmic protein and a *sepF ezrA* double mutant still being able form *Z* rings in *B. subtilis* (Hamoen et al., 2006), seem to discard them as essential for tethering the *Z* ring. Since it has been shown that FtsA is also not required for such role during *Z* ring assembly, this important event in cell division in *B. subtilis* is still not elucidated.

Another interesting observation is that, despite efficient *Z* ring formation in *ftsA*-deleted cells, the *Z* rings did not constrict immediately. In fact, they persisted into the second cycle of division, unlike wild-type cells that showed *Z* ring constriction and septum formation (see diagram in Figure 3.9). This observation hinted that *Z* ring constriction may be severely affected in the absence of FtsA, thus pointing to a novel perspective on the function of this protein in *B. subtilis*. It was also important to exclude the possibility that the efficient formation of the first *Z* ring in outgrown spores, in the absence of FtsA, was caused by a unique characteristic of the spore outgrowth system. Thus, FtsA was

transiently depleted in vegetatively-growing cells and the same fate of Z rings was observed, confirming that the formation of the first Z rings was not due to the spore outgrowth system. The results obtained here, with the observation of the formation of the first Z rings in the cells, emphasise how misleading a phenotype can be if its origin is not properly investigated.

At this point in the work, it was important to examine the fate of Z rings once they are formed in the absence of FtsA. According to the observed roles in the literature for FtsA in *E. coli* (Pichoff and Lutkenhaus, 2002; Corbin *et al.*, 2004; Rico *et al.*, 2004), and suggested in *B. subtilis* (Errington *et al.*, 2003), FtsA is responsible for the recruitment of the later division proteins to the Z ring. DivIB was used as a reference for divisome assembly at midcell in the absence of FtsA and the efficiency and timing of its recruitment became the focus of the work presented in Chapter 4. Notably, the results obtained with the spore outgrowth system revealed that DivIB, and presumably the other later-assembly proteins, localises to the midcell site with wild-type efficiency in the absence of FtsA. It is important to note that some localisation of divisome components was expected to occur since cell division is impaired, but still occurs in *ftsA* mutants of *B. subtilis*. The important observation of this work is that wild-type levels of DivIB assembly occurred in the absence of FtsA. However, it was verified that there was a notable delay in the DivIB recruitment process under these conditions. These facts are suggesting that, rather than being required for the localisation of DivIB, FtsA is required for the correct timing of its localisation. The existence of a conserved sub-complex of later division proteins seems to validate the extrapolation of the results presented here for DivIB localisation to other proteins as DivIC, FtsL and PBP 2B (Daniel *et al.*, 2000; Goehring and Beckwith, 2005; Gamba *et al.*, 2009). Furthermore, the requirement of late division proteins by FtsA in *E. coli* can be bypassed by the premature targeting of the division protein FtsQ to the Z ring (Goehring *et al.*, 2005), thus restoring localisation of downstream proteins in cells lacking FtsA and/or FtsK.

However, the same assumption made above, regarding the recruitment of downstream proteins of DivIB, cannot be made for other division proteins that are known to assemble to the Z ring later than the above-mentioned sub-complex, and are dependent on it. An example is the DivIVA protein that localises at the division site slightly after the localisation of other late division proteins (Gamba *et al.*, 2009). Therefore, it is

possible that, without the presence of FtsA at midcell, DivIVA localisation and function is obstructed. A follow up work on this matter will be of most importance. As an extension of the study of divisome assembly in the absence of FtsA, septum formation was also analysed. Despite the normal efficiency of DivIB recruitment, and presumably the other later-assembling division proteins, septation was still significantly inefficient in absence of FtsA.

Overall, the results presented in Chapters 3 and 4 expose FtsA as a key protein in the later stages of cell division in *B. subtilis*, possibly in Z ring constriction during cytokinesis. Two phenotypic observations were considered at this stage. First, an *ftsA* deletion is not lethal to the cells; however, cell division occurs at low frequency. Therefore, Z ring constriction is inefficient but still happens when FtsA is absent. Second, the frequency of Z rings observed between outgrown spores and vegetative cells is very different. It became clear that to better understand how the absence of FtsA affects the process of Z ring constriction, the fate of the initially-formed Z rings needed to be determined. In Chapter 5, a time-lapse fluorescence microscopy approach was used to visualise the fate of individual Z rings in filamentous FtsA-depleted cells. Four different fates for the Z ring were observed. These include normal but slower Z ring constriction, disassembly of the Z ring, persistence of the Z ring for long periods of time without constriction, and possible Z ring constriction without septation (time-lapse movies of each Z ring fate are available as supplementary material). Taken together, these observations showed that, in the absence of FtsA, constriction is either significantly delayed or never occurs, resulting in destabilisation of the Z ring. Therefore, FtsA is required for efficient Z ring constriction in *B. subtilis*.

When studying the Z ring it becomes clear that the dynamics of this bacterial structure are vital for its functionality (Erickson, 2009). Following this notion, it became imperative to further analyse these dynamics in an attempt to identify how FtsA affects Z ring constriction. A certain level of FtsZ turnover appears to be required for Z ring constriction (Li *et al.*, 2007; Osawa and Erikson, 2011). This knowledge, together with the observations made earlier of defective Z ring constrictions in the absence of FtsA, propelled the hypothesis that FtsA may be affecting constriction by altering the FtsZ turnover in the Z rings. To validate this idea, the rate of FtsZ turnover in Z rings of *ftsA* mutant cells was investigated using FRAP. This analysis demonstrated that FtsZ

turnover in the Z ring decreases in the absence of FtsA. Although small, a difference of 1.6-fold slower rate was calculated to be significant and it may be enough to cause an effect on Z ring constriction; or even perhaps it may be delaying the recruitment of the late division proteins as discussed in Chapter 4.

Collectively, the novel results from Chapter 5 favour a role for FtsA in promoting efficient Z ring constriction. However, the mechanism behind it is still not clear. Several possibilities were raised, taking into account what is known and carefully extrapolating with comparative data (discussed in Section 5.3, Chapter 5). In a succinct manner, the key possibilities discussed were divided between a direct or indirect role for FtsA in Z ring constriction. In a direct role, FtsA may be assisting in FtsZ turnover in the Z ring, thus affecting its dynamics; or in providing a membrane tether for the Z ring required for its contraction. On the other hand, FtsA may be acting indirectly on Z ring constriction, ensuring the correct assembly of other divisome proteins, or even enabling them to efficiently interact with FtsZ. Critically, it is important to acknowledge that there is most probably an overlap of these functions. A common aspect of several essential proteins is the ability to provide the cell with different functions. Another important characteristic to consider is that some of the cell division genes are redundant and can be deleted without a significant effect to cell division. However, only when combined with other essential genes are their roles often revealed. This makes the overall cell division process more efficient, and the study of the individual protein functions much more complicated.

Of all the new data collected, one observation already discussed above that was particularly interesting; the initial observation of wild-type efficiency formation of the first Z rings in the absence of FtsA. It became clear that Z ring assembly and its tethering to the membrane do not require FtsA. When taking into account that *B. subtilis* does not have a ZipA homolog and that simultaneous deletion of *ftsA* and *eZR*A still produces Z rings, what is tethering Z ring to the membrane? Does the Z ring really require a physical anchoring to the membrane or can the Z ring be stably formed without it? Also, can the anchoring of the Z ring to the membrane differ depending on the stage of cell division? The observation of Z ring constriction without septation, a phenotype visualised during time-lapse microscopy in 23% of the cells, seems to point to a requirement for FtsA in coupling Z ring constriction with cell wall ingrowth. In

fact, bacteria that don't have FtsZ don't have FtsA either, and this may highlight the importance of the interaction between these two proteins, further suggesting a role for FtsA in coupling Z ring constriction with septal peptidoglycan synthesis. A second piece of evidence that supports this role for FtsA is the observation of abnormally thin polar (asymmetric) septa formed in a *B. subtilis ftsA* mutant during sporulation (Kemp *et al.*, 2002). This phenotype lead to the suggestion that FtsA may be playing two distinct roles, depending on the cell cycle processes, most likely in connecting Z ring constriction with cell wall synthesis. A daring but interesting idea would be that the requirement for FtsA during Z ring constriction, besides physically anchoring it, would be to work as a motor for the constriction process to occur. The polymerisation of FtsA and its ATPase hydrolase activity could be involved in delivering the necessary force for efficient Z ring constriction. This line of thought should be developed and tested in the laboratory in the future.

An obvious question arises from the observations of the spore outgrowth system in the absence of FtsA. Since FtsA is not required for Z ring assembly, why is there only one Z ring per cell in the absence of FtsA? All the strains used have normal expression of FtsZ; so it is safe to assume that this result is not due to inappropriate levels of FtsZ. Perhaps even though FtsA is not required for Z ring formation during spore outgrowth, it appears to rely on constriction of Z rings to form the next ones. This suggests that a defect in Z ring constriction, caused by the absence of FtsA, prevents subsequent Z ring assembly. This would explain why vegetative cells contain fewer Z rings in the absence of FtsA. The proposed speculation is that the inability of Z rings to constrict causes a shortage of cytoplasmic FtsZ that is available for new Z ring formation at the future division sites. In other words, for new Z ring formation is essential that the FtsZ from the constricting Z ring is recycled into the new Z ring. In the absence of FtsA, during spore outgrowth, the first Z ring is able to form normally because there is no previous Z ring from which FtsZ needs to be recycled. In the absence of this recycling mechanism, subsequent Z rings are not able to form. Following this idea, it is possible that the FtsZ constituent of the Z ring, which has been through the processes of polymerisation and dynamic turnover, acts differently to that in the cytoplasmic pool. To gain some insight into this theory, future work could be done using photo-convertible fluorescent proteins linked to FtsZ. This technique would allow the analyses of the trajectory and fate of FtsZ from the constricting Z ring out into the cytoplasm and possibly into a new Z ring,

in the presence and absence of FtsA (Matsuda *et al.*, 2008; Hoi *et al.*, 2010; Patterson *et al.*, 2010). It is also important to keep in mind that it might not just be an issue of FtsZ recycling the previous ring but the FtsA activity that specifically affects its; otherwise the same phenotype would also be seen with other division mutants. One possibility is that FtsA controls the number of Z rings forming at any one time.

In conclusion, the data gathered in this thesis adds a significant contribution to the general knowledge of one of the most important proteins in bacterial cell division; further enlightening the role for FtsA in *B. subtilis* cell division. It also clearly reveals that *B. subtilis* FtsA has more in common with *E. coli* FtsA than previously thought. It is shown for the first time that FtsA is not required for Z ring assembly in *B. subtilis* and its role in divisome recruitment seems to be only related to the correct timing of assembly. Furthermore, FtsA is essential for efficient Z ring constriction.

Supplementary Material

Accompanying this thesis is a CD containing four movies that correspond with the time-lapse microscopy images presented in Chapter 5. The movies are in Audio Video Interleave (AVI) format. The movies include all acquired images from each time-lapse, inclusive of images of lesser quality (unfocused).

Figure S5.1 Movie corresponds with the time-lapse microscopy presented in Figure 5.3. The movie shows normal Z ring constriction in *B. subtilis* SU570 (*ftsZ-gfp*) cells. Images were acquired at 5-min intervals over a 150-min period.

Figure S5.2 Movie corresponds with the time-lapse microscopy presented in Figure 5.4. The movie shows two different Z ring constriction fates in *B. subtilis* SU638 (FtsA-depletion) cells. The top cell shows a non-constricting Z ring that persists for longer than wild-type Z rings, while the bottom cell shows a Z ring disassembling and then disappearing. Images were acquired at 5-min intervals over a 140-min period.

Figure S5.3 Movie corresponds with the time-lapse microscopy presented in Figure 5.5. It should be noted that this movie shows a 90° rotation from time-lapse images presented in Chapter 5. The movie shows a slow constricting Z ring, but with no apparent cell wall constriction, in a *B. subtilis* SU638 (FtsA-depletion) cell. Images were acquired at 5-min intervals over a 130-min period.

Figure S5.4 Movie corresponds with the time-lapse microscopy presented in Figure 5.6. The movie shows a constricting Z ring in a *B. subtilis* SU638 (FtsA-depletion) cell. The new Z rings are then observed to assemble in the corresponding daughter cells, within 60 minutes. Images were acquired at 5-min intervals over a 150-min period.

References

- Adams, D. W. and Errington, J. (2009) Bacterial cell division: assembly, maintenance and disassembly of the Z ring. *Nature Reviews Microbiology* 7: 642-653.
- Addinall, S. G. and Holland, B. (2002) The tubulin ancestor, FtsZ, draughtsman, designer and driving force for bacterial cytokinesis. *Journal of Molecular Biology* 318: 219-236.
- Addinall, S. G., Bi, E. and Lutkenhaus, J. (1996) FtsZ ring formation in *fts* mutants. *Journal of Bacteriology* 178: 3877-3884.
- Alexeeva, S., Gadella, T. W. J., Verheul, J., Verhoeven, G. S. and den Blaauwen, T. (2010) Direct interactions of early and late assembling division proteins in *Escherichia coli* cells resolved by FRET. *Molecular Microbiology* 77(2): 384-398.
- Allard, J. F. and Cytrynbaum E. N. (2009) Force generation by a dynamic Z ring in *Escherichia coli* cell division. *Proceedings of the National Academy of Sciences of the United States of America* 106(1): 145-150.
- Anderson, D. E., Gueiros-Filho, F. J. and Erickson, H. P. (2004) Assembly dynamics of FtsZ rings in *Bacillus subtilis* and *Escherichia coli* and effects of FtsZ-regulating proteins. *Journal of Bacteriology* 186: 5775-5781.
- Axelrod, D., Koppel, D. E., Schlessinger, J., Elson, E., and Webb, W. (1976) Mobility measurement by analysis of fluorescence photobleaching recovery kinetics. *Biophysical Journal* 16: 1055-1069.
- Barák, I., Muchova, K., Wilkinson, A. J., O'Toole, P. J. and Pavlendova, N. (2008) Lipid spirals in *Bacillus subtilis* and their role in cell division. *Molecular Microbiology* 68(5): 1315-1327.
- Barák, I., Ricca, E. and Cutting, S. M. (2005) From fundamental studies of sporulation to applied spore research. *Molecular Microbiology* 55: 330-338.
- Beall, B. and Lutkenhaus, J. (1989) Nucleotide sequence and insertional inactivation of a *Bacillus subtilis* gene that affects cell division, sporulation, and temperature sensitivity. *Journal of Bacteriology* 171(12): 6821-6834.
- Beall, B. and Lutkenhaus, J. (1991) FtsZ in *Bacillus subtilis* is required for vegetative septation and for asymmetric septation during sporulation. *Genes and Development* 5: 447-455.
- Beall, B. and Lutkenhaus, J. (1992) Impaired cell division and sporulation of a *Bacillus subtilis* strain with the *ftsA* gene deleted. *Journal of Bacteriology* 174: 2398-2403.

- Beall, B., Lowe, M. and Lutkenhaus, J. (1988) Cloning and characterization of *Bacillus subtilis* homologs of *Escherichia coli* cell division genes *ftsZ* and *ftsA*. *Journal of Bacteriology* 170(10): 4855-4864.
- Begg, K. J. and Donachie W. D. (1985) Cell shape and division in *Escherichia coli*: Experiments with shape and division mutants. *Journal of Bacteriology* 163: 615-622.
- Begg, K., Nikolaichik, Y., Crossland, N. and Donachie, W. D. (1998) Roles of FtsA and FtsZ in activation of division sites. *Journal of Bacteriology* 180: 881-884.
- Beuria, T. K., Mullapudi, S., Mileykovskaya, E., Sadasivam, M., Dowhan, W. and Margolin, W. (2009) Adenine nucleotide-dependent regulation of assembly of bacterial tubulin-like FtsZ by a hypermorph of bacterial Actin-like FtsA. *ASBMB The Journal of Biological Chemistry* 284(21): 14079–14086.
- Ben-Yehuda, S. and Losick, R. (2002) Asymmetric cell division in *Bacillus subtilis* involves a spiral-like intermediate of the cytokinetic protein FtsZ. *Cell* 109: 257-266.
- Bermudes, D., Hinkle, G. and Margulis, L. (1994) Do prokaryotes contain microtubules? *Microbiological Reviews* 58: 387-400.
- Bernhardt, T. G. and de Boer, P. A. (2005) SlmA, a nucleoid-associated, FtsZ binding protein required for blocking septal ring assembly over chromosomes in *Escherichia coli*. *Molecular Cell* 18: 555-564.
- Bi, E. and Lutkenhaus, J. (1991) FtsZ ring structure associated with division in *Escherichia coli*. *Nature* 354: 161-164.
- Bork, P., Sander, C. and Valencia, A. (1992) An ATPase domain common to prokaryotic cell cycle proteins, sugar kinases, actin, and Hsp70 heat shock proteins. *Proceedings of the National Academy of Sciences of the United States of America* 89: 7290-7294.
- Bramhill, D. (1997) Bacterial cell division. *Annual Review of Cellular Biology* 13: 395-424.
- Bramhill, D. and Thompson, C. M. (1994) GTP-dependent polymerization of *Escherichia coli* FtsZ protein to form tubules. *Proceedings of the National Academy of Sciences of the United States of America* 91: 5813-5817.
- Bramkamp, M., Emmins, R., Weston, L., Donovan, C., Daniel, R. A. and Errington, J. (2008) A novel component of the division site selection system of *Bacillus subtilis* and a new mode of action for the division inhibitor MinCD. *Molecular Microbiology* 70: 1556-1569.

- Buddelmeijer, N. and Beckwith, J. (2004) A complex of the *Escherichia coli* division proteins FtsL, FtsB and FtsQ forms independently of its localization to the septal region. *Molecular Microbiology* 52: 1315-1327.
- Callister, H. (1982) The initiation of cell division in *Bacillus subtilis*. PhD Thesis, University of Sydney, Australia.
- Callister, H. and Wake, R. G. (1974) Completed chromosomes in thymine-requiring *Bacillus subtilis* spores. *Journal of Bacteriology* 120: 579-582.
- Cha, J. H. and Stewart, G. C. (1997) The *divIVA* minicell locus of *Bacillus subtilis*. *Journal of Bacteriology* 179: 1671-1683.
- Chauhan, A., Madiraju, M. V. V. S., Fol, M., Lofton, H., Maloney, E., Reynolds, R. and Rajagopalan, M. (2006) *Mycobacterium tuberculosis* cells growing in macrophages are filamentous and deficient in FtsZ rings. *Journal of Bacteriology* 188: 1856-1865.
- Chen, Y. and Erickson, H. P. (2005) Rapid in vitro assembly dynamics and subunit turnover of FtsZ demonstrated by Fluorescence Resonance Energy Transfer. *Journal of Biological Chemistry* 280: 22549-22554.
- Cho, H., McManus, H. R., Dove, S. L. and Bernhardt, T. G. (2011) Nucleoid occlusion factor SlmA is a DNA-activated FtsZ polymerization antagonist. *Proceedings of the National Academy of Sciences of the United States of America* 108: 3773-3778.
- Chung, K., Hsu, H., Govindan, S. and Chang, B. (2004) Transcription regulation of *ezrA* and its effect on cell division of *Bacillus subtilis*. *Journal of Bacteriology* 186(17): 5926-5932.
- Chung, K., Hsu, H., Yeh, H. Y. and Chang, B. Y. (2007) Mechanism of regulation of prokaryotic tubulin-like GTPase FtsZ by membrane protein EzrA. *Journal of Biological Chemistry* 282: 14891-14897.
- Claessen, D., Emmins, R., Hamoen, L. W., Daniel, R. A., Errington, J. and Edwards, D. H. (2008) Control of the cell elongation–division cycle by shuttling of PBP1 protein in *Bacillus subtilis*. *Molecular Microbiology* 68(4): 1029-1046.
- Corbin, B. D., Geissler, B., Sadasivam, M. and Margolin, W. (2004) Z ring-independent interaction between a subdomain of FtsA and late septation proteins as revealed by a polar recruitment assay. *Journal of Bacteriology* 186: 7736-7744.
- Cutting, S. M. and Vander Horn, P. B. (1990) Genetic analysis. In *Molecular Biology Methods for Bacillus*. Harwood, C. R., and Cutting, S. M. (eds). Chichester, UK: John Wiley and Sons Limited, pp. 27-60.

- Dai, K. and Lutkenhaus, J. (1991) *ftsZ* is an essential cell division gene in *Escherichia coli*. *Journal of Bacteriology* 173: 3500-3506.
- Dai, K. and Lutkenhaus, J. (1992) The proper ratio of FtsZ to FtsA is required for cell division to occur in *Escherichia coli*. *Journal of Bacteriology* 174: 6145-6151.
- Dajkovic, A. and Lutkenhaus, J. (2006) Z ring as executor of bacterial cell division. *Journal of Molecular Microbiology and Biotechnology* 11: 140-151.
- Dajkovic, A., Lan, G., Sun, S. X., Wirtz, D. and Lutkenhaus, J. (2008) MinC spatially controls bacterial cytokinesis by antagonizing the scaffolding function of FtsZ. *Current Biology* 18: 235-244.
- Dajkovic, A., Pichoff, S., Lutkenhaus, J. and Wirtz, D. (2010) Cross-linking FtsZ polymers into coherent Z rings. *Molecular Microbiology* 78(3): 651-668.
- Daniel, R. A., Harry, E. J. and Errington, J. (2000) Role of penicillin-binding protein PBP 2B in assembly and functioning of the division machinery of *Bacillus subtilis*. *Molecular Microbiology* 35: 299-311.
- de Boer, P. (2010) Advances in understanding *E. coli* cell fission. *Current Opinion in Microbiology* 13: 730-737.
- de Boer, P., Crossley, R. and Rothfield, L. (1992) The essential bacterial cell division protein FtsZ is a GTPase. *Nature* 359: 254-256.
- den Blaauwen, T., Buddelmeijer, N., Aarsman, M. E., Hameete, C. M. and Nanninga, N. (1999) Timing of FtsZ assembly in *Escherichia coli*. *Journal of Bacteriology* 181: 5167-5175.
- Dewar, S. J., Begg, K. J. and Donachie, W. D. (1992) Inhibition of cell division initiation by an imbalance in the ratio of FtsA to FtsZ. *Journal of Bacteriology* 174: 6314-6316.
- Di Lallo, G., Fagioli, M., Barionovi, D., Ghelardini, P. and Paolozzi, L. (2003) Use of a two-hybrid assay to study the assembly of a complex multicomponent protein machinery: Bacterial septosome differentiation. *Microbiology* 149: 3353-3359.
- Din, N., Quardokus, E. M., Sackett, M. J. and Brun, Y. V. (1998) Dominant C-terminal deletions of FtsZ that affect its ability to localize in *Caulobacter* and its interaction with FtsA. *Molecular Microbiology* 27: 1051-1063.
- Donachie, W. D., Begg, K. J., Lutkenhaus, J. F., Salmond, G. P. C., Martinez-Salas, E. and Vincente, M. (1979) Role of the *ftsA* gene product in control of *Escherichia coli* cell division. *Journal of Bacteriology* 140: 388-394.

- Edwards, D. H. and Errington, J. (1997) The *Bacillus subtilis* DivIVA protein targets to the division septum and controls the site specificity of cell division. *Molecular Microbiology* 24: 905-915.
- Eichenberger, P. (2007) Genomics and cellular biology of endospore formation. In *Bacillus: Cellular and Molecular Biology*. Graumann, P. (ed.). Wymondham, UK: Caister Academic Press, pp. 375-418.
- Erickson, H. P. (1995) FtsZ, a prokaryotic homolog of tubulin? *Cell* 80: 367-370.
- Erickson, H. P. (1997) FtsZ, a tubulin homologue in prokaryote cell division. *Trends in Cell Biology* 7: 362-367.
- Erickson, H. P. (2007) Evolution of the cytoskeleton. *Bioessays* 29: 668-677.
- Erickson, H. P. (2009) Modeling the physics of FtsZ assembly and force generation. *Proceedings of the National Academy of Sciences of the United States of America* 106(23): 9238-9243.
- Erickson, H. P., Anderson, D. E. and Osawa, M. (2010) FtsZ in bacterial cytokinesis: cytoskeleton and force generator all in one. *Microbiology and Molecular Biology Reviews* 74(4): 504-528.
- Erickson, H. P. and Stoffler, D. (1996) Protofilaments and rings, two conformations of the tubulin family conserved from bacterial FtsZ to alpha/beta and gamma tubulin. *Journal of Cell Biology* 135: 5-8.
- Erickson, H. P., Taylor, D. W., Taylor, K. A. and Bramhill, D. (1996) Bacterial cell division protein FtsZ assembles into protofilament sheets and minirings, structural homologs of tubulin polymers. *Proceedings of the National Academy of Sciences of the United States of America* 93: 519-523.
- Errington, J. (1984) Efficient *Bacillus subtilis* cloning system using bacteriophage vector phi 105J9. *Journal of General Microbiology* 130: 2615-2628
- Errington, J. (2003) Dynamic proteins and a cytoskeleton in bacteria. *Nature Cell Biology* 5: 175-178.
- Errington, J. and Daniel, R. A. (2002) Cell division during growth and sporulation. In *Bacillus subtilis and its Closest Relatives: From Genes to Cells*. Sonenshein, A. L., Hoch, J. A., and Losick, R. (eds). Washington DC, USA: American Society for Microbiology Press, pp. 97-109.
- Errington, J., Daniel, R. A. and Scheffers, D. J. (2003) Cytokinesis in bacteria. *Microbiology and Molecular Biology Reviews* 67: 52-65.

- Feucht, A. and Errington, J. (2005) *ftsZ* mutations affecting cell division frequency, placement and morphology in *Bacillus subtilis*. *Microbiology* 151: 2053-2064.
- Feucht, A. and Lewis, P. J. (2001) Improved plasmid vectors for the production of multiple fluorescent protein fusions in *Bacillus subtilis*. *Gene* 264: 289-297.
- Fu, G., Huang, T., Buss, J., Coltharp, C. and Hensel, Z. (2010) In vivo structure of the *E. coli* FtsZ-ring revealed by Photoactivated Localization Microscopy (PALM). *PLoS ONE* 5: e12680.
- Gamba, P., Veening, J. W., Saunders, N. J., Hamoen, L. W. and Daniel, R. A. (2009) Two-step assembly dynamics of the *Bacillus subtilis* divisome. *Journal of Bacteriology* 191(13): 4186-4194.
- Garner, E. C., Bernard, R., Wang, W., Zhuang, X., Rudner, D. Z. and Mitchison, T. (2011) Coupled, circumferential motions of the cell wall synthesis machinery and MreB filaments in *B. subtilis*. *Science* 333: 222-225.
- Geissler, B. and Margolin, W. (2005) Evidence for functional overlap among multiple bacterial cell division proteins: compensating for the loss of FtsK. *Molecular Microbiology* 58(2): 596-612.
- Geissler, B., Elraheb, D. and Margolin, W. (2003) A gain-of-function mutation in *ftsA* bypasses the requirement for the essential cell division gene *zipA* in *Escherichia coli*. *Proceedings of the National Academy of Sciences of the United States of America* 100: 4197-4202.
- Geissler, B., Shiomi, D. and Margolin, W. (2007) The *ftsA** gain-of-function allele of *Escherichia coli* and its effects on the stability and dynamics of the Z ring. *Microbiology* 153: 814-825.
- Gerding, M. A., Liu, B., Bendezú, F. O., Hale, C. A., Bernhardt, T. G. and de Boer P. A. J. (2009) Self-enhanced accumulation of FtsN at division sites and roles for other proteins with a SPOR Domain (DamX, DedD, and RlpA) in *Escherichia coli* cell constriction. *Journal of Bacteriology* 191(24): 7383-7401.
- Ghigo, J. M., Weiss, D. S., Chen, J. C., Yarrow, J. C. and Beckwith, J. (1999) Localization of FtsL to the *Escherichia coli* septal ring. *Molecular Microbiology* 31(2): 725-737.
- Gholamhoseinian, A., Shen, Z., Wu, J. J. and Piggot, P. (1992) Regulation of transcription of the cell division gene *ftsA* during sporulation of *Bacillus subtilis*. *Journal of Bacteriology* 174: 4647-4656.
- Ghosh, B. and Sain, A. (2008) Origin of contractile force during cell division of bacteria. *Physical Review Letters* 101: 178101.

- Glass, J. I., Lefkowitz, E. J., Glass, J. S., Heiner, C. R., Chen, E. Y. and Cassell, G. H. (2000) The complete sequence of the mucosal pathogen *Ureaplasma urealyticum*. *Nature* 407: 757-762.
- Goehring, N. W. and Beckwith, J. (2005) Diverse paths to midcell: assembly of the bacterial cell division machinery. *Current Biology* 15: 514-526.
- Goehring, N. W., Gonzalez, M. D. and Beckwith, J. (2006) Premature targeting of cell division proteins to midcell reveals hierarchies of protein interactions involved in divisome assembly. *Molecular Microbiology* 61(1): 33-45.
- Goehring, N. W., Gueiros-Filho, F. and Beckwith, J. (2005) Premature targeting of a cell division protein to midcell allows dissection of divisome assembly in *Escherichia coli*. *Genes and Development* 19: 127-137.
- Gonzalez, J. M., Jimenez, M., Velez, M., Mingorance, J., Andreu, J. M., Vicente, M. and Rivas, G. (2003) Essential cell division protein FtsZ assembles into one monomer-thick ribbons under conditions resembling the crowded intracellular environment. *Journal of Biological Chemistry* 278: 37664-37671.
- Gonzy-Tréboul, G., Karmazyn-Campelli, C. and Stragier, P. (1992) Developmental regulation of transcription of the *Bacillus subtilis* *ftsAZ* operon. *Journal of Molecular Biology* 224: 967-979.
- Grantcharova, N., Lustig, U. and Flardh, K. (2005) Dynamics of FtsZ assembly during sporulation in *Streptomyces coelicolor* A3(2). *Journal of Bacteriology* 187: 3227-3237.
- Gregory J. A., Becker E. C. and Pogliano, K. (2008) *Bacillus subtilis* MinC destabilizes FtsZ-rings at new cell poles and contributes to the timing of cell division. *Genes and Development* 22: 3475-3488.
- Gueiros-Filho, F. J. (2007) Cell division. In *Bacillus: Cellular and Molecular Biology*. Graumann, P. (ed.). Wymondham, UK: Caister Academic Press, pp. 33 1-373.
- Gueiros-Filho, F. J. and Losick, R. (2002) A widely conserved bacterial cell division protein that promotes assembly of the tubulin-like protein FtsZ. *Genes and Development* 16: 2544-2556.
- Gullbrand, B. and Nordstrom, K. (2000) FtsZ ring formation without subsequent cell division after replication runout in *Escherichia coli*. *Molecular Microbiology* 36: 1349-1359.
- Gündoğdu, M. E., Kawai, Y., Pavlendova, N., Ogasawara, N., Errington, J., Scheffers, D. and Hamoen, L. W. (2011) Large ring polymers align FtsZ polymers for normal septum formation. *The EMBO Journal* 30: 617-626.

- Gupta, R., Beg, Q. K. and Lorenz, P. (2002) Bacterial alkaline proteases: molecular approaches and industrial applications. *Applied Microbiology and Biotechnology* 59: 15–32
- Haeusser, D. P. and Margolin, W. (2011) Prokaryotic Cytokinesis: Little rings bring big cylindrical things. *Current Biology* 21(6): 221-223.
- Haeusser, D. P., Schwartz, R. L., Smith, A. M., Oates, M. E. and Levin, P. A. (2004) EzrA prevents aberrant cell division by modulating assembly of the cytoskeletal protein FtsZ. *Molecular Microbiology* 52: 801-814.
- Hale, C. A. and de Boer, P. A. (1997) Direct binding of FtsZ to ZipA, an essential component of the septal ring structure that mediates cell division in *Escherichia coli*. *Cell* 88: 175-185.
- Hale, C. A. and de Boer, P. A. (1999) Recruitment of ZipA to the septal ring of *Escherichia coli* is dependent on FtsZ and independent of FtsA. *Journal of Bacteriology* 181: 167-176.
- Hamoen, L. W. and Errington, J. (2003) Polar targeting of DivIVA in *Bacillus subtilis* is not directly dependent on FtsZ or PBP 2B. *Journal of Bacteriology* 185: 693-697.
- Hamoen, L. W., Meile, J. C., Jong, W. D., Noirot, P. and Errington, J. (2006) SepF, a novel FtsZ-interacting protein required for a late step in cell division. *Molecular Microbiology* 59: 989-999.
- Harry, E. J. (2001) Bacterial cell division: Regulating Z ring formation. *Molecular Microbiology* 40: 795-803.
- Harry, E. J. and Lewis, P. J. (2003) Early targeting of Min proteins to the cell poles in germinated spores of *Bacillus subtilis*: Evidence for division apparatus-independent recruitment of Min proteins to the division site. *Molecular Microbiology* 47: 37-48.
- Harry, E. J., Monahan, L. and Thompson, L. (2006) Bacterial cell division: The mechanism and its precision. In *International Review of Cytology: A Survey of Cell Biology*. Jeon, K. W. (ed.). San Diego, USA: Academic Press, vol. 253, pp. 27-94.
- Harry, E. J., Pogliano, K. and Losick, R. (1995) Use of immunofluorescence to visualize cell-specific gene expression during sporulation in *Bacillus subtilis*. *Journal of Bacteriology* 177: 3386-3393.
- Harry, E. J., Rodwell, J. and Wake, R. G. (1999) Co-ordinating DNA replication with cell division in bacteria: A link between the early stages of a round of replication and mid-cell Z ring assembly. *Molecular Microbiology* 33: 33-40.

- Harry, E. J., Stewart, B. J. and Wake, R. G. (1993) Characterization of mutations in *divIB* of *Bacillus subtilis* and cellular localization of the DivIB protein. *Molecular Microbiology* 7(4): 611-621.
- Hauser, P. and Errington, J. (1995) Characterization of cell cycle events during the onset of sporulation in *Bacillus subtilis*. *Journal of Bacteriology* 177: 3923-3931.
- Haydon, D. J., Stokes, N. R., Ure, R., Galbraith, G., Bennett, J. M., Brown, D. R., Baker, P. J., Barynin, V. V., Rice, D. W., Sedelnikova, S. E., Heal, J. R., Sheridan, J. M., Aiwale, S. T., Chauhan, P. K., Srivastava, A., Taneja, A., Collins, I., Errington, J. and Czaplewski, L. G. (2008) An inhibitor of FtsZ with potent and selective anti-Staphylococcal activity. *Science* 321: 1673-1675.
- Hirota, Y., Ryter, A. and Jacob, F. (1968) Thermosensitive mutants of *Escherichia coli* affected in the process of DNA synthesis and cellular division. *Cold Spring Harbor Symposia on Quantitative Biology* 33: 677-693.
- Hoi, H., Shaner, N. C., Davidson, M. W., Cairo, C. W., Wang, J. and Campbell, R. E. (2010) A monomeric photoconvertible fluorescent protein for imaging of dynamic protein localization. *Journal of Molecular Biology* 401: 776-791.
- Horger, I., Campelo, F., Hernandez-Machado, A. and Tarazona, P. (2010) Constricting force of filamentary protein rings evaluated from experimental results. *Physical Review. E Statistical, Nonlinear, and Soft Matter Physics* 81: 031922.
- Huecas, S., Schaffner-Barbero, C., Garcia, W., Yebenes, H., Palacios, J. M., Diaz, J. F., Menendez, M. and Andreu, J. M. (2007) The interactions of cell division protein FtsZ with guanine nucleotides. *Journal of Biological Chemistry* 282: 37515-37528.
- Ishikawa, S., Kawai, Y., Hiramatsu, K., Kuwano, M. and Ogasawara, N. (2006) A new FtsZ-interacting protein, YlmF, complements the activity of FtsA during progression of cell division in *Bacillus subtilis*. *Molecular Microbiology* 60: 1364-1380.
- Jensen, S. O., Thompson, L. S. and Harry, E. J. (2005) Cell division in *Bacillus subtilis*: FtsZ and FtsA association is Z ring independent, and FtsA is required for efficient midcell Z ring assembly. *Journal of Bacteriology* 187: 6536-6544.
- Jones, L. J. F., Carballido-López, R. and Errington, J. (2001) Control of cell shape in bacteria: helical, Actin-like filaments in *Bacillus subtilis*. *Cell* 104: 913-922.
- Kalman, S., Mitchell, W., Marathe, R., Lammel, C., Fan, J., Hyman, R. W., Olinger, L., Grimwood, J., Davis, R. W. and Stephens, R. S. (1999) Comparative genomes of *Chlamydia pneumoniae* and *C. trachomatis*. *Nature Genetics* 21: 385-389.

- Karimova, G., Dautin, N. and Ladant, D. (2005) Interaction network among *Escherichia coli* membrane proteins involved in cell division as revealed by bacterial two-hybrid analysis. *Journal of Bacteriology* 187: 2233-2243.
- Katis, V. L., Wake, R. G. and Harry, E. J. (2000) Septal localization of the membrane-bound division proteins of *Bacillus subtilis* DivIB and DivIC is codependent only at high temperatures and requires FtsZ. *Journal of Bacteriology* 182(12): 3607-3611.
- Kemp, J. T., Driks, A. and Losick, R. (2002) FtsA mutants of *Bacillus subtilis* impaired in sporulation. *Journal of Bacteriology* 184(14): 3856-3863.
- Kobayashi, K., Ehrlich, S. D., Albertini, A., Amati, G., Andersen, K. K., Arnaud, M., Asai, K., Ashikaga, S., Aymerich, S., Bessieres, P., Boland, F., Brignell, S. C., Bron, S., Bunai, K., Chapuis, J., Christiansen, L. C., Danchin, A., Debarbouille, M., Dervyn, E., Deuerling, E., Devine, K., Devine, S. K., Dreesen, O., Errington, J., Fillinger, S., Foster, S. J., Fujita, Y., Galizzi, A., Gardan, R., Eschevins, C., Fukushima, T., Haga, K., Harwood, C. R., Hecker, M., Hosoya, D., Hullo, M. F., Kakeshita, H., Karamata, D., Kasahara, Y., Kawamura, F., Koga, K., Koski, P., Kuwana, R., Imamura, D., Ishimaru, M., Ishikawa, S., Ishio, I., Le Coq, D., Masson, A., Mauel, C., Meima, R., Mellado, R. P., Moir, A., Moriya, S., Nagakawa, E., Nanamiya, H., Nakai, S., Nygaard, P., Ogura, M., Ohanan, T., O'Reilly, M., O'Rourke, M., Pragai, Z., Pooley, H. M., Rapoport, G., Rawlins, J. P., Rivas, L. A., Rivolta, C., Sadaie, A., Sadaie, Y., Sarvas, M., Sato, T., Saxild, H. H., Scanlan, E., Schumann, W., Seegers, J. F., Sekiguchi, J., Sekowska, A., Seror, S. J., Simon, M., Stragier, P., Studer, R., Takamatsu, H., Tanaka, T., Takeuchi, M., Thomaidis, H. B., Vagner, V., van Dijl, J. M., Watabe, K., Wipat, A., Yamamoto, H., Yamamoto, M., Yamamoto, Y., Yamane, K., Yata, K., Yoshida, K., Yoshikawa, H., Zuber, U. and Ogasawara, N. (2003) Essential *Bacillus subtilis* genes. *Proceedings of the National Academy of Sciences of the United States of America* 100: 4678-4683.
- Kolin D. L. and Wiseman, P. W. (2007) Advances in image correlation spectroscopy: measuring number densities, aggregation states, and dynamics of fluorescently labeled macromolecules in cells. *Cell Biochemistry and Biophysics* 49: 141-164.
- Kunst, F., Ogasawara, N., Moszer, I., Albertini, A. M., Alloni, G., Azevedo, V., Bertero, G., Bessières, P., Bolotin, A., Borchert, S., Borriss, R., Boursier, L., Brans, A., Braun, M., Brignell, S. C., Bron, S., Brouillet, S., Bruschi, C. V., Caldwell, B., Capuano, V., Carter, N. M., Choi, S. K., Codani, J. J., Connerton, I. F., Cummings, J., Daniel, R. A., Denizot, F., Devine, K. M., Düsterhöft, A., Ehrlich, S. D., Emmerson, P. T., Entian, K. D., Errington, J., Fabret, C., Ferrari, E., Foulger, D., Fritz, C., Fujita, M., Fujita, Y., Fuma, S., Galizzi, A., Galleron, N., Ghim, S. Y., Glaser, P., Goffeau, A., Golightly, E. J., Grandi, G., Guiseppi, G., Guy, B. J., Haga, K., Haiech, J., Harwood, C. R., Hénaut, A., Hilbert, H., Holsappel, S., Hosono, S., Hullo, M. F., Itaya, M., Jones, L., Joris, B., Karamata, D., Kasahara, Y., Klaerr-

- Blanchard, M., Klein, C., Kobayashi, Y., Koetter, P., Koningstein, G., Krogh, S., Kumano, M., Kurita, K., Lapidus, A., Lardinois, S., Lauber, J., Lazarevic, V., Lee, S. M., Levine, A., Liu, H., Masuda, S., Mauël, C., Médigue, C., Medina, N., Mellado, R. P., Mizuno, M., Moestl, D., Nakai, S., Noback, M., Noone, D., O'Reilly, M., Ogawa, K., Ogiwara, A., Oudega, B., Park, S. H., Parro, V., Pohl, T. M., Portetelle, D., Porwollik, S., Prescott, A. M., Presecan, E., Pujic, P., Purnelle, B., Rapoport, G., Rey, M., Reynolds, S., Rieger, M., Rivolta, C., Rocha, E., Roche, B., Rose, M., Sadaie, Y., Sato, T., Scanlan, E., Schleich, S., Schroeter, R., Scoffone, F., Sekiguchi, J., Sekowska, A., Seror, S. J., Serror, P., Shin, B. S., Soldo, B., Sorokin, A., Tacconi, E., Takagi, T., Takahashi, H., Takemaru, K., Takeuchi, M., Tamakoshi, A., Tanaka, T., Terpstra, P., Tognoni, A., Tosato, V., Uchiyama, S., Vandenbol, M., Vannier, F., Vassarotti, A., Viari, A., Wambutt, R., Wedler, E., Wedler, H., Weitzenegger, T., Winters, P., Wipat, A., Yamamoto, H., Yamane, K., Yasumoto, K., Yata, K., Yoshida, K., Yoshikawa, H. F., Zumstein, E., Yoshikawa, H. and Danchin, A. (1997) The complete genome sequence of the gram-positive bacterium *Bacillus subtilis*. *Nature* 390: 249-256.
- Laemmli, U. K. (1970) Cleavage of structural proteins during the assembly of the head of bacteriophage T4. *Nature* 227: 680-685.
- Lan, G., Wolgemuth, C. W. and Sun, S. X. (2007) Z ring force and cell shape during division in rod-like bacteria. *Proceedings of the National Academy of Sciences of the United States of America* 104: 16110-16115.
- Lan, G., Daniels, B. R., Dobrowsky, T. M., Wirtz, D. and Sun, S. X. (2009) Condensation of FtsZ filaments can drive bacterial cell division. *Proceedings of the National Academy of Sciences of the United States of America* 106: 121-126.
- Lappchen, T., Hartog, A. F., Pinas, V. A., Koomen, G. J. and den Blaauwen, T. (2005) GTP analogue inhibits polymerization and GTPase activity of the bacterial protein FtsZ without affecting its eukaryotic homologue tubulin. *Biochemistry* 44: 7879-7884.
- Lara, B., Rico, A. I., Petruzzelli, S., Santona, A., Dumas, J., Biton, J., Vicente, M., Mingorance, J. and Massidda, O. (2005) Cell division in cocci: Localization and properties of the *Streptococcus pneumoniae* FtsA protein. *Molecular Microbiology* 55: 699-711.
- Leaver, M., Domínguez-Cuevas, P., Coxhead, J. M., Daniel, R. A. and Errington, J. (2009) Life without a wall or division machine in *Bacillus subtilis*. *Nature* 457: 849-853.
- Lemon, K. P., Earl, A. M., Vlamakis, H. C., Aguilar, C. and Kolter, R. (2008) Biofilm development with an emphasis on *Bacillus subtilis*. *Current Topics in Microbiology and Immunology* 322: 11-16.

- Lemon, K. P., Moriya, S., Ogasawara, N. and Grossman, A. D. (2002) Chromosome replication and segregation. In *Bacillus subtilis and its Closest Relatives: From Genes to Cells*. Sonenshein, A. L., Hoch, J. A., and Losick, R. (eds). Washington DC, USA: American Society for Microbiology Press, pp. 73-86.
- Lenarcic, R., Halbedel, S., Visser, L., Shaw, M., Wu, L. J., Errington, J., Marenduzzom, D. and Hamoen, L. W. (2009) Localization of DivIVA by targeting to negatively curved membranes. *EMBO Journal* 28: 2272-2282.
- Levin, P. A. and Losick, R. (1996) Transcription factor SpoOA switches the localization of the cell division protein FtsZ from a medial to a bipolar pattern in *Bacillus subtilis*. *Genes and Development* 10: 478-488.
- Levin, P. A., Kurtser, I. G. and Grossman, A. D. (1999) Identification and characterization of a negative regulator of FtsZ ring formation in *Bacillus subtilis*. *Proceedings of the National Academy of Sciences of the United States of America* 96: 9642-9647.
- Li, G. W. and Xie, X. S. (2011) Central dogma at the single-molecule level in living cells. *Nature* 475: 308-315.
- Li, Z., Trimble, M. J., Brun, Y. V. and Jensen, G. J. (2007) The structure of FtsZ filaments *in vivo* suggests a force-generating role in cell division. *EMBO Journal* 26: 4694-4708.
- Lippincott-Schwartz, J., Snapp, E. and Kenworthy, A. (2001) Studying protein dynamics in living cells. *Nature Reviews. Molecular Cell Biology* 2(6): 444-456.
- Lock, R. L. and Harry, E. J. (2008) Cell-division inhibitors: new insights for future antibiotics. *Nature Reviews Drug Discovery* 7: 324-338.
- Low, H. H., Moncrieffe, M. C. and Löwe, J. (2004) The crystal structure of ZapA and its modulation of FtsZ polymerisation. *Journal of Molecular Biology* 341: 839-852.
- Löwe, J. and Amos, L. A. (1998) Crystal structure of the bacterial cell-division protein FtsZ. *Nature* 391: 203-206.
- Löwe, J. and Amos, L. A. (1999) Tubulin-like protofilaments in Ca²⁺-induced FtsZ sheets. *EMBO Journal* 18: 2364-2371.
- Lutkenhaus, J. (2007) Assembly dynamics of the bacterial MinCDE system and spatial regulation of the Z ring. *Annual Review of Biochemistry* 76: 1411-1424.
- Lutkenhaus, J. (2009) Bacterial Cell Division. In: *Encyclopedia of Life Sciences (ELS)*. John Wiley & Sons, Ltd: Chichester.

- Lutkenhaus, J. F. and Donachie, W. D. (1979) Identification of the *ftsA* gene product. *Journal of Bacteriology* 137: 1088-1094.
- Lutkenhaus, J. F., Hans Wolf-Watz and Donachie, W. D. (1980) Organization of the genes in the *ftsA-envA* region of the *Escherichia coli* genetic map and identification of a new *fts* locus (*ftsZ*). *Journal of Bacteriology* 142: 615-620.
- Lu, C. and Erickson, H. P. (1999) The straight and curved conformation of FtsZ protofilaments-evidence for rapid exchange of GTP into the curved protofilament. *Cell Structure and Function* 24: 285-290.
- Lu, C., Reedy, M. and Erickson, H. P. (2000) Straight and curved conformations of FtsZ are regulated by GTP hydrolysis. *Journal of Bacteriology* 182(1): 164-170.
- Ma, X. and Margolin, W. (1999) Genetic and functional analyses of the conserved C-terminal core domain of *Escherichia coli* FtsZ. *Journal of Bacteriology* 181: 7531-7544.
- Ma, X. L., Ehrhardt, D. W. and Margolin, W. (1996) Colocalization of cell division proteins FtsZ and FtsA to cytoskeletal structures in living *Escherichia coli* cells by using green fluorescent protein. *Proceedings of the National Academy of Sciences of the United States of America* 93: 12998-13003.
- Margolin, W. (2000) Themes and variations in prokaryotic cell division. *FEMS Microbiology Reviews* 24: 531-548.
- Margolin, W. (2001) Spatial regulation of cytokinesis in bacteria. *Current Opinion in Microbiology* 4: 647-652.
- Margolin, W. (2005) FtsZ and the division of prokaryotic cells and organelles. *Nature Reviews Molecular Cell Biology* 6: 862-871.
- Margolin, W. and Bernander, R. (2004) How do prokaryotic cells cycle? *Current Biology* 14(18): 768-770.
- Marston, A. L. and Errington, J. (1999) Selection of the midcell division site in *Bacillus subtilis* through MinD-dependent polar localization and activation of MinC. *Molecular Microbiology* 33: 84-96.
- Marston, A. L., Thomaidis, H. B., Edwards, D. H., Sharpe, M. E. and Errington, J. (1998) Polar localization of the MinD protein of *Bacillus subtilis* and its role in selection of the mid-cell division site. *Genes and Development* 12: 3419-3430.
- Matsuda, T., Miyawaki, A. and Nagai, T. (2008) Direct measurement of protein dynamics inside cells using a rationally designed photoconvertible protein. *Nature Methods* 5(4): 339-345.

- Meyer, P. and Dworkin, J. (2007) Applications of fluorescence microscopy to single bacterial cells. *Research in Microbiology* 158: 187-194.
- Migocki, M. D., Freeman, M. K., Wake, R. G. and Harry, E. J. (2002) The Min system is not required for precise placement of the midcell Z ring in *Bacillus subtilis*. *EMBO Reports* 3: 1163-1167.
- Mingorance, J., Tadros, M., Vicente, M., Gonzalez, J. M., Rivas, G. and Velez, M. (2005) Visualization of single *Escherichia coli* FtsZ filament dynamics with atomic force microscopy. *Journal of Biological Chemistry* 280: 20909-20914.
- Mingorance, J., Rivas, G., Velez, M., Gomez-Puertas, P. and Vicente, M. (2010) Strong FtsZ is with the force: mechanisms to constrict bacteria. *Trends in Microbiology* 18: 348-356.
- Monahan, L. G. (2008) PhD Thesis: Cell division in *Bacillus subtilis*: New insights from an old mutant. University of Technology, Sydney.
- Monahan, L. G., D'Elia, M. A. and Harry, E. J. (2011) Mining bacterial cell division for new antibacterial drugs. In *Emerging Trends in Antibacterial Discovery: Answering the Call to Arms*. Caister Academic Press.
- Monahan, L., Robinson, A. and Harry, E. J. (2009) Lateral FtsZ association and the assembly of the cytokinetic Z ring in bacteria. *Molecular Microbiology* 74: 1004-1017.
- Moriya, S., Rashid, R. A., Rodrigues, C. D. and Harry, E. J. (2010) Influence of the nucleoid and the early stages of DNA replication on positioning the division site in *Bacillus subtilis*. *Molecular Microbiology* 76: 634-647.
- Mosyak, L., Zhang, Y., Glasfeld, E., Haney, S., Stahl, M., Seehra, J. and Somers, W. S. (2000) The bacterial cell division protein ZipA and its interaction with an FtsZ fragment revealed by X-ray crystallography. *EMBO Journal* 19: 3179-3191.
- Mukherjee, A. and Lutkenhaus, J. (1994) Guanine nucleotide-dependent assembly of FtsZ into filaments. *Journal of Bacteriology* 176: 2754-2758.
- Mukherjee, A. and Lutkenhaus, J. (1999) Analysis of FtsZ assembly by light scattering and determination of the role of divalent metal cations. *Journal of Bacteriology* 181: 823-832.
- Mukherjee, A., Cao, C. and Lutkenhaus, J. (1998) Inhibition of FtsZ polymerization by SulA, an inhibitor of septation in *Escherichia coli*. *Proceedings of the National Academy of Sciences of the United States of America* 95: 2885-2890.

- Mukherjee, A., Dai, K. and Lutkenhaus, J. (1993) *Escherichia coli* cell division protein FtsZ is a guanine nucleotide binding protein. *Proceedings of the National Academy of Sciences of the United States of America* 90: 1053-1057.
- Nicholson, W. L. (2003) Using thermal inactivation kinetics to calculate the probability of extreme spore longevity: Implications for paleomicrobiology and lithopanspermia. *Origins of Life and Evolution of the Biosphere* 33: 621-631.
- Niu, L. and Yu, J. (2008) Investigating intracellular dynamics of FtsZ cytoskeleton with photoactivation single-molecule tracking. *Biophysical Journal* 95: 2009-2016.
- Nogales, E., Downing, K. H., Amos, L. A. and Löwe, J. (1998) Tubulin and FtsZ form a distinct family of GTPases. *Nature Structural Biology* 5: 451-458.
- Nukushina, J. I. and Ikeda, Y. (1969) Genetic analysis of the developmental processes during germination and outgrowth of *Bacillus subtilis* spores with temperature sensitive mutants. *Genetics* 63: 63-74.
- Oliva, M. A., Cordell, S. C. and Löwe, J. (2004) Structural insights into FtsZ protofilament formation. *Nature Structural and Molecular Biology* 11: 1243-1250.
- Oliva, M. A., Halbedel, S., Freund, S. M., Dutow, P., Leonard, T. A., Veprintsev, D. B., Hamoen, L. W. and Löwe, J. (2010) Features critical for membrane binding revealed by DivIVA crystal structure. *EMBO Journal* 29(12): 1988-2001.
- Oliva, M. A., Huecas, S., Palacios, J. M., Martin-Benito, J., Valpuesta, J. M. and Andreu, J. M. (2003) Assembly of archaeal cell division protein FtsZ and a GTPase-inactive mutant into double-stranded filaments. *Journal of Biological Chemistry* 278: 33562-33570.
- Oliva, M. A., Trambaiolo, D. and Löwe, J. (2007) Structural insights into the conformational variability of FtsZ. *Journal of Molecular Biology* 373: 1229-1242.
- Osawa, M. and Erickson, H. P. (2005) Probing the domain structure of FtsZ by random truncation and insertion of GFP. *Microbiology* 151: 4033-4043.
- Osawa, M. and Erickson, H. P. (2011) Inside-out Z rings – constriction with and without GTP hydrolysis. *Molecular Microbiology* 81(2): 571–579.
- Osawa, M., Anderson, D. E. and Erickson, H. P. (2008) Reconstitution of contractile FtsZ rings in liposomes. *Science* 320: 792-794.
- Osawa, M., Anderson, D. E. and Erickson, H. P. (2009) Curved FtsZ protofilaments generate bending forces on liposome membranes. *EMBO Journal* 28: 3476-3484.

- Otter, T., King, S. M. and Witman, G. M. (1987) A two step procedure for efficient electro-transfer of both high-molecular weight (> 400000 Da) and low-molecular weight (< 20000 Da) proteins. *Analytical Biochemistry* 162: 370-377.
- Paradis-Bleau, C., Beaumont, M., Sanschagrín, F., Voyer, N. and Levesque, R. C. (2007) Parallel solid synthesis of inhibitors of the essential cell division FtsZ enzyme as a new potential class of anti bacterials. *Bioorganic & Medicinal Chemistry* 15(3): 1330-1340.
- Partridge, S. R. and Wake, R. G. (1995) FtsZ and Nucleoid Segregation during Outgrowth of *Bacillus subtilis* Spores. *Journal of Bacteriology* 177(9): 2560–2563.
- Patrick, J. E. and Kearns, D. B. (2008) MinJ (YvjD) is a topological determinant of cell division in *Bacillus subtilis*. *Molecular Microbiology* 70: 1166-1179.
- Patterson, G., Davidson, M., Manley, S. and Lippincott-Schwartz, J. (2010) Superresolution imaging using single-molecule localization. *Annual Review of Physic Chemistry* 61: 345-367.
- Peters, P. C., Migocki, M. D., Thoni, C. and Harry, E. J. (2007) A new assembly pathway for the cytokinetic Z ring from a dynamic helical structure in vegetatively growing cells of *Bacillus subtilis*. *Molecular Microbiology* 64: 487-499.
- Phair, R. D. and Misteli, T. (2001) Kinetic modelling approaches to *in vivo* imaging. *Nature Reviews. Molecular Cell Biology* 2(12): 898-907.
- Pichoff, S. and Lutkenhaus, J. (2002) Unique and overlapping roles for ZipA and FtsA in septal ring assembly in *Escherichia coli*. *EMBO Journal* 21: 685-693.
- Pichoff, S. and Lutkenhaus, J. (2005) Tethering the Z ring to the membrane through a conserved membrane targeting sequence in FtsA. *Molecular Microbiology* 55: 1722-1734.
- Pichoff, S. and Lutkenhaus, J. (2007) Identification of a region of FtsA required for interaction with FtsZ. *Molecular Microbiology* 64: 1129-1138.
- Pla, J., Dopazo, A. and Vicente, M. (1990) The native form of FtsA, a septal protein of *Escherichia coli*, is located in the cytoplasmic membrane. *Journal of Bacteriology* 172(9): 5097-5102.
- Pogliano, J., Osborne, N., Sharp, M. D., Mello, A. A., Perez, A., Sun, Y. and Pogliano, K. (1999) A vital stain for studying membrane dynamics in bacteria: a novel mechanism controlling septation during *Bacillus subtilis* sporulation. *Molecular Microbiology* 31(4): 1149–1159.

- RayChaudhuri, D. (1999) ZipA is a MAP-Tau homolog and is essential for structural integrity of the cytokinetic FtsZ ring during bacterial cell division. *EMBO Journal* 18: 2372-2383.
- RayChaudhuri, D. and Park, J. T. (1992) *Escherichia coli* cell division gene *ftsZ* encodes a novel GTP-binding protein. *Nature* 359: 251-254.
- Reeve, J. N., Mendelson, N. H., Coyne, S. I., Hallock, L. L. and Cole, R. M. (1973) Minicells of *Bacillus subtilis*. *Journal of Bacteriology* 114: 860-873.
- Rico, A. I., Garcia-Ovalle, M., Mingorance, J. and Vicente, M. (2004) Role of two essential domains of *Escherichia coli* FtsA in localization and progression of the division ring. *Molecular Microbiology* 53: 1359-1371.
- Rico, A. I., García-Ovalle, M., Palacios, P., Casanova, M. and Vicente, M. (2010) Role of *Escherichia coli* FtsN protein in the assembly and stability of the cell division ring. *Molecular Microbiology* 76(3): 760–771.
- Rivas, G., López, A., Mingorance, F., Ferrándiz, M. J., Zorrilla, S., Minton, A. P., Vicente, M. and Andreu, J. M. (2000) Magnesium-induced linear self-association of the FtsZ bacterial cell division protein monomer. The primary steps for FtsZ assembly. *Journal of Biological Chemistry* 275(16): 11740-11749.
- Robinson, A. C., Kenan, D. J., Hatfull, G. F., Sullivan, N. F., Spiegelberg, R. and Donachie, W. D. (1984) DNA sequence and transcriptional organization of essential cell division genes *ftsQ* and *ftsA* of *Escherichia coli*: Evidence for overlapping transcriptional units. *Journal of Bacteriology* 160: 546-555.
- Robson, S. A., Michie, K. A., Mackay, J. P., Harry, E. and King, G. F. (2002) The *Bacillus subtilis* cell division proteins FtsL and DivIC are intrinsically unstable and do not interact with one another in the absence of other septasomal components. *Molecular Microbiology* 44(3): 663–674.
- Rodrigues, C. D. A. (2011) PhD Thesis: Establishing how bacterial cells position the division site. University of Technology, Sydney.
- Romberg, L. and Levin, P. A. (2003) Assembly dynamics of the bacterial cell division protein FtsZ: Poised at the edge of stability. *Annual Review of Microbiology* 57: 125-154.
- Romberg, L. and Mitchison, T. J. (2004) Rate-limiting guanosine 5'-triphosphate hydrolysis during nucleotide turnover by FtsZ, a prokaryotic tubulin homologue involved in bacterial cell division. *Biochemistry* 43: 282-288.
- Rothfield, L., Justice, S. and García-Lara, J. (1999) Bacterial cell division. *Annual Review of Genetics* 33: 423-448.

- Rothfield, L., Taghbalout, A. and Shih, Y. L. (2005) Spatial control of bacterial division-site placement. *Nature Reviews Microbiology* 3: 959-968.
- Rowland, S. L., Katis, V. L., Partridge, S. R. and Wake, R. G. (1997) DivIB, FtsZ and cell division in *Bacillus subtilis*. *Molecular Microbiology* 23(2): 295-302.
- Rudner, D. Z. and Losick, R. (2010) Protein subcellular localization in bacteria. *Cold Spring Harbor Perspectives in Biology* 2(4): a000307.
- Rueda, S., Vicente, M. and Mingorance, J. (2003) Concentration and assembly of the division ring proteins FtsZ, FtsA, and ZipA during the *Escherichia coli* cell cycle. *Journal of Bacteriology* 185: 3344-3351.
- Ryan, K. R. and Shapiro, L. (2003) Temporal and spatial regulation in prokaryotic cell cycle progression and development. *Annual Review of Biochemistry* 72: 367-394.
- Sambrook, J., Fritsch, E. F. and Maniatis, T. (1989) *Molecular Cloning: A Laboratory Manual*. 2nd ed. Cold Spring Harbor, USA: Cold Spring Harbor Laboratory Press.
- Sanchez, M., Valencia, A., Ferrandiz, M. J., Sander, C. and Vicente, M. (1994) Correlation between the structure and biochemical activities of FtsA, an essential cell division protein of the actin family. *EMBO Journal* 13: 4919-4925.
- Sánchez-Pullido, L., Devos, D., Genevrois, S., Vicente, M. and Valencia, A. (2003) POTRA: a conserved domain in the FtsQ family and a class of beta-barrel outer membrane proteins. *Trends in Biochemical Science* 28(10): 523-526.
- Scheffers, D.J. (2008) The effect of MinC on FtsZ polymerization is pH dependent and be counteracted by ZapA. *FEBS letters* 582: 2601-2608.
- Shapiro, L. (1993) Protein localization and asymmetry in the bacterial cell. *Cell* 73(5): 841-855.
- Shapiro, L. and Losick, R. (2000) Dynamic spatial regulation in the bacterial cell. *Cell* 100: 89-98.
- Shapiro, L., McAdams, H. H. and Losick, R. (2009) Why and how bacteria localize proteins. *Science* 326: 1225-1228.
- Shen, B. and Lutkenhaus, J. (2009) The conserved C-terminal tail of FtsZ is required for the septal localization and division inhibitory activity of MinC(C)/MinD. *Molecular Microbiology* 72: 410-424.
- Shih, Y.-L. and Rothfield, L. (2006) The bacterial cytoskeleton. *Microbiology and Molecular Biology Reviews* 70: 729-754.

- Shiomi, D. and Margolin, W. (2007) Dimerization or oligomerization of the actin-like FtsA protein enhances the integrity of the cytokinetic Z ring. *Molecular Microbiology* 66: 1396-1415.
- Shiomi, D. and Margolin, W. (2008) Compensation for the loss of the conserved membrane targeting sequence of FtsA provides new insights into its function. *Molecular Microbiology* 67(3): 558–569.
- Singh, J. K., Makde, R. D., Kumar, V. and Panda, D. (2007) A membrane protein, EzrA, regulates assembly dynamics of FtsZ by interacting with the C-terminal tail of FtsZ. *Biochemistry* 46: 11013-11022.
- Singh, J. K., Makde R. D., Kumar V. and Panda D. (2008) SepF increases the assembly and bundling of FtsZ polymers and stabilizes FtsZ protofilaments by binding along its length. *The Journal of Biological Chemistry* 283(45): 31116-31124.
- Small, E., Marrington, R., Rodger, A., Scott, D. J., Sloan, K., Roper, D. I., Dafforn, T. R. and Addinall, S. G. (2007) FtsZ polymer-bundling by the *Escherichia coli* ZapA orthologue, YgfE, involves a conformational change in bound GTP. *Journal of Molecular Biology* 369: 210-221.
- Sprague, B. L. and McNally, J. G. (2005) FRAP analysis of binding: proper and fitting. *TRENDS in Cell Biology* 15(2): 84-91.
- Stephens, R. S., Kalman, S., Lammel, C., Fan, J., Marathe, R., Aravind, L., Mitchell, W., Olinger, L., Tatusov, R. L. and Zhao, Q. (1998) Genome sequence of an obligate intracellular pathogen of humans *Chlamydia trachomatis*. *Science* 282: 754- 759.
- Stokes, N. R., Sievers, J., Barker, S., Bennett, J. M., Brown, D. R., Collins, I., Errington, V. M., Foulger, D., Hall, M., Halsey, R., Johnson, H., Rose, V., Thomaidis, H. B., Haydon, D. J., Czaplewski, L. G. and Errington, J. (2005) Novel inhibitors of bacterial cytokinesis identified by a cell-based antibiotic screening assay. *Journal of Biological Chemistry* 280: 39709-39715.
- Strahl, H. and Hamoen, L. W. (2010) Membrane potential is important for bacterial cell division. *Proceedings of the National Academy of Sciences of the United States of America* 107(27): 12281-12286.
- Stricker, J. and Erickson, H. P. (2003) *In vivo* characterization of *Escherichia coli* ftsZ mutants: Effects on Z ring structure and function. *Journal of Bacteriology* 185: 4796-4805.
- Stricker, J., Maddox, P. S., Salmon, E. D. and Erickson, H. P. (2002) Rapid assembly dynamics of the *Escherichia coli* FtsZ-ring demonstrated by fluorescence recovery

- after photobleaching. *Proceedings of the National Academy of Sciences of the United States of America* 99: 3171-3175.
- Sun, Q. and Margolin, W. (1998) FtsZ dynamics during the division cycle of live *Escherichia coli* cells. *Journal of Bacteriology* 180: 2050-2056.
- Sun, Q. and Margolin, W. (2001) Influence of the nucleoid on placement of FtsZ and MinE rings in *Escherichia coli*. *Journal of Bacteriology* 183: 1413–1422.
- Surovtsev, I. V., Morgan, J. J. and Lindahl, P. A. (2008) Kinetic modeling of the assembly, dynamic steady state, and contraction of the FtsZ ring in prokaryotic cytokinesis. *PLoS Computational Biology* 4(7): e1000102.
- Tamames, J., Gonzalez-Moreno, M., Mingorance, J., Valencia, A. and Vicente, M. (2001) Bringing gene order into bacterial shape. *Trends in Genetics* 17: 124-126.
- Tavares, J. R., de Souza, R. F., Meira, G. L. and Gueiros-Filho, F. J. (2008) Cytological characterization of YpsB, a novel component of the *Bacillus subtilis* divisome. *Journal of Bacteriology* 190: 7096-7107.
- Teleman, A. A., Graumann, P. L., Chi-Hong Lin, D., Grossman, A. D. and Losick, R. (1998) Chromosome arrangement within a bacterium. *Current Biology* 8: 1102-1109.
- Thanbichler, M. and Shapiro, L. (2006) MipZ, a spatial regulator coordinating chromosome segregation with cell division in *Caulobacter*. *Cell* 126: 147-162.
- Thanedar, S. and Margolin, W. (2004) FtsZ exhibits rapid movement and oscillation waves in helix-like patterns in *Escherichia coli*. *Current Biology* 14: 1167-1173.
- van Baarle, S. and Bramkamp, M. (2010) The MinCDJ System in *Bacillus subtilis* Prevents Minicell Formation by Promoting Divisome Disassembly. *PLoS ONE* 5(3): e9850.
- van den Ent, F. and Löwe, J. (2000) Crystal structure of the cell division protein FtsA from *Thermotoga maritima*. *EMBO Journal* 19: 5300-5307.
- van de Putte, P., van Dillewijn, A. and Roersch, A. (1964) The selection of mutants of *Escherichia coli* with impaired cell division at elevated temperature. *Mutation Research* 106: 121-128.
- Varley, A. W. and Stewart, G. C. (1992) The *divIVB* region of the *Bacillus subtilis* chromosome encodes homologs of *Escherichia coli* septum placement (MinCD) and cell shape (MreBCD) determinants. *Journal of Bacteriology* 174: 6729-6742.

- Vaughan, S., Wickstead, B., Gull, K. and Addinall, S. G. (2004) Molecular evolution of FtsZ protein sequences encoded within the genomes of archaea, bacteria, and eukaryota. *Journal of Molecular Evolution* 58: 19-29.
- Veiga, H., Jorge, A. M. and Pinho, M. G. (2011) Absence of nucleoid occlusion effector Noc impairs formation of orthogonal FtsZ rings during *Staphylococcus aureus* cell division. *Molecular Microbiology* 80: 1366-1380.
- Vollmer, W. (2008) Targeting the bacterial Z ring. *Chemistry and Biology* 15: 93-94.
- Wang, H. C. and Gayda, R. C. (1990) High-level expression of the FtsA protein inhibits cell septation in *Escherichia coli* K-12. *Journal of Bacteriology* 172(8): 4736-4740.
- Wang, X. and Lutkenhaus, J. (1993) The FtsZ protein of *Bacillus subtilis* is localized at the division site and has GTPase activity that is dependent upon FtsZ concentration. *Molecular Microbiology* 9: 435-442.
- Wang, X. and Lutkenhaus, J. (1996) Characterization of the *ftsZ* gene from *Mycoplasma pulmonis*, an organism lacking a cell wall. *Journal of Bacteriology* 178: 2314-2319.
- Wang, X., Huang, J., Mukherjee, A., Cao, C. and Lutkenhaus, J. (1997) Analysis of the interaction of FtsZ with itself, GTP, and FtsA. *Journal of Bacteriology* 179: 5551-5559.
- Weart, R. B., Nakano, S., Lane, B. E., Zuber, P. and Levin, P. A. (2005) The ClpX chaperone modulates assembly of the tubulin-like protein FtsZ. *Molecular Microbiology* 57: 238-249.
- Weart, R. B., Lee, A. H., Chien, A. C., Haeusser, D. P., Hill, N. S. and Levin, P. A. (2007) A metabolic sensor governing cell size in bacteria. *Cell* 130: 335-347.
- Weiss, D. S. (2004) Bacterial cell division and the septal ring. *Molecular Microbiology* 54: 588-597.
- Wells, W. A. (2004) Man the Nanoscopes. *The Journal of Cell Biology* 164(3): 337-340.
- Woldringh, C. L., Mulder, E., Huls, P. G. and Vischer, N. O. E. (1991) Toporegulation of bacterial division according to the nucleoid occlusion model. *Research in Microbiology* 142: 309-320.
- Woldringh, C. L., Mulder, E., Valkenburg, J. A. C., Wientjes, F. B., Zaritsky, A. and Nanninga, N. (1990) Role of the nucleoid in the toporegulation of division. *Research in Microbiology* 141: 39-49.
- Wu, L. J. and Errington, J. (2004) Coordination of cell division and chromosome segregation by a nucleoid occlusion protein in *Bacillus subtilis*. *Cell* 117: 915-925.

- Wu, L. J., Franks, A. H. and Wake, R. G. (1995) Replication through the terminus region of the *Bacillus subtilis* chromosome is not essential for the formation of a division septum that partitions the DNA. *Journal of Bacteriology* 177: 5711-5715.
- Wu, L. J., Ishikawa, S., Kawai, Y., Oshima, T., Ogasawara, N. and Errington, J. (2009) Noc protein binds to specific DNA sequences to coordinate cell division with chromosome segregation. *EMBO Journal* 28: 1940-1952.
- Yan, K., Pearce, K. H. and Payne, D. J. (2000) A conserved residue at the extreme C-terminus of FtsZ is critical for the FtsA-FtsZ interaction in *Staphylococcus aureus*. *Biochemical and Biophysical Research Communications* 270: 387-392.
- Yim, L., Vandebussche, G., Mingorance, J., Rueda, S., Casanova, M., Ruyschaert, J. M. and Vicente, M. (2000) Role of the carboxy terminus of *Escherichia coli* FtsA in self-interaction and cell division. *Journal of Bacteriology* 182: 6366-6373.
- Yu, X. C. and Margolin, W. (1997) Ca²⁺-mediated GTP-dependent dynamic assembly of bacterial cell division protein FtsZ into asters and polymer networks *in vitro*. *EMBO Journal* 16: 5455-5463.
- Yu, X. C. and Margolin, W. (1999) FtsZ ring clusters in *min* and partition mutants: Role of both the Min system and the nucleoid in regulating FtsZ ring localization. *Molecular Microbiology* 32: 315-326.